

Ice nucleation by mineral dusts

by

Alexander David Harrison

Submitted in accordance with the requirements for the degree of
Doctor of Philosophy

The University of Leeds
School of Earth and Environment

September 2019

The candidate confirms that the work submitted is his/her own, except where work which has formed part of jointly-authored publications has been included. The contribution of the candidate and the other authors to this work has been explicitly indicated below. The candidate confirms that appropriate credit has been given within the thesis where reference has been made to the work of others.

Harrison, A. D., Lever, K., Sanchez-Marroquin, A., Holden, M. A., Whale, T. F., Tarn, M. D., McQuaid, J. B. and Murray, B. J. ‘The ice-nucleating ability of quartz immersed in water and its atmospheric importance compared to K-feldspar’, Published in Atmospheric Chemistry and Physics 2019). This publication forms chapter two. I designed the study in conjunction with BJM. Scientific discussions with TFW and JBM further progressed the design of the experiments. I selected and sourced the materials for this study, designed the experimental protocol and analysed the resulting data. Together with BJM, I supervised KL who assisted with many of the experiments. AS completed calculations used in figures 7b and 8a and assisted in the calculation of errors for the active site density measurements. MAH performed Raman analysis of the chalcedony samples and MDT helped in the collection of literature data. I led the writing of the paper with contributions from all co-authors.

Harrison, A. D., O’Sullivan, D. O., Adams, M. P., Porter, G. C. E., Brathwaite, C. Lucas-Chewitt, R., Prospero, J. M., Sealy, A., Sealy, P., Whitehall, S., Sanchez-Marroquin, A., Tarn, M. D., Hawker, R., McQuaid, J. B. and Murray, B. J. ‘Ice-Nucleating Particle Activity in Transported Desert Dust in the Western Atlantic’, in preparation for submission to Geophysical Research Letters. The manuscript for this submission makes up chapter three. I conceived the initial concept of the campaign and together with BJM and DO designed the experiments. I managed the project with DO, BJM, MPA, GCEP, JBM, MDT, JMP, RC and AS assisting in the logistical planning of the campaign. Field experiments were conducted by OS, MPA, GCEP, CB, SW and myself. AS provided SEM analysis of filters taken back to the University of Leeds. RH performed all modelling of INP concentrations and aerosol global distributions. I led the writing of the manuscript with contributions from all authors.

Harrison, A. D., Whale, T. F., Rutledge, R., Lamb, S., Tarn, M. D., Porter, G. C. E., Adams, M. P., McQuaid, J. B., Morris, G. J., and Murray, B. J. ‘An instrument for quantifying heterogeneous ice nucleation in multiwell plates using infrared emissions to detect freezing’, published in Atmospheric Measurement Techniques (2018). This publication forms chapter four. The initial concept of the instrument was conceived by TFW, JGM and BJM which was further advanced by myself. I led the development of the instrument

, performed the bulk of the experiments and led the writing of the paper. RR and SL assisted with the development of the IR-NIPI and the analysis code with SL also performing initial proof-of-principle experiments. MDT, GCEP and MPA collected and analysed the atmospheric sample. All authors contributed to the writing of the paper.

This copy has been supplied on the understanding that it is copyright material and that no quotation from the thesis may be published without proper acknowledgement.

The right of Alexander David Harrison to be identified as Author of this work has been asserted by him in accordance with the Copyright, Designs and Patents Act 1988.

© 2019 The University of Leeds and Alexander David Harrison

Acknowledgements

I would like to thank my supervisors Benjamin Murray, James McQuaid and John Morris for all of their support and guidance during this project. I would also like to thank all members of the Murray group who have assisted me with their scientific discussions and also for their support and company for the duration of the project: Mark Tarn, Grace Porter, Michael Adams, Mark Holden, Thomas Whale, Alberto Sanchez-Marroquin, Jesus Vergara Temprado, Daniel O'Sullivan, Rachel Hawker, Martin Daily, Elena Maters, Sandy James, Seb Sikora, Beth Wyld, Sarah Barr and Tom Mangan.

A special thanks to all of my family and friends who have helped me throughout. In particular I thank my parents, David and Kim Harrison, for their support and guidance.

I would also like to take the time to thank my financial sponsors the National Environmental Research Council and Asymptote Ltd. whom without the project would not have been possible.

Abstract

Heterogeneous ice nucleation in the immersion mode plays a vital, yet poorly understood, role in the development of ice in mixed-phase clouds. From recent work it is thought that mineral dusts are a major, globally important source of ice-nucleating particles (INP). However, field observations to support this are sparse and the prediction of INP concentrations is challenging. This thesis expands on our current knowledge of the ice-nucleating characteristics of various components of mineral dust with the ultimate goal of being able to better predict INP concentrations globally and improve our fundamental understanding. These laboratory based experiments are then used to guide fieldwork studies and develop an interpretation of the observations. In addition to this, presented here is the development and characterisation of a new immersion mode assay for the detection of low concentrations of INP.

From previous work K-feldspar is thought to be the dominant component in mineral dusts for ice nucleation. However, the quartzes have not been extensively surveyed although they make up a much larger proportion of mineral dusts than K-feldspar (in most instances). The investigation of 10 α -quartz samples show quartz to be ice active with a large variability in activity and sensitivity to time spent in water and air. The development of four new parameterisations supports evidence that K-feldspar is the dominant mineral INP in the atmosphere and we can predict field collected dust sample measurements well with the proposed K-feldspar parameterisation.

We also make the first field measurements of INP at Barbados where desert dust aerosol is present which has been transported for many days after being emitted from dust sources in Africa. We show the activity of the dust to have decreased on transport across the Atlantic. Using XRD, SEM and INP modelling we attribute the deactivation to the preferential loss of the K-feldspar component on transport.

The last section of this project describes the development of a 50 μ L drop assay which is more sensitive to the detection of low concentrations of INP active at warm temperatures ($> -15^{\circ}\text{C}$) and lends itself to future use in field campaigns. This instrument is novel in that it uses an infrared camera to make temperature measurements and to automatically detect freezing.

Table of Contents

Acknowledgements	iv
Abstract	v
Table of Contents	vi
List of Tables	x
List of Figures	xi
List of Abbreviations	xiv
1. Introduction	2
1.1 Clouds in the Earth's climate system.....	2
1.2 Ice nucleation in the atmosphere	5
1.2.1 Atmospheric ice-nucleating particles.....	7
1.3 Mineral dust in the climate system.....	10
1.4 Modes of ice nucleation	14
1.4.1 Experimental methods.....	16
1.4.1.1 Wet dispersion.....	16
1.4.1.2 Dry dispersion	17
1.5 Classical Nucleation Theory (CNT)	18
1.5.1. Homogenous classical nucleation theory	19
1.5.2 Heterogeneous classical nucleation theory.....	20
1.6 Describing ice nucleation.....	21
1.7 Minerals as ice-nucleating particles	22
1.8 Feldspars	28
1.9 Quartz.....	30
1.10 Project objectives.....	32
1.11 Thesis overview.....	33
1.12 Other work completed during the course of my PhD	34

References	37
2. The ice-nucleating ability of quartz immersed in water and its atmospheric importance compared to K-feldspar.....	55
2.1 Introduction.....	56
2.2 Quartz, the mineral.....	59
2.3 Materials and Methods.....	61
2.3.1 Samples and preparation.....	61
2.3.2 Ice nucleation experiments.....	64
2.4 Results and discussion.....	66
2.4.1 The variable ice-nucleating ability of α -quartz.....	66
2.4.2 The sensitivity of ice-nucleating activity with time spent in water and air.....	70
2.4.3 Discussion of the nature of active sites on quartz.....	73
2.5 The importance of quartz relative to feldspar for ice nucleation in the atmosphere.....	75
2.5.1 Comparison to the literature data for quartz and feldspar.....	75
2.5.2 New parameterisations for the ice-nucleating ability of quartz, K-feldspar, plagioclase and albite.....	78
2.5.3 Testing the new parameterisations against literature laboratory and field measurements of the ice-nucleating ability of desert dust.....	83
2.6 Conclusions.....	87
References.....	89
3. Ice-nucleating activity of desert dust decreases on transport across the Atlantic.....	101
3.1 Introduction.....	101
3.2 Methods.....	104
3.2.1 Project overview.....	104

3.2.2 Aerosol sampling and measurements.....	104
3.2.2 Ice nucleation experiments.....	105
3.3 Results and discussion.....	106
3.3.1 Ice-nucleating particle concentrations and activity.....	106
3.3.2 Characterisation of aerosol in Barbados.....	110
3.3.3 Discussion of what leads to the lower activity of dust in Barbados...	112
3.4 Conclusions.....	117
References.....	118
Supporting information.....	127
References.....	146
4. An instrument for quantifying heterogeneous ice nucleation in multiwell plates using infrared emissions to detect freezing.....	147
4.1 Introduction.....	148
4.2 Instrument design.....	150
4.2.1 Operating principle.....	150
4.2.2 IR-NIPI design.....	151
4.2.3 Temperature measurements with an infrared camera.....	155
4.2.4 Temperature calibration.....	155
4.3 Test experiments and analysis.....	160
4.3.1 Control experiments.....	160
4.3.2 Feldspar chips.....	162
4.3.3 NX-illite.....	164
4.3.4 Atmospheric aerosol sample.....	167
4.4 Summarray and conclusions.....	169
References.....	170
5. Conclusions.....	179

5.1 Overview.....	179
5.2 Objective one: Mineral characteristics and their influence on the ice-nucleating ability of mineral dust.....	179
5.3 Objective two: Taking field measurements of transported mineral dust and constraining INP predictions.....	184
5.4 Objective three: Develop an immersion mode instrument capable of detecting rare INP.....	187
5.5 Concluding remarks.....	189
References.....	190
Appendix 1.....	195

List of Tables

Table 1.1: A list of aerosol-cloud interactions and their resulting effects. Table modified from an insert from Storelvmo (2017).....	4
Table 1.2: List of materials initially active above -18 °C. Table modified from Mason and Maybank (1958).....	23
Table 2.1: Table showing the relative concentrations of different minerals within each sample and the respective BET specific surface area of the ground sample and derived spherical equivalent average surface area.....	62
Table S1: Sampling durations and the volume of air sampled for 28 runs and their corresponding symbols used in figure 3.2a.....	127

List of Figures

Figure 1.1: A representation of the appearance, composition, typical midlatitude altitude, and radiative effects of (a) cirrus and (b) mixed-phase clouds. Figure taken from Storelvmo (2017).....	2
Figure 1.2: Schematic of the process leading to marine organic aerosol being emitted to the atmosphere. Diagram is taken from Wilson et al. (2015).....	9
Figure 1.3: Compilation of the active site densities of various materials which are known to nucleate ice. Figure taken from Murray et al. (2012).....	10
Figure 1.4: Average composition of atmospheric dusts. Diagram is taken from Murray et al. (2012).....	12
Figure 1.5: Modes of sediment transport in air where saltation can lead to ejected particles being suspended in airflow and emitted to the atmosphere. Diagram modified from Pye (1994).....	13
Figure 1.6: Schematic showing the various ice nucleation pathways which occur in the atmosphere. Figure taken from Kanji et al. (2017).....	15
Figure 1.7: Ternary diagram displaying the range of compositions in the feldspar group of minerals. Diagram taken from Harrison et al. (2016).....	26
Figure 1.8: Images displaying two feldspar samples, one with and one without perthitic texture, when observed under C-P microscopy, SEM and EDX. Images are taken from Whale et al. (2017).....	27
Figure 1.9: Schematic representation of the structure of α-quartz along its c-axis where each Si is bonded to four oxygens. Schematic modified from Gibbs (1926).....	31
Figure 1.10: Phase diagram showing the stability fields of various silica polymorphs. The diagram is based on Swamy et al. (1994).....	32
Figure 2.1: Illustration of the geological processes that lead to the creation of a mineral dust and its emission to the atmosphere.....	59
Figure 2.2: Pictures of the various quartz samples explored in this study showing their varying appearances and characteristics.....	63

Figure 2.3: Fraction frozen and active site densities for ten quartz suspensions (1 wt%).....	69
Figure 2.4: Plots showing the sensitivity of quartz activity, expressed as n_s, to time spent in water and air.....	72
Figure 2.5: Plot of n_s versus temperature for the available literature data for quartz compared to the data collected in this study.....	76
Figure 2.6: Plot of n_s versus temperature for quartz and feldspar literature data, together with the quartz data from this study.....	77
Figure 2.7: Parameterizations developed for various silicate minerals.....	79
Figure 2.8: Comparison of the newly developed parameterisations.....	82
Figure 2.9: Testing the newly developed K-feldspar and quartz parameterisations against literature data for desert dust.....	86
Figure 3.1: Schematic of the processes which may alter the ice-nucleating ability of a mineral dust during transport.....	104
Figure 3.2: INP measurements from Barbados from the 24th July-24th August.....	109
Figure 3.3: [INP] per litre for heated versus unheated samples.....	110
Figure 3.4: Composite of the merged size distributions (from both the APS and SMPS) for the duration of the campaign.....	111
Figure 3.5: Predictions versus the observations at Barbados.....	116
Figure S1: $\text{Log}(k(T))$ for the baselines of the experiments and the exponential fit and standard deviation used to represent the baseline in subsequent error calculations and background subtractions.....	131
Figure S2: $k(T)$ versus temperature for two examples of collected aerosol.....	132
Figure S3: The calculated $K(T)$ values for the examples from Figure S2 and their corresponding errors.....	133
Figure S4: HYSPLIT back trajectories for the date and times of the filter samples in this study.....	134-138
Figure S5: The fraction frozen curves for heated versus unheated suspensions.....	139

Figure S6: Time series for the relative humidity, wind direction and INP(T) at 0.01L^{-1}.....	140
Figure S7: Compilation of the sized resolved composition and the contribution of mineral dust to the overall surface area retrieved from SEM analysis of four aerosol filter samples.....	141
Figure S8: XRD analysis of aerosol collected in rain water from the 3rd-4th of August. The limit of detection of this technique was $\sim 2\%$.....	142
Figure S9: GLOMAP model simulation of the mass fraction of K-feldspar relative to aerosolised mineral dust.....	143
Figure S10: The GLOMAP simulated and APS measured aerosol mass daily averages for the duration of the campaign.....	144
Figure S11: The effect of sea salt on K-feldspars ability to nucleate ice.....	145
Figure 4.1: Schematic diagram of the IR-NIPI system (not to scale).....	152
Figure 4.2: Illustration of the use of the IR camera to measure temperature and freezing events.....	152
Figure 4.3: Tests of the IR temperature measurement using aluminium wells with embedded thermocouples.....	157
Figure 4.4: Tests of the IR temperature measurements using thermocouples positioned in a multiwall plate.....	159
Figure 4.5: The fraction of droplets frozen as a function of temperature on cooling for a range of samples.....	161
Figure 4.6: Comparison of nucleation induced by feldspar chips in the IR-NIPI and μL-NIPI instruments.....	163
Figure 4.7: Active site densities, $n_s(T)$, for NX-illite.....	166
Figure 4.8: The active site density, $n_s(T)$, for a $0.01\text{wt}\%$ NX-illite suspension and $n_s(T)$ from a corresponding second freezing run with the same droplets after they had been thawed out and refrozen.....	167
Figure 4.9. INP concentrations per litre of air samples on the 5th November 2017 in Leeds.....	169

List of Abbreviations

INP	Ice-Nucleating Particle
BET	Brunauer-Emmett-Teller surface area
CCN	Cloud Condensation Nuclei
CFDC	Continuous Flow Diffusion Chamber
CNT	Classical Nucleation Theory
IPCC	Intergovernmental Panel on Climate
μ L-NIPI	microliter Nucleation by Immersed Particle Instrument
IR-NIPI	InfraRed Nucleation by Immersed Particle Instrument
IR	InfraRed
ETA	Eastern Tropical Atlantic
APS	Aerodynamic Particle Sizer
SMPS	Scanning Mobility Particle Sizer

1. Introduction

1.1 Clouds in the Earth's climate system

Clouds are an essential component in determining the Earth's climate and radiative budget. Their physical properties are a determining factor to what influence a cloud will have on the Earth's climate with both incoming shortwave and outgoing long wave radiation being influenced (Storelvmo, 2017; Tan et al., 2016), see figure 1. Clouds can also effect wind patterns as well as play a key role in the hydrological cycle through processes such as water transport and precipitation (Hoose and Mohler, 2012; Murray et al., 2012a). There is much uncertainty on the impact of clouds on the global energy budget (Lohmann and Feichter, 2005; Wild et al., 2019) but the 2013 Intergovernmental Panel on Climate change (IPCC) report would suggest that clouds result in a net cooling effect of up to -20 W m^{-3} (Boucher et al., 2013). (Ipcc, 2014) attribute this uncertainty to the unknowns of interactions between clouds and aerosols.

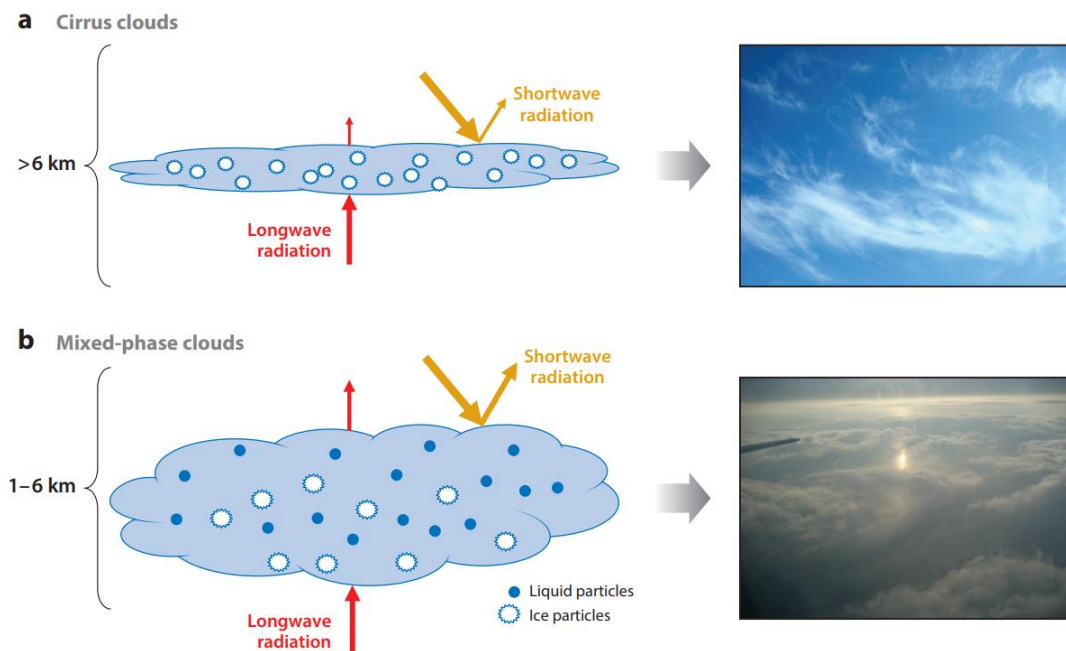


Figure 1.1: A representation of the appearance, composition, typical midlatitude altitude, and radiative effects of (a) cirrus and (b) mixed-phase clouds. Figure taken from Storelvmo (2017).

Aerosol can exist as a primary product (such as mineral dust, anthropogenic emissions and sea salt) or as secondary aerosol as the result of condensing gases. The properties of the aerosol present impacts the clouds size, liquid water content, lifetime and amount of ice vs supercooled droplets. These impacts are otherwise known as aerosol indirect effects (Denman et al., 2007) and the work by Köhler (1936) formed the basis for our current understanding of cloud droplet formation and growth. This work suggested that cloud droplets could not form under atmospheric humidity's without the presence of hygroscopic particles to act as a cloud condensation nuclei (CCN). If the atmosphere was completely aerosol free then extreme supersaturations could develop and lead to homogeneous droplet formation but in reality there are many anthropogenic and naturally occurring aerosol that can act as CCN and activate aerosol to form droplets at much lower humidity's. Once relative humidity reaches 100% cloud droplet formation occurs with the amount of CCN hardly ever being a limiting factor (Storelvmo, 2017). Based on the work of (Köhler, 1936) it is then understandable that a clouds reflective properties can be determined by the CCN concentration. If a cloud was to form in the presence of a high concentration of CCN then the droplets would be small but abundant. Likewise if a cloud, of a similar water content, was to form under low CCN concentrations then the cloud would develop less but larger water droplets and therefore be optically thinner than the cloud developed with high CCN concentrations. This effect is often referred to as the Twomey effect (Twomey, 1977), the first aerosol indirect effect, or the cloud albedo effect (Storelvmo, 2017). The Twomey effect can then have an impact on a clouds water content and life time as the size of the droplets can affect the rate of droplet collisions and coalescence (with smaller droplet sizes tending to be less efficient) and has been termed the Albrecht effect, the cloud lifetime effect or the second indirect aerosol effect (Albrecht, 1989). This effect is particularly important for warm rain processes. The above mentioned effects demonstrate the sensitivity of a clouds properties to the presence of CCN aerosol.

However, under the right conditions aerosol can also act as ice-nucleating particles (INP) to initiate cloud glaciation, which also influences a clouds liquid water content and albedo. The presence and morphology of ice in clouds influences its properties such as its lifetime and optical thickness (Hartmann et al., 1992; Lohmann and Feichter, 2005). A list of aerosol effects on different cloud types can be seen in table 1. Vergara-Temprado et al. (2018) have

demonstrated the importance of these aerosol indirect effects by explaining the large biases of model simulated cloud reflectivity over the Southern Ocean. They show that the low concentrations of ice-nucleating particles are not represented in models and that these concentrations are vital for understanding the life time of the clouds and therefore their impact on the radiative budget. This is particularly important when modelling the effect of anthropogenic influences for climate change in the future. Tan et al. (2016) have shown that the climate sensitivity is underestimated in models where INP are poorly constrained and the equilibrium climate sensitivity can be up to 1.3 °C higher in models that are constrained by liquid-ice observations from satellites. This is linked directly to the reduction in the amount of glaciation with a warming climate which leads to a weakened cloud-phase feedback. It is then clear that in order to make better climate predictions we need to understand the process of ice nucleation in the atmosphere.

Aerosol-Cloud Interaction Definitions

Aerosol Effects on Liquid Clouds

The **Twomey effect** refers to the increased albedo associated with clouds forming in environments with an abundance of CCN; these consist of more, but smaller, cloud droplets compared with similar clouds forming in clean environments. It is also known as the cloud albedo effect or the first indirect aerosol effect.

The **Albrecht effect** refers to the prolonged lifetime of clouds in response to the reduced warm-rain production efficiency expected to accompany an aerosol-induced reduction in cloud droplet size. The effect, Also known as the cloud lifetime effect or the second indirect aerosol effect, is thought to yield a net cooling by causing liquid clouds to be more extensive, whether spatially, temporally, or both.

Aerosol Effects on Mixed-Phase Clouds

The **cloud glaciation effect** is hypothesised to occur in response to an increase in aerosol particles that can act as INP. Additional INP would be expected to nucleate more ice crystals, which could in turn lead to a more rapid conversion from liquid ice to ice through diffusional growth or riming. This more rapid cloud glaciation would decrease cloud optical thickness and likely produce precipitation.

The **deactivation effect** could occur as a result of an increase in aerosol precursor gases, which when condensing onto INP could in fact deactivate their ice-nucleating ability either temporarily or permanently. This could reduce cloud glaciation through the mechanisms described above.

A **mixed-phase cloud lifetime effect** would work in much the same way as the lifetime effect for liquid clouds described above.

Aerosol Effects on Cirrus Clouds

INP effects on cirrus clouds: Additional INP could increase the heterogeneous ice nucleation rate and suppress homogeneous nucleation, which would yield fewer but larger ice crystals and optically thinner clouds. That is, assuming there is sufficient homogeneous nucleation to suppress, an increase in INP abundance would have a cooling effect on climate. The opposite would be true if heterogeneous nucleation dominated cirrus cloud formation.

Sulphate effects on cirrus clouds: Sulphur emissions should increase the number concentration of small solution droplets available for homogeneous nucleation in the upper troposphere, which could in theory produce effects similar to the Twomey and Albrecht effects for warm clouds by increasing the number of ice crystals formed once the criteria for homogenous nucleation are met.

Table 1.1: A list of aerosol-cloud interactions and their resulting effects. Table modified from an insert from Storelvmo (2017).

1.2 Ice nucleation in the atmosphere

Ice nucleation is thought to be important for both cirrus and mixed-phase clouds. Where cirrus clouds are composed entirely of ice crystals and mixed-phase clouds are a combination of the ice and liquid water phases. The nucleation of ice crystals straight from the vapour phase is not favourable in the troposphere and so an aerosol particle is often needed to act as an INP which highlights the importance of understanding heterogeneous ice nucleation for mixed-phase clouds in the regime of 0 to about $-37\text{ }^{\circ}\text{C}$ (Forster et al., 2007; Kanji et al., 2017). Although an INP is beneficial for ice formation it is worth noting that ice can form homogeneously in the atmosphere at temperatures sufficiently cold enough, below around $-33\text{ }^{\circ}\text{C}$ (Herbert et al., 2015; Riechers et al., 2013). Cirrus clouds form in the upper troposphere at temperatures roughly below $-38\text{ }^{\circ}\text{C}$. Ice nucleation under cirrus conditions is thought to occur by both the immersion and the deposition mode, which are discussed in more depth in section 1.4. Mixed-phase clouds form in the mid to lower troposphere at temperatures between 0 to $-38\text{ }^{\circ}\text{C}$. For mixed-phase clouds heterogeneous ice nucleation above $\sim -33\text{ }^{\circ}\text{C}$ is thought to be dominated by the immersion mode process (Cui et al., 2006; de Boer et al., 2011). In this project my studies are focused on the immersion mode for this reason.

Although supercooled water can exist in clouds well-below $-33\text{ }^{\circ}\text{C}$ we often see clouds glaciating at much warmer temperatures (Ansmann et al., 2009; Kanitz et al., 2011). This demonstrates the importance INP have for ice formation in clouds with Choi et al. (2010) reporting that roughly 50 % of clouds globally are glaciated at $-20\text{ }^{\circ}\text{C}$. It should be noted that INP in the atmosphere are much rarer than CCN. It has also been found that the number of aerosol particles capable of acting as an INP increases with decreasing temperature (Mason, 1971; Meyers et al., 1992; Pruppacher and Klett, 1997). INP concentrations are typically measured to be on the order of 10^{-4} to 10^{-1} cm^{-3} depending on location and temperature (where the limits are defined by the experimental limitations) (DeMott et al., 2010; Mason, 1971; Pruppacher and Klett, 1997), with values in excess of 1 cm^{-3} being recorded in desert dust plumes (DeMott et al., 2003). Vergara-Temprado et al. (2018b) demonstrated that concentrations much lower than 0.1 L^{-1} can deplete the liquid water content of shallow clouds in the Southern Ocean which strongly changes their radiative properties. Remote marine regions appear to have the lowest INP concentrations recorded (DeMott et al., 2016; Rosinski and Morgan, 1988) and no correlation between the concentration of CCN and INP is apparent (Rogers et al., 1998).

For a particle to act as an effective INP Pruppacher and Klett (1997) suggest that the particle should: (1) be insoluble in water; (2) have sufficient size; (3) have the ability to make chemical bonds between the INP surface and water; (4) have a crystallographic match to the shape of ice, i.e. lattice match. Exceptions to these guidelines have been found which means caution should be applied when investigating a material using these criteria. At present the understanding of INPs is limited and the only way to determine the ice-nucleating efficiency of a material is to carry out quantitative experimentation (Murray et al., 2012). More recent work has attributed the activity of some minerals to the presence of defects on the crystals surface with high speed microscopy finding preferred locations for ice nucleation to occur (Holden et al., 2019; Whale et al., 2017). The nature of these defects is on the nanoscale and so there they are still poorly understood but may lead to new studies which can probe into the nature of their ice-nucleating ability and provide a basis for predicting the ice-nucleating ability of a material.

The presence of these active sites/INP can lead to the initial formation of ice via a heterogeneous pathway and have drastic effects on the ice crystal size and content in a cloud

as well as leading to secondary ice formation. Initial ice crystals will grow at the expense of the surrounding supercooled water droplets (known as the Wegener-Bergeron-Findeisen process) until they are large enough to fall out (Pruppacher and Klett, 1997). If many ice crystals were to form in the presence of supercooled water then the lifetime of the cloud would be longer than that of a cloud which had fewer ice crystals. This is because the fewer ice crystals would be able to grow larger at the expense of the supercooled droplets, due to less competition from other growing crystals, and therefore become denser and fall out, dissipating the cloud. The amount, size and concentration of the ice crystals significantly changes the radiative properties of the cloud and is directly affected by the concentration of INP in regimes where homogeneous ice formation is not possible (Lohmann and Feichter, 2005). Primary ice formation can also be the catalyst for secondary ice formation processes which can increase the concentration of ice crystals by several orders of magnitude (Field et al., 2017; Phillips et al., 2003). The most well understood of these secondary ice formation processes is the Hallett-Mossop process which occurs at temperatures between -3 to -8 °C (Hallett and Mossop, 1974). These secondary ice formation processes are thought to explain field observations where ice crystal concentrations are orders of magnitude higher than the INP concentrations (Mignani et al., 2019).

1.2.1 Atmospheric-ice nucleating particles

Electron microscope work has analysed snowflakes and found mineral dust to be commonly found within them which would suggest that mineral dust acts as an effective INP in the atmosphere (Eriksen Hammer et al., 2018; Iwata and Matsuki, 2018; Pratt et al., 2009). In these studies biological, soot and salt components have also been found with evidence for the deactivation of INP by the presence of the salt component (Iwata and Matsuki, 2018; Si et al., 2019). Climate model simulations by Hoose et al. (2010) have proposed that up to 77% of INP active between 0 to -38°C are accounted for by mineral dusts making mineral dusts a globally important source of INP. At present there is an understanding that the K-feldspar component is responsible for the generally high ice-nucleating ability of mineral dust (Atkinson et al., 2013b). A fuller review of mineral dusts can be found in section 1.3.

Primary biological aerosol particles (PBAPs) have been known to nucleate ice for half a century and come from living organisms (Matthias-Maser and Jaenicke, 1995; Schnell and Vali, 1973). PBAPs can be pollen, viruses, bacteria, fungal spores, or fragments of plants and animals. The exact concentration of these PBAPs in the atmosphere is difficult to quantify but it has been estimated that up to 1000 Tg a year of PBAPs are emitted to the atmosphere (Jaenicke, 2005; Jaenicke et al., 2007). Other studies have attributed ~20%, by number (< 0.4 μm), of aerosol sampled is attributable to PBAPs (Graham et al., 2003; Gruber et al., 1999; Matthias-Maser and Jaenicke, 1995; Morris et al., 2011). The effect of biological components in transported mineral dusts is still poorly understood but there is evidence to suggest that mineral dusts can act as carriers for ice-nucleation active biological species. O’Sullivan et al. (2014) showed that dusts extracted from fertile soils can have high ice-nucleating efficiencies which decrease in activity with heat treatment. This provides evidence for the presence of biogenic ice-nucleating material combined with mineral dusts. Further work by O’Sullivan et al. (2016) has proven that proteins from a common soil borne fungus (*Fusarium avenaceum*) can actively bind to kaolinite particles and the ice-nucleating activity of the protein can be sustained once adsorbed onto the clay surface. Schnell (1974) found that there were biological INP present in soil dusts in the Sahel, but it is unclear if this biological component is important once airborne. However, O’Sullivan et al. (2018) recently measured airborne aerosol at an agricultural site in the U.K. and suggested the presence of biological INP internally mixed with mineral dust. This has potential significance for the activity of mineral dusts at warm temperatures if biological INP are present. The relative contributions of mineral and biogenic components as INP is still poorly understood.

More recently marine organics have been proven to be effective INP, especially in remote areas with low concentrations of aerosols (DeMott et al., 2016; Wilson et al., 2015). A bubble bursting process on the water surface is thought to eject material from the microlayer of the ocean and provide a source of efficient INP to the atmosphere (DeMott et al., 2016; Wilson et al., 2015), see figure 1.2. Although mineral dusts are the major source of INP globally there are instances in remote areas, such as the southern ocean, where marine organics are thought to become the dominant INP (Vergara-Temprado et al., 2017).

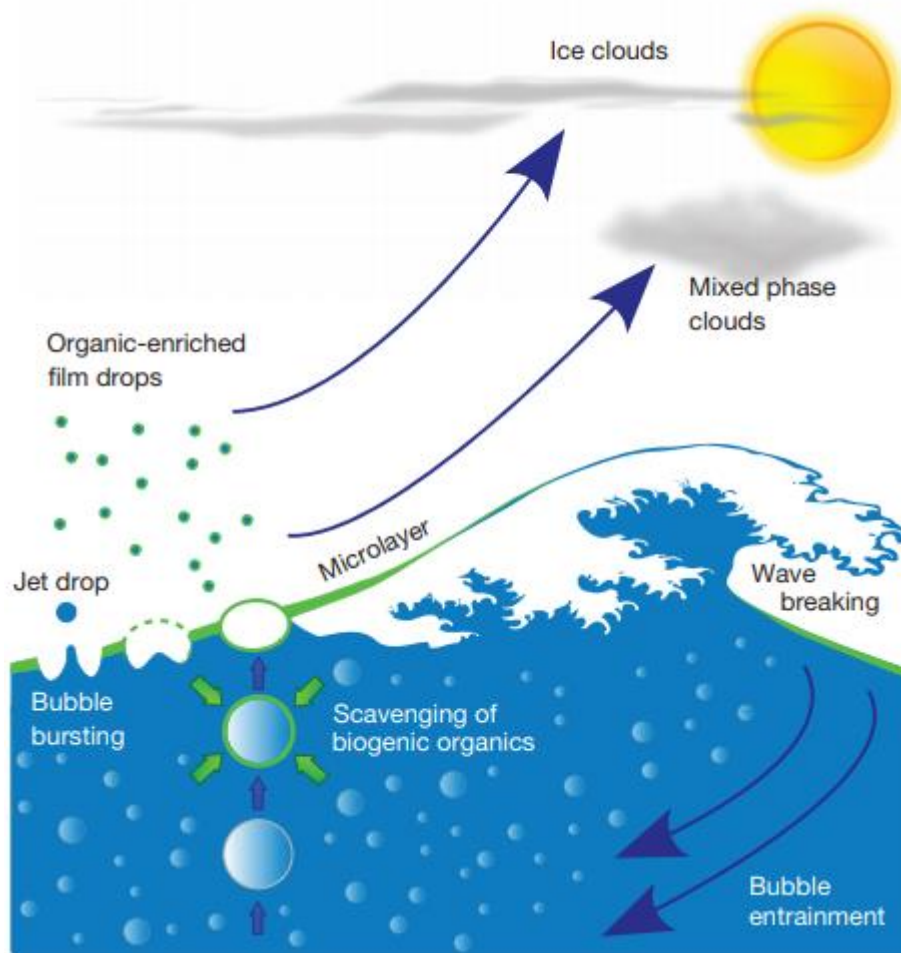


Figure 1.2: Schematic of the process leading to marine organic aerosol being emitted to the atmosphere. Rising bubbles scavenge organic material when rising to the surface resulting in an enrichment of organic material at the air-sea interface. The bubbles may then burst which allows for the ejection of organic material as organic-rich film drops. Diagram is taken from Wilson et al. (2015).

At current there is much debate and discussion on the role of anthropogenic combustion aerosol as INP (Ardon-Dryer and Levin, 2014; Chen et al., 2018; Demott, 1990; Grawe et al., 2018; McCluskey et al., 2014; Schill et al., 2016; Ullrich et al., 2017; Umo et al., 2015). Contradicting measurements have been made which has led to an unclear role of this aerosol type as an INP in the atmosphere. For example, Twohy et al. (2010) observed increased ice crystal concentrations correlating to black carbon content in mixed-phase clouds. In contradiction to this Pratt et al. (2009) observed no enhancement of combustion aerosol in ice crystal residues from the very same campaign. At present there is still much uncertainty in the role of

combustion aerosol as INP but there is a general consensus that mineral dust is the major global source of INP along with contributions from marine organics and other possible sources. This is supported by the work of Vergara-Temprado et al. (2018a) who completed a recent laboratory investigation into the ice-nucleating ability of soot and found results to be in agreement with other recent studies (Schill et al., 2016; Ullrich et al., 2017). These results were implemented into a global model which demonstrated that BC was unlikely to contribute substantially to atmospheric INP populations with BC INP concentrations being several orders of magnitude lower than mineral dust and marine organic INP concentrations. A compilation of the ice-nucleating ability of various materials can be seen in figure 1.3, (Murray et al., 2012).

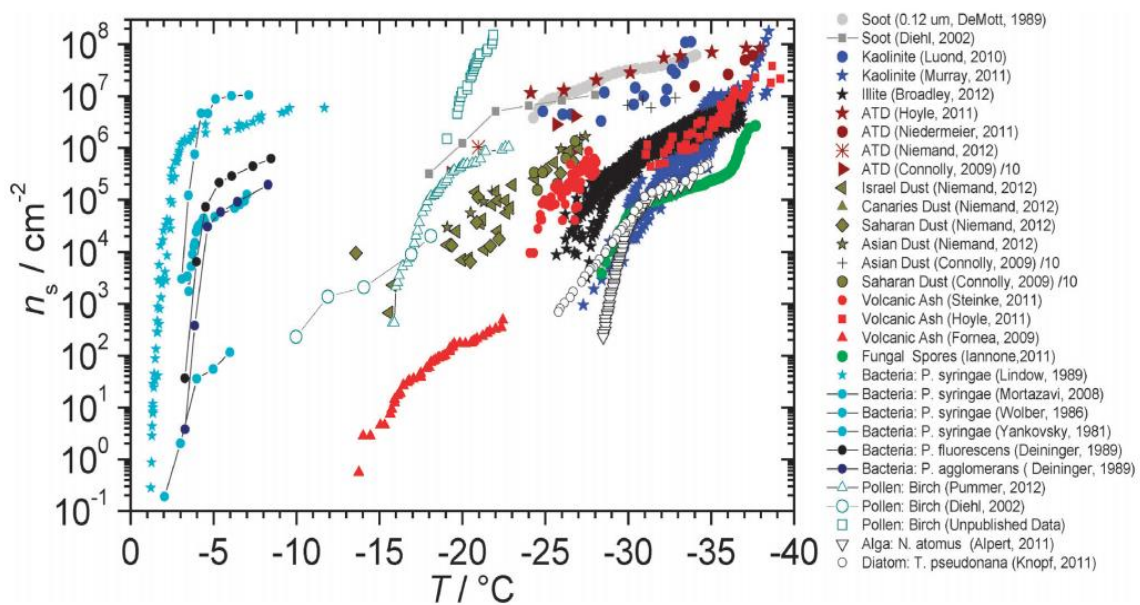


Figure 1.3: Compilation of the active site densities of various materials which are known to nucleate ice. It can be seen that biogenic materials are extremely efficient at nucleating ice, however mineral dusts are more prominent as INP in the atmosphere due to their abundance. Figure taken from Murray et al. (2012).

1.3 Mineral dust in the climate system

Mineral dusts are composed of various minerals with the three most abundant mineral groups in the atmosphere being the clays, quartz and feldspars respectively, see figure 1.2 (Murray et al., 2012). These dusts are created by the scavenging of material from the surface layer of the earth and therefore mineral dusts are similar in composition to the crust. When subject to

weathering crustal rocks can break down into fragments (silts, sands and gravels) to form soils (Press et al., 2003). If these soils are not lithified then erosion can transport these mineral fragments and hence these minerals can be lofted into the atmosphere where they can play a role in the glaciation of clouds. Creep or reptation, saltation and suspension are the three major modes of sediment transport in Aeolian systems (Pye, 1994), figure 1.5. Saltation, in particular, is important for the ejection of material to the atmosphere and is controlled by elastic impacts as a result of moving grains colliding with stationary grains on a surface. It is estimated that between 1000 to 3000 Tg of mineral dust is aerosolised in the atmosphere each year (Zender et al., 2004) commonly being sourced from arid regions such as Asia, Africa and the middle East, referred to as the Dust Belt (Prospero et al., 2002). The amount of mineral dust emitted to the atmosphere may change in future years as anthropogenic land use changes (e.g. deforestation and desertification) (Ginoux et al., 2012; Mahowald, 2007), with estimates suggesting that mineral dust emissions have doubled during the twentieth century (Mahowald et al., 2010). Estimates have attributed up to 50% of aerosolised mineral dust as a result of anthropogenic influences (Sokolik and Toon, 1996; Tegen and Fung, 1995) with a more recent study reporting roughly 25% of mineral dust is produced as a result of human influences (Ginoux et al., 2012).

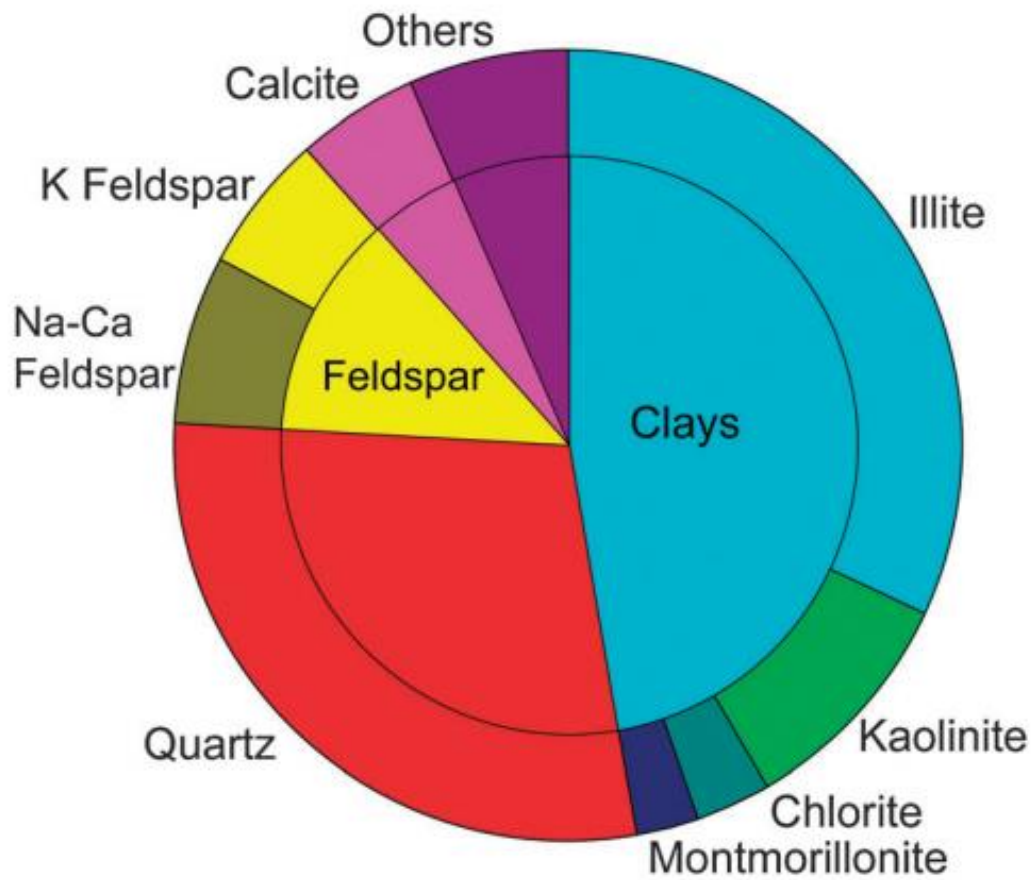


Figure 1.4: Average composition of atmospheric dusts. The heading ‘other’ includes materials such as gypsum, goethite, haematite, palygorskite and halite. Diagram is taken from Murray et al. (2012).

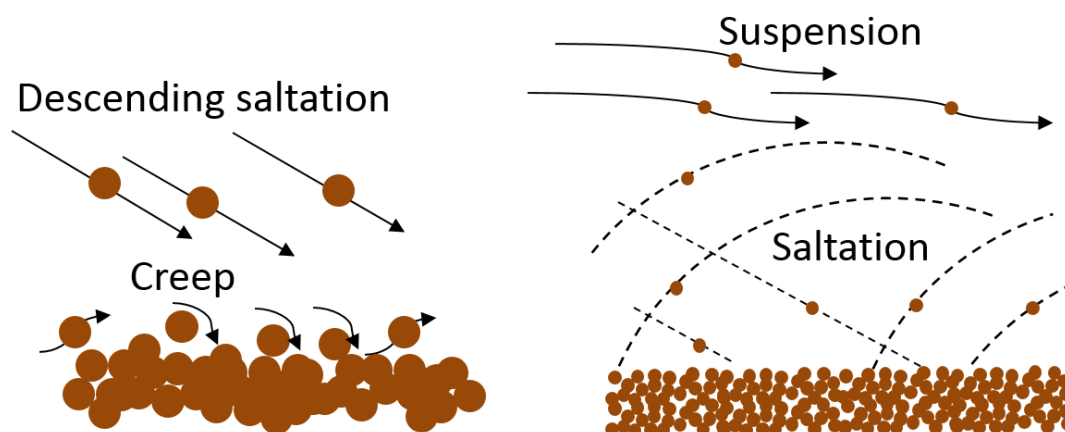


Figure 1.5: Modes of sediment transport in air where saltation can lead to ejected particles being suspended in airflow and emitted to the atmosphere. Diagram modified from Pye (1994).

As mentioned earlier the three most commonly found minerals in aerosolised mineral dusts are clay, quartz and feldspar. As soils (and therefore mineral dusts) are the result of weathering and erosion processes it is not surprising that quartz and feldspar are found in abundance as these minerals are relatively hard and make up a large component of the continental crust (Mohs scale 6.5-7) (Deer et al., 1992). Quartz is also chemically inert and hence is commonly the major constituent in sand found on coastal beaches where the sediments have been vigorously weathered. However, in most mineral dusts it is the clay minerals which dominate. Clays are often formed as reaction products from the breakdown of other minerals, such as feldspar, and hence are found in abundance in soils (Press et al., 2003). Clays are a softer (meaning they wear down to smaller aerosol sizes) and less dense mineral than both the quartz and feldspar minerals and so are more easily lofted into the atmosphere and have greater residence times. This is partly why for a number of years the clay group was targeted for ice nucleation studies and considered to be the most important component in mineral dusts for ice nucleation (Broadley et al., 2011; Mason and Maybank, 1958; Murray et al., 2011; Pinti et al., 2012; Roberts and Hallett, 1968; Wex et al., 2014).

As alluded to earlier, although clays are the dominant component of mineral dusts there is a general consensus that it is the K-feldspar component which is important for ice nucleation (Atkinson et al., 2013b). However, the general emission of the mineral components of dust are not constant over geologic time and can vary dependent on factors such as climate, volcanism and meteorite impacts. Interesting studies have shown how these factors can potentially alter

the relative concentrations of minerals, in particularly K-feldspar, and impact the amount of effective INP that are present for ice formation in clouds through geological time (Coldwell and Pankhurst, 2019; Pankhurst, 2017). This demonstrates that no one mineral dust can be treated the same and that the mineralogy can vary greatly depending on the source rock and conditions under which it was weathered.

In addition to this it has also been suggested that the formation processes involved in the crystallisation of the minerals themselves may have an impact on the nucleating ability of dust. Whale et al. (2017) have shown that the microtexture in alkali feldspars is important in determining their ice-nucleating ability. The perthitic texture, which is thought to relate to an alkali feldspars ability to nucleate ice, forms under conditions which allow the melt to cool over long periods of time so that the alkali and plagioclase components of feldspar may separate during crystallisation. Erosion processes which have access to minerals which have formed under conditions which favour their ability to nucleate ice can thus produce dusts which are more effective as INP.

1.4 Modes of ice nucleation

The descriptions outlined here are based on the recent work of Vali et al. (2015) who consolidated the various definitions used in the literature.

The modes of ice nucleation can be separated in to two broad categories, deposition and freezing. Deposition ice nucleation is a gas to solid phase transition and refers to the process of ice nucleation from a supersaturated water vapour on to a substrate. There should be no intermediate step between the water vapour to ice transition, i.e. water vapour should not condense as a liquid before ice formation occurs. Freezing ice nucleation is a liquid to solid phase transition and described as ice nucleation within a body of supercooled water as the result of the presence of an INP. Freezing ice nucleation can be further subdivided in to three subgroups. Immersion freezing is the process of an INP being fully immersed within a body of supercooled water before initiating ice formation. Contact freezing is the nucleation of ice at the water-air interface as a result of an INP coming in contact with a supercooled droplet. A further 'inside-out' nucleation process has been identified in which ice formation only occurs once a solid particle immersed in a supercooled liquid comes in contact with the liquid-air

interface (Durant and Shaw, 2005). This is likely to happen when a droplet is evaporating (Durant and Shaw, 2005). Condensation freezing (sometimes referred to as deliquescence freezing) is the third freezing mode and is the result of water vapour condensing in parallel with ice formation. Condensation freezing is the topic of much debate as it could be a form of immersion freezing on a microscopic scale, i.e. microscopic amounts of water first condenses onto an INP before immersion freezing takes place. A similar argument could be made for deposition freezing in which condensation of the vapour phase happens prior to ice nucleation and ice grows at the expense of the surrounding water vapour (Marcolli, 2014). A schematic of the various modes can be seen in figure 1.6.

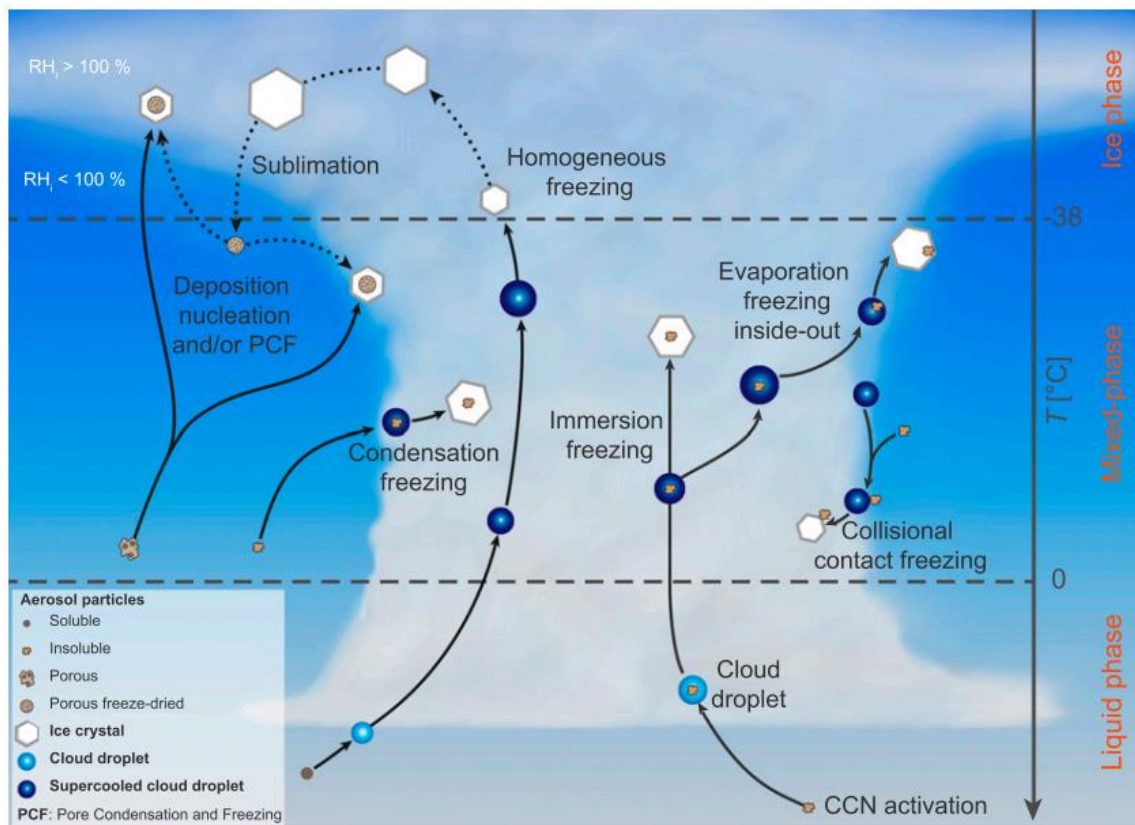


Figure 1.6: Schematic showing the various ice nucleation pathways which occur in the atmosphere. Figure taken from Kanji et al. (2017).

It is thought that immersion and contact modes are the most relevant processes in mixed phase clouds as water saturation is a prerequisite for ice formation in mid-low level clouds (Murray et al., 2012). However Philips et al. (2007) suggest that contact freezing is likely to be of secondary importance with immersion freezing being the dominant process. Contact freezing

is reliant on Brownian motion, thermophoresis, and diffusiophoresis. As aerosol are small in size they are often diverted around droplets in the moving air stream as their size and density do not allow for enough momentum to impact the droplet. However, contact freezing may become the dominant process under specific conditions, i.e. if aerosol were to become charged. In this project we are mainly interested in the immersion mode and all the experiments presented are designed around immersion freezing.

1.4.1 Experimental methods

Many experimental methods have been used to determine the ice-nucleating ability of materials. For the study of ice nucleation in the immersion mode there are two main experimental categories; Dry and wet dispersion techniques (Hiranuma et al., 2015). These differ in that wet dispersion methods submerge and disperse particles, or a single particle, in water which is then frozen. Dry dispersion techniques suspend INP in air and activate them as water droplets before freezing. Murray *et al.* (2012) also distinguished by those which support droplets within an oil or on a substrate and those which suspend droplets in gas. This however is a very similar classification to the dry and wet dispersed. Both of these styles of techniques monitor droplet freezing in respect to temperature. Common variables are the cooling rate of the system, fraction of droplets frozen at a given temperature, type of INP and the concentration of the nucleator per droplet.

1.4.1.1 Wet dispersion

Wet dispersion methods usually involve an array of droplets supported on a substrate or within an oil or emulsion, also referred to as droplet freezing assays in the literature (Beall et al., 2017; Budke and Koop, 2015; Häusler et al., 2018; Knopf and Alpert, 2013; Murray et al., 2011; Vali, 2008b; Whale et al., 2015). For these experiments an array of droplets is sub divided from a bulk sample and the array is cooled down until the droplets freeze. For homogenous studies the bulk sample is pure water but for heterogeneous studies the bulk is an amount of nucleator immersed within water. The droplets can be monitored with optical cameras (Beall et al., 2017; Budke and Koop, 2015; Häusler et al., 2018; Whale et al., 2015), calorimetry (Marcolli et al., 2007; Pinti et al., 2012) and more recently with infrared thermometry (Zarogotas et al., 2016). The droplet size can be altered depending on the scope of the study with volumes from millilitres (Beall et al., 2017; Bigg, 1953; Vali, 1971) to picolitres (Murray et al., 2010; Tarn

et al., 2018). Larger droplets are more sensitive to rarer, but more active INP, and so are advantageous for field studies (DeMott et al., 2016). However, these systems struggle to quantify INP down to the homogenous limit due to a greater sensitivity to impurities and so smaller droplets (nano-picolitre) are typically used for homogeneous studies (Murray et al., 2010; Stan et al., 2009). The droplets are often placed on a substrate (Lindow et al., 1982; Whale et al., 2015) or placed within wells of a plate (Beall et al., 2017). More recently chips for microfluidics have been used to generate droplets with freezing occurring within the chip (with the droplets immersed in oil) (Riechers et al., 2013; Stan et al., 2009; Tarn et al., 2018). Emulsions of droplets immersed in oil have also been used by other studies (Atkinson et al., 2013b; Zolles et al., 2015). Droplets are either trapped between two immiscible oil layers (Hoffer, 1961) or within an emulsion (Marcolli et al., 2007). Using this technique allows droplets to be exposed to a series of well-defined conditions for extended periods of time, i.e. without evaporation of droplets. A linear cooling rate is used for most studies but isothermal cooling rates have also been used to investigate the time dependence aspect of nucleation (Broadley et al., 2012; Herbert et al., 2014; Sear, 2014).

1.4.1.2 Dry dispersion

Cloud expansion chambers can perform deposition, condensation and immersion mode nucleation experiments. In order to carry out immersion mode experiments the chamber is first brought to water saturation so water can condense onto particles making them into immersed droplets. Pumping is then used to expand the gas within the chamber to cause a decrease in temperature. Ice can then crystallise and grow. These ice crystals may then fall to the base of the chamber due to their density and are detected and related to the temperature of formation (Cotton et al., 2007; Niemand et al., 2012).

Continuous Flow Diffusion Chambers (CFDCs) can be used to study IN concentrations in both field and laboratory studies (Garimella et al., 2016; Hagen et al., 1981; Kanji and Abbatt, 2009; Kohn et al., 2016; Rogers et al., 2001; Salam et al., 2006; Stetzer et al., 2008). Two ice coated plates, set at different temperatures, control the humidity and temperature of the chamber by forming a gradient between the two plates. Injection of aerosol particles into a directed flow stream then allows for aerosol to be exposed to a specific set of conditions within the vessel. Aerosol particles which nucleate ice within the time spent in the supersaturated region can be

counted and related to conditions they were exposed to. Aerosol particles can be activated into droplets prior to being injected into the chamber which allows the study of immersion mode nucleation (Luond et al., 2010).

Wind tunnels can suspend single droplets within a gas with a control on temperature. The study of many droplets can lead to INP studies (Diehl et al., 1998; Pitter and Pruppacher, 1973).

Flow chambers mix a cool dry flow of gas mixed aerosol with a warmer wetter air which generates supersaturation (Niedermeier et al., 2010). The activation of ice is then observed and related to the conditions of formation to determine INP efficiencies.

Free falling droplet systems allow the study of micron sized droplets (Wood et al., 2002). Droplets are created and then allowed to fall downwards into a cold chamber. The temperature of ice formation is then recorded using a polarised laser system.

Other systems less commonly used are *electrodynamic levitation* of micron sized droplets (Kramer et al., 1999) and *aerosol flow tubes* to study nanometer sized particles within droplets (Hung et al., 2003).

It should be highlighted that work by (Hiranuma et al., 2015) and (Emersic et al., 2015) demonstrated a discrepancy between both suspension and dry dispersed methods for quantifying ice nucleation for some materials. A more recent comparison with a more systematic sampling of material has shown that good agreement between different instruments can be achieved (DeMott et al., 2018). This highlights that it is key to use a standardised material and sampling strategy. If we wish to advance our knowledge in ice nucleation further work in this area would be beneficial. Consistent results between varying instruments is needed so that we can access the full regime of applicable conditions for ice nucleation in the atmosphere.

1.5 Classical Nucleation Theory (CNT)

Classical nucleation theory (CNT) is used to describe the development of a new phase from a metastable phase and has been utilised by many different fields (Kashchiev, 2011). CNT estimates the rate at which a new phase forms using macroscopic quantities and reproduces observed trends with surprising accuracy even with the assumptions made.

1.5.1 Homogeneous classical nucleation theory

Clusters form and dissipate, in pure water, through the addition and subtraction of water molecules (Murray et al., 2012). Above 0 °C this process is thermodynamically unstable as cluster formation is dependent on temperature and the stability of the clusters. For these clusters, also termed embryos or germs (Vali et al., 2015), to grow spontaneously in supercooled water a critical size must be met. When the embryo is below the critical size the addition of water molecules to the cluster is an endothermic process but above this size and the reaction becomes exothermic and so crystal growth is favourable. The Gibbs free energy for cluster formation (ΔG_{cl}) is determined by the sum of the Gibbs free energy for making an interface (ΔG_s , is always positive and hence is always unfavourable) and the Gibbs free energy needed for forming bonds between water molecules within the bulk cluster (ΔG_v , is negative, and therefore favourable, if the saturation phase with respect to a specific condensed phase is larger than 1) (Mullin, 2001).

$$\Delta G_{cl} = \Delta G_s + \Delta G_v \quad (1)$$

It can then be shown that

$$\Delta G_{cl} = \frac{-4\pi r^3}{3v} kT \ln S + 4\pi r^2 \gamma \quad (2)$$

This applies for a spherical cluster with a radius r . k is the Boltzmann constant, γ the energy between the new and parent phases (also referred to as the surface tension), and v is the molecular volume of the condensed phase (Murray et al., 2012). The saturation ratio, S , can be derived from vapour pressures for liquid water and ice.

The critical radius of the embryo can be defined by:

$$r_g = \frac{2\gamma v}{kT \ln S} \quad (3)$$

By combining equations 2 and 3 we can create an expression to define the Gibbs free energy of formation for the critical embryo size.

$$\Delta G^* = \frac{16\pi\gamma^3 v^2}{3(kT \ln S)^2} \quad (4)$$

The equation shows that the interfacial energy strongly influences the nucleation energy barrier. This means that a metastable phase may form over a stable phase if its interfacial energy

is lower. This explains why studies have recognised the nucleation of a metastable phase of ice preferentially to a more stable hexagonal ice which has a higher surface tension (Huang and Bartell, 1995; Malkin et al., 2012).

The Gibbs energy needed to form a critical cluster can also be related to the rate coefficient (J , nucleation events per unit volume per unit time) at which ice crystals occur in supercooled water in the form of:

$$J = A \exp\left(-\frac{\Delta G^*}{kT}\right) \quad (5)$$

Which can then be expressed as:

$$\ln J = \ln A - \frac{16\pi\gamma^3 v^2}{3k^3 T^3 (\ln S)^2} \quad (6)$$

CNT makes the assumptions that interfacial energy, saturation ratio and density are consistent between the nanometer sized clusters to the macroscopic. This assumption is important to consider when it is thought that interfacial energy is size dependent (Bogdan, 1997). Another assumption made is that the initial cluster is spherical but never the less CNT is a useful tool for understanding ice nucleation and can reproduce observed results.

1.5.2 Heterogeneous classical nucleation theory

A surface in contact with supercooled liquid water can act to catalyse ice formation by reducing the energy barrier needed for formation. The Arrhenius equation (5) can be changed to represent heterogeneous nucleation in the form of:

$$J_{het}(T) = A_{het} \exp\left(-\frac{\Delta G^* \varphi}{kT}\right) \quad (7)$$

$A_{het}(T)$ is a pre-exponential factor with the units $\text{cm}^{-2}\text{s}^{-1}$ and φ is the factor which describes the reduction in the homogeneous energy barrier in consequence to the presence of the solid surface. φ can be expressed as :

$$\varphi = \frac{(2+m)(1-m)^2}{4} \quad (8)$$

The value m in equation 8 is equal to $\cos \theta$, where θ is the contact angle between a spherical ice nucleus and a flat surface. A value of $m = 1$ ($\theta = 0^\circ$) would suggest a perfect ice nucleus, where as $m = -1$ would suggest that a material does not nucleate ice. This equation, although

useful, does assume that a critical ice cluster will adopt a spherical form. By making use of equations (7) and (8) we can express heterogeneous nucleation as:

$$\ln J = \ln A_{het} - \frac{16\pi\gamma^3 v^2 (2+m)(1-m)^2}{3k^3 4} \quad (9)$$

1.6 Describing Ice Nucleation

Early experiments relied on presenting results in the form of the relative humidity reached for ice formation under a given set of conditions. Although this works on a single experiment basis it does not allow comparison between different experiments. This has caused a need for a new means of defining ice nucleation efficiency. Ice nucleation is a stochastic process which means that the number of ice-nucleating particles present in a droplet and also time effect the probability of nucleation. This stochastic nature makes quantifying ice nucleation complicated and it has therefore been suggested that the time dependence element of ice nucleation be neglected to create a singular approach (Murray et al. 2012). Singular Component Stochastic (SCS) methods have proven to work well for some materials, such as kaolinite (Murray et al., 2011), but not for others, for example illite (Broadley et al., 2012), showing that care needs to be taken with the SCS description. A Multiple Component Stochastic approach is possible which takes into account the variability of particles, within each droplet in an immersion experiment, and their contrasting ice-nucleating capabilities.

A commonly used approach to characterise an immersed sample is using the singular description. This method assumes that time dependence aspect of nucleation is a less important factor than the distribution and type of ice nucleation sites (Pruppacher and Klett, 1997). In this description there is a characteristic freezing temperature for an INP (t_c) above which freezing will not occur. If multiple INP types are present then the INP with the highest t_c will dominate ice nucleation and cause freezing. In this method the fraction of droplets frozen at a given temperature $f_{ice}(T)$ can be expressed as:

$$f_{ice}(T) = \frac{n_{ice}(T)}{N_{tot}} = 1 - \exp(-n_s(T)s) \quad (10)$$

$N_{ice}(T)$ is the number of frozen droplets at temperature T and N_{tot} is the total of droplets in the experiment. Again s is the surface area of material within each droplet and $n_s(T)$ is the number

of sites that become active at a certain temperature per unit surface area. $n_s(T)$ is a cumulative measure. Others have measured the density of active sites per unit volume $K(T)$ rather than by surface area (Vali, 1971):

$$f_{ice}(T) = \frac{n_{ice}(T)}{N_{tot}} = 1 - \exp(-K(T)V) \quad (11)$$

Experiments by Vali (2008) and Vali and Stansbury (1966) showed that this approach was still influenced by the stochastic nature of freezing where by freeze thaw experiments did not see droplets freeze at the exact same temperatures and that the rate of cooling influenced the results. This led Vali (1994) to modify this singular description to:

$$f_{ice}(T) = \frac{n_{ice}(T)}{N_{tot}} = 1 - \exp(-n_s(T - \alpha)s) \quad (12)$$

where α encompasses the offset in temperature compared to an experiment run with a ramp rate of 1 Kmin^{-1} . α is related to the cooling rate (r) with an empirical parameter β :

$$\alpha = \beta \log(|r|) \quad (13)$$

β can be calculated experimentally but appears to be dependent on material as different studies have given varying values of β (Herbert et al., 2014; Murray et al., 2012b).

1.7 Minerals as ice-nucleating particles

Early work by Mason (1950) tentatively suggested that aerosol responsible for ice nucleation above $-30 \text{ }^\circ\text{C}$ were solid, insoluble particles which likely originated from the ground as particles of soil and other mineral dusts. Isono (1955) and Kumai (1951) also supported this hypothesis with the observation of the presence of siliceous particles within snow crystals. With this in mind, Mason and Maybank (1958) probed the ice-nucleating ability of 28 naturally-occurring mineral dusts. These experiments showed common aluminosilicates to be active including biotite, kaolinite, microcline, anorthoclase and a variety of silica named tridymite (see table 1). The study suggested that kaolinite was the most active commonly found mineral with microcline also being active which was in agreement with later work by Zimmermann et al. (2008).

Substance	Threshold temperature (°C)
Covellite	-5
Vaterite	-7
β - Tridymite	-7
Kaolinite	-9
Microcline	-9.5
Glacial debris	-9.5
hematite (Specularite)	-10
Aquadag (colloidal graphite)	-12
Volcanic ash	-13
Halloysite	-13
Dolomite	-14
Biotite	-14
Vermiculite	-15
Phlogopite	-15
Cinnabar	-16
Gypsum	-16
Graphite	-16
Anorthoclase	-17
Stony meteorite (1 out of 3)	-17
Substances inactive above -18 °C include: Montmorillonite, sepiolite, albite, muscovite, orthoclase, talc, sand, quartz, α - tridymite, and two stony meteorites	

Table 1.2: List of materials initially active above -18 °C. Table modified from Mason and Maybank (1958).

Since these early studies there have been a series of investigations probing the ice-nucleating activity of atmospherically relevant minerals to determine their importance. A review of these studies was presented by Murray et al. (2012b) which, at the time, suggested that clay minerals were still the most important INP type within mineral dusts for the majority of mixed-phase clouds. This was supported by other studies at the time (Broadley et al., 2012; Hiranuma et al., 2014; Hoose and Möhler, 2012; Mason and Maybank, 1958; Murray et al., 2011; Pinti et al., 2012; Roberts and Hallett, 1968; Wex et al., 2014; Zimmermann et al., 2008). When comparing clays such as kaolinite and NX-illite (a mixture of illite and other minor mineral components) with actual dust samples it was found that clays nucleated ice rather effectively (Murray et al.,

2012b). Given the clay minerals proved to be ice nucleation active and make up roughly 50 % of mineral dusts, they were the major focus for studies at this time.

However, work by Atkinson et al. (2013) investigated other common components of dust. Chlorite, calcite and two other clay groups (montmorillonite and mica) proved to be less effective at nucleating ice than kaolinite. However, quartz and feldspar were more effective than kaolinite as an INP with potassium feldspar being highly active. It should be noted that the feldspars are a complex mineral group with varying compositions (more in depth discussion of the feldspars can be found in section 1.8). The ternary diagram for the feldspars is shown as figure 1.7, where the three end-members are Anorthite (Ca rich), Albite (Na rich) and Orthoclase (K rich). The feldspars can be grouped into two categories, the alkali feldspars (Na-K rich) and the plagioclases (Na-Ca rich). Atkinson et al. (2013) had only experimented with one potassium feldspar and one plagioclase feldspar for the study and so a more thorough investigation into the feldspars was needed to fully determine whether the majority of potassium feldspars were ice-active and if so why?

To answer these questions I investigated 15 feldspars which covered a range of compositions (Harrison et al., 2016). The work from this paper can be found in Appendix 1. The initial results showed that the feldspar group as a whole showed a large variability in ice-nucleating ability. 5 out of 6 K-feldspars had a similar activity to the K-feldspar tested by Atkinson et al. (2013) and supported the evidence that K-feldspars were better ice nucleators than the plagioclase feldspars (in most instances). In addition to this study further work supported the evidence that K-feldspar was extremely ice active (Augustin-Bauditz et al., 2015; Emersic et al., 2015a; Niedermeier et al., 2015; Peckhaus et al., 2016; Zolles et al., 2015). Harrison et al. (2016) described two instances of ‘hyper-active’ feldspars. One microcline sample and one albite (belonging to the plagioclase family). This showed that not all feldspars were the same at nucleating ice and although composition appeared to be important it was not the only determining factor in the ice-nucleating ability of the feldspars. Harrison et al. (2016) also showed that feldspar samples had varying degrees of sensitivity to aging in water, in terms of their ice-nucleating ability. This observation first showed that there must be different types of sites found on feldspar, and secondly that feldspar may weather in the atmosphere and change its ice-nucleating ability. However, the microcline sample that seemed most representative of K-feldspars, in terms of ice-nucleating ability, showed little sensitivity to time spent in water.

Given the observations of different types of active sites and that the K-feldspars were the most active of the feldspar mineral group Harrison et al. (2016) proposed that the high ice-nucleating ability of the K-feldspars may be a result of microtexture. In particular Harrison et al. (2016) refers to the exsolution lamella which are commonly found in alkali feldspars as a result of a solid solution series which forms between the albite and orthoclase endmembers. This results in the development of a perthitic texture (Na rich and K rich zones) within the alkali feldspars, figure 1.8. It is plausible that the boundaries between the Na rich and K rich zones can act as planes of weakness to release stress and so microstructures, such as pits and cracks, may occur which may act as sites for nucleation. Whale et al. (2017) probed this theory and showed that feldspars which had the microtextures related to phase separation showed exceptional ice-nucleating activities opposed to those that did not. Further to this Holden et al. (2019) showed that topographical features located close to the boundaries between the phase separations were predominantly the sites for ice nucleation. It has been suggested that these defects may expose high energy crystal planes, such as the (100) plane in feldspar, which act as active sites for nucleation (Kiselev et al., 2017). Further to this a molecular dynamics study has proposed that high energy sites, such as the (100) plane, have H-bonding groups which form strong water-surface interactions and can initiate ice formation (Pedevilla et al., 2017).

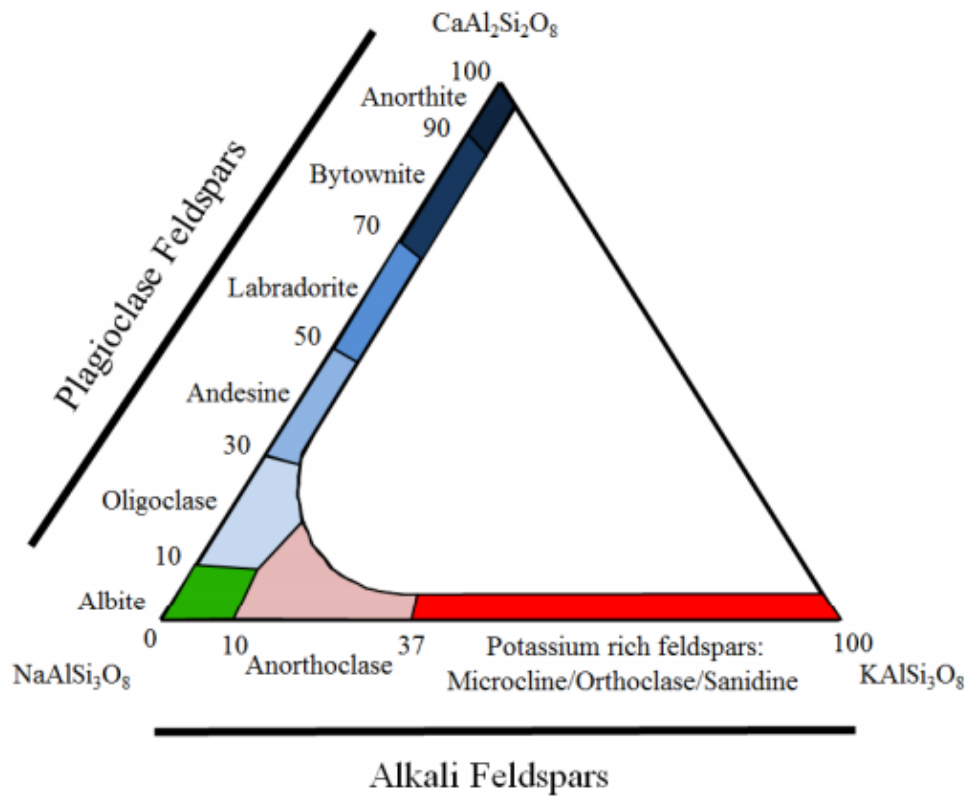


Figure 1.7: Ternary diagram displaying the range of compositions in the feldspar group of minerals. Diagram taken from Harrison et al. (2016).

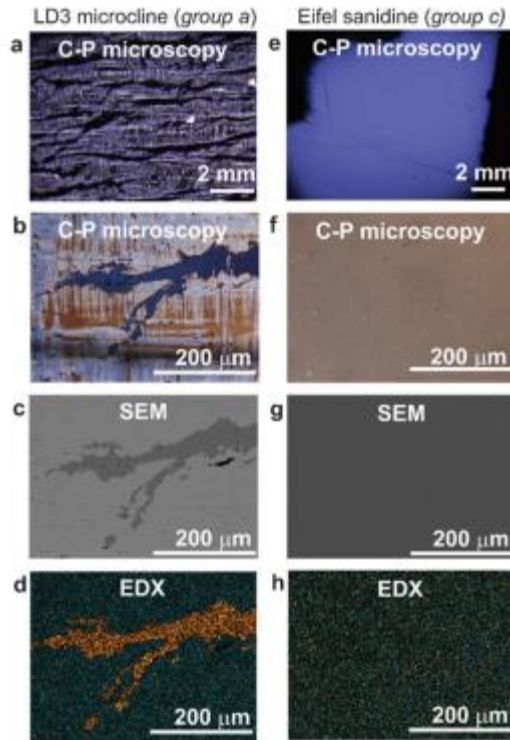


Figure 1.8: Images displaying two feldspar samples, one with and one without perthitic texture, when observed under C-P microscopy, SEM and EDX. Both samples have a similar composition and crystal structure but LD3 microcline (a-d) has undergone phase separation whereas Eifel sanidine (e-h) has not. Images are taken from Whale et al. (2017).

The work described above showed that the ice-nucleating ability of K-feldspar made it the dominant INP in mineral dusts, even though it is roughly five times less in abundance than the clay group of minerals. Recent field observations have supported Atkinson et al. (2013) by showing strong correlations between the observations and the predicated INP concentrations based on the lab based K-feldspar parameterisation created by Atkinson et al. (2013) (Boose et al., 2016; Price et al., 2018). Boose et al. (2016) present the correlation between K-feldspar content and the ice-nucleating ability of various mineral dusts. However, this correlation is only true at 253K and the role of quartz combined with K-feldspar becomes important at lower temperatures between 238 and 245 K. These findings display the complexities of ice nucleation in relation to mineral dusts as there is still a dearth of observations for minerals as a whole. It

is becoming clear that K-feldspar plays an important role in the ice-nucleating activity of mineral dusts but it is still unclear to what extent and if other minerals (such as quartz) can possibly contribute to the INP population in the atmosphere.

The question of which minerals dominate ice nucleation in the atmosphere becomes even more complex when considering transported mineral dusts. These transported dusts may become exposed to ageing processes for prolonged periods of time which may deactivate the ice-nucleating ability of the mineral dust. Evidence from Harrison et al. (2016) has already shown that some feldspars can become deactivated when exposed to water for a period of time, although the most representative K-feldspar showed little sensitivity. Zolles et al. (2015) investigated quartz minerals and found that the milling process could lead to enhanced ice-nucleation. This was supported by Kumar et al. (2019) who also showed the quartz was sensitive to time left in water. The exposure of fresh sites was thought to lead to the increased ice-nucleating ability of the material on milling which could then be aged by exposure to water (in glass vials). This demonstrated the possible effect ageing processes may have on components of mineral dusts. From the limited literature it appears that quartz is more sensitive to these milling and ageing processes than K-feldspar. However, K-feldspar has been shown to be sensitive to acids which may decrease its ice-nucleating ability in the atmosphere (Boose et al., 2019; Kumar et al., 2018). Conversely, Whale et al. (2018) showed that solutes could both suppress and enhance the ice-nucleating ability of K-feldspar. With this in mind the complex geological/ageing history of mineral particles in the atmosphere could impact their ice-nucleating ability and thus affect which minerals dominate the INP population.

1.8 Feldspars

From the previous section it is clear that the K-feldspars are an important INP species in the atmosphere. The feldspars are the most common rock forming mineral and are a complex mineral group belonging to the tectosilicates (also known as the framework silicates) (Deer et al., 1992; MacKenzie and Adams, 2011). They have the general formula $XAl(SiAl)Si_2O_8$, where X is commonly either Na, Ca or K, or less commonly NH_4^+ and Ba^{2+} . The silica tetrahedra form a 3D framework where the tetrahedra are bonded at the corners to a shared oxygen (Deer et al., 1992). Cations fill the interstitial sites with the charge being balanced by the substitution of Si by Al. Na cations within the interstitial sites can readily substitute for Ca given the cations have a similar size and K can substitute for Na given their similar charge.

This leads to a series of feldspars with feldspars. Those that have Ca and Na in their interstitial sites are named the plagioclase feldspars and those that have Na and K are named the alkali feldspars. However, the size and charge of Ca and K are too different to allow substitution and hence there is no feldspar series between Ca and K. Three end members of feldspar exist: orthoclase (KAlSi_3O_8), albite ($\text{NaAlSi}_3\text{O}_8$) and anorthite ($\text{CaAlSi}_3\text{O}_8$). As albite can form a series between both anorthite and orthoclase a ternary diagram can be used to represent the composition of feldspar where the plagioclase and alkali feldspars are conjoined at the corner by the endmember albite. It should be noted that all plagioclase feldspars contain a small amount of potassium feldspar, usually less than 5%, and all alkali feldspars contain a small amount of calcium feldspar (<5%) so that a band is drawn to represent the compositions of feldspars rather than a straight line (MacKenzie and Adams, 2011).

For the plagioclases there is a series of intermediate members and endmembers including albite (0-10% Ca), oligoclase (10-30% Ca), andesine (30-50% Ca), labradorite (50-70% Ca), bytownite (70-90% Ca) and anorthite (90-100% Ca). For the alkali series there are the members albite (0-10% K), anorthoclase (10-37% K) and orthoclase (37-100% K). With a sufficiently long cooling rate intermediate members of the alkali feldspars separate into zones of potassium rich feldspar and sodium rich feldspar. These intergrowths are often referred to as perthites (or microperthites depending on how coarse the intergrowths are), which lead to perthitic texture (MacKenzie and Adams, 2011).

Depending on the temperature of formation the silica tetrahedra can be ordered or disordered. This leads to various polymorphs of the various feldspars. At high temperatures the Si, Al tetrahedra are positioned randomly through the lattice and this results in polymorphs such as sanidine and high albite (Deer et al., 1992). With a lower temperature of formation and slower cooling rate there is more time to order the tetrahedra so that Si and Al tetrahedra are consistently positioned through the structure and hence the formation of polymorphs such as microcline and low albite can occur. Orthoclase is an intermediate polymorph between high temperature sanidine and low formation temperature microcline and so is semi-ordered. Given the lower formation temperatures and slower cooling rates needed for the formation of microcline it is not surprising that perthitic textures are commonly found within this polymorph.

1.9 Quartz

Quartz is the second most abundant mineral found in the Earth's crust after the feldspar group of minerals. Quartz is a common component in most deposits with it often being found as an accessory mineral (i.e. within hydrothermal veins). Its tough physical (Moh's scale 7) and chemical nature, and absence of a cleavage plane mean it is also a common constituent to sands and soils as it is resistant to most weathering processes. Quartz does not have cleavage and this is used as the main identifier when looking to characterise an unknown mineral sample. However, it does exhibit conchoidal fractures which lead to smooth curved surfaces (Deer et al., 1966).

Quartz is composed of nearly 100 % SiO_2 . SiO_2 tetrahedra are bonded together with each silicon being bound to four oxygens which forms a 3D framework of six or eight membered loops (Deer et al., 1992), see figure 1.9. Depending on the temperature and pressure of formation quartz has various polymorphs such as: cristobalite, tridymite, stishovite and coesite, figure 1.10 (Koike et al., 2013; Swamy et al., 1994). Stishovite and coesite are rarer forms associated with high pressure environments and so are a common metamorphic mineral found at meteor impact sites. The polymorphs quartz, cristobalite and tridymite can exist in two metastable forms, both a high temperature (β) and low temperature (α) state. The transformation of β -quartz to α -quartz is a minor atomic movement, which involves no breakage amongst Si-O bonds or interchange of atoms, also known as a displacive transformation (Dolino, 1990). This takes next to no energy to occur as no bonds are broken (Dolino, 1990). In comparison, to tridymite and cristobalite, quartz is densely packed in its arrangement of tetrahedra (Deer et al, 1966). The transition from cristobalite to tridymite, tridymite to quartz and cristobalite to quartz is reconstructive, i.e. bonds need to be broken (Dmitriev et al., 1998). This means for both cristobalite and tridymite (and also stishovite and coesite) to be found at the Earth's surface they have to cross their stability boundaries rapidly to exist as a metastable phase. Hence α -quartz is the most commonly found silica mineral at the Earth's surface.

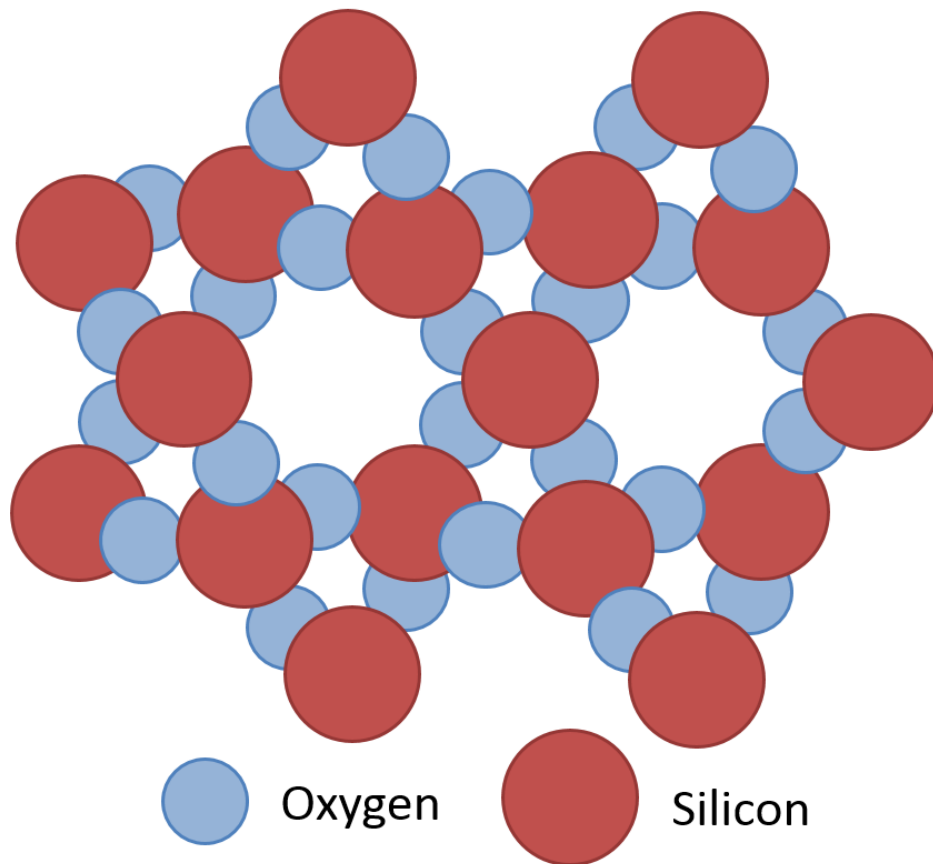


Figure 1.9: Schematic representation of the structure of α -quartz along its c-axis where each Si is bonded to four oxygens. Schematic modified from Gibbs (1926).

α -quartz are the focus of section 1.4 as they are the most atmospherically significant forms of silica. It is common to find small amounts of oxides as inclusions or liquid infillings within cavities which leads to a variety of α -quartzs. The substitution of Al^{3+} for Si^{4+} allows for the introduction of alkali ions such as Li^+ and Na^+ . These subtle impurities can lead to a variety of colours. A common cause of these colours is the natural exposure of quartz (and its impurities) to radiation causing colour centres. Colour centres are caused by unpaired electrons in the structure, also known as “hole defects”, as a result of radioactive sources causing the emission of a pair of electrons (for example from an oxygen atom adjacent to Al). A fuller description of varieties of α -quartzs can be seen in section 1.4.2.

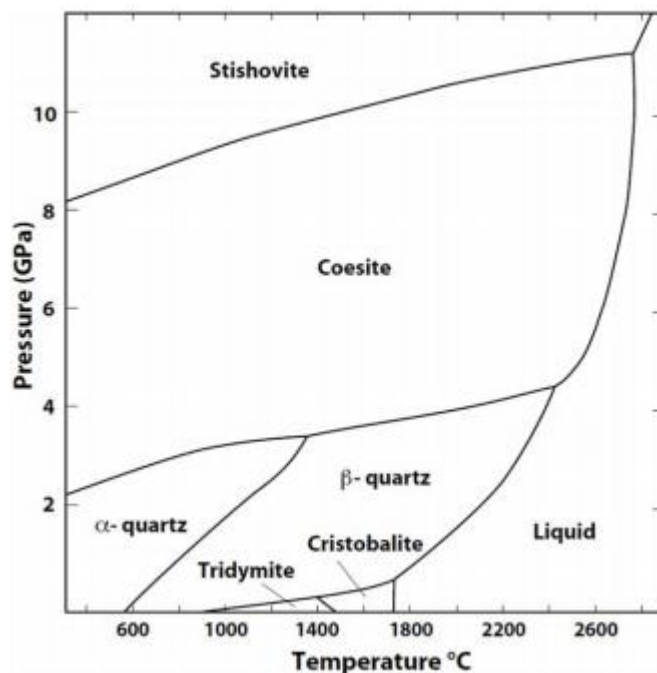


Figure 1.10: Phase diagram showing the stability fields of various silica polymorphs. The diagram is based on Swamy et al. (1994).

1.10 Project objectives

There are 3 overarching aims for the project presented in this thesis with the first objective being to further the fundamental understanding of mineral nucleators in the atmosphere. With this in mind I aim to a) understand how their physical and chemical differences influence their ability to nucleate ice and b) understand their relative importance in the atmosphere as INPs. To do this I decided to investigate a common mineral found in atmospheric mineral dusts which has been poorly characterised in the past for its ice-nucleating ability, quartz. Further to this I would find varieties of quartz which were similar, but non-identical, in nature so that I could try and correlate their ice-nucleating abilities to their varying properties. Once an understanding of the ice-nucleating ability of quartz is established I can then infer the potential significance of this mineral dust component opposed to other mineral types, for example K-feldspar.

My second objective is to make field measurements in a dusty environment to constrain laboratory based paramterisations which are used in the global model (GLOMAP) to predict INP concentrations. From My laboratory studies I will be able to build an understanding of which minerals may be important for ice nucleation in the atmosphere which I can then use to improve our INP predictions in global models. However, there are other processes (i.e. acid

ageing) which could potentially alter the nucleating ability of the mineral dusts on transport. To justify the use of these models using laboratory based parameterisations I need to test the predictions against real world observations. Here I decided to make the first measurements of INP in Barbados in order to answer vital questions regarding mineral dust activity on transport and to refine model predictions.

Finally, a third aim was to construct an instrument capable of making ice nucleation measurements of rare INP. Typically drop assays have used nano-picoliter sized droplets in experiments to better represent the droplet sizes present in clouds. The disadvantage of using such small droplet sizes is that the amount of aerosol in the droplet is reduced and so it is much harder to replicate the amount of aerosol present in clouds and hence it is less sensitive to the rarest (and most active) INP. Microliter droplet experiments have proven to be advantageous and extended datasets to warmer regimes but there are still few field measurements made above $\sim -15^{\circ}\text{C}$ although we see that clouds often glaciate above this temperature (Kanitz et al., 2011; Seifert et al., 2015). It should also be considered that around -3 to -8°C (a regime we currently do not consistently access) the potentially important Hallett-Mossop secondary ice formation process may occur (Hallett and Mossop, 1974). Given this, it is clear that an even larger volume assay is needed to increase the sensitivity of INP measurements in the field to access these important temperature regimes. Ideally, the instrument needs to be an order of magnitude (or greater) in sensitivity to INP than a typical microliter experiment, be affordable, adaptable and portable. In addition to this it would ideally be simple to use and automatable. Here I attempt to build such an instrument making use of infrared technology to help in the automation of the process.

1.11 Thesis overview

Chapter two of this thesis is a published manuscript while chapter three is in preparation and chapter four is a published paper.

Chapter two consists of the paper *'The ice-nucleating ability of quartz immersed in water and its atmospheric importance compared to K-feldspar'* (Harrison et al., 2019). This chapter presents a survey of the ice-nucleating ability of 10 α -quartz samples. We show that although the 10 samples have a near identical crystal structure and composition they have a wide range

of ice-nucleating abilities which we attribute to the presence of small impurities in the structure. We also demonstrate the extraordinary sensitivity of some quartz samples to time spent in water and in air. We then go on to compile literature data to construct four new parameterisations for the minerals quartz, K-feldspar, plagioclase and albite. Using these new parameterisations we demonstrate that K-feldspar is the most important component in mineral dusts for galciating clouds. Using this knowledge we then predict the INP concentrations in the tropical atlantic using the newly developed K-feldspar paramterisation and reproduce the field observations well.

Chapter three contains the manuscript *'Ice-nucleating particle activity in transported desert dust in the western Atlantic'* (Harrison *et al.* In Prep.). In this chapter we present the measurements made in the dusty environment of Barbados. We compare the field observations to measurements obtained from the eastern tropical Atlantic and find the INP concentrations and the ice-nucleating activity of the aerosol present in Barbados to be lower than in the eastern tropical Atlantic. We use the XRD analysis of mineral dust collected from rain samplers during the campaign, measurements of mineralogy made by Glaccum and Prospero (1980), and predications of INP concentrations via the new K-feldspar parameterisation presented in chapter four to understand why the mineral dust has deactivated. We hypothesise that the drop in mineral dust activity with transport across the Atlantic can be attributed to the preferential removal of the K-feldspar component on transport.

Chapter four consists of the paper *'An instrument for quantifying heterogeneous ice nucleation in multiwell plates using infrared emissions to detect freezing'* (Harrison *et al.*, 2018). Here we describe the IR-NIPI instrument, a large volume drop assay system. We present the development of a new calibration technique for the infrared camera used in the system and validate its use by investigating various materials and comparing the results to literature data for other instruments. In general we find good agreement to other characterised instruments.

1.12 Other work completed during the course of my PhD

During the course of the project, which has resulted in this thesis, I have had the opportunity to be involved in a number of other exciting studies, some of which are cited in the above introduction.

Harrison et al. (2016) carried out an extensive survey of the ice-nucleating ability of the feldspar group of minerals. This study showed the variability in ice-nucleating ability of the feldspar group and that although composition is important for determining the minerals activity it is not the sole determining factor. This work helped establish the consensus that generally the alkali feldspars are more active than the plagioclases. For this paper I conducted all the experiments, handled all the data analysis, proposed the time series investigation and was heavily involved in the writing and presentation of the paper. This paper has been omitted from the thesis chapters on the technicality of it being a joint first author paper. However, given the relevance of this paper to the rest of the chapter presented in this thesis it is included in Appendix 1.

Tarn et al. (2018) presented a new microfluidics device for the generation of picolitre sized droplets to be used in a drop assay system. For this study I helped in the collection of aerosol samples during two campaigns and advised in the selection of minerals for characterisation of the instrument.

O'Sullivan et al. (2018) carried out a field study of INP sampled at an agricultural site in Tadcaster, England. The study provided evidence for the internal mixing of biogenic INP with mineral dusts and suggested the potential for a missing biogenic source of INP from our current climate models. For this paper I helped in the logistical planning of the campaign, the development of a sampling protocol, the collection of field samples during the course of the campaign and also was involved in the analysis of data.

Daily et al. (In Prep.) investigated the role of manually seeding ice nucleation in multiwell plates on the survival of primary mammalian cells for cryopreservation purposes. The study proved that the survival of granulosa cells increased with the control of nucleation in the plates. For this study I collected and analysed the background freezing data to determine the variability in the baseline nucleation of Milli-Q water in the IR-NIPI system which was used for the freezing of the granulosa containing multiwell plates in previous experiments.

Tarn et al. (In Prep.) has developed on a previous microfluidics system to freeze droplets in a continuous flow. This techniques paper presents the new instrument (LOC-NIPI) and validates the technique with measurements of lab prepared samples and data collected during a field campaign to the eastern Mediterranean. For this manuscript I was involved in the logistics and design of experiments for the field study and provided scientific discussions.

Tarn et al. (In Prep.) collected aerosol during a field campaign in Israel. The aerosol were tested for their ice-nucleating ability on both a microliter drop assay system and microfluidics device. As dust emissions which reach Israel come from various sources it is thought that a correlation can be made between dust source location and INP activity. Heat tests of aerosol samples and DNA aim to provide evidence for the presence of a biogenic component in aerosol which has passed over agricultural sites. For this study I was heavily involved in the logistics of the campaign and provided scientific advice in regards to the objectives and experimental plan. I also helped in the calculation of INP predictions.

Adams et al. (In Prep.) led a field study to Hyytiala, Finland. The study made measurements during the course of 2 months to monitor INP during the seasonal progression from a winter to spring. Hyytiala is also famous for aerosol nucleation events and so it was the objective of the campaign to try and capture such an event and determine its influence on the INP concentration. For this campaign I have heavily involved in the logistical preparation and the experimental design and setup. I conducted all microliter immersion mode experiments for the first half of the campaign and also completed the analysis of these runs.

Porter et al. (In Prep.) sampled aerosol at an arctic location making use of ground based and airborne (balloon) samplers. The objective of the study was to monitor the INP concentrations at various heights over the arctic and correlate these with any meteorological factors or back trajectory sources. I was involved in the logistics of the campaign, provided technical instrument training and was involved in scientific discussions which assisted the campaign work flow.

Porter et al. (In Prep.) developed a small portable sampling device. The novel device makes use of cascade impactor and has been specifically designed to minimise its weight. The reduction in weight allows for the device to be suspended from a weather balloon and to sample aerosol at varying heights, and make aerosol size measurements via an OPC, at heights relevant for mixed-phase clouds. In this study I was involved in the collection of field samples to validate the instruments use.

Adams et al. (In Prep.) completed a case study of INP concentrations across an anthropogenic aerosol emission event, 'Bonfire night'. Bonfire night is a British holiday celebrating the failed gunpowder plot on the houses of parliament. To mark this occasion, around the 5th of November, it is customary to light bonfires and fireworks which leads to an increased emission

of aerosol. This studies focus was to investigate whether this increase in black carbon aerosol would increase the INP concentration. For this study I was involved in the logistics and analysis of some of the field collected data.

References

Albrecht, B. A.: Aerosols, Cloud Microphysics, and Fractional Cloudiness, *Science*, 245, 1227-1230, 1989.

Ansmann, A., Tesche, M., Seifert, P., Althausen, D., Engelmann, R., Fruntke, J., Wandinger, U., Mattis, I., and Müller, D.: Evolution of the ice phase in tropical altocumulus: SAMUM lidar observations over Cape Verde, *Journal of Geophysical Research: Atmospheres*, 114, D17208, 2009.

Ardon-Dryer, K. and Levin, Z.: Ground-based measurements of immersion freezing in the eastern Mediterranean, *Atmospheric Chemistry and Physics*, 14, 5217-5231, 2014.

Atkinson, J. D., Murray, B. J., Woodhouse, M. T., Whale, T. F., Baustian, K. J., Carslaw, K. S., Dobbie, S., O'Sullivan, D., and Malkin, T. L.: The importance of feldspar for ice nucleation by mineral dust in mixed-phase clouds, *Nature*, 498, 355-358, 2013a.

Atkinson, J. D., Murray, B. J., Woodhouse, M. T., Whale, T. F., Baustian, K. J., Carslaw, K. S., Dobbie, S., O'Sullivan, D., and Malkin, T. L.: The importance of feldspar for ice nucleation by mineral dust in mixed-phase clouds, *Nature*, 498, 355-358, 2013b.

Augustin-Bauditz, S., Wex, H., Denjean, C., Hartmann, S., Schneider, J., Schmidt, S., Ebert, M., and Stratmann, F.: The immersion freezing behavior of mineral dust particles mixed with biological substances, *Atmospheric Chemistry and Physics Discussions*, 15, 29639-29671, 2015.

Beall, C. M., Stokes, M. D., Hill, T. C., DeMott, P. J., DeWald, J. T., and Prather, K. A.: Automation and heat transfer characterization of immersion mode spectroscopy for analysis of ice nucleating particles, *Atmospheric Measurement Techniques*, 10, 2613-2626, 2017.

Bigg, E. K.: The supercooling of water, *Proc.Phys. Soc.*, 66, 688-694, 1953.

Bogdan, A.: Thermodynamics of the curvature effect on ice surface tension and nucleation theory, *The Journal if Chemical Physics*, 106, 1921-1929, 1997.

Boose, Y., Baloh, P., Plötze, M., Ofner, J., Grothe, H., Sierau, B., Lohmann, U., and Kanji, Z. A.: Heterogeneous ice nucleation on dust particles sourced from nine deserts worldwide – Part 2: Deposition nucleation and condensation freezing, *Atmospheric Chemistry and Physics*, 19, 1059-1076, 2019.

Boose, Y., Welti, A., Atkinson, J., Ramelli, F., Danielczok, A., Bingemer, H. G., Plötze, M., Sierau, B., Kanji, Z. A., and Lohmann, U.: Heterogeneous ice nucleation on dust particles sourced from nine deserts worldwide – Part 1: Immersion freezing, *Atmospheric Chemistry and Physics*, 16, 15075-15095, 2016.

Boucher, O., Randall, D., Artaxo, P., Bretherton, C., Feingold, G., Forster, P., Kerminen, V.-M., Kondo, Y., Liao, H., and Lohmann, U.: Clouds and aerosols. In: *Climate change 2013: The physical science basis. Contribution of working group I to the fifth assessment report of the intergovernmental panel on climate change*, Cambridge University Press, 2013.

Broadley, S. L., Murray, B. J., Herbert, R. J., Atkinson, J. D., Dobbie, S., Condliffe, E., and Neve, L.: Immersion mode heterogeneous ice nucleation by an illite rich powder representative of atmospheric mineral dust, *Atmos. Chem. Phys. Discuss.*, 11, 22801-22856, 2011.

Broadley, S. L., Murray, B. J., Herbert, R. J., Atkinson, J. D., Dobbie, S., Malkin, T. L., Condliffe, E., and Neve, L.: Immersion mode heterogeneous ice nucleation by an illite rich powder representative of atmospheric mineral dust, *Atmospheric Chemistry and Physics*, 12, 287-307, 2012.

Budke, C. and Koop, T.: BINARY: an optical freezing array for assessing temperature and time dependence of heterogeneous ice nucleation, *Atmos. Meas. Tech.*, 8, 689-703, 2015.

Chen, J., Wu, Z., Augustin-Bauditz, S., Grawe, S., Hartmann, M., Pei, X., Liu, Z., Ji, D., and Wex, H.: Ice-nucleating particle concentrations unaffected by urban air pollution in Beijing, China, *Atmospheric Chemistry and Physics*, 18, 3523-3539, 2018.

Choi, Y.-S., Lindzen, R. S., Ho, C.-H., and Kim, J.: Space observations of cold-cloud phase change, *Proceedings of the National Academy of Sciences, USA*, 107, 11211-11216, 2010.

Coldwell, B. C. and Pankhurst, M. J.: Evaluating the influence of meteorite impact events on global potassium feldspar availability to the atmosphere since 600 Ma, *Journal of the Geological Society*, 176, 209-224, 2019.

Cotton, R. J., Benz, S., Field, P. R., Mohler, O., and Schnaiter, M.: Technical note: A numerical test-bed for detailed ice nucleation studies in the AIDA cloud simulation chamber, *Atmos. Chem. Phys.*, 7, 243-256, 2007.

Cui, Z. Q., Carslaw, K. S., Yin, Y., and Davies, S.: A numerical study of aerosol effects on the dynamics and microphysics of a deep convective cloud in a continental environment, *Journal of Geophysical Research-Atmospheres*, 111, 2006.

de Boer, G., Morrison, H., Shupe, M. D., and Hildner, R.: Evidence of liquid dependent ice nucleation in high-latitude stratiform clouds from surface remote sensors, *Geophys. Res. Lett.*, 38, L01803, 2011.

Deer, W. A., Howie, R. A., and Zussman, J.: An introduction to the rock forming minerals, Addison Wesley Longman, Harlow, UK, 1992.

Deer, W. A., Howie, R. A., and Zussman, J.: An introduction to the rock forming minerals, Longman group limited, London, 1966.

Demott, P. J.: An Exploratory-Study of Ice Nucleation by Soot Aerosols, *Journal of Applied Meteorology*, 29, 1072-1079, 1990.

DeMott, P. J., Hill, T. C., McCluskey, C. S., Prather, K. A., Collins, D. B., Sullivan, R. C., Ruppel, M. J., Mason, R. H., Irish, V. E., Lee, T., Hwang, C. Y., Rhee, T. S., Snider, J. R., McMeeking, G. R., Dhaniyala, S., Lewis, E. R., Wentzell, J. J., Abbatt, J., Lee, C., Sultana, C. M., Ault, A. P., Axson, J. L., Diaz Martinez, M., Venero, I., Santos-Figueroa, G., Stokes, M. D., Deane, G. B., Mayol-Bracero, O. L., Grassian, V. H., Bertram, T. H., Bertram, A. K., Moffett, B. F., and Franc, G. D.: Sea spray aerosol as a unique source of ice nucleating particles, *Proceedings of the National Academy of Sciences of the United States of America*, 113, 5797-5803, 2016.

DeMott, P. J., Möhler, O., Cziczo, D. J., Hiranuma, N., Petters, M. D., Petters, S. S., Belosi, F., Bingemer, H. G., Brooks, S. D., Budke, C., Burkert-Kohn, M., Collier, K. N., Danielczok, A., Eppers, O., Felgitsch, L., Garimella, S., Grothe, H., Herenz, P., Hill, T. C. J., Höhler, K., Kanji, Z. A., Kiselev, A., Koop, T., Kristensen, T. B., Krüger, K., Kulkarni, G., Levin, E. J. T., Murray, B. J., Nicosia, A., and others, Sullivan, D., Peckhaus, A., Polen, M. J., Price, H. C., Reicher, N., Rothenberg, D. A., Rudich, Y., Santachiara, G., Schiebel, T., Schrod, J., Seifried, T. M., Stratmann, F., Sullivan, R. C., Suski, K. J., Szakáll, M., Taylor, H. P., Ullrich, R., Vergara-Temprado, J., Wagner, R., Whale, T. F., Weber, D., Welti,

A., Wilson, T. W., Wolf, M. J., and Zenker, J.: The Fifth International Workshop on Ice Nucleation phase 2 (FIN-02): laboratory intercomparison of ice nucleation measurements, *Atmospheric Measurement Techniques*, 11, 6231-6257, 2018.

DeMott, P. J., Prenni, A. J., Liu, X., Kreidenweis, S. M., Petters, M. D., Twohy, C. H., Richardson, M. S., Eidhammer, T., and Rogers, D. C.: *Proc. Natl. Acad. Sci. U. S. A.*, 107, 11217-11222, 2010.

DeMott, P. J., Sassen, K., Poellot, M. R., Baumgardner, D., Rogers, D. C., Brooks, S. D., Prenni, A. J., and Kreidenweis, S. M.: *Geophys. Res. Lett.*, 30, 1732, 2003.

Denman, K. L., Brasseur, G., Chidthaisong, A., Ciais, P., Cox, P. M., Dickinson, R. E., Hauglustaine, D., Heinze, C., Holland, E., Jacob, D., Lohmann, U., Ramachandran, S., da Silva Dias, P. L., Wofsy, S. C., and Zhang, X.: Couplings Between Changes in the Climate System and Biogeochemistry. In: *Climate Change 2007: The Physical Science Basis. Contribution of Working Group I to the Fourth Assessment Report of the Intergovernmental Panel on Climate Change*, Cambridge University Press, Cambridge, United Kingdom, 2007.

Diehl, K., Mitra, S. K., and Pruppacher, H. R.: A laboratory study on the uptake of HCl, HNO₃ and SO₂ gas by ice crystals and the effect of these gases on the evaporation rate of the crystals, *Atmospheric Research*, 48, 235-244, 1998.

Dmitriev, V. P., Tolédano, P., Torgashev, V. I., and Salje, E. K. H.: Theory of reconstructive phase transitions between SiO₂ polymorphs, *Physical Review B*, 58, 11911-11921, 1998.

Dolino, G.: The α -inc- β transitions of quartz: A century of research on displacive phase transitions, *Phase Transitions*, 21, 59-72, 1990.

Durant, A. J. and Shaw, R. A.: *Geophys. Res. Lett.*, 32, 2005.

Emersic, C., Connolly, P. J., Boulton, S., Campana, M., and Li, Z.: Investigating the discrepancy between wet-suspension- and dry-dispersion-derived ice nucleation efficiency of mineral particles, *Atmospheric Chemistry and Physics*, 15, 11311-11326, 2015a.

Emersic, C., J. Connolly, P., Boulton, S., Campana, M., and Li, Z.: Investigating the discrepancy between wet-suspension and dry-dispersion derived ice nucleation efficiency of mineral particles, *Atmos. Chem. Phys. Discuss.*, 15, 887-929, 2015b.

Eriksen Hammer, S., Mertes, S., Schneider, J., Ebert, M., Kandler, K., and Weinbruch, S.: Composition of ice particle residuals in mixed-phase clouds at Jungfrauoch (Switzerland): enrichment and depletion of particle groups relative to total aerosol, *Atmospheric Chemistry and Physics*, 18, 13987-14003, 2018.

Field, C. B., Barros, V. R., Mach, K. J., Mastrandrea, M. D., Aalst, M. v., Adger, W. N., Arent, D. J., Barnett, J., Betts, R., Bilir, T. E., Birkmann, J., Carmin, J., Chadee, D. D., Challinor, A. J., Chatterjee, M., Cramer, W., Davidson, D. J., Estrada, Y. O., Gattuso, J. P., Hijikawa, Y., Hoegh-Guldberg, O., Huang, H. Q., Insarov, G. E., Jones, R. N., Kovats, R. S., Lankao, P. R., Larsen, J. N., Losada, I. J., Marengo, J. A., McLean, R. F., Mearns, L. O., Mechler, R., Morton, J. F., Niang, I., Oki, T., Olwoch, J. M., Opondo, M., Poloczanska, E. S., Pörtner, H. O., Redsteer, M. H., Reisinger, A., Revi, A., Schmidt, D. N., Shaw, M. R., Solecki, W., Stone, D. A., Stone, J. M. R., Strzepek, K. M., Suarez, A. G., Tschakert, P., Valentini, R., Vicuña, S., Villamizar, A., Vincent, K. E., Warren, R., White, L. L., Wilbanks, T. J., Wong, P. P., and Yohe, G. W.: Technical Summary. In: *Climate Change 2014: Impacts, Adaptation, and Vulnerability. Part A: Global and Sectoral Aspects. Contribution of Working Group II to the Fifth Assessment Report of the Intergovernmental Panel on Climate Change*, Field, C. B., Barros, V. R., Dokken, D. J., Mach, K. J., Mastrandrea, M. D., Bilir, T. E., Chatterjee, M., Ebi, K. L., Estrada, Y. O., Genova, R. C., Girma, B., Kissel, E. S., Levy, A. N., MacCracken, S., Mastrandrea, P. R., and White, L. L. (Eds.), Cambridge University Press, Cambridge, United Kingdom and New York, NY, USA, 2014.

Field, P. R., Lawson, R. P., Brown, P. R. A., Lloyd, G., Westbrook, C., Moisseev, D., Miltenberger, A., Nenes, A., Blyth, A., Choularton, T., Connolly, P., Buehl, J., Crosier, J., Cui, Z., Dearden, C., DeMott, P., Flossmann, A., Heymsfield, A., Huang, Y., Kalesse, H., Kanji, Z. A., Korolev, A., Kirchgassner, A., Lasher-Trapp, S., Leisner, T., McFarquhar, G., Phillips, V., Stith, J., and Sullivan, S.: Chapter 7. Secondary Ice Production - current state of the science and recommendations for the future, *Meteorological Monographs*, doi: 10.1175/amsmonographs-d-16-0014.1, 2017. 2017.

Forster, P., Ramaswamy, P., Artaxo, T., Bernsten, R., Betts, R., Fahey, D. W., Haywood, J., Lean, J., Lowe, D. C., Myhre, G., Nganga, J., Prinn, R., Raga, G., Schulz, M., and Van Dorland, R.: *Climate Change 2007: The Physical Science Basis. Contribution of Working Group I to the Fourth assessment Report of the Intergovernmental Panel on Climate Change*, Cambridge University Press, Cambridge, 2007.

Garimella, S., Kristensen, T. B., Ignatius, K., Welti, A., Voigtländer, J., Kulkarni, G. R., Sagan, F., Kok, G. L., Dorsey, J., Nichman, L., Rothenberg, D., Rösch, M., Kirchgäßner, A., Ladkin, R., Wex, H., Wilson, T. W., Ladino, L. A., Abbatt, J. P. D., Stetzer, O., Lohmann, U., Stratmann, F., and Cziczo, D. J.: The SPectrometer for Ice Nuclei (SPIN): An instrument to investigate ice nucleation, *Atmos. Meas. Tech. Discuss.*, 2016, 1-37, 2016.

Gibbs, R. E.: Structure of Formula Quartz, *Proceedings of the Royal Society A: Mathematical, Physical and Engineering Sciences*, 110, 443-455, 1926.

Ginoux, P., Prospero, J. M., Gill, T. E., Hsu, N. C., and Zhao, M.: Global-scale attribution of anthropogenic and natural dust sources and their emission rates based on MODIS Deep Blue aerosol products, *Reviews of Geophysics*, 50, RG3005, 2012.

Glaccum, R. A. and Prospero, J. M.: Saharan aerosols over the tropical North Atlantic — Mineralogy, *Marine Geology*, 37, 295-321, 1980.

Graham, B., Guyon, P., Maenhaut, W., Taylor, P. E., Ebert, M., Matthias-Maser, S., Mayol-Bracero, O. L., Godoi, R. H. M., Artaxo, P., Meixner, F. X., Moura, M. A. L., Rocha, C. H. E. D. A., Grieken, R. V., Glosky, M. M., Flagan, R. C., and Andreae, M. O.: Composition and diurnal variability of the natural Amazonian aerosol, *Journal of Geophysical Research: Atmospheres*, 108, n/a-n/a, 2003.

Grawe, S., Augustin-Bauditz, S., Clemen, H.-C., Ebert, M., Eriksen Hammer, S., Lubitz, J., Reicher, N., Rudich, Y., Schneider, J., Staacke, R., Stratmann, F., Welti, A., and Wex, H.: Coal fly ash: linking immersion freezing behavior and physicochemical particle properties, *Atmospheric Chemistry and Physics*, 18, 13903-13923, 2018.

Gruber, S., Matthias-Maser, S., and Jaenicke, R.: Concentration and chemical composition of aerosol particles in marine and continental air, *Journal of Aerosol Science*, 30, S9-S10, 1999.

Hagen, D. E., Anderson, R. J., and Kassner, J. L.: Homogeneous Condensation—Freezing Nucleation Rate Measurements for Small Water Droplets in an Expansion Cloud Chamber, *Journal of the Atmospheric Sciences*, 38, 1236-1243, 1981.

Hallett, J. and Mossop, S. C.: Production of secondary ice particles during the riming process, *Nature*, 249, 26-28, 1974.

Harrison, A. D., Lever, K., Sanchez-Marroquin, A., Holden, M. A., Whale, T. F., Tarn, M. D., McQuaid, J. B., and Murray, B. J.: The ice-nucleating ability of quartz immersed in water and its atmospheric importance compared to K-feldspar, *Atmospheric Chemistry and Physics Discussions*, doi: 10.5194/acp-2019-288, 2019. 1-23, 2019.

Harrison, A. D., Whale, T. F., Carpenter, M. A., Holden, M. A., Neve, L., apos, Sullivan, D., Vergara Temprado, J., and Murray, B. J.: Not all feldspars are equal: a survey of ice nucleating properties across the feldspar group of minerals, *Atmospheric Chemistry and Physics*, 16, 10927-10940, 2016.

Harrison, A. D., Whale, T. F., Rutledge, R., Lamb, S., Tarn, M. D., Porter, G. C. E., Adams, M. P., McQuaid, J. B., Morris, G. J., and Murray, B. J.: An instrument for quantifying heterogeneous ice nucleation in multiwell plates using infrared emissions to detect freezing, *Atmospheric Measurement Techniques*, 11, 5629-5641, 2018.

Hartmann, D. L., Ockert-Bell, M. E., and Michelsen, M. L.: The Effect of Cloud Type on Earth's Energy Balance: Global Analysis, *Journal of Climate*, 5, 1281-1304, 1992.

Häusler, T., Witek, L., Felgitsch, L., Hitzenberger, R., and Grothe, H.: Freezing on a Chip—A New Approach to Determine Heterogeneous Ice Nucleation of Micrometer-Sized Water Droplets, *Atmosphere*, 9, 140, 2018.

Herbert, R. J., Murray, B. J., Dobbie, S. J., and Koop, T.: Sensitivity of liquid clouds to homogenous freezing parameterizations, *Geophysical Research Letters*, 42, 1599-1605, 2015.

Herbert, R. J., Murray, B. J., Whale, T. F., Dobbie, S. J., and Atkinson, J. D.: Representing time-dependent freezing behaviour in immersion mode ice nucleation, *Atmospheric Chemistry and Physics*, 14, 8501-8520, 2014.

Hiranuma, N., Augustin-Bauditz, S., Bingemer, H., Budke, C., Curtius, J., Danielczok, A., Diehl, K., Dreischmeier, K., Ebert, M., and Frank, F.: A comprehensive laboratory study on the immersion freezing behavior of illite NX particles: a comparison of seventeen ice nucleation measurement techniques, *Atmospheric Chemistry and Physics Discussions*, 14, 22045-22116, 2014.

Hiranuma, N., Augustin-Bauditz, S., Bingemer, H., Budke, C., Curtius, J., Danielczok, A., Diehl, K., Dreischmeier, K., Ebert, M., Frank, F., Hoffmann, N., Kandler, K., Kiselev, A., Koop, T., Leisner, T., Möhler, O., Nillius, B., Peckhaus, A., Rose, D., Weinbruch, S., Wex, H., Boose, Y., DeMott, P. J., Hader,

J. D., Hill, T. C. J., Kanji, Z. A., Kulkarni, G., Levin, E. J. T., McCluskey, C. S., Murakami, M., Murray, B. J., Niedermeier, D., Petters, M. D., O'Sullivan, D., Saito, A., Schill, G. P., Tajiri, T., Tolbert, M. A., Welti, A., Whale, T. F., Wright, T. P., and Yamashita, K.: A comprehensive laboratory study on the immersion freezing behavior of illite NX particles: a comparison of 17 ice nucleation measurement techniques, *Atmos. Chem. Phys.*, 15, 2489-2518, 2015.

Hoffer, T. E.: *J. Meteorol.*, 18, 766-778, 1961.

Holden, M. A., Whale, T. F., Tarn, M. D., O'Sullivan, D., Walshaw, R. D., Murray, B. J., Meldrum, F. C., and Christenson, H. K.: High-speed imaging of ice nucleation in water proves the existence of active sites, *Sci. Adv.*, 2019. 2019.

Hoose, C., Kristjansson, J. E., Chen, J. P., and Hazra, A.: *J. Atmos. Sci.*, 67, 2483-2503, 2010.

Hoose, C. and Mohler, O.: Heterogeneous ice nucleation on atmospheric aerosols: a review of results from laboratory experiments, *Atmospheric Chemistry and Physics*, 12, 9817-9854, 2012.

Hoose, C. and Möhler, O.: Heterogeneous ice nucleation on atmospheric aerosols: a review of results from laboratory experiments, *Atmos. Chem. Phys.*, 12, 9817-9854, 2012.

Huang, J. and Bartell, L. S.: Kinetics of Homogeneous Nucleation in the Freezing of Large Water Clusters, *The Journal of Physical Chemistry*, 99, 3924-3931, 1995.

Hung, H. M., Malinowski, A., and Martin, S. T.: *J. Phys. Chem. A*, 107, 1296-1306, 2003.

Ipcc: Climate Change 2014: Impacts, Adaptation, and Vulnerability. Part A: Global and Sectoral Aspects. Contribution of Working Group II to the Fifth Assessment Report of the Intergovernmental Panel on Climate Change [Field, C.B., V.R. Barros, D.J. Dokken, K.J. Mach, M.D. Mastrandrea, T.E. Bilir, M. Chatterjee, K.L. Ebi, Y.O. Estrada, R.C. Genova, B. Girma, E.S. Kissel, A.N. Levy, S. MacCracken, P.R. Mastrandrea, and L.L. White (eds.)], Cambridge University Press, Cambridge, United Kingdom and New York, NY, USA, 2014.

Isono, K.: On Ice-Crystal Nuclei and Other Substances Found in Snow Crystals, *Journal of Meteorology*, 12, 456-462, 1955.

Iwata, A. and Matsuki, A.: Characterization of individual ice residual particles by the single droplet freezing method: a case study in the Asian dust outflow region, *Atmospheric Chemistry and Physics*, 18, 1785-1804, 2018.

Jaenicke, R.: Abundance of cellular material and proteins in the atmosphere, *Science*, 308, 73, 2005.

Jaenicke, R., Matthias-Maser, S., and Gruber, S.: Omnipresence of biological material in the atmosphere, *Environmental Chemistry*, 4, 217, 2007.

Kanitz, T., Seifert, P., Ansmann, A., Engelmann, R., Althausen, D., Casiccia, C., and Rohwer, E. G.: Contrasting the impact of aerosols at northern and southern midlatitudes on heterogeneous ice formation, *Geophys. Res. Lett.*, 38, L17802, 2011.

Kanji, Z. A. and Abbatt, J. P. D.: The University of Toronto Continuous Flow Diffusion Chamber (UT-CFDC): A Simple Design for Ice Nucleation Studies, *Aerosol Science and Technology*, 43, 730-738, 2009.

Kanji, Z. A., Ladino, L. A., Wex, H., Boose, Y., Burkert-Kohn, M., Cziczo, D. J., and Krämer, M.: Overview of Ice Nucleating Particles, *Meteorological Monographs*, 58, 1.1-1.33, 2017.

Kashchiev, D.: *Nucleation: Basic Theory with Applications*, Butterworth-Heinemann, Oxford, 2011.

Kiselev, A., Bachmann, F., Pedevilla, P., Cox, S. J., Michaelides, A., Gerthsen, D., and Leisner, T.: Active sites in heterogeneous ice nucleation-the example of K-rich feldspars, *Science*, 355, 367-371, 2017.

Knopf, D. A. and Alpert, P. A.: A water activity based model of heterogeneous ice nucleation kinetics for freezing of water and aqueous solution droplets, *Faraday Discuss*, 165, 513-534, 2013.

Köhler, H.: The nucleus in and the growth of hygroscopic droplets, *Trans. Faraday. Soc.*, 32, 1152-1161, 1936.

Kohn, M., Lohmann, U., Welti, A., and Kanji, Z. A.: Immersion mode ice nucleation measurements with the new Portable Immersion Mode Cooling Chamber (PIMCA), *Journal of Geophysical Research: Atmospheres*, 121, 4713-4733, 2016.

Koike, C., Noguchi, R., Chihara, H., Suto, H., Ohtaka, O., Imai, Y., Matsumoto, T., and Tsuchiyama, A.: Infrared Spectra of Silica Polymorphs and the Conditions of Their Formation, *The Astrophysical Journal*, 778, 60, 2013.

Kramer, B., Hubner, O., Vortisch, H., Woste, L., Leisner, T., Schwell, M., Ruhl, E., and Baumgartel, H.: *J. Chem. Phys.*, 111, 6521-6527, 1999.

Kumai, M.: Electron-microscope study of snow-crystal nuclei, *Journal of Meteorology*, 8, 151-156, 1951.

Kumar, A., Marcolli, C., Luo, B., and Peter, T.: Ice nucleation activity of silicates and aluminosilicates in pure water and aqueous solutions – Part 1: The K-feldspar microcline, *Atmospheric Chemistry and Physics*, 18, 7057-7079, 2018.

Kumar, A., Marcolli, C., and Peter, T.: Ice nucleation activity of silicates and aluminosilicates in pure water and aqueous solutions – Part 2: Quartz and amorphous silica, *Atmospheric Chemistry and Physics*, 19, 6035-6058, 2019.

Lindow, S. E., Arny, D. C., and Upper, C. D.: Bacterial ice nucleation: a factor in frost injury to plants, *Plant Physiology*, 70, 1084-1089, 1982.

Lohmann, U. and Feichter, J.: Global indirect aerosol effects: a review, *Atmospheric Chemistry and Physics*, 5, 715-737, 2005.

Luond, F., Stetzer, O., Welti, A., and Lohmann, U.: *J. Geophys. Res.*, 115, 2010.

MacKenzie, W. S. and Adams, A. E.: *A colour Atlas of rocks and minerals in thin section*, Manson Publishing Ltd, Barcelona, Spain, 2011.

Mahowald, N. M.: Anthropocene changes in desert area: Sensitivity to climate model predictions, *Geophysical Research Letters*, 34, 2007.

Mahowald, N. M., Kloster, S., Engelstaedter, S., Moore, J. K., Mukhopadhyay, S., McConnell, J. R., Albani, S., Doney, S. C., Bhattacharya, A., Curran, M. A. J., Flanner, M. G., Hoffman, F. M., Lawrence, D. M., Lindsay, K., Mayewski, P. A., Neff, J., Rothenberg, D., Thomas, E., Thornton, P. E., and Zender, C. S.: Observed 20th century desert dust variability: impact on climate and biogeochemistry, *Atmos. Chem. Phys.*, 10, 10875-10893, 2010.

Malkin, T. L., Murray, B. J., Brukhno, A. V., Anwar, J., and Salzmann, C. G.: Structure of ice crystallized from supercooled water, *Proceedings of the National Academy of Sciences*, 109, 1041-1045, 2012.

Marcolli, C.: Deposition nucleation viewed as homogeneous or immersion freezing in pores and cavities, *Atmos. Chem. Phys.*, 14, 2071-2104, 2014.

Marcolli, C., Gedamke, S., Peter, T., and Zobrist, B.: Efficiency of immersion mode ice nucleation on surrogates of mineral dust, *Atmos. Chem. Phys.*, 7, 5081-5091, 2007.

Mason, B. J.: The nature of ice-forming nuclei in the atmosphere, *Quarterly Journal of the Royal Meteorological Society*, 76, 59-74, 1950.

Mason, B. J.: *The Physics of Clouds*, Claredon Press, Oxford, 1971.

Mason, B. J. and Maybank, J.: ICE-NUCLEATING PROPERTIES OF SOME NATURAL MINERAL DUSTS, *Quarterly Journal of the Royal Meteorological Society*, 84, 235-241, 1958.

Matthias-Maser, S. and Jaenicke, R.: The size distribution of primary biological aerosol particles with radii $> 0.2 \mu\text{m}$ in an urban/rural influenced region, *Atmospheric Research*, 39, 279-286, 1995.

McCluskey, C. S., DeMott, P. J., Prenni, A. J., Levin, E. J. T., McMeeking, G. R., Sullivan, A. P., Hill, T. C. J., Nakao, S., Carrico, C. M., and Kreidenweis, S. M.: Characteristics of atmospheric ice nucleating particles associated with biomass burning in the US: Prescribed burns and wildfires, *Journal of Geophysical Research: Atmospheres*, 119, 10458-10470, 2014.

Meyers, M. P., DeMott, P. J., and Cotton, W. R.: *J. Appl. Meteorol.*, 31, 708-721, 1992.

Mignani, C., Creamean, J. M., Zimmermann, L., Alewell, C., and Conen, F.: New type of evidence for secondary ice formation at around $-15\text{ }^\circ\text{C}$ in mixed-phase clouds, *Atmospheric Chemistry and Physics*, 19, 877-886, 2019.

Morris, C. E., Sands, D. C., Bardin, M., Jaenicke, R., Vogel, B., Leyronas, C., Ariya, P. A., and Psenner, R.: Microbiology and atmospheric processes: research challenges concerning the impact of airborne micro-organisms on the atmosphere and climate, *Biogeosciences*, 8, 17-25, 2011.

Mullin, J. W.: *Crystallization*, Elsevier, Oxford, UK, 2001.

Murray, B. J., Broadley, S. L., Wilson, T. W., Atkinson, J. D., and Wills, R. H.: Heterogeneous freezing of water droplets containing kaolinite particles, *Atmospheric Chemistry and Physics*, **11**, 4191-4207, 2011.

Murray, B. J., Broadley, S. L., Wilson, T. W., Bull, S. J., Wills, R. H., Christenson, H. K., and Murray, E. J.: Kinetics of the homogeneous freezing of water, *Phys. Chem. Chem. Phys.*, **12**, 10380-10387, 2010.

Murray, B. J., O'Sullivan, D., Atkinson, J. D., and Webb, M. E.: Ice nucleation by particles immersed in supercooled cloud droplets, *Chemical Society reviews*, **41**, 6519-6554, 2012a.

Murray, B. J., O'Sullivan, D., Atkinson, J. D., and Webb, M. E.: Ice nucleation by particles immersed in supercooled cloud droplets, *Chemical Society Reviews*, **41**, 6519-6554, 2012b.

Niedermeier, D., Augustin-Bauditz, S., Hartmann, S., Wex, H., Ignatius, K., and Stratmann, F.: Can we define an asymptotic value for the ice active surface site density for heterogeneous ice nucleation?, *Journal of Geophysical Research: Atmospheres*, **120**, 5036-5046, 2015.

Niedermeier, D., Hartmann, S., Shaw, R. A., Covert, T. F., Mentel, J., Schneider, J., Poulain, L., Reitz, P., Spindler, C., Clauss, T., Kiselev, A., Hallbauer, E., Wex, H., Mildnerberger, K., and Stratmann, F.: *Atmos. Chem. Phys.*, **10**, 3601-3614, 2010.

Niemand, M., Möhler, O., Vogel, B., Vogel, H., Hoose, C., Connolly, P., Klein, H., Bingemer, H., DeMott, P. J., Skrotzki, J., and Leisner, T.: A particle-surface-area-based parameterization of immersion freezing on desert dust particles, *Journal of the Atmospheric Sciences*, **69**, 2012.

O'Sullivan, D., Adams, M. P., Tarn, M. D., Harrison, A. D., Vergara-Temprado, J., Porter, G. C. E., Holden, M. A., Sanchez-Marroquin, A., Carotenuto, F., Whale, T. F., McQuaid, J. B., Walshaw, R., Hedges, D. H. P., Burke, I. T., Cui, Z., and Murray, B. J.: Contributions of biogenic material to the atmospheric ice-nucleating particle population in North Western Europe, *Sci Rep*, **8**, 13821, 2018.

O'Sullivan, D., Murray, B. J., Malkin, T. L., Whale, T. F., Umo, N. S., Atkinson, J. D., Price, H. C., Baustian, K. J., Browse, J., and Webb, M. E.: Ice nucleation by fertile soil dusts: relative importance of mineral and biogenic components, *Atmos. Chem. Phys.*, **14**, 1853-1867, 2014.

- O'Sullivan, D., Murray, B. J., Ross, J., and Webb, M. E.: The adsorption of fungal ice-nucleating proteins on mineral dusts: a terrestrial reservoir of atmospheric ice-nucleating particles, *Atmos. Chem. Phys. Discuss.*, 2016, 1-22, 2016.
- Pankhurst, M. J.: Atmospheric K-feldspar as a potential climate modulating agent through geologic time, *Geology*, 45, 379-382, 2017.
- Peckhaus, A., Kiselev, A., Hiron, T., Ebert, M., and Leisner, T.: A comparative study of K-rich and Na/Ca-rich feldspar ice nucleating particles in a nanoliter droplet freezing assay, *Atmospheric Chemistry and Physics Discussions*, doi: 10.5194/acp-2016-72, 2016. 1-43, 2016.
- Pedevilla, P., Fitzner, M., and Michaelides, A.: What makes a good descriptor for heterogeneous ice nucleation on OH-patterned surfaces, *Physical Review B*, 96, 2017.
- Phillips, V., Choulaton, T., Illingworth, A., Hogan, R., and Field, P.: Simulations of the glaciation of a frontal mixed-phase cloud with the Explicit Microphysics Model, *Quarterly Journal of the Royal Meteorological Society*, 129, 1351-1371, 2003.
- Phillips, V. T. J., Donner, L. J., and Garner, S. T.: *J. Atmos. Sci.*, 64, 2007.
- Pinti, V., Marcolli, C., Zobrist, B., Hoyle, C. R., and Peter, T.: Ice nucleation efficiency of clay minerals in the immersion mode, *Atmospheric Chemistry and Physics*, 12, 5859-5878, 2012.
- Pitter, R. L. and Pruppacher, H. R.: *Q. J. R. Meteorol. Soc.*, 99, 540-550, 1973.
- Pratt, K. A., DeMott, P. J., French, J. R., Wang, Z., Westphal, D. L., Heymsfield, A. J., Twohy, C. H., Prenni, A. J., and Prather, K. A.: In situ detection of biological particles in cloud ice-crystals, *Nature Geosci*, 2, 398-401, 2009.
- Press, F., Siever, R., Grotzinger, J., and Jordan, T. H.: *Understanding Earth: Fourth edition*, W. H. Freeman and Company, New York, 2003.
- Price, H. C., Baustian, K. J., McQuaid, J. B., Blyth, A., Bower, K. N., Choulaton, T., Cotton, R. J., Cui, Z., Field, P. R., Gallagher, M., Hawker, R., Merrington, A., Miltenberger, A., Neely, R. R., Parker, S. T., Rosenberg, P. D., Taylor, J. W., Trembath, J., Vergara-Temprado, J., Whale, T. F., Wilson, T. W., Young, G., and Murray, B. J.: Atmospheric Ice-Nucleating Particles in the Dusty Tropical Atlantic, *Journal of Geophysical Research: Atmospheres*, 123, 2175-2193, 2018.

Prospero, J. M., Ginoux, P., Torres, O., Nicholson, S. E., and Gill, T. E.: Environmental characterization of global sources of atmospheric soil dust identified with the NIMBUS 7 Total Ozone Mapping Spectrometer (TOMS) absorbing aerosol product, *Rev. Geophys.*, 40, 1002, 2002.

Pruppacher, H. R. and Klett, J. D.: *Microphysics of Clouds and Precipitation*, Kluwer Academic Publishers, 1997.

Pye, K.: *Sediment transport and depositional processes*. Pye, K. (Ed.), Blackwell scientific publications, Oxford, Boston, 1994.

Riechers, B., Wittbracht, F., Hütten, A., and Koop, T.: The homogeneous ice nucleation rate of water droplets produced in a microfluidic device and the role of temperature uncertainty, *Physical Chemistry Chemical Physics*, 15, 5873-5887, 2013.

Roberts, P. and Hallett, J.: A laboratory study of the ice nucleating properties of some mineral particulates, *Quarterly Journal of the Royal Meteorological Society*, 94, 25-34, 1968.

Rogers, D. C., DeMott, P. J., Kreidenweis, S. M., and Chen, Y. L.: A continuous-flow diffusion chamber for airborne measurements of ice nuclei, *J. Atmos. Ocean. Tech.*, 18, 725-741, 2001.

Rogers, D. C., DeMott, P. J., Kreidenweis, S. M., and L., C. Y.: *Geophys. Res. Lett.*, 25, 1383-1386, 1998.

Rosinski, J. and Morgan, G. M.: *J. Aerosol Sci.*, 19, 531-538, 1988.

Salam, A., Lohmann, U., Crenna, B., Lesins, G., Klages, P., Rogers, D., Irani, R., MacGillivray, A., and Coffin, M.: Ice nucleation studies of mineral dust particles with a new continuous flow diffusion chamber, *Aerosol. Sci. Tech.*, 40, 134-143, 2006.

Schill, G. P., Jathar, S. H., Kodros, J. K., Levin, E. J. T., Galang, A. M., Friedman, B., Link, M. F., Farmer, D. K., Pierce, J. R., Kreidenweis, S. M., and DeMott, P. J.: Ice-nucleating particle emissions from photochemically aged diesel and biodiesel exhaust, *Geophysical Research Letters*, 43, 5524-5531, 2016.

Schnell, R. C.: *Biogenic and inorganic sources for ice nuclei in the drought-stricken areas of the Sahel*, Rockefeller Foundation, New York, 1974.

Schnell, R. C. and Vali, G.: World-wide Source of Leaf-derived Freezing Nuclei, *Nature*, 246, 212-213, 1973.

Sear, R. P.: Quantitative studies of crystal nucleation at constant supersaturation: experimental data and models, *CrystEngComm*, 16, 6506-6522, 2014.

Seifert, P., Kunz, C., Baars, H., Ansmann, A., Bühl, J., Senf, F., Engelmann, R., Althausen, D., and Artaxo, P.: Seasonal variability of heterogeneous ice formation in stratiform clouds over the Amazon Basin, *Geophysical Research Letters*, 42, 5587-5593, 2015.

Si, M., Evoy, E., Yun, J., Xi, Y., Hanna, S. J., Chivulescu, A., Rawlings, K., Veber, D., Platt, A., Kunkel, D., Hoor, P., Sharma, S., Leaitch, W. R., and Bertram, A. K.: Concentrations, composition, and sources of ice-nucleating particles in the Canadian High Arctic, *Atmos. Chem. and Phys.*, 19, 3007-3024, 2019.

Sokolik, I. N. and Toon, O. B.: Direct radiative forcing by anthropogenic airborne mineral aerosols, *Nature*, 381, 681-683, 1996.

Stan, C. A., Schneider, G. F., Shevkoplyas, S. S., Hashimoto, M., Ibanescu, M., Wiley, B. J., and Whitesides, G. M.: A microfluidic apparatus for the study of ice nucleation in supercooled water drops, *Lab on a Chip*, 9, 2293-2305, 2009.

Stetzer, O., Baschek, B., Lüönd, F., and Lohmann, U.: The Zurich Ice Nucleation Chamber (ZINC)-A new instrument to investigate atmospheric ice formation, *Aerosol Science and Technology*, 42, 64-74, 2008.

Storelvmo, T.: Aerosol Effects on Climate via Mixed-Phase and Ice Clouds, *Annual Review of Earth and Planetary Sciences*, 45, 199-222, 2017.

Swamy, V., Saxena, S. K., Sundman, B., and Zhang, J.: A thermodynamic assessment of silica phase diagram, *Journal of Geophysical Research: Solid Earth*, 99, 11787-11794, 1994.

Tan, I., Storelvmo, T., and Zelinka, M. D.: Observational constraints on mixed-phase clouds imply higher climate sensitivity, *Science*, 352, 224-227, 2016.

Tarn, M. D., Sikora, S. N. F., Porter, G. C. E., O'Sullivan, D., Adams, M., Whale, T. F., Harrison, A. D., Vergara-Temprado, J., Wilson, T. W., Shim, J. U., and Murray, B. J.: The study of atmospheric ice-nucleating particles via microfluidically generated droplets, *Microfluid Nanofluidics*, 22, 52, 2018.

- Tegen, I. and Fung, I.: Contribution to the atmospheric mineral aerosol load from land surface modification, *J. Geophys. Res.*, 100, 18707-18726, 1995.
- Twohy, C. H., DeMott, P. J., Pratt, K. A., Subramanian, R., Kok, G. L., Murphy, S. M., Lersch, T., Heymsfield, A. J., Wang, Z., Prather, K. A., and Seinfeld, J. H.: Relationships of Biomass-Burning Aerosols to Ice in Orographic Wave Clouds, *Journal of the Atmospheric Sciences*, 67, 2437-2450, 2010.
- Twomey, S.: The influence of pollution on shortwave albedo of clouds, *Journal of the Atmospheric Sciences*, 34, 1149-1152, 1977.
- Ullrich, R., Hoose, C., Möhler, O., Niemand, M., Wagner, R., Höhler, K., Hiranuma, N., Saathoff, H., and Leisner, T.: A New Ice Nucleation Active Site Parameterization for Desert Dust and Soot, *Journal of the Atmospheric Sciences*, 74, 699-717, 2017.
- Umo, N. S., Murray, B. J., Baeza-Romero, M. T., Jones, J. M., Lea-Langton, A. R., Malkin, T. L., O'Sullivan, D., Neve, L., Plane, J. M. C., and Williams, A.: Ice nucleation by combustion ash particles at conditions relevant to mixed-phase clouds, *Atmos. Chem. Phys.*, 15, 5195-5210, 2015.
- Vali, G.: *J. Atmos. Sci.*, 8, 5017-5031, 2008a.
- Vali, G.: Freezing Rate Due to Heterogeneous Nucleation, *Journal of the Atmospheric Sciences*, 51, 1843-1856, 1994.
- Vali, G.: Quantitative Evaluation of Experimental Results on the Heterogeneous Freezing Nucleation of Supercooled Liquids, *Journal of the Atmospheric Sciences*, 28, 402-409, 1971.
- Vali, G.: Repeatability and randomness in heterogeneous freezing nucleation, *Atmos. Chem. Phys.*, 8, 5017-5031, 2008b.
- Vali, G., DeMott, P. J., Möhler, O., and Whale, T. F.: Technical Note: A proposal for ice nucleation terminology, *Atmospheric Chemistry and Physics*, 15, 10263-10270, 2015.
- Vali, G. and Stansbury, E. J.: *Can. J. Phys.*, 44, 477-502, 1966.
- Vergara-Temprado, J., Holden, M. A., Orton, T. R., O'Sullivan, D., Umo, N. S., Browse, J., Reddington, C., Baeza-Romero, M. T., Jones, J. M., Lea-Langton, A., Williams, A., Carslaw, K. S., and Murray, B. J.:

Is Black Carbon an Unimportant Ice-Nucleating Particle in Mixed-Phase Clouds?, *J Geophys Res Atmos*, 123, 4273-4283, 2018a.

Vergara-Temprado, J., Miltenberger, A. K., Furtado, K., Grosvenor, D. P., Shipway, B. J., Hill, A. A., Wilkinson, J. M., Field, P. R., Murray, B. J., and Carslaw, K. S.: Strong control of Southern Ocean cloud reflectivity by ice-nucleating particles, *Proceedings of the National Academy of Sciences of the United States of America*, 115, 2687-2692, 2018b.

Vergara-Temprado, J., Murray, B. J., Wilson, T. W., amp, apos, Sullivan, D., Browse, J., Pringle, K. J., Ardon-Dryer, K., Bertram, A. K., Burrows, S. M., Ceburnis, D., DeMott, P. J., Mason, R. H., amp, apos, Dowd, C. D., Rinaldi, M., and Carslaw, K. S.: Contribution of feldspar and marine organic aerosols to global ice nucleating particle concentrations, *Atmos. Chem. Phys.*, 17, 3637-3658, 2017.

Wex, H., DeMott, P. J., Tobo, Y., Hartmann, S., Rösch, M., Clauss, T., Tomsche, L., Niedermeier, D., and Stratmann, F.: Kaolinite particles as ice nuclei: learning from the use of different kaolinite samples and different coatings, *Atmos. Chem. Phys.*, 14, 5529-5546, 2014.

Whale, T. F., Holden, M. A., Kulak, A. N., Kim, Y. Y., Meldrum, F. C., Christenson, H. K., and Murray, B. J.: The role of phase separation and related topography in the exceptional ice-nucleating ability of alkali feldspars, *Phys Chem Chem Phys*, 19, 31186-31193, 2017.

Whale, T. F., Holden, M. A., Wilson, T. W., O'Sullivan, D., and Murray, B. J.: The enhancement and suppression of immersion mode heterogeneous ice-nucleation by solutes, *Chem Sci*, 9, 4142-4151, 2018.

Whale, T. F., Murray, B. J., O'Sullivan, D., Wilson, T. W., Umo, N. S., Baustian, K. J., Atkinson, J. D., Workneh, D. A., and Morris, G. J.: A technique for quantifying heterogeneous ice nucleation in microlitre supercooled water droplets, *Atmos. Meas. Tech.*, 8, 2437-2447, 2015.

Wild, M., Hakuba, M. Z., Folini, D., Dorig-Ott, P., Schar, C., Kato, S., and Long, C. N.: The cloud-free global energy balance and inferred cloud radiative effects: an assessment based on direct observations and climate models, *Clim Dyn*, 52, 4787-4812, 2019.

Wilson, T. W., Ladino, L. A., Alpert, P. A., Breckels, M. N., Brooks, I. M., Browse, J., Burrows, S. M., Carslaw, K. S., Huffman, J. A., Judd, C., Kalthau, W. P., Mason, R. H., McFiggans, G., Miller, L. A., Najera, J. J., Polishchuk, E., Rae, S., Schiller, C. L., Si, M., Temprado, J. V., Whale, T. F., Wong, J. P. S.,

Wurl, O., Yakobi-Hancock, J. D., Abbatt, J. P. D., Aller, J. Y., Bertram, A. K., Knopf, D. A., and Murray, B. J.: A marine biogenic source of atmospheric ice-nucleating particles, *Nature*, 525, 234-238, 2015.

Wood, S. E., Baker, M. B., and Swanson, B. D.: *Rev. Sci. Instrum.*, 73, 3988-3996, 2002.

Zaragotas, D., Liolios, N. T., and Anastassopoulos, E.: Supercooling, ice nucleation and crystal growth: a systematic study in plant samples, *Cryobiology*, 72, 239-243, 2016.

Zender, C. S., Miller, R. L. R. L., and Tegen, I.: Quantifying mineral dust mass budgets: Terminology, constraints, and current estimates, *Eos Trans. AGU*, 85, 2004.

Zimmermann, F., Weinbruch, S., Schütz, L., Hofmann, H., Ebert, M., Kandler, K., and Worringer, A.: Ice nucleation properties of the most abundant mineral dust phases, *Journal of Geophysical Research: Atmospheres*, 113, D23204, 2008.

Zolles, T., Burkart, J., Häusler, T., Pummer, B., Hitzemberger, R., and Grothe, H.: Identification of Ice Nucleation Active Sites on Feldspar Dust Particles, *The Journal of Physical Chemistry A*, 119, 2692-2700, 2015.

2. The ice-nucleating ability of quartz immersed in water and its atmospheric importance compared to K-feldspar

This chapter has been accepted for publication in *Atmospheric Chemistry and Physics* as:

Harrison, A. D., Lever, K., Sanchez-Marroquin, A., Holden, M. A., Whale, T. F., Tarn, M. D., McQuaid, J. B. and Murray, B. J. ‘The ice-nucleating ability of quartz immersed in water and its atmospheric importance compared to K-feldspar’, ACP (2019).

Abstract. Mineral dust particles are thought to be an important type of ice-nucleating particle (INP) in the mixed-phase cloud regime around the globe. While K-feldspar has been identified as being a particularly important component of mineral dust for ice nucleation, it has been shown that quartz is also relatively ice nucleation active. Given quartz typically makes up a substantial proportion of atmospheric desert dust it could potentially be important for cloud glaciation. Here, we survey the ice-nucleating ability of 10 α -quartz samples (the most common quartz polymorph) when immersed in microlitre supercooled water droplets. Despite all samples being α -quartz, the temperature at which they induce freezing varies by around 12°C for a constant active site density. We find that some quartz samples are very sensitive to ageing in both aqueous suspension and air, resulting in a loss of ice-nucleating activity, while other samples are insensitive to exposure to air and water over many months. For example, the ice nucleation temperatures for one quartz sample shift down by ~2°C in 1 hour and 12°C after 16 months in water. The sensitivity to water and air is perhaps surprising as quartz is thought of as a chemically resistant mineral, but this observation suggests that the active sites responsible for nucleation are less stable than the bulk of the mineral. We find that the quartz group of minerals are generally less active than K-feldspars by roughly 7 °C, although the most active quartz samples are of a similar activity to some K-feldspars with an active site density, $n_s(T)$, of 1 cm⁻² at -9 °C. We also find that the freshly milled quartz samples are generally more active by roughly 5 °C than the plagioclase feldspar group of minerals and the albite end-member has an intermediate activity. Using both the new and literature data, active site density parameterisations have been proposed for freshly milled quartz, K-feldspar, plagioclase and albite. Combining these parameterisations with the typical atmospheric abundance of each mineral supports previous work that suggests that K-feldspar is the most important ice-nucleating mineral in airborne mineral dust.

2.1 Introduction

The formation of ice in supercooled clouds strongly affects hydrometeor size which in turn impacts cloud lifetime, precipitation and radiative properties (Kanji et al., 2017). There are a number of primary and secondary mechanisms through which ice can form in clouds. Homogeneous freezing of cloud droplets becomes increasingly important below $-33\text{ }^{\circ}\text{C}$ (Herbert et al., 2015), but clouds commonly glaciate at much warmer temperatures (Kanitz et al., 2011; Ansmann et al., 2009). Freezing at these warmer temperatures can occur through secondary ice production (Field et al., 2017) or heterogeneous freezing on ice-nucleating particles (INPs) (Murray et al., 2012; Hoose and Möhler, 2012). The presence of INPs, which tend to comprise only a small fraction of cloud condensation nuclei, can dramatically reduce the lifetime of shallow clouds (Vergara-Temprado et al., 2018), and alter the development of deep convective clouds through, for example, the release of latent heat which invigorates the updraft thus altering cloud structure (Lohmann, 2017; Rosenfeld et al., 2011). It is also recognised that an accurate representation of cloud phase is important for assessments of climate sensitivity (Tan et al., 2016; Ceppi et al., 2017). However, our understanding of which type of aerosol particles serve as effective INPs is incomplete (Vergara-Temprado et al., 2017; Kanji et al., 2017).

Mineral dust has been inferred to be an effective INP in the atmosphere from field, model and laboratory studies (Hoose and Möhler, 2012; Vergara-Temprado et al., 2017). Observations of aerosol within ice crystals have shown that mineral dust is often present, suggesting they act as INPs within mixed phase clouds (Iwata and Matsuki, 2018; Eriksen Hammer et al., 2018; Pratt et al., 2009). Laboratory studies also demonstrate mineral dusts are relatively effective at nucleating ice (Hoose and Möhler, 2012; Murray et al., 2012; DeMott et al., 2015). Atmospheric mineral dusts are composed of several components. Clay is a major component of airborne mineral dust and is sufficiently small that its atmospheric lifetime is relatively long. Hence, historically ice nucleation studies have focused on the clay group of minerals (e.g. Broadley et al., 2012; Murray et al., 2011; Wex et al., 2014; Mason and Maybank, 1958; Pinti et al., 2012; Roberts and Hallett, 1968; Hoose and Möhler, 2012). However, more recent work shows that K-rich feldspars (K-feldspars) are very effective INPs when immersed in supercooled water (Whale et al., 2017; Zolles et al., 2015; Tarn et al., 2018; Peckhaus et al., 2016; DeMott et al., 2018; Reicher et al., 2018; Harrison et al., 2016; Niedermeier et al.,

2015;Atkinson et al., 2013). However, there are other minerals present in the atmosphere, many of which are relatively poorly characterised in terms of their ice-nucleating activity.

Quartz is a major component of aerosolised atmospheric mineral dust (Perlwitz et al., 2015;Glaccum and Prospero, 1980) and studies have shown that it can be active as an INP (Zolles et al., 2015;Atkinson et al., 2013;Isono and Ikebe, 1960;Holden et al., 2019;Kumar et al., 2019a;Losey et al., 2018). Boose et al. (2016b) showed a correlation between the INP activity of nine desert dusts and the concentration of K-feldspar at temperatures of -20°C . However, at lower temperatures (-35 to -28°C) the ice-nucleating activity of the dusts correlated with the combined concentration of quartz and K-feldspar. Boose et al. (2016bb) thus emphasised the importance of understanding quartz and feldspars present in the atmosphere for the modelling of INPs. Recently, Kumar et al. (2018) investigated five milled quartz samples (two synthetic, three naturally occurring) for their ice-nucleating activity, demonstrating the activity of milled quartz. Very recently, Holden et al. (2019) demonstrated that nucleation on quartz is indeed site specific, through repeated freezing experiments with high-speed cryomicroscopy, and found that micron sized defects tended to be collocated with the nucleation sites. While our understanding of ice nucleation by quartz has improved recently, it is still unclear how variable quartz samples are in their ice-nucleating ability, which prevents an assessment of its atmospheric importance as an ice-nucleating particle relative to other minerals.

When designing experiments focused on understanding the ice-nucleating activity of atmospheric mineral dusts, we must consider the processes that lead to the production of dust in the atmosphere (these processes are illustrated in Figure 2.1). It is common practice to mill relatively pure samples to fine powders which can be studied in the laboratory (Atkinson et al., 2013;Harrison et al., 2016;Peckhaus et al., 2016;Zolles et al., 2015;DeMott et al., 2018;Kumar et al., 2018;Niedermeier et al., 2015) for the purposes of characterising the ice-nucleating ability of individual minerals, but the relevance of this mechanical milling process to natural airborne mineral dusts needs some discussion. Ultimately, atmospheric mineral dust is derived from bulk rocks which are mechanically broken down to finer particles through erosion processes (Blatt et al., 1980). The finer material that results can be transported by rivers or wind and forms soils in deserts or fertile regions. The particles in these soils undergo complex ageing chemistry (and biology), which converts certain minerals into clay minerals (Wilson,

2004). Minerals such as pyroxenes and amphiboles are relatively readily converted to clays over geological timescales, but quartz and to a lesser extent feldspars are relatively inert and therefore persist in soils (Goldich, 1938; Wilson, 2004). However, the ageing state of the surfaces of these minerals is unclear. While ageing processes may modify the surfaces relative to the original fresh surfaces, these aged materials are continually exposed to aeolian processes that involve grains mechanically abrading against one another, resulting in rounding of grains and the break-up of aggregates (Bagnold, 1941; Pye, 1994). These vigorous aeolian processes result in the generation of small airborne dust particles which most likely have fresh surfaces. Hence, the commonly applied practice of mechanically milling rock samples for laboratory characterisation has some justification, but it would be wise to test how sensitive the active sites on these surfaces are to exposure to air and water. Previous studies indicate that K-feldspars tend to be relatively insensitive to exposure to water and air (Harrison et al., 2016; Whale et al., 2017), although acids can deactivate K-feldspars (Kumar et al., 2018). Hence, in the absence of strong acids, freshly milled K-feldspar is thought to be relevant for atmospheric mineral dust. Quartz on the other hand has been shown to be very sensitive to exposure to water and re-milling these samples appears to readily expose or create new active sites (Zolles et al., 2015; Kumar et al., 2019a).

In this study we present a survey of the ice-nucleating ability of 10 naturally occurring quartz samples and demonstrate the variability in ice-nucleating ability within natural quartz. We also explore the stability of a subset of these samples to time spent in water or exposed to air confirming that the activity of some quartz samples are very sensitive to ageing, in contrast to K-feldspars. Then, in order to compare the potential contribution of quartz to the atmospheric INP population to that of other minerals we have generated a parameterisation for freshly milled quartz based on the experimental work in this study. In addition we present new parameterisations for K-feldspar, plagioclase feldspar, and albite feldspar based on datasets available in the literature. This allows us to compare the potential contribution of quartz, albite, plagioclase and K-feldspar to the atmospheric INP population.

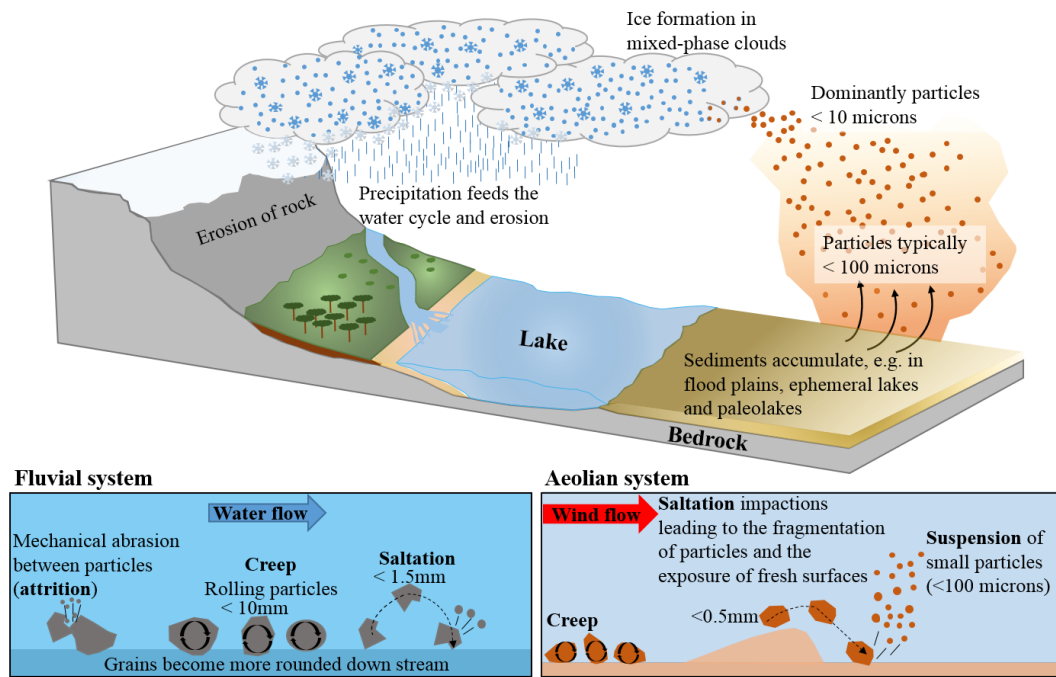


Figure 2.1: Illustration of the geological processes that lead to the creation of a mineral dust and its emission to the atmosphere. Saltation and creep occur both in fluvial and aeolian systems and are processes responsible for the movement of material. There is typically more energy in a fluvial system and hence the particle sizes moved in these systems are larger. Attrition between particles causes them to fragment and to become more rounded on transport with small particles becoming suspended in water or air. The particles smaller than $\sim 10 \mu\text{m}$ in air can be transported for long distances and may interact with clouds, serving as INP, many 100s or 1000s of kilometres away from the source regions.

2.2 Quartz, the mineral

Quartz is the second most abundant mineral in the Earth's crust after the feldspar group of minerals. Its hardness (Moh's scale 7) and chemical nature along with its lack of cleavage planes mean it is also a common constituent of sands and soils as it is resistant to weathering processes. Although quartz does not have cleavage planes it does exhibit conchoidal fracturing meaning particles tend to have smoothly curving surfaces as a result of fracturing (Deer et al., 1966), rather than planes with steps that might be expected on a cleavage plane. As it is a common constituent to soils, including desert soils, it can be lofted into the atmosphere and is

found within transported mineral dusts (Caquineau et al., 1998; Avila et al., 1997; Kandler et al., 2011; Kandler et al., 2009).

The silica minerals are composed of SiO_2 tetrahedra with each silicon being bonded to four oxygen atoms and these tetrahedra form a 3D framework which can be in six or eight membered loops (Deer et al., 1992). There are three principle crystalline types of SiO_2 : quartz, cristobalite and tridymite, with stishovite and coesite being other high pressure polymorphs. The polymorph that is present depends on the temperature and pressure during formation (Koike et al., 2013; Swamy et al., 1994). All three crystalline silica types (quartz, cristobalite and tridymite) can exist in two polymorphs, both a high temperature (β) and low temperature (α) state. α -quartz is most commonly found at or near the Earth's surface due to it being the most stable at atmospheric conditions and thus is the dominant polymorph of quartz found in soils and in atmospheric desert dust aerosol (Deer et al., 1992). In fact, α -quartz is so common that by convention it is referred to simply as quartz.

Generally, quartz samples tend to be close to 100 % SiO_2 although it is common to find small amounts of oxides as inclusions or liquid infillings within cavities (Deer et al., 1966). The substitution of Al^{3+} for Si^{4+} allows for the introduction of alkali ions such as Li^+ and Na^+ . These subtle impurities can lead to a variety of colours. If quartz with impurities (for example Al) is exposed to low levels of naturally occurring radiation then one pair of electrons from an oxygen adjacent to Al can be emitted leaving unpaired electrons otherwise known as "hole defects" (Nassau, 1978). This forms the basis for colour centres, which cause the colouration of amethyst. Amethyst is typically violet in colour and differs from standard α -quartz in that it has a larger proportion of Fe_2O_3 inclusions and marginally more TiO_2 and Al_2O_3 in its structure (Deer et al., 1966). Rose quartz generally contains higher amounts of alkali oxides, Fe_2O_3 , TiO_2 and MnO_2 (Deer et al., 1966). It has a pinkish colour which is thought to be attributed to the presence of a fibrous mineral which was first suggested to be dumortierite (Kibar et al., 2007; Applin and Hicks, 1987) but has been suggested to be a different, unclassified type of mineral (Goreva et al., 2001). Smoky quartz has a black colour which is caused by colour centres created by the irradiation of iron (Nassau, 1978). Chalcedony is a form of cryptocrystalline or microcrystalline α -quartz (Deer et al., 1966). It has been suggested that it is also commonly intergrown with another polymorph of quartz known as moganite (Heaney and Post, 1992; Götze et al., 1998). Moganite has a monoclinic crystal structure opposed to the

trigonal crystal system of quartz. Chalcedony often includes micropores within its structure due to its microcrystalline nature (Deer et al., 1966).

2.3 Materials and Methods

2.3.1 Samples and preparation

10 α -quartz samples were tested for their ice-nucleating ability. These included four typical α -quartzes, two amethysts, two microcrystalline quartzes (chalcedony), one rose quartz and one smoky quartz, as summarised in Table 1. Photographs of the samples are presented in Figure 2.2. These samples were selected to investigate the natural variability of the ice-nucleating ability of α -quartz.

These samples were sourced from various gem sellers. The minerals were visually inspected, using their colour, crystal habit, lustre and cleavage to confirm whether the mineral was quartz and, if so, what type of quartz. Rietveld refinement of powder X-ray diffraction (XRD) patterns was then used to verify the silica polymorph and identify any significant crystalline impurities. The results of this process are presented in Table 1. Raman spectroscopy was used in conjunction with XRD to test for the presence of moganite within the two chalcedony samples based on the work of Götze et al. (1998). However, both methods indicated that no moganite was present above the limit of detection (~ 1 wt%).

Eight of the samples were prepared from bulk rock or crystal samples by first rinsing the rock surface with isopropanol and pure water and placing in a clean sealed plastic bag before chipping off fragments and then grinding them into a powder with

<i>Sample</i>	<i>XRD analysis</i>	<i>BET surface area (m²g⁻¹)</i>	<i>Spherical equivalent diameter (μm)</i>
<i>Bombay chalcedony</i>	α-quartz: 100%	1.23 ± 0.01	1.88
<i>Grape chalcedony</i>	α-quartz: 100%	4.39 ± 0.01	0.53
<i>Smoky quartz</i>	α-quartz: 98.3% Haematite: 0.1% Albite: 1.6%	1.23 ± 0.01	1.88
<i>Rose quartz</i>	α-quartz: 100%	1.13 ± 0.01	2.04
<i>Atkinson quartz</i>	α-quartz: 99.9% Calcite: 0.1%	4.20 ± 0.01	0.55
<i>Fluka quartz</i>	α-quartz: 100%	0.91 ± 0.01	2.54
<i>Mexico quartz</i>	α-quartz: 96.4% Dolomite: 3.6%	1.74 ± 0.01	1.33
<i>LD1 quartz</i>	α-quartz: 100%	0.94 ± 0.01	2.45
<i>Uruguay amethyst</i>	α-quartz: 99.9% Calcite: 0.1%	1.46 ± 0.01	1.58
<i>Brazil amethyst</i>	α-quartz: 100%	2.76 ± 0.01	0.84

Table 2.1: Table showing the relative concentrations of different minerals within each sample and the respective BET specific surface area of the ground sample and derived spherical equivalent average surface area. The uncertainty in the XRD analysis is on the order of 0.1 %, hence the identification of some trace constituents in some samples is tentative. The mineral density was assumed to be 2.6 gcm⁻³ for the calculation of spherical equivalent diameter.

an agate mortar and pestle. The mortar and pestle were cleaned before use by scrubbing them with quartz sand (Fluka) and rinsing thoroughly with pure deionised water and isopropanol. A similar method was employed by Harrison et al. (2016) who investigated less ice-active minerals (plagioclase feldspars) and found that contamination from the cleaning process was not observed. Atkinson quartz (the same quartz sample as used by Atkinson et al. (2013)) and Fluka quartz were supplied as a powder, although Atkinson quartz was originally ground via the same milling process (Atkinson et al. 2013).



Figure 2.2: Pictures of the various quartz samples explored in this study showing their varying appearances and characteristics. Samples supplied in a milled state are not shown.

These samples were reground to ensure all samples initially had freshly exposed surfaces for ice nucleation experiments. The milling process was used to break down mineral crystals/powders to a sufficient size so that they may be suspended in water. We argue that these freshly milled samples are relevant in that they represent the fresh surfaces which are

likely produced by mechanical processes in nature as rocks are broken down and particles aerosolised through the saltation process (see Figure 2.1 and discussion in the introduction). We therefore suggest that the results from these freshly ground samples of quartz represent an upper limit to the ice-nucleating ability of quartz in atmospheric mineral dust since ageing processes may reduce this activity.

The specific surface areas of the quartz samples were measured using the Brunauer-Emmett-Teller (BET) N₂ adsorption method with a Micromeritics TriStar 3000 instrument (Table 1). Heating of the sample overnight at 100 °C was performed under a steady flow of dry nitrogen to evaporate any moisture in the sample before the surface area measurement. After BET analysis, 1 wt% suspensions for all the samples were prepared gravimetrically by suspending a known amount of material in purified water (18.2 MΩ cm at 25 °C) in a 10 mL glass vial. As quartz is a hard mineral the use of magnetic stirrer bars was avoided when suspending the material as preliminary experiments showed the potential for the Teflon coating to abrade off the stirrer bars and become mixed with the suspension. We also chose not to use glass stirrer bars, partly because glass is softer than quartz and partly because we have noted in the past that it can be a source of contamination. Therefore particles were suspended by vortexing for 5 min prior to ice nucleation experiments. Only small amounts of sample were available for Mexico quartz and Uruguay amethyst and so the powder used for BET analysis was then used to prepare the suspensions for ice nucleation experiments. The BET analysis and subsequent suspension in water was carried out within a week of grinding the sample.

2.3.2 Ice nucleation experiments

The microlitre Nucleation by Immersed Particle Instrument (μL-NIPI) was employed to test the ice-nucleating ability of the various quartz samples in the immersion mode (Whale et al., 2015). This technique has been used in several previous ice nucleation studies e.g. (Atkinson et al., 2013; O'Sullivan et al., 2014; Harrison et al., 2016). In brief, 1 μL droplets of a suspension were pipetted onto a hydrophobic glass cover slip atop a cold plate (EF600, Asymptote, UK). During pipetting, the suspension was vigorously shaken manually every 10 droplets (with roughly 40 droplets per experiment) to keep the quartz particles suspended and to ensure that the amount of mineral in each droplet was similar. The cold plate and glass slide were then enclosed within a Perspex chamber and a digital camera was used to image the droplets. The temperature of the cold plate was decreased at a rate of 5 °C min⁻¹ to 0 °C (from room

temperature), then at $1\text{ }^{\circ}\text{C min}^{-1}$ until all the droplets were frozen. Whilst cooling the system, a gentle flow of zero-grade dry nitrogen ($<0.2\text{ L min}^{-1}$) was passed across the cold plate to reduce condensation onto the glass slide, which can cause interference between freezing droplets and the surrounding unfrozen droplets (Whale et al., 2015). As the droplets were cooled, images were recorded with the digital camera and freezing events identified in post analysis to calculate the fraction of droplets frozen as a function of temperature $\pm 0.4\text{ }^{\circ}\text{C}$. A second run for each sample suspension, with a fresh array of droplets, was performed immediately after the first experiment with approximately 1 hour between the two runs. Prior to the start of each experimental day droplets of pure water (no dust) were used to determine the background freezing signal. Umo et al. (2015) compiled a large collection of background freezing results to create a fit which represents the variability of the background in the $\mu\text{L-NIPI}$ instrument. The background signal measured in this study was in line with the lower bound set by Umo et al. (2015).

We assume that nucleation on quartz occurs at specific active sites, as supported by the work of Holden et al. (2019) who showed that nucleation occurs preferentially at specific sites on α -quartz and feldspar using high-speed cryomicroscopy of ice crystal growth on thin sections of mineral. The cumulative ice-nucleating active site density $n_s(T)$, on cooling from $0\text{ }^{\circ}\text{C}$ to a temperature, T , was determined for each quartz sample. Standardising the active site density to the surface area of nucleant allows for comparison of the ice-nucleating ability of different materials (Connolly et al., 2009;Vali et al., 2015). It should be noted that this model neglects the time dependence of nucleation, which can have some influence on the nucleation temperature (Herbert et al., 2014;Holden et al., 2019). $n_s(T)$ is calculated using:

$$\frac{n(T)}{N} = 1 - \exp(-n_s(T)A), \quad (1)$$

where $n(T)$ is the cumulative number of frozen droplets on cooling to temperature T , N is the total number of droplets in the experiment. A is the surface area of nucleant per droplet calculated based on the mass of quartz per droplet (assumed to be the same as in the bulk suspension) and the specific surface area determined via BET analysis.

We conducted Monte Carlo simulations to estimate the error in $n_s(T)$ as a result of the randomness of the distribution of active sites in the droplet freezing experiments. These simulations consider the possible distribution of active sites throughout the droplets that

explain each fraction frozen and quantify this uncertainty, which is then combined with the uncertainty in the pipetting and BET measurements. This methodology was based on the work of Wright and Petters (2013).

2.4 Results and discussion

2.4.1 The variable ice-nucleating ability of α -quartz

The cumulative fraction of droplets frozen ($n(T)/N$) on cooling is shown in Fig. 2.3a for arrays of droplets containing the quartz samples. Comparison of these curves with the fraction frozen curves for droplets without added particles in the $\mu\text{L-NIPI}$ system (Umo et al., 2015), shows that all quartz samples heterogeneously nucleate ice since the freezing temperatures for droplets containing quartz are always much higher than the pure water droplets. These fraction frozen curves are then translated into $n_s(T)$ in Fig. 2.3b-c. In Fig. 2.3b we show n_s for freshly prepared samples where the particles were suspended in water for ~ 10 minutes before carrying out an experiment. The variability in the ice-nucleating ability of these α -quartz samples is striking. Bombay chalcedony and Atkinson quartz are substantially more active than the other samples with the activity spanning roughly 10°C at $n_s(T) = 10\text{ cm}^{-2}$. While the overall spread is large, it is also notable that the droplet freezing temperatures of 8 out of 10 of the samples fall between -17°C and -20°C at $n_s(T) = 10\text{ cm}^{-2}$.

In Fig. 2.3c we show n_s for both the first (fresh) run and a subsequent run performed approximately one hour after the first experiment for each quartz sample. In the cases of Bombay chalcedony, Brazil amethyst and Smoky quartz, the first and second runs were identical within the uncertainties, whereas in the other cases there was a systematic decrease in freezing temperature. For example, the temperature at which Atkinson quartz had an $n_s(T)$ of 1 cm^{-2} decreased by $\sim 3^\circ\text{C}$ between the first experiment and the second experiment run. In the past, using this technique with mineral particles of a similar grain size has mostly resulted in consistent results from run-to-run (e.g. Atkinson et al., 2013; Whale et al., 2015). This suggests that the decrease in activity seen for some quartz samples is a real change in the activity of the quartz rather than artefacts such as, for example, the settling of particles out of suspension leading to less surface area in each droplet. The finding that the activity of many of the α -quartz samples decrease with time spent in water is perhaps surprising given quartz is typically regarded as an inert material. We come back to this issue of ageing of active sites in water and air in section 2.4.2 where we describe a dedicated set of experiments to explore this topic.

The Bombay chalcedony sample stands out as being one of the most active quartz samples. For $n_s = 1 \text{ cm}^{-2}$ the Bombay chalcedony nucleates ice at $-9 \text{ }^\circ\text{C}$ which is comparable to K-feldspar (see section 2.5.1 for a comparison with other minerals). As described in section 2.2, chalcedony is a microcrystalline form of α -quartz and commonly has micropores. It is possible that these micropores contain ice nucleation active sites or create zones of weakness which allow defects to be created when ground. In order to test if the superior ice-nucleating ability of Bombay chalcedony is inherent to chalcedony, we located, characterised and tested a second chalcedony sample. Grape chalcedony has a similar microcrystalline form to Bombay chalcedony, but behaves more like the other quartz samples we have tested, both in having a lower ice-nucleating activity, but also in the decrease in its activity with time spent in water. One possibility is that the Bombay chalcedony sample is contaminated with another very active ice-nucleating component. The X-ray diffraction results suggest that there is not enough inorganic crystalline material, for example K-feldspar, to account for the result. In addition, we washed a $\sim 2 \text{ g}$ sample of unground Bombay chalcedony in 10 mL pure water (shaking vigorously for ~ 2 minutes) and tested the water. A droplet freezing assay with this washing water indicated that there was no significant detachable contamination. This suggests that the ice-nucleating activity of the Bombay chalcedony is inherent to the material rather than associated with an impurity, although the presence of an ice-nucleating impurity cannot be categorically excluded. These results suggests that a subtle difference between the two chalcedony samples causes the Bombay chalcedony to be much more active.

The second most active quartz sample, fresh Atkinson quartz, does not have any obvious differences with the other less active quartz samples which might explain its activity. It is almost entirely pure α -quartz with only a minor component of calcite (0.2%). It is unlikely that the calcite component is responsible for nucleation since Uruguay amethyst contains the same percent impurity of calcite and is much less ice active.

Overall, the results in Fig. 2.3 show a surprising diversity in ice nucleation behaviour. As mentioned above, quartz is a relatively uniform material which is chemically and physically stable, hence we might have expected its ice-nucleating ability to be uniform and insensitive to ageing processes (in fact, this was our original hypothesis when we started this project). However, the results clearly demonstrate neither of these expectations is correct. Since all these quartz samples are α -quartz we might have expected all of these quartz samples to exhibit

similar nucleating properties. This variability indicates that these quartz samples do not nucleate through a lattice matching mechanism. This is consistent with the recent observation that nucleation on quartz occurs at active sites (Holden et al., 2019). Our results suggest that these active sites have diverse properties, with different activities, different site densities and some being sensitive to ageing processes where others are not. In the next section we present a set of experiments designed to further probe the ageing of the ice nucleation sites on quartz samples.

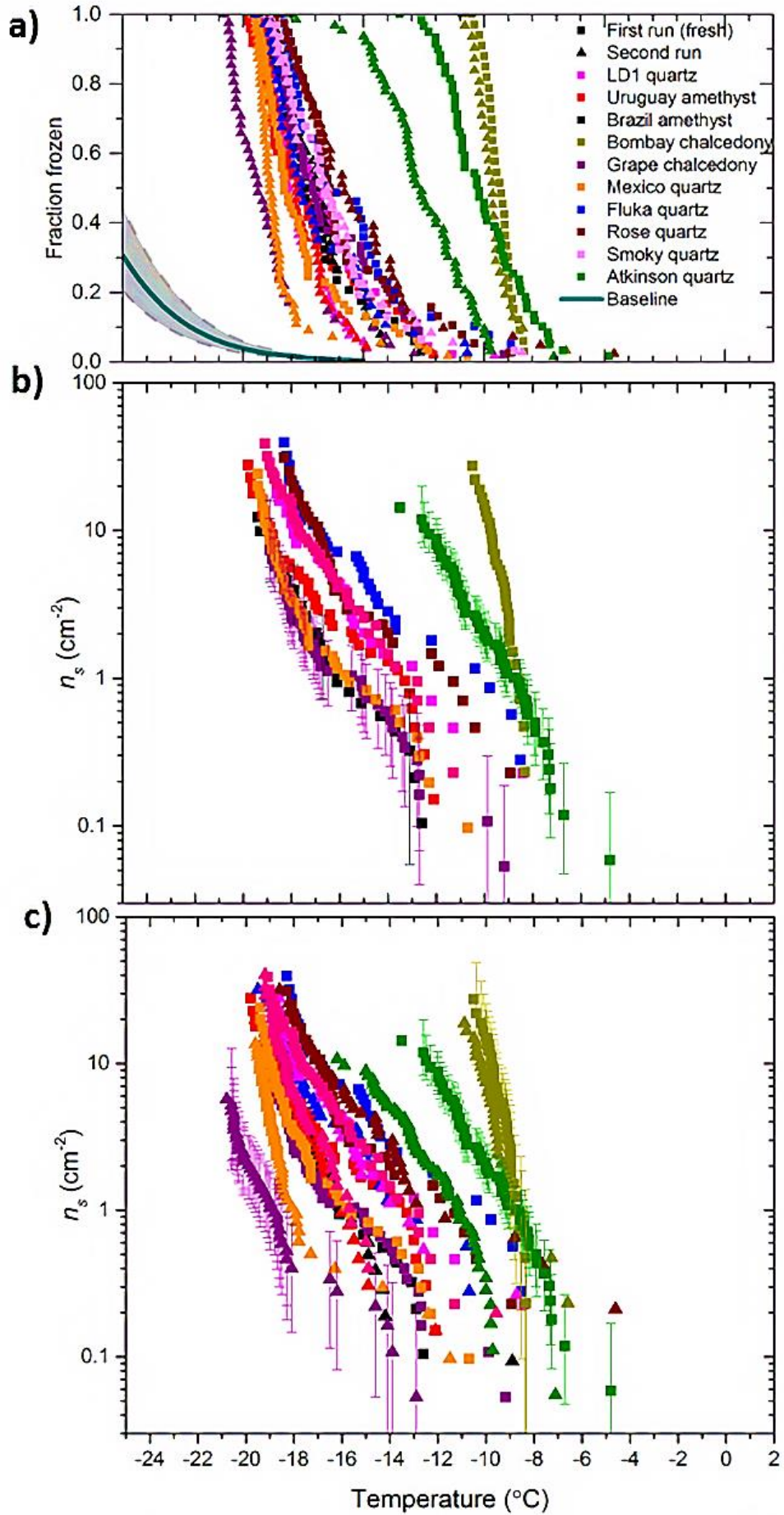


Figure 2.3: Fraction frozen and active site densities for ten quartz suspensions (1 wt%).
a) The fraction frozen versus temperature for the different quartz samples investigated in this study. The range of freezing for the baseline is highlighted in the grey shaded region (Umo et al., 2015). (b) The active site density (n_s) for the range of quartz samples in this study. In this plot only the first run of each sample is displayed. These samples are considered to be fresh as they have only spent roughly 10 minutes in suspension. (c) The active site density (n_s) versus temperature for the quartz samples on their initial runs and their corresponding second runs. The second runs were carried out roughly an hour after the first run. A sample of the error bars are shown in Fig. 2.3b/c.

2.4.2 The sensitivity of ice-nucleating activity with time spent in water and air

The results presented in Fig. 2.3 clearly indicate that the activity of many of the samples of quartz decreases by several degrees within an hour (Fig. 2.3b). In initial experiments we also showed that the quartz powder used by Atkinson et al. (2013) had lost its activity since it was initially tested. The sample had been stored in air within a sealed glass vial under dark conditions for ~5 years. However, milling of the powder dramatically increased its activity, which suggests that milling can (re)expose surfaces with the most effective active sites. This observation is similar to that described by Zolles et al. (2015) who noted that two out of three quartz samples increased in activity by up to 5 °C on milling. This supports the hypothesis that fresh surfaces are often key to maximising a quartz sample's ice-nucleating ability. Very recently, Kumar et al. (2018) have also observed that milling quartz increases its ice nucleation activity and suggest that this may be a result of defects created during the process.

In order to further explore the stability of active sites we tested how the activity of three samples of quartz varied when exposed for a range of times to water and air. For this investigation we tested: i) Smoky quartz, as it is a representative quartz in terms of its ice-nucleating ability, lying within the middle of the spread of $n_s(T)$; ii) Bombay chalcedony, as it was the most active sample and iii) Atkinson quartz, since initial experiments indicated it was highly sensitive to ageing in both water and air. The dry powder and suspension samples were stored at room

temperature in a dark cupboard in sealed glass vials. Prior to the droplet freezing experiment, wet samples were agitated to re-suspend the particles and the dry powders were added to water in the standard manner described above. The $n_s(T)$ of the various quartz samples aged in both water and in air for varying times are displayed in Fig. 2.4.

Each of the three samples responded in a distinct manner to time spent in water. Inspection of Fig. 2.4 (a, c and e) reveals that while the ice-nucleating ability of Smoky quartz did not significantly decrease after ~1 h, its activity decreased by about 3 °C after four months in water which is well outside the uncertainties of the experiment. Bombay chalcedony was far more stable in water, with no substantial change in the $n_s(T)$ curve after four months, being within 1 °C of the fresh sample (close to the uncertainties of the experiment). In contrast, the activity of Atkinson quartz decreased dramatically on exposure to water. Even after only ~1 hour in suspension the $n_s(T)$ curve decreased by 2 °C, but after 16 months in water the activity decreased by 12 °C. These results point to populations of very different active sites on these three different quartz samples.

We also found that the activity of some quartz samples decreased even when they were stored in air (Fig. 2.4b, d and e). Dry Smoky quartz and Bombay chalcedony powders were tested after being left in a glass vial for 20 months and showed no decrease in activity. In contrast the activity of Atkinson quartz decreased by ~5 °C in half of this time period (10 months). Fig. 2.4f also shows the initial freezing temperatures obtained using the same sample from the Atkinson *et al.* (2013) study which had been stored for ~5 years in a glass vial. This sample was ~10 °C less active compared to the freshly ground powder.

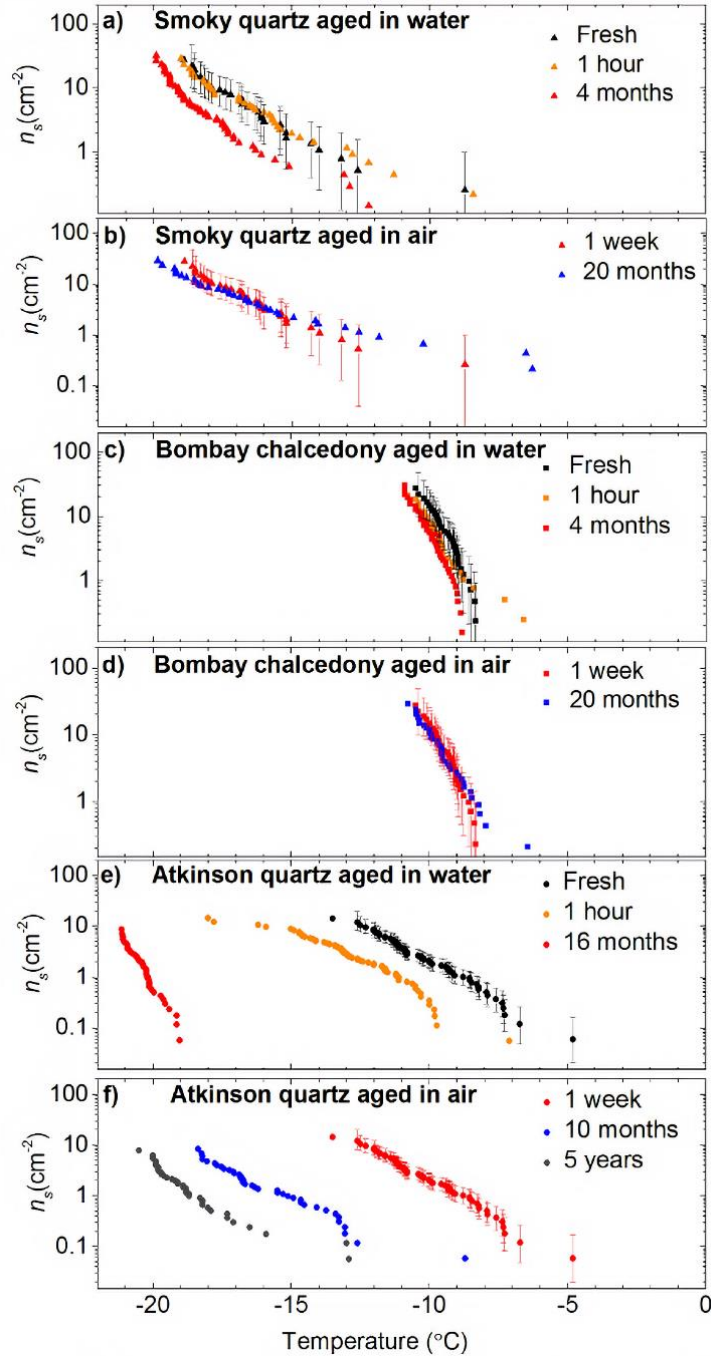


Figure 2.4: Plots showing the sensitivity of quartz activity, expressed as n_s , to time spent in water and air. Data are shown for (a and b) Smoky quartz, (c and d) Bombay chalcedony and (e and f) Atkinson quartz. Error bars for the first run of each time series are shown, but omitted for the other datasets for clarity. The n_s values for the fresh (~10 min) and one hour suspensions were taken from Fig. 2.3.

2.4.3 Discussion of the nature of active sites on quartz

These results paint a complex picture of the properties of the active sites on quartz samples. Not only is the absolute activity of the samples variable, but the sensitivity of the sites to time spent in water and air is also highly variable. The active sites of the Atkinson quartz are far more susceptible to ageing in water and air than both the Smoky quartz and Bombay Chalcedony. The sites on Bombay chalcedony are stable in both air and water, whereas those on Smoky quartz are somewhat intermediate in stability, being sensitive to water only after an extended period of time beyond 1 hour.

Very recently, Kumar et al. (2018) also described the deactivation of quartz in suspension over a period of five days. However, they noted that time series experiments carried out within glass vials showed deactivation of quartz in pure water whereas experiments within polypropylene falcon tubes did not. They suggested that silicic acid leached from the glass vial walls allows the quartz fragments to slowly grow and the active sites to be lost during the process. The explanation of Kumar et al. (2018) is consistent with our observation that the nucleating ability of many samples decreases with time spent in water. However, it is inconsistent with the stability of Bombay chalcedony and it cannot explain the loss of activity seen for Atkinson quartz when aged in air.

The physical and chemical characteristics which lead to the large variability in the properties of the ice nucleation sites on quartz are challenging to define. Classical nucleation theory suggests that ice critical clusters at the nucleation temperatures observed in this study are likely to be on the order of several nanometres across (Pummer et al., 2015). It therefore seems reasonable to think that the relevant ice nucleation sites will be on a similar scale but the nature of these sites remains unclear. A molecular dynamics study by Pedevilla et al. (2017) suggested that surfaces with strong substrate-water interaction and high densities of OH groups (or other H-bonding groups) give rise to effective sites for ice nucleation. However, sites with high densities of surface OH groups are also inherently thermodynamically unstable and will have a tendency to either react with, for example, moisture in air, or rearrange to a more stable configuration. Hence, it may be at defects in the crystal structure where such sites become stabilised when the thermodynamic cost of having a nanoscale region with a high density of

H-bonding groups is outweighed by the gain from relaxing strain in a structure. For example, in K-feldspar, it has been suggested that active sites are related to strain induced by exsolution into K and Na rich regions, which is known to result in an array of nanoscale topographical features (Whale et al., 2017). Consistent with this idea, Kiselev et al. (2016) reported that nucleation on K-feldspar was related to exposed patches of the high energy surface plane (100) and Holden et al. (2019) demonstrated that nucleation on K-feldspar always occurs within micrometre scale surface imperfections. Holden et al. (2019) reports that topographic features were observed on quartz, at some of the nucleation sites, but they have not been further characterised.

Larger nanoscale patches of surface H-bonding groups should be better at nucleating ice, but these larger high energy patches will also be less energetically stable. Hence, one might expect that the sites responsible for nucleation at the highest temperatures would also be the least stable and most sensitive to time spent in water or air. But, this does not hold for Bombay chalcedony which is the most active quartz we studied and also the most insensitive to exposure to water and air (Fig. 2.4). This indicates that the sites in this case are either of a completely different chemistry (perhaps a different high energy crystal plane), or the topography and strain associated with a defect imparts a greater stability on these sites. The fact that Bombay chalcedony is distinct from the bulk of the samples in being a microcrystalline quartz may be related to this, however, Grape chalcedony also has a similar morphology and does not possess the population of very active sites.

The increased ice nucleation associated with milling may be caused by the mechanical fracturing of the quartz leading to exposure of high energy but unstable sites, which decay away through a structural rearrangement process when exposed to air or liquid water. Alternatively, milling may simply result in the removal of reaction products to leave exposed active sites. Kumar et al. (2018) suggest the milling process causes the breakage of Si-O bonds which act as high energy sites for ice nucleation. Quartz does not exhibit a preferential plane of weakness (cleavage) to break along and it therefore fractures. The presence of small impurities distributed throughout the lattice, as described in sections 2.2 and 2.3, may influence the nature of fracturing and hence create differing defects and high energy sites. Gallagher (1987) classified impurities as a form of structural weakness. The impurities can create zones of weakness and stress within the crystal structure and therefore act as a pathway of least resistance resulting in

the breakage of bonds and development of microtexture. Alternatively, in some instances the impurities may create areas of greater strength and so fracturing occurs around these zones. Hence, it is possible that the presence of impurities influences the way in which individual quartz samples fracture and therefore influence the presence of active sites.

Inherently, quartz is rather simple in terms of naturally occurring defects compared to other minerals, such as feldspar. In fact, in the past quartz has been considered to be in the ‘perfect crystal class’, i.e. lacking imperfections. However, quartz does have defects, albeit at a lower density than other minerals (Spencer and Smith (1966)). Quartz minerals can be subject to varying conditions and stresses after their formation and so the geological history of the quartz may also influence the degree of microtexture. For example, a quartz sample which has undergone stress at a fault boundary is more likely to exhibit microtextural features than one that has not (Mahaney et al., 2004). It may be these microtextural differences that lead to the observed variability in ice-nucleating ability. This hypothesis might be tested in the future if quartz samples could be obtained with well characterised geological histories.

It has also been observed in the past that, for other minerals, the specifics of the mineral formation mechanism are critical for determining its ice-nucleating ability. Whale et al. (2017) demonstrated that a sample of K-feldspar, which had cooled sufficiently quickly during its formation that it did not undergo exsolution and therefore lacked the associated microtextures, had very poor ice nucleation properties. This was in contrast to the more common K-feldspars which do have exsolution microtexture and nucleate ice very effectively. Despite having very different ice-nucleating properties, their crystal structures and compositions are very similar. A similar formation pathway dependence may be true for quartz, such as strain introduced in geological fault systems. But one thing is clear: while bulk mineralogy is a guide to ice-nucleating activity, in some cases details of the formation pathway may be more important.

2.5 The importance of quartz relative to feldspar for ice nucleation in the atmosphere

2.5.1 Comparison to the literature data for quartz and feldspar

The data from the present study are contrasted with literature active site density data for quartz (Zolles et al., 2015; Atkinson et al., 2013; Losey et al., 2018) in Fig. 2.5. This data is also compared with $n_s(T)$ parameterisations for desert dust samples (Niemand et al., 2012; Ullrich et al., 2017) and K-feldspar (Atkinson et al., 2013). The variability within the α -quartz samples

that we report is also reflected in the literature data for quartz. It is striking that two of the quartz samples in this study, Bombay chalcedony and Atkinson quartz, have an activity approaching or equal to K-feldspar. Nevertheless, it is apparent that quartz is never substantially more active than K-feldspar or desert dust in terms of $n_s(T)$.

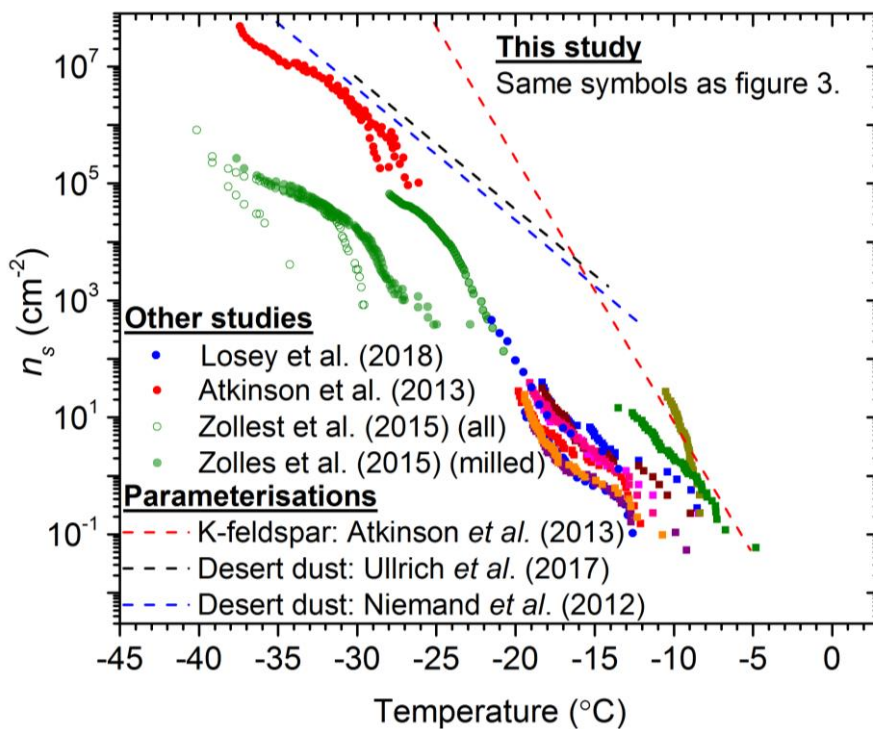
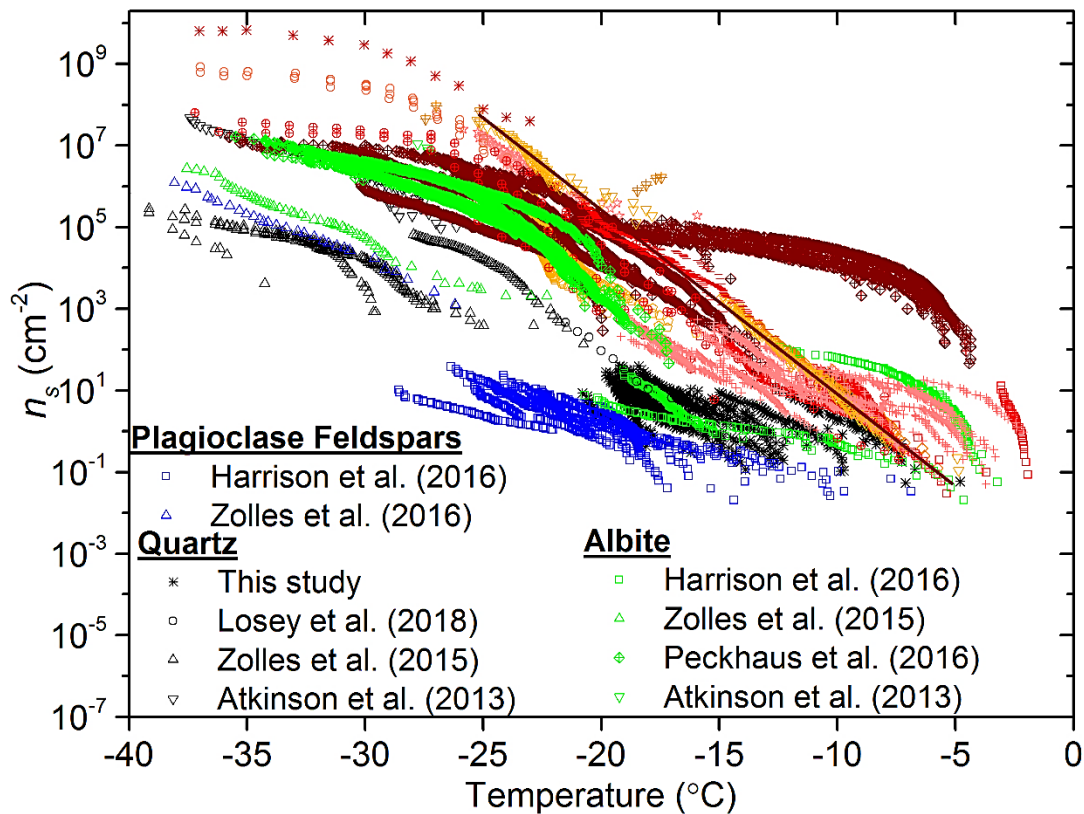


Figure 2.5: Plot of n_s versus temperature for the available literature data for quartz compared to the data collected in this study. The symbols for this study’s data are displayed the same as in Fig. 2.2 and only the first runs (fresh samples) from this study are plotted. The data from Zolles et al. (2015) has been split into quartz samples which were milled for fresh surfaces and all the combined data (both milled and un-milled quartz).

Since one of our objectives is to determine how effective quartz is at nucleating ice in comparison to feldspars, we contrast the literature active site density data for feldspars and

quartz in Fig. 2.6. The feldspars have been colour coded into the plagioclase (blue), albite (green) and the K-feldspar (orange-reds) groups. We note that, by convention, albite is considered part of the plagioclase solid solution series. However, Harrison et al. (2016) demonstrated that albites had a distinct nucleating activity and therefore we plot them here as a separate group. The K-feldspars presented here represent the K-rich samples from the alkali feldspar group (i.e. >10 % K). Overall, there is a general trend in that plagioclase feldspars are the least active of the four mineral groups and K-feldspar is the most active. Both albite and quartz show similar, intermediate, activities. K-feldspars from Whale et al. (2017) which did not exhibit the common phase separation were excluded from this plot as they are unrepresentative of common K-feldspars and are rare in nature. Although quartz is an ice active mineral, Fig. 2.6 supports the consensus that it is the K-feldspars that are the most active mineral for ice nucleation that is commonly found in mineral dusts in the atmosphere.



K-feldspars

- Harrison et al. (2016)
- △ Zolles et al. (2015)
- ◇ Whale et al. (2015)
- Tarn et al. (2018)
- ◇ Peckhaus et al. (2016)
- Demott et al. (2018)
- + Whale et al. (2017)
- Reicher et al. (2018)
- ☆ O'Sullivan et al. (2014)
- Niedermeier et al. (2015)
- * Augustin-Bauditz et al. (2014)
- Atkinson et al. (2013)
- ▽ Atkinson et al. (2013)
- ◇ Emersic et al. (2015)

Figure 2.6: Plot of n_s versus temperature for quartz and feldspar literature data, together with the quartz data from this study.

2.5.2 New parameterisations for the ice-nucleating activity of quartz, K-feldspar, plagioclase and albite

In order to be able to determine which mineral is most important in the atmosphere we need the activity of each mineral (expressed as $n_s(T)$) in combination with estimates of the abundance of each mineral in the atmosphere. In this section we produce new $n_s(T)$ parameterisations for quartz, K-feldspar, plagioclase and albite using data from the present study in addition to literature data.

The new set of parameterisations are shown in Fig. 2.7. In order to derive these parameterisations we compiled data for representative samples of quartz, K-feldspar, plagioclase and albite. To create these parameterisations we binned the data within each dataset into 1 °C intervals and then fitted a polynomial line through the log averages of the data. We binned the data in an attempt to remove bias towards datasets with relatively high data density. In addition, we only applied a fit in the temperature range where multiple datasets were present (with the exception of plagioclase, where the available data is so sparse in some temperature regimes that we had to relax this criterion in order to produce a parameterisation). We used polynomial fits to represent the data since the data is quite complex and alternatives such as a straight line would produce a very poor representation of the data. These fits were constrained at the warmest and coldest temperatures in order to obtain a reasonable representation of the data at these limits. We stress that these fits must not be extrapolated to higher and lower temperatures. The standard deviation for each parameterisation was calculated by taking the average of the standard deviations of the log $n_s(T)$ values for each 1 °C temperature interval. The corresponding value was then used to approximate the standard deviation from each fit, which is represented by the dashed lines and shaded area in Fig. 2.7.

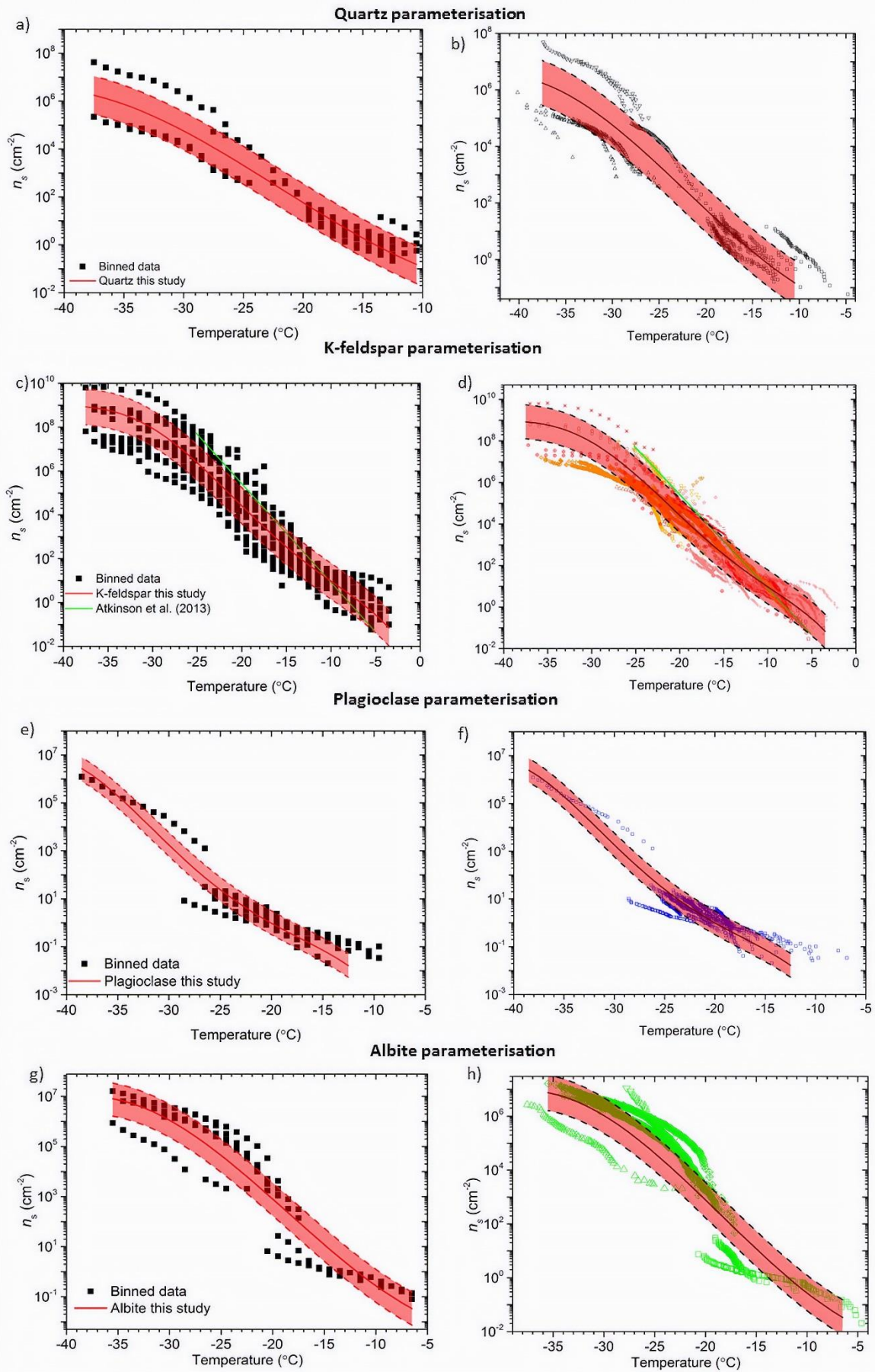


Figure 2.7: Parameterizations developed for various silicate minerals. Panels (a), (c), (g) and (e) show the temperature-binned n_s data used to derive the parameterizations. Panels (b),(d), (f), and (g) show the new parameterizations plotted with the original non-binned data. The standard deviation is highlighted in the red-shaded area for each parameterization. The green line in panel (d) indicates the K-feldspar parameterization from Atkinson et al. (2013). See Fig. 2.6 for the sources of the raw data. The new parameterizations (validity T ranges and standard deviation for $\log(n_s(T))$), where n_s is in units of cm^{-2} , are as follows. Quartz: $\log(n_s(T)) = -1.709 + (2.66 \times 10^{-4}T^3) + (1.75 \times 10^{-2}T^2) + (7 \times 10^{-2}T)$, (-10.5 to -37.5 °C; 0.8); K-feldspar: $\log(n_s(T)) = -3.25 + (-0.793T) + (-6.91 \times 10^{-2}T^2) + (-4.17 \times 10^{-3}T^3) + (-1.05 \times 10^{-4}T^4) + (-9.08 \times 10^{-7}T^5)$, (-3.5 to -37.5 °C; 0.8); plagioclase feldspar: $\log(n_s(T)) = (-3.24 \times 10^{-5}T^4) + (-3.17 \times 10^{-3}T^3) + (-0.106T^2) + (-1.71T) - 12$, (-12.5 to -38.5 °C; 0.5); albite: $\log(n_s(T)) = (3.41 \times 10^{-4}T^3) + (1.89 \times 10^{-2}T^2) + (-1.79 \times 10^{-2}T) - 2.29$, (-6.5 to -35.5 °C; 0.7)

For the quartz fit, the chalcedony samples were excluded given these microcrystalline minerals are unrepresentative of most quartz in nature and that they are therefore likely to be in negligible abundances in the atmosphere. We also only include the runs with freshly made quartz suspensions in the parameterisation since the second runs often showed signs of deactivation in suspension. By only using the relatively fresh suspension data, our parameterisation is representative of freshly milled quartz dust. The new parameterisation can be seen in Fig. 2.7a-b and covers a temperature range of -10.5 °C to -37.5 °C and nine orders of magnitude in $n_s(T)$. This is the first robust $n_s(T)$ parameterisation developed for this mineral that can be used to determine its role as an INP in the atmosphere.

The K-feldspar parameterisation developed by Atkinson et al. (2013) has been used extensively within the ice nucleation community. However, this parameterisation was created with data from one K-feldspar sample and does not reflect the variability we now know to exist. The parameterisation developed as part of this study can be seen in Fig. 2.7c-d. We excluded K-feldspar samples which did not exhibit phase separation from the Whale et al. (2017) study from this parameterisation as these types of alkali feldspar are rare and unlikely to be found in significant quantities in the atmosphere. The data included in these plots includes all three polymorphs of K-feldspar (microcline, orthoclase and sanidine), although most of the data is

for microcline. The strongly hyperactive TUD #3, examined by Harrison et al. (2016) and Peckhaus et al. (2016), was excluded as it exhibited extremely high activity and appears to be an exceptional case which is generally unrepresentative of the K-feldspar group of minerals. With this in mind we have developed a parameterisation which represents K-feldspars that possess exsolution microtexture. It should be noted that all of the studies used BET derived surface areas for the calculation of $n_s(T)$ other than DeMott et al. (2018) and Augustin-Bauditz *et al.* (2014) who used geometric surface areas. However, while the difference between BET and geometric surface areas is substantial for clay samples (Hiranuma et al., 2015), the discrepancy is much smaller for materials with larger grain sizes like feldspar (Atkinson et al. 2013). When the new K-feldspar parameterisation is compared to the literature data (Fig. 2.7d) it represents the variability of K-feldspar, as well as the curvature in the datasets. In particular, the new parameterisation captures the observed plateau in $n_s(T)$ below about $-30\text{ }^\circ\text{C}$. In addition, the new parameterisation produces higher $n_s(T)$ values at temperatures warmer than $-10\text{ }^\circ\text{C}$ relative to that of Atkinson et al. (2013). Below $-10\text{ }^\circ\text{C}$ this new parameterisation gives lower values of $n_s(T)$. The temperature range of the parameterisation is also extended, covering $-3.5\text{ }^\circ\text{C}$ to $-37.5\text{ }^\circ\text{C}$.

The parameterisation proposed here to represent plagioclase feldspar is shown in Fig. 2.7e-f. The parameterisation spans a temperature range of $-12.5\text{ }^\circ\text{C}$ to $-38.5\text{ }^\circ\text{C}$. Only one dataset was available to represent the plagioclase feldspars in the lowest temperature regime (Zolles et al., 2015), hence this parameterisation needs to be used cautiously, but it is nonetheless a best estimate at present given the current data available. A similar caution must be accepted when using the albite parameterisation displayed in Fig. 2.7g-h which spans a range of $-6.5\text{ }^\circ\text{C}$ to $-35.5\text{ }^\circ\text{C}$. For the albite parameterisation, the hyperactive Amelia albite from the Harrison et al. (2016) study was excluded due to its exceptional ice-nucleating ability making it unrepresentative of the other five albite samples. Hence, this parameterisation is representative of the non-hyperactive albites.

The parameterisations are summarised in Fig. 2.8a and are then combined with a typical abundance of each mineral to estimate the INP concentration ($[\text{INP}]_T$) associated with each of the four minerals in Fig. 2.8b. On average, roughly $3\pm 6\%$ (by mass) of atmospheric transported mineral dust particles are K-feldspar whereas $16\pm 15\%$ are quartz and $8\pm 3\%$ are plagioclase (see compilations of measurements in (Atkinson et al., 2013), which are consistent

with more recent measurements (Boose et al., 2016b)). Albite is often grouped with plagioclase feldspars when determining the mineralogy of atmospheric mineral dusts rather than being reported on its own. For the purposes of this estimate we have assumed that albite has a concentration equal to 10 % of that of plagioclase. $[\text{INP}]_T$ was derived from the $n_s(T)$ parameterisations assuming a surface area concentration of mineral dust of $50 \mu\text{m}^2 \text{cm}^{-3}$ (a moderately dusty environment) and assuming that the mass fraction of each mineral is equivalent to its surface area fraction. In order to approximate the size distribution of dust, a lognormal size distribution centred around particles of $1 \mu\text{m}$ in diameter with a standard deviation of $0.3 \mu\text{m}$ was used. We have also assumed that each mineral is externally mixed (see Atkinson et al. (2013) for details of how to treat the mixing state of mineral dust), which is the assumption that has been made when modelling the global distribution of INPs in the past (Atkinson et al., 2013 and Vergara-Temprado et al., 2017). In reality, desert dust aerosol will be somewhat internally mixed. The opposing assumption of full internal mixing produces 1-2 orders more INP at the lowest temperatures, but produces the same INP concentration above about -25°C (Atkinson et al. 2013). The upper and lower bounds for each line in Fig. 2.8b are derived from the range of mineral mass concentrations.

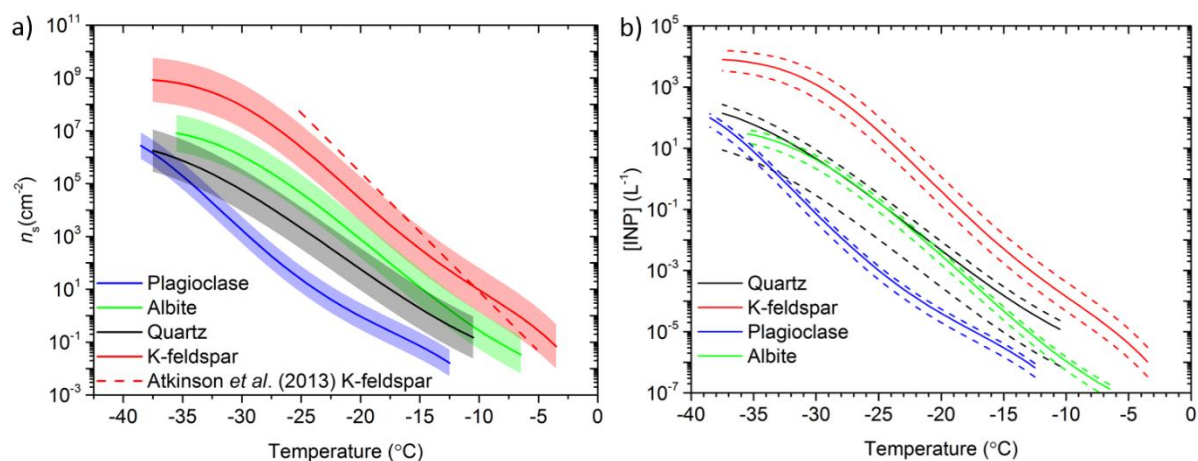


Figure 2.8: Comparison of the newly developed parameterisations. (a) n_s versus temperature for the four newly created parameterisations from this study and the K-feldspar parameterisation proposed by Atkinson et al. (2013). The standard deviation of

each parameterisation is shown by the shaded regions. (b) INP per litre predictions using the quartz, K-feldspar, albite and plagioclase parameterisations. The solid lines represent the predicted INP concentration associated with the average mineral proportion and the dashed lines represent the upper and lower proportions based on the variability of mineral proportions of atmospheric desert dust (see section 2.5.2 for details). An aerosol surface area concentration of $50 \mu\text{m}^2 \text{cm}^{-3}$ and an external mixing assumption were used.

The $[\text{INP}]_T$ curves in Fig. 2.8b confirm that, under most atmospheric situations, K-feldspar has the main contribution to the ice-nucleating particle population in desert dust. Quartz is the next most important mineral, with plagioclase the least important. The contribution of pure albite is rather uncertain given the amount of pure albite in desert dust is poorly constrained, but it is unlikely to compete with K-feldspar. Nevertheless, while K-feldspar is the most important contributor to the INP population, the estimates in Fig. 2.8b do suggest that quartz may make a non-negligible contribution to the INP budget at temperatures between about -20 and -12.5 °C. This is particularly so when we consider the variability in the ice-nucleating ability of the K-feldspar and quartz groups. However, it should also be considered that the estimated $[\text{INP}]_T$ curves in Fig. 2.8b are based on the assumption that quartz has the activity of fresh quartz. We know from the work presented above that the activity of quartz is sensitive to ageing processes. We cannot quantify ageing of atmospheric quartz, but the parameterisation we present here probably represents an upper limit to its activity. In contrast, the activity of K-feldspar does not decrease with time spent in water or air (Kumar et al., 2018; Harrison et al., 2016; Whale et al., 2017). Overall, we conclude that K-feldspar contributes the bulk of the INPs associated with desert dust, because it is more active and it is less sensitive to ageing processes. However, we should not rule out quartz making a significant contribution to the INP population in a minority of cases.

2.5.3 Testing the new parameterisations against literature laboratory and field measurements of the ice-nucleating ability of desert dust

We now test the quartz and K-feldspar parameterisations to see if they are consistent with literature data of the ice-nucleating ability of desert dust (Fig. 2.9). In Fig. 2.9a we contrast the predicted $n_s(T)$ values, based on the quartz and K-feldspar parameterisations, against a variety

of literature datasets for desert dust. For the K-feldspar based prediction, we have presented lines where 20 %, 1 % and 0.1 % of the surface area of dust is made up of K-feldspar. For the 20 % prediction, which is consistent with measurements in Cape Verde (Kandler et al., 2011), we have also shown the natural variability in K-feldspar activity as the shaded region. The line assuming quartz is the dominant ice-nucleating mineral in desert dust is for 12 % quartz which again is consistent with measurements made in Cape Verde (Kandler et al., 2011).

From Fig. 2.9a it is clear that quartz does not account for the $n_s(T)$ measurements of desert dusts sampled directly from the atmosphere and suspended in laboratory studies. However, the new K-feldspar parameterisation is consistent with the ice-nucleating activity of dusts over a wide range of temperatures. The K-feldspar parameterisation reasonably represents the majority of mineral dust measurements when taking into account that typically ~1 % to 25 % of atmospheric desert dust can be attributed to K-feldspar (Atkinson et al., 2013) and that there is a natural variability in the ice-nucleating ability of K-feldspar (as represented by the shaded area around the 20 % K-feldspar prediction). The shape of the parameterisation represents the bulk of the data well and plateaus at the lowest temperatures in agreement with the observations.

Fig. 2.9b shows INP concentrations measured from an aircraft in the eastern tropical Atlantic (Price et al., 2018) plotted with the predicted INP concentrations based on the K-feldspar parameterisation developed by Atkinson et al. (2013) (in black dashed lines), the parameterisation for desert dust by Niemand et al. (2012) (blue dashed lines) and the K-feldspar parameterisation proposed here (red solid lines). The parameterisations were calculated assuming an externally mixed scenario (although both internal and external mixing assumptions produce a similar result in the regime where the measurements were made). The upper and lower bounds were calculated by incorporating the maximum and minimum in the aerosol surface area concentrations corresponding to the various aircraft measurements ($23.8 \mu\text{m}^2 \text{cm}^{-3}$ to $1874 \mu\text{m}^2 \text{cm}^{-3}$) (Price et al, 2018). K-feldspar was assumed to represent 20 % of the aerosol surface area, based on measurements by Kandler et al. (2011). Note that the small number of data points above $\sim -11^\circ\text{C}$ have a very high uncertainty due to Poisson counting issues and should be regarded as upper limits. Price et al. (2018) and Sanchez-Marroquin et al. (2019) have described a sub-isokinetic sampling bias in the aircraft inlet which results in an enhancement of aerosol surface area by roughly a factor of 2.5 for the used sampling

conditions. We have therefore corrected the Price et al. (2018) data downwards by a factor of 2.5 (although on the log scale this makes a relatively small difference).

We can see that the Atkinson et al. (2013) parameterisation is a relatively poor predictor of the INP concentration, especially at temperatures colder than about $-15\text{ }^{\circ}\text{C}$. The parameterisation by Niemand et al. (2012) tends to over-predict INP concentrations relative to the Price et al. (2018) data by about one order of magnitude. The K-feldspar parameterisation proposed here better represents the magnitude, the range and the slope of the aircraft data. Overall, the new K-feldspar parameterisation provides a good representation of the ice-nucleating activity of dust from field and laboratory studies and further makes it clear that quartz is of second order importance for desert dust's ice-nucleating ability.

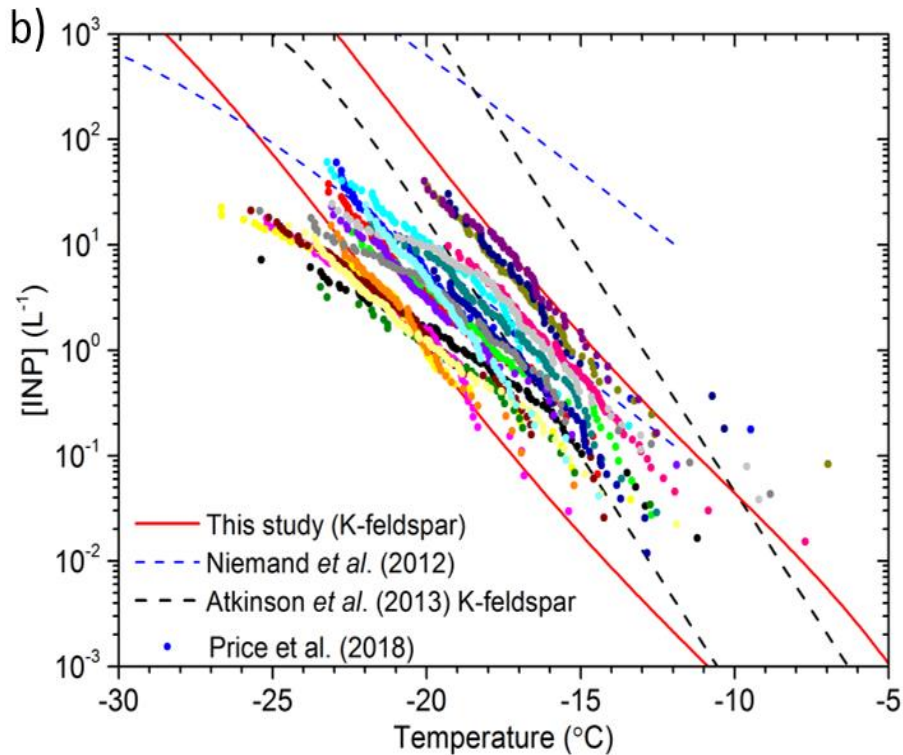
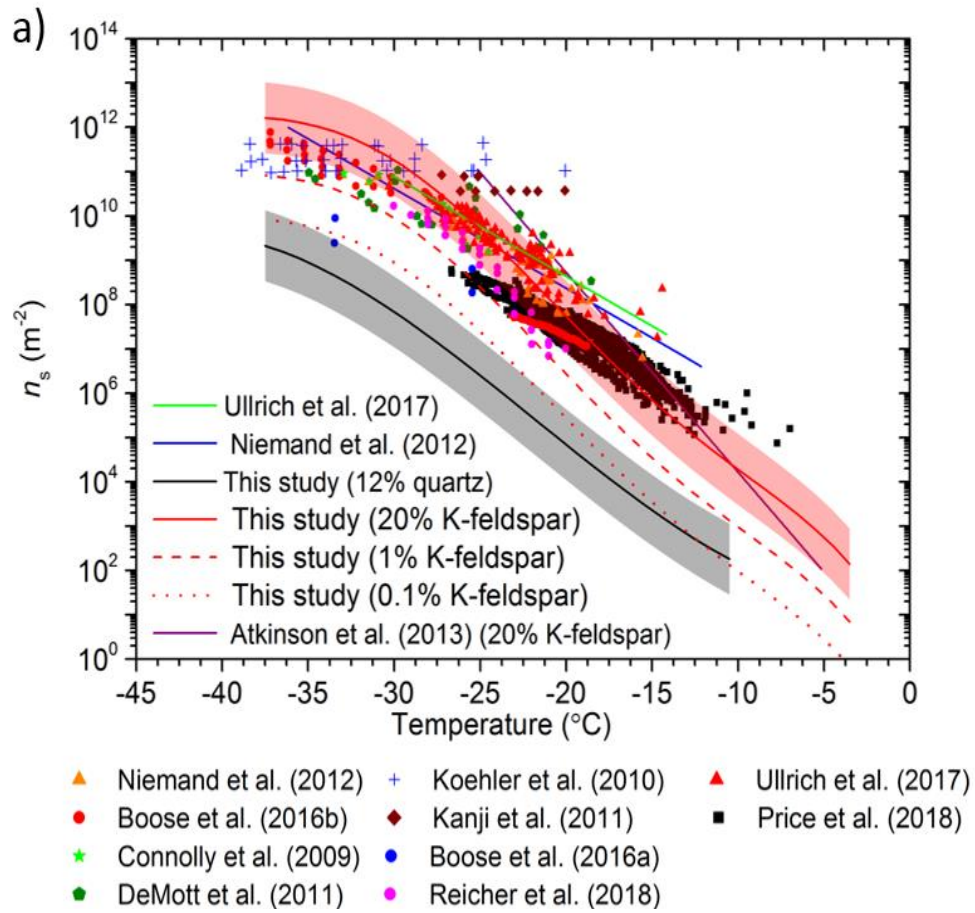


Figure 2.9: Testing the newly developed K-feldspar and quartz parameterisations against literature data for desert dust. a) Comparison of n_s versus temperature for mineral dust from laboratory and field studies against the K-feldspar and quartz parameterisations. The red lines are n_s values where 0.1, 1 and 20 % of the aerosol surface area is assumed to be K-feldspar. The standard deviation of the K-feldspar parameterisation from this study is represented as the shaded area around the 20 % K-feldspar prediction: this is to show the natural variability in mineral activity. The prediction for 12 % quartz is shown using a black line, with the natural mineral variability of freshly milled quartz highlighted by the shaded region. Literature data and parameterisations have been plotted from (Niemand et al., 2012;Boose et al., 2016b;Boose et al., 2016a;Connolly et al., 2009;DeMott et al., 2011;Koehler et al., 2010;Kanji et al., 2011;Reicher et al., 2018;Ullrich et al., 2017;Price et al., 2018). b) Comparison of the INP concentrations predicted by several parameterisations with the INP concentrations measured in the dusty eastern tropical Atlantic region by Price et al. (2018). The predictions were made assuming that 20% of the dust was K-feldspar, consistent with Kandler et al. (2011). For this calculation we assumed that the dust is externally mixed in terms of its mineralogy, although in this regime an internal versus external mixing state assumption makes very little difference (see Atkinson et al. (2013)). The upper and lower bounds of the predicted INP concentrations are based on the lowest and highest aerosol surface area concentrations corresponding to the INP data in Price et al. (2018). Note that the measured INP concentrations from Price et al. (2018) have been corrected downwards by a factor of 2.5 based on the work presented by Price et al. (2018) and Sanchez-Marroquin et al. (2019).

2.2 Conclusions

We have studied 10 quartz samples for their ice-nucleating ability in order to better understand and define the ice-activity of this abundant mineral. The chosen samples were all α -quartz, the most common silica polymorph found at the Earth's surface, but included a variety of α -quartz types with varying degrees of impurities and different crystal habits. We found that the ice-nucleating activity of these samples is surprisingly variable, spanning about 10 °C. Eight out

of ten of the quartz samples lay within $-17\text{ }^{\circ}\text{C}$ to $-20\text{ }^{\circ}\text{C}$ at $n_s(T) = 10\text{ cm}^{-2}$, with two quartz samples, Bombay chalcedony and Atkinson quartz, being much more active (as active as K-feldspar). Overall, the quartz group of minerals tends to be less active than the K-feldspars, slightly less active than albite, but more active than the plagioclase feldspars. In the future it would be interesting to probe the nature of the active sites on the two most active samples and to try to contrast these sites to those on the less active samples in order to further understand the nature of active sites and why they have such strongly contrasting characteristics.

Although quartz is regarded as a relatively chemically inert mineral the activity of some samples decreases with time spent in air and water. Most of the samples were sensitive to time spent in water, but interestingly, the most active sample's activity did not change significantly even after many months in water. We note that the sensitivity to time in water displayed by most of the quartz samples studied here is in strong contrast to K-feldspars, which tend to be much more stable. Related to this, we also note that solutes can alter the ice-nucleating ability of mineral samples (Whale et al., 2018; Kumar et al., 2018; Kumar et al., 2019a, b). Sensitivity to these ageing processes and solutes could be very important in determining the dominant INP types globally (Boose et al., 2019). Hence, we suggest further studies aim to build a better understanding of the relationship between the experimental observations and field collected samples to determine the role of ageing in the atmosphere.

To investigate the relative importance of quartz to feldspars in the atmosphere we have proposed new active site density parameterisations for quartz, K-feldspar, plagioclase and albite. These parameterisations are based on a combination of the data presented here for quartz along with data available in the literature. Sparse data sets available for the albite and plagioclase mineral groups lead to lower confidence when creating parameterisations for these mineral groups. It is suggested that future studies expand on the current datasets of the ice-nucleating behaviour of minerals to improve these parameterisations. When using the newly developed parameterisations to predict INP concentrations in combination with typical atmospheric abundances of minerals, it is found that K-feldspar typically produces more INP than milled quartz (or any other mineral). Also note that the parameterisation for quartz is for freshly milled quartz and the ageing results presented here and elsewhere (Zolles et al., 2015; Kumar et al., 2019a) suggest that the active sites on quartz are removed on exposure to air and water. Therefore the parameterisation for milled quartz should be regarded as an upper

limit. Even with this upper limit, quartz is of secondary importance relative to K-feldspars which appear to be less sensitive to ageing processes. In addition, we find that the newly developed K-feldspar parameterisation is consistent with $n_s(T)$ literature measurements on desert dusts and better represents field measurements of INP concentrations in the dusty tropical Atlantic compared to the parameterisations by Atkinson et al. (2013) and Niemand et al. (2012). We hereby propose the use of this new K-feldspar parameterisation when predicting INP concentrations related to mineral dusts.

Data availability. Data for the various quartz samples presented in this paper are available at <http://dx.doi.org/10.5285/171726739bb54d0ba84cdde15c5b17ae>, (Harrison et al., 2019).

Author contributions. ADH designed the experiments with help from scientific discussions with BJM, TFW and JBM. Both KL and ADH performed the experiments. AS completed the calculations for the external mixing assumption used in figures 2.8b and 2.9a and assisted in the calculation of errors for the active site density measurements. MAH carried out Raman analysis of the chalcedony samples and MDT helped in the assembly of the literature data. ADH prepared the manuscript with contributions from all co-authors.

Acknowledgements. We would like to take the opportunity to thank Lesley Neve for her contribution in the XRD analysis. The authors acknowledge the European Research Council (ERC, MarineIce: 648661), Engineering and Physical Sciences Research Council (EPSRC, EP/M003027/1) and the Natural Environment Research Council (NERC, NE/M010473/1) along with Asymptote Ltd. (now part of GE Healthcare) for funding this research.

References

- Ansmann, A., Tesche, M., Seifert, P., Althausen, D., Engelmann, R., Fruntke, J., Wandinger, U., Mattis, I., and Müller, D.: Evolution of the ice phase in tropical altocumulus: SAMUM lidar observations over Cape Verde, *J. Geophys. Res. Atmos.*, 114, D17208, 10.1029/2008jd011659, 2009.
- Applin, K. R., and Hicks, B. D.: Fibers of dumortierite in quartz, *Am. Mineral.*, 72, 170-172, 1987.

Atkinson, J. D., Murray, B. J., Woodhouse, M. T., Whale, T. F., Baustian, K. J., Carslaw, K. S., Dobbie, S., O'Sullivan, D., and Malkin, T. L.: The importance of feldspar for ice nucleation by mineral dust in mixed-phase clouds, *Nature*, 498, 355-358, 10.1038/nature12278, 2013.

Avila, A., Queralt-Mitjans, I., and Alarcón, M.: Mineralogical composition of African dust delivered by red rains over northeastern Spain, *J. Geophys. Res. Atmos.*, 102, 21977-21996, 10.1029/97jd00485, 1997.

Bagnold, R. A.: *The Physics of blown sand and desert dunes*, Dover publicationsm Inc., New York, 10-37, 1941.

Blatt, H., Middleton, G., and Murray, R.: *Origin of sedimentary rocks*, Prentice-Hall, Inc., New Jersey, 245-275, 1980.

Boose, Y., Sierau, B., Garcia, I. M., Rodriguez, S., Alastuey, A., Linke, C., Schnaiter, M., Kupiszewski, P., Kanji, Z. A., and Lohmann, U.: Ice nucleating particles in the Saharan Air Layer, *Atmos. Chem. Phys.*, 16, 9067-9087, <https://doi.org/10.5194/acp-16-9067-2016>, 2016a.

Boose, Y., Welti, A., Atkinson, J., Ramelli, F., Danielczok, A., Bingemer, H. G., Plötze, M., Sierau, B., Kanji, Z. A., and Lohmann, U.: Heterogeneous ice nucleation on dust particles sourced from nine deserts worldwide – Part 1: Immersion freezing, *Atmos. Chem. Phys.*, 16, 15075-15095, 10.5194/acp-16-15075-2016, 2016b.

Boose, Y., Baloh, P., Plötze, M., Ofner, J., Grothe, H., Sierau, B., Lohmann, U., and Kanji, Z. A.: Heterogeneous ice nucleation on dust particles sourced from nine deserts worldwide – Part 2: Deposition nucleation and condensation freezing, *Atmos. Chem. Phys.*, 19, 1059-1076, 10.5194/acp-19-1059-2019, 2019.

Broadley, S. L., Murray, B. J., Herbert, R. J., Atkinson, J. D., Dobbie, S., Malkin, T. L., Condliffe, E., and Neve, L.: Immersion mode heterogeneous ice nucleation by an illite rich powder representative of atmospheric mineral dust, *Atmos. Chem. Phys.*, 12, 287-307, 10.5194/acp-12-287-2012, 2012.

Caquineau, S., Gaudichet, A., Gomes, L., Magonthier, M.-C., and Chatenet, B.: Saharan dust: Clay ratio as a relevant tracer to assess the origin of soil-derived aerosols, *Geophys. Res. Lett.*, 25, 983-986, 10.1029/98gl00569, 1998.

Ceppi, P., Brient, F., Zelinka, M. D., and Hartmann, D. L.: Cloud feedback mechanisms and their representation in global climate models, *WIREs Cli. Change*, 8, doi: 10.1002/wcc.465, 1-21, 2017.

Connolly, P. J., Möhler, O., Field, P. R., Saathoff, H., Burgess, R., Choularton, T., and Gallagher, M.: Studies of heterogeneous freezing by three different desert dust samples, *Atmos. Chem. Phys.*, 9, 2805-2824, 10.5194/acp-9-2805-2009, 2009.

Deer, W. A., Howie, R. A., and Zussman, J.: An introduction to the rock forming minerals, Longman group limited, London, 340-355, 1966.

Deer, W. A., Howie, R. A., and Zussman, J.: An introduction to the rock forming minerals, 2nd ed., Addison Wesley Longman, Harlow, UK, 457-472, 1992.

DeMott, P. J., Möhler, O., Stetzer, O., Vali, G., Levin, Z., Petters, M. D., Murakami, M., Leisner, T., Bundke, U., Klein, H., Kanji, Z. A., Cotton, R., Jones, H., Benz, S., Brinkmann, M., Rzesanke, D., Saathoff, H., Nicolet, M., Saito, A., Nillius, B., Bingemer, H., Abbatt, J., Ardon, K., Ganor, E., Georgakopoulos, D. G., and Saunders, C.: Resurgence in Ice Nuclei Measurement Research, *B. Am. Meteorol. Soc.*, 92, 1623-1635, 10.1175/2011bams3119.1, 2011.

DeMott, P. J., Prenni, A. J., McMeeking, G. R., Sullivan, R. C., Petters, M. D., Tobo, Y., Niemand, M., Möhler, O., Snider, J. R., Wang, Z., and Kreidenweis, S. M.: Integrating laboratory and field data to quantify the immersion freezing ice nucleation activity of mineral dust particles, *Atmos. Chem. Phys.*, 15, 393-409, 10.5194/acp-15-393-2015, 2015.

DeMott, P. J., Möhler, O., Cziczo, D. J., Hiranuma, N., Petters, M. D., Petters, S. S., Belosi, F., Bingemer, H. G., Brooks, S. D., Budke, C., Burkert-Kohn, M., Collier, K. N., Danielczok, A., Eppers, O., Felgitsch, L., Garimella, S., Grothe, H., Herenz, P., Hill, T. C. J., Höhler, K., Kanji, Z. A., Kiselev, A., Koop, T., Kristensen, T. B., Krüger, K., Kulkarni, G., Levin, E. J. T., Murray, B. J., Nicosia, A., and Sullivan, D., Peckhaus, A., Polen, M. J., Price, H. C., Reicher, N., Rothenberg, D. A., Rudich, Y., Santachiara, G., Schiebel, T., Schrod, J.,

- Seifried, T. M., Stratmann, F., Sullivan, R. C., Suski, K. J., Szakáll, M., Taylor, H. P., Ullrich, R., Vergara-Temprado, J., Wagner, R., Whale, T. F., Weber, D., Welti, A., Wilson, T. W., Wolf, M. J., and Zenker, J.: The Fifth International Workshop on Ice Nucleation phase 2 (FIN-02): laboratory intercomparison of ice nucleation measurements, *Atmos. Meas. Tech.*, 11, 6231-6257, 10.5194/amt-11-6231-2018, 2018.
- Eriksen Hammer, S., Mertes, S., Schneider, J., Ebert, M., Kandler, K., and Weinbruch, S.: Composition of ice particle residuals in mixed-phase clouds at Jungfraujoch (Switzerland): enrichment and depletion of particle groups relative to total aerosol, *Atmos. Chem. Phys.*, 18, 13987-14003, 10.5194/acp-18-13987-2018, 2018.
- Field, P. R., Lawson, R. P., Brown, P. R. A., Lloyd, G., Westbrook, C., Moisseev, D., Miltenberger, A., Nenes, A., Blyth, A., Choulaton, T., Connolly, P., Buehl, J., Crosier, J., Cui, Z., Dearden, C., DeMott, P., Flossmann, A., Heymsfield, A., Huang, Y., Kalesse, H., Kanji, Z. A., Korolev, A., Kirchgaessner, A., Lasher-Trapp, S., Leisner, T., McFarquhar, G., Phillips, V., Stith, J., and Sullivan, S.: Chapter 7. Secondary Ice Production - current state of the science and recommendations for the future, *Meteor. Mon.*, 58, 1-20, 10.1175/amsmonographs-d-16-0014.1, 2017.
- Gallagher, J. J.: Fractography of sand grains broken by uniaxial compression, *Clastic particles: scanning electron microscopy and shape analysis of sedimentary and volcanic clasts*, edited by: Marshall, J. R., Van Nostrand Reinhold, New York, USA, 189-228, 1987.
- Glaccum, R. A., and Prospero, J. M.: Saharan aerosols over the tropical North Atlantic — Mineralogy, *Mar. Geol.*, 37, 295-321, 10.1016/0025-3227(80)90107-3, 1980.
- Goldich, S. S.: A Study in Rock-Weathering, *J. Geo.*, 46, 17-58, 10.1086/624619, 1938.
- Goreva, J. S., Ma, C., and Rossman, G. R.: Fibrous nanoinclusions in massive rose quartz: The origin of rose coloration, *Am. Mineral.*, 86, 466-472, 10.2138/am-2001-0410, 2001.
- Götze, J., Nasdala, L., Kleeberg, R., and Wenzel, M.: Occurrence and distribution of "moganite" in agate/chalcedony: a combined micro-Raman, Rietvel and cathodoluminescence study, *Contrib. Mineral. Petr.*, 133, 96-105, doi.org/10.1007/s004100050, 1998.

Harrison, A. D., Whale, T. F., Carpenter, M. A., Holden, M. A., Neve, L., apos, Sullivan, D., Vergara Temprado, J., and Murray, B. J.: Not all feldspars are equal: a survey of ice nucleating properties across the feldspar group of minerals, *Atmos. Chem. Phys.*, 16, 10927-10940, 10.5194/acp-16-10927-2016, 2016.

Harrison, A.D.; Lever, K.; Sanchez-Marroquin, A.; Holden, M.; Whale, T.F.; Tarn, M.D.; McQuaid, J.B.; Murray, B.J. (2019): Ice-nucleating ability measurements of quartz samples. Centre for Environmental Data Analysis, 25 June, doi:10.5285/171726739bb54d0ba84cdde15c5b17ae, 2019.

Heaney, P. J., and Post, J. E.: The widespread distribution of a novel silica polymorph in microcrystalline quartz varieties, *Science*, 255, 441-443, doi: 10.1126/science.255.5043.441, 1992.

Herbert, R. J., Murray, B. J., Whale, T. F., Dobbie, S. J., and Atkinson, J. D.: Representing time-dependent freezing behaviour in immersion mode ice nucleation, *Atmos. Chem. Phys.*, 14, 8501-8520, 10.5194/acp-14-8501-2014, 2014.

Herbert, R. J., Murray, B. J., Dobbie, S. J., and Koop, T.: Sensitivity of liquid clouds to homogenous freezing parameterizations, *Geo. Phys. Lett.*, 42, 1599-1605, 10.1002/2014gl062729, 2015.

Hiranuma, N., Augustin-Bauditz, S., Bingemer, H., Budke, C., Curtius, J., Danielczok, A., Diehl, K., Dreischmeier, K., Ebert, M., Frank, F., Hoffmann, N., Kandler, K., Kiselev, A., Koop, T., Leisner, T., Möhler, O., Nillius, B., Peckhaus, A., Rose, D., Weinbruch, S., Wex, H., Boose, Y., DeMott, P. J., Hader, J. D., Hill, T. C. J., Kanji, Z. A., Kulkarni, G., Levin, E. J. T., McCluskey, C. S., Murakami, M., Murray, B. J., Niedermeier, D., Petters, M. D., O'Sullivan, D., Saito, A., Schill, G. P., Tajiri, T., Tolbert, M. A., Welti, A., Whale, T. F., Wright, T. P., and Yamashita, K.: A comprehensive laboratory study on the immersion freezing behavior of illite NX particles: a comparison of 17 ice nucleation measurement techniques, *Atmos. Chem. Phys.*, 15, 2489-2518, 10.5194/acp-15-2489-2015, 2015.

Holden, M. A., Whale, T. F., Tarn, M. D., O'Sullivan, D., Walshaw, R. D., Murray, B. J., Meldrum, F. C., and Christenson, H. K.: High-speed imaging of ice nucleation in water proves the existence of active sites, *Sci. Adv.*, 5, eaav4316, 10.1126/sciadv.aav4316, 2019.

Hoose, C., and Möhler, O.: Heterogeneous ice nucleation on atmospheric aerosols: a review of results from laboratory experiments, *Atmos. Chem. Phys.*, 12, 9817-9854, 10.5194/acp-12-9817-2012, 2012.

Isono, K., and Ikebe, Y.: On the Ice-nucleating Ability of Rock-forming Minerals and Soil Particles, *J. Meteorol. Soc. Jpn. . Ser. II*, 38, 213-230, 10.2151/jmsj1923.38.5_213, 1960.

Iwata, A., and Matsuki, A.: Characterization of individual ice residual particles by the single droplet freezing method: a case study in the Asian dust outflow region, *Atmos. Chem. Phys.*, 18, 1785-1804, 10.5194/acp-18-1785-2018, 2018.

Kandler, K., Schütz, L., Deutscher, C., Ebert, M., Hofmann, H., Jäckel, S., Jaenicke, R., Knippertz, P., Lieke, K., Massling, A., Petzold, A., Schladitz, A., Weinzierl, B., Wiedensohler, A., Zorn, S., and Weinbruch, S.: Size distribution, mass concentration, chemical and mineralogical composition and derived optical parameters of the boundary layer aerosol at Tinfou, Morocco, during SAMUM 2006, *Tellus*, 61B, 32-50, 10.1111/j.1600-0889.2008.00385.x, 2009.

Kandler, K., SchÜTz, L., JÄCkel, S., Lieke, K., Emmel, C., MÜLler-Ebert, D., Ebert, M., Scheuvens, D., Schladitz, A., ŠEgviĆ, B., Wiedensohler, A., and Weinbruch, S.: Ground-based off-line aerosol measurements at Praia, Cape Verde, during the Saharan Mineral Dust Experiment: microphysical properties and mineralogy, *Tellus*, 63B, 459-474, 10.1111/j.1600-0889.2011.00546.x, 2011.

Kanitz, T., Seifert, P., Ansmann, A., Engelmann, R., Althausen, D., Casiccia, C., and Rohwer, E. G.: Contrasting the impact of aerosols at northern and southern midlatitudes on heterogeneous ice formation, *Geophys. Res. Lett.*, 38, L17802, 10.1029/2011gl048532, 2011.

Kanji, Z. A., DeMott, P. J., Möhler, O., and Abbatt, J. P. D.: Results from the University of Toronto continuous flow diffusion chamber at ICIS 2007: instrument intercomparison and ice onsets for different aerosol types, *Atmos. Chem. Phys.*, 11, 31-41, 10.5194/acp-11-31-2011, 2011.

- Kanji, Z. A., Ladino, L. A., Wex, H., Boose, Y., Burkert-Kohn, M., Cziczo, D. J., and Krämer, M.: Overview of Ice Nucleating Particles, *Meteorol. Mon.*, 58, 1.1-1.33, 10.1175/amsmonographs-d-16-0006.1, 2017.
- Kibar, R., Garcia-Guinea, J., Çetin, A., Selvi, S., Karal, T., and Can, N.: Luminescent, optical and color properties of natural rose quartz, *Radiat. Meas.*, 42, 1610-1617, 10.1016/j.radmeas.2007.08.007, 2007.
- Koehler, K. A., Kreidenweis, S. M., DeMott, P. J., Petters, M. D., Prenni, A. J., and Möhler, O.: Laboratory investigations of the impact of mineral dust aerosol on cold cloud formation, *Atmos. Chem. Phys.*, 10, 11955-11968, 10.5194/acp-10-11955-2010, 2010.
- Koike, C., Noguchi, R., Chihara, H., Suto, H., Ohtaka, O., Imai, Y., Matsumoto, T., and Tsuchiyama, A.: Infrared Spectra of Silica Polymorphs and the Conditions of Their Formation, *Astrophys. J.*, 778, 60, 1-12, 10.1088/0004-637x/778/1/60, 2013.
- Kumar, A., Marcolli, C., Luo, B., and Peter, T.: Ice nucleation activity of silicates and aluminosilicates in pure water and aqueous solutions – Part 1: The K-feldspar microcline, *Atmos. Chem. Phys.*, 18, 7057-7079, 10.5194/acp-18-7057-2018, 2018.
- Kumar, A., Marcolli, C., and Peter, T.: Ice nucleation activity of silicates and aluminosilicates in pure water and aqueous solutions – Part 2: Quartz and amorphous silica, *Atmos. Chem. Phys.*, 19, 6035-6058, 10.5194/acp-19-6035-2019, 2019a.
- Kumar, A., Marcolli, C., and Peter, T.: Ice nucleation activity of silicates and aluminosilicates in pure water and aqueous solutions – Part 3: Aluminosilicates, *Atmos. Chem. Phys.*, 19, 6059-6084, 10.5194/acp-19-6059-2019, 2019b.
- Lohmann, U.: Anthropogenic Aerosol Influences on Mixed-Phase Clouds, *Curr. Clim. Change Rep.*, 3, 32-44, 10.1007/s40641-017-0059-9, 2017.
- Losey, D. J., Sihvonen, S. K., Veghte, D. P., Chong, E., and Freedman, M. A.: Acidic processing of fly ash: chemical characterization, morphology, and immersion freezing, *Environ. Sci. Process Impacts*, 20, 1581-1592, 10.1039/c8em00319j, 2018.
- Mahaney, W. C., Dirszowsky, R. W., Milner, M. W., Menzies, J., Stewart, A., Kalm, V., and Bezada, M.: Quartz microtextures and microstructures owing to deformation of

- glaciolacustrine sediments in the northern Venezuelan Andes, *J. Quaternary Sci.*, 19, 23-33, 10.1002/jqs.818, 2004.
- Mason, B. J., and Maybank, J.: ICE-NUCLEATING PROPERTIES OF SOME NATURAL MINERAL DUSTS, *Q. J. Roy. Meteor. Soc.*, 84, 235-241, 1958.
- Murray, B. J., Broadley, S. L., Wilson, T. W., Atkinson, J. D., and Wills, R. H.: Heterogeneous freezing of water droplets containing kaolinite particles, *Atmos. Chem. Phys.*, 11, 4191-4207, 10.5194/acp-11-4191-2011, 2011.
- Murray, B. J., O'Sullivan, D., Atkinson, J. D., and Webb, M. E.: Ice nucleation by particles immersed in supercooled cloud droplets, *Chem. Soc. Rev.*, 41, 6519-6554, 10.1039/C2CS35200A, 2012.
- Nassau, K.: The origins of color in minerals, *Am. Mineral.*, 63, 219-229, 1978.
- Niedermeier, D., Augustin-Bauditz, S., Hartmann, S., Wex, H., Ignatius, K., and Stratmann, F.: Can we define an asymptotic value for the ice active surface site density for heterogeneous ice nucleation?, *J. Geophys. Res. Atmos.*, 120, 5036-5046, 10.1002/2014jd022814, 2015.
- Niemand, M., Möhler, O., Vogel, B., Vogel, H., Hoose, C., Connolly, P., Klein, H., Bingemer, H., DeMott, P. J., Skrotzki, J., and Leisner, T.: A particle-surface-area-based parameterization of immersion freezing on desert dust particles, *J. Atmos. Sci.*, 69, 3077-3092, 10.1175/jas-d-11-0249.1, 2012.
- O'Sullivan, D., Murray, B. J., Malkin, T. L., Whale, T. F., Umo, N. S., Atkinson, J. D., Price, H. C., Baustian, K. J., Browse, J., and Webb, M. E.: Ice nucleation by fertile soil dusts: relative importance of mineral and biogenic components, *Atmos. Chem. Phys.*, 14, 1853-1867, 10.5194/acp-14-1853-2014, 2014.
- Peckhaus, A., Kiselev, A., Hiron, T., Ebert, M., and Leisner, T.: A comparative study of K-rich and Na/Ca-rich feldspar ice-nucleating particles in a nanoliter droplet freezing assay, *Atmos. Chem. Phys.*, 16, 11477-11496, 10.5194/acp-16-11477-2016, 2016.

- Pedevilla, P., Fitzner, M., and Michaelides, A.: What makes a good descriptor for heterogeneous ice nucleation on OH-patterned surfaces, *Phys. Rev. B*, 96, 115441, 10.1103/PhysRevB.96.115441, 2017.
- Perlwitz, J. P., Pérez García-Pando, C., and Miller, R. L.: Predicting the mineral composition of dust aerosols – Part 1: Representing key processes, *Atmos. Chem. Phys.*, 15, 11593-11627, 10.5194/acp-15-11593-2015, 2015.
- Pinti, V., Marcolli, C., Zobrist, B., Hoyle, C. R., and Peter, T.: Ice nucleation efficiency of clay minerals in the immersion mode, *Atmos. Chem. Phys.*, 12, 5859-5878, 10.5194/acp-12-5859-2012, 2012.
- Pratt, K. A., DeMott, P. J., French, J. R., Wang, Z., Westphal, D. L., Heymsfield, A. J., Twohy, C. H., Prenni, A. J., and Prather, K. A.: In situ detection of biological particles in cloud ice-crystals, *Nature Geosci.*, 2, 398-401, 10.1038/ngeo521, 2009.
- Price, H. C., Baustian, K. J., McQuaid, J. B., Blyth, A., Bower, K. N., Choularton, T., Cotton, R. J., Cui, Z., Field, P. R., Gallagher, M., Hawker, R., Merrington, A., Miltenberger, A., Neely III, R. R., Parker, S. T., Rosenberg, P. D., Taylor, J. W., Trembath, J., Vergara-Temprado, J., Whale, T. F., Wilson, T. W., Young, G., and Murray, B. J.: Atmospheric Ice-Nucleating Particles in the Dusty Tropical Atlantic, *J. Geophys. Res. Atmos.*, 123, 2175-2193, 10.1002/2017jd027560, 2018.
- Pummer, B. G., Budke, C., Augustin-Bauditz, S., Niedermeier, D., Felgitsch, L., Kampf, C. J., Huber, R. G., Liedl, K. R., Loerting, T., Moschen, T., Schauperl, M., Tollinger, M., Morris, C. E., Wex, H., Grothe, H., Pöschl, U., Koop, T., and Fröhlich-Nowoisky, J.: Ice nucleation by water-soluble macromolecules, *Atmos. Chem. Phys.*, 15, 4077-4091, 10.5194/acp-15-4077-2015, 2015.
- Pye, K.: Sediment transport and depositional processes, in, edited by: Pye, K., Blackwell scientific publications, Oxford, Boston, 1-58, 1994.
- Reicher, N., Segev, L., and Rudich, Y.: The Weizmann Supercooled Droplets Observation on a Microarray (WISDOM) and application for ambient dust, *Atmos. Meas. Tech.*, 11, 233-248, 10.5194/amt-11-233-2018, 2018.

- Roberts, P., and Hallett, J.: A laboratory study of the ice nucleating properties of some mineral particulates, *Q. J. Roy. Meteor. Soc.*, 94, 25-34, 10.1002/qj.49709439904, 1968.
- Rosenfeld, D., Yu, X., Liu, G., Xu, X., Zhu, Y., Yue, Z., Dai, J., Dong, Z., Dong, Y., and Peng, Y.: Glaciation temperatures of convective clouds ingesting desert dust, air pollution and smoke from forest fires, *Geophys. Res. Lett.*, 38, L2104, 10.1029/2011gl049423, 2011.
- Sanchez-Marroquin, A., Hedges, D. H. P., Hiscock, M., Parker, S. T., Rosenberg, P. D., Trembath, J., Walshaw, R., Burke, I. T., McQuaid, J. B., and Murray, B. J.: Characterisation of the filter inlet system on the BAE-146 research aircraft and its use for size resolved aerosol composition measurements, *Atmos. Meas. Tech. Disc.*, 1-35, 10.5194/amt-2019-196, 2019.
- Spencer, W. J., and Smith, W. L.: Defects in Natural Quartz, *J. of Appl. Phys.*, 37, 2557-2563, 10.1063/1.1782083, 1966.
- Swamy, V., Saxena, S. K., Sundman, B., and Zhang, J.: A thermodynamic assessment of silica phase diagram, *J. Geophys. Res. Solid*, 99, 11787-11794, 10.1029/93jb02968, 1994.
- Tan, I., Storelvmo, T., and Zelinka, M. D.: Observational constraints on mixed-phase clouds imply higher climate sensitivity, *Science*, 352, 224-227, 10.1126/science.aad5300, 2016.
- Tarn, M. D., Sikora, S. N. F., Porter, G. C. E., O'Sullivan, D., Adams, M., Whale, T. F., Harrison, A. D., Vergara-Temprado, J., Wilson, T. W., Shim, J. U., and Murray, B. J.: The study of atmospheric ice-nucleating particles via microfluidically generated droplets, *Microfluid. Nanofluid.*, 22, 52, 10.1007/s10404-018-2069-x, 2018.
- Ullrich, R., Hoose, C., Möhler, O., Niemand, M., Wagner, R., Höhler, K., Hiranuma, N., Saathoff, H., and Leisner, T.: A New Ice Nucleation Active Site Parameterization for Desert Dust and Soot, *J. Atmos. Sci.*, 74, 699-717, 10.1175/jas-d-16-0074.1, 2017.
- Umo, N. S., Murray, B. J., Baeza-Romero, M. T., Jones, J. M., Lea-Langton, A. R., Malkin, T. L., O'Sullivan, D., Neve, L., Plane, J. M. C., and Williams, A.: Ice nucleation by combustion ash particles at conditions relevant to mixed-phase clouds, *Atmos. Chem. Phys.*, 15, 5195-5210, 10.5194/acp-15-5195-2015, 2015.

Vali, G., DeMott, P. J., Möhler, O., and Whale, T. F.: Technical Note: A proposal for ice nucleation terminology, *Atmos. Chem. Phys.*, 15, 10263-10270, 10.5194/acp-15-10263-2015, 2015.

Vergara-Temprado, J., Murray, B. J., Wilson, T. W., amp, apos, Sullivan, D., Browse, J., Pringle, K. J., Ardon-Dryer, K., Bertram, A. K., Burrows, S. M., Ceburnis, D., DeMott, P. J., Mason, R. H., amp, apos, Dowd, C. D., Rinaldi, M., and Carslaw, K. S.: Contribution of feldspar and marine organic aerosols to global ice nucleating particle concentrations, *Atmos. Chem. Phys.*, 17, 3637-3658, 10.5194/acp-17-3637-2017, 2017.

Vergara-Temprado, J., Miltenberger, A. K., Furtado, K., Grosvenor, D. P., Shipway, B. J., Hill, A. A., Wilkinson, J. M., Field, P. R., Murray, B. J., and Carslaw, K. S.: Strong control of Southern Ocean cloud reflectivity by ice-nucleating particles, *P. Natl. Acad. Sci. USA*, 115, 2687-2692, 10.1073/pnas.1721627115, 2018.

Wex, H., DeMott, P. J., Tobo, Y., Hartmann, S., Rösch, M., Clauss, T., Tomsche, L., Niedermeier, D., and Stratmann, F.: Kaolinite particles as ice nuclei: learning from the use of different kaolinite samples and different coatings, *Atmos. Chem. Phys.*, 14, 5529-5546, 10.5194/acp-14-5529-2014, 2014.

Whale, T. F., Murray, B. J., O'Sullivan, D., Wilson, T. W., Umo, N. S., Baustian, K. J., Atkinson, J. D., Workneh, D. A., and Morris, G. J.: A technique for quantifying heterogeneous ice nucleation in microlitre supercooled water droplets, *Atmos. Meas. Tech.*, 8, 2437-2447, 10.5194/amt-8-2437-2015, 2015.

Whale, T. F., Holden, M. A., Kulak, A. N., Kim, Y. Y., Meldrum, F. C., Christenson, H. K., and Murray, B. J.: The role of phase separation and related topography in the exceptional ice-nucleating ability of alkali feldspars, *Phys. Chem. Chem. Phys.*, 19, 31186-31193, 10.1039/c7cp04898j, 2017.

Whale, T. F., Holden, M. A., Wilson, T. W., O'Sullivan, D., and Murray, B. J.: The enhancement and suppression of immersion mode heterogeneous ice-nucleation by solutes, *Chem. Sci.*, 9, 4142-4151, 10.1039/c7sc05421a, 2018.

Wilson, M. J.: Weathering of the primary rock-forming minerals: processes, products and rates, *Clay Minerals*, 39, 233-266, 10.1180/0009855043930133, 2004.

Wright, T. P., Petters, M. D., Hader, J. D., Morton, T., and Holder, A. L.: Minimal cooling rate dependence of ice nuclei activity in the immersion mode, *J. Geophys. Res. Atmos.*, 118, 10535-10543, 10.1002/jgrd.50810, 2013.

Zolles, T., Burkart, J., Häusler, T., Pummer, B., Hitzenberger, R., and Grothe, H.: Identification of Ice Nucleation Active Sites on Feldspar Dust Particles, *J. Phys. Chem. A*, 119, 2692-2700, 10.1021/jp509839x, 2015.

3. Ice-nucleating activity of desert dust decreases on transport across the Atlantic

This chapter is in preparation to be submitted to *Geophysical research letters* as:

A. D. Harrison, D. O’Sullivan, M. P. Adams, G. C. E. Porter, C. Brathwaite, R. Chewitt-Lucas, R. Hawker, O. O. Krueger, L. Neve, M. L. Pohlker, C. Pohlker, U. Poschl, J. M. Prospero, A. Sanchez-Marroquin, A. Sealy, P. Sealy, M. D. Tarn, S. Whitehall, J. B. McQuaid and B. J. Murray ‘Ice-Nucleating Particle Activity in Transported Desert Dust in the Western Atlantic’, GRL (2020).

Abstract

Mineral dust is known to act as an ice-nucleating particle (INP) in the atmosphere, but little is known about the influence of the transportation process on its activity. Dust plumes emitted from Africa typically pass over the eastern tropical Atlantic before reaching Barbados (5-7 days later). Here we present the first INP concentrations measured at Barbados and contrast them to measurements made around Cape Verde. INP concentrations in Barbados are lower than observed in the eastern tropical Atlantic and the activity of the aerosol has decreased during transportation. The GLOMAP model over predicts INP concentrations at Barbados which we attribute to the over prediction of K-feldspar at this location. We suggest that K-feldspar is preferentially removed during transportation, resulting in mineral dust aerosol with a lower activity. On this basis we recommend that future modeling studies refine their approaches to predicting K-feldspar concentrations on transport.

3.1 Introduction

Immersion freezing is the process where a particle becomes immersed within a water droplet before initiating freezing (Pruppacher and Klett, 1997; Vali et al., 2015) and it is thought to be the dominant pathway for ice formation in mixed-phase clouds (Ansmann et al., 2009). The presence of ice crystals opposed to liquid water droplets has large effects on a cloud’s radiative properties and lifetime (Lohmann et al., 2006; Storelvmo et al., 2011). Pure water cloud droplets, in the absence of particles which have ice-nucleating capabilities, will supercool to temperatures below -33 °C before freezing homogeneously to form ice crystals (Herbert et al., 2015; Riechers et al., 2013). However, the confidence in the description of aerosol-cloud

interactions in models remains low (Boucher et al., 2013; Field et al., 2014; Pachauri et al., 2014; Tan et al., 2016).

Observations of atmospheric ice crystals have commonly found mineral dust to be a residual component which would suggest that mineral dust acts as an effective ice-nucleating particle (INP) in the atmosphere (Eriksen Hammer et al., 2018; Iwata and Matsuki, 2018; Pratt et al., 2009). Further studies attribute tens of per cent of atmospheric INP as mineral dust (Cziczo et al., 2003; Pratt et al., 2009) and climate model simulations by Hoose et al. (2010) suggest that up to 77% of INP active between 0 to -38°C are accounted for by mineral dusts. Mineral dusts are composed of various minerals with the three most abundant groups in the atmosphere being clay, quartz and feldspar respectively (Murray et al., 2012). These dusts are created by the weathering of the Earth's surface and are commonly sourced from arid regions such as Africa, the Middle East and Asia, otherwise referred to as the Dust Belt (Prospero et al., 2012).

Atkinson et al. (2013) found that K-feldspar was the most effective ice nucleator of any major mineral component found in mineral dust. Further work has confirmed that K-feldspar is an extremely active INP (Augustin-Bauditz et al., 2014; Emersic et al., 2015; Harrison et al., 2019; Harrison et al., 2016; Niedermeier et al., 2015; Peckhaus et al., 2016; Zolles et al., 2015). These findings have led to mineral dust INP being modelled with the activity being related to the amount K-feldspar in the dust (Perlwitz et al., 2015; Vergara-Temprado et al., 2017). This assumption has given reasonable predictions of INP concentrations in the past (Harrison et al., 2019; O'Sullivan et al., 2018; Price et al., 2018).

However, there are sparse field studies which have observed the effect of transport on mineral dust INP and there are a number of possible processes which could potentially alter the ice-nucleating ability of mineral dust in the atmosphere (Figure 3.1). For example, Harrison et al. (2016) showed that feldspar could lose its ice-nucleating ability when left suspended in water. Recent studies have demonstrated that solutes and acids, such as atmospherically present NaCl and H_2SO_4 , can alter the ice-nucleating ability of K-feldspar (Kumar et al., 2018; Kumar et al., 2019; Whale et al., 2018). The influence of such ageing processes in the atmosphere have been discussed by Boose et al. (2019) and Kumar et al. (2018). However, there is still much uncertainty on this topic due to the lack of field observations of transported mineral dusts.

INP measurements have been made close to dust source regions in the eastern tropical Atlantic (ETA) by Price et al. (2018). These observations (which investigate minimally transported

mineral dust) are predicted well by the K-feldspar parameterizations created by Atkinson et al. (2013) and Harrison et al. (2019). However, Iwata and Matsuki (2018) suggest that transported mineral dust measured in Japan is deactivated by an internal mixing with sea-salt. This depression of mineral dust activity by sea-salt is further supported by the work of Si et al. (2019) in the high Arctic and is in line with laboratory findings (Kumar et al., 2018; Kumar et al., 2019; Whale et al., 2018). Given the above findings, there is still much uncertainty on the effect of transportation on the ice-nucleating ability of INP and it is clear that further studies of transported mineral dust are needed.

It typically takes 5-7 days for desert dust plumes to reach Barbados once leaving the west coast of Africa and there are only sea spray sources of INP, which are relatively ineffective INP, on the passage across the ocean. Hence Barbados is an ideal location to investigate the transportation effect on mineral dust. Desert dust plumes pass over the Eastern tropical Atlantic (ETA) before reaching Barbados where mineral dust will have undergone multiple days of processing. Therefore a comparison can be drawn between the two locations as aircraft INP measurements from the ETA are already available (Price et al., 2018). Recently, Haarig et al. (2019) used LIDAR ground retrievals and aircraft aerosol size distribution measurements to infer the INP concentrations at Barbados. The inferred INP concentrations at Barbados were slightly lower than those measured in the ETA, which is to be expected given the aerosol concentration was also lower (Haarig et al., 2019; Price et al., 2018). However, as of yet there have not been any direct measurements of INP concentrations at Barbados.

Here we present the first INP measurements made in Barbados and contrast them with previous observations from the ETA to determine the effect of long-range transport on the ice-nucleating activity of mineral dusts. Further to this we contrast our measurements with the results of a global INP model (Vergara-Temprado et al., 2017) and make recommendations for how this model could be improved in the future.

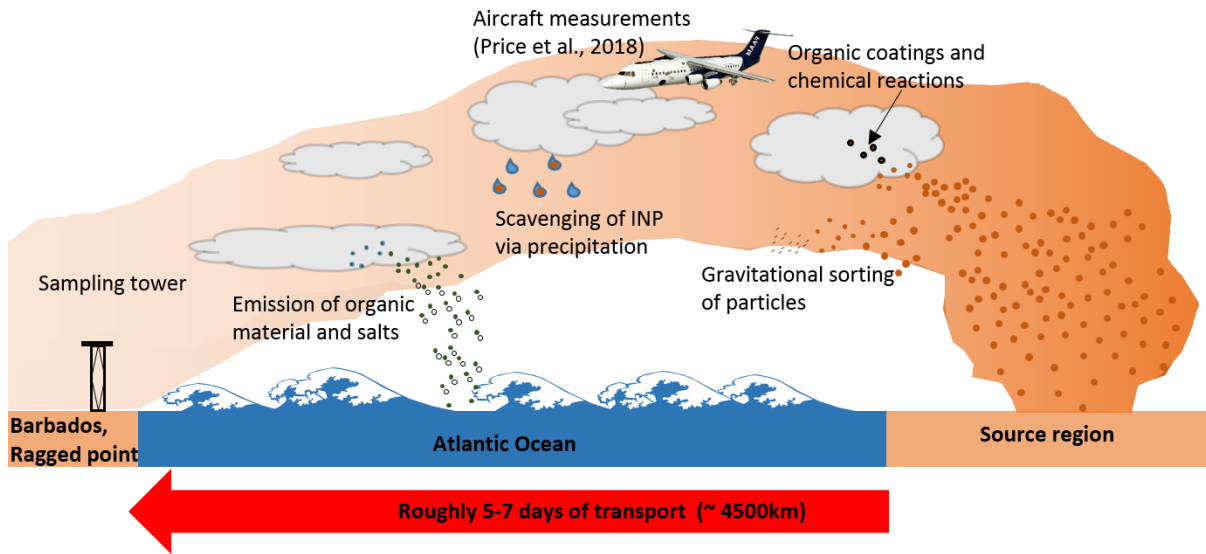


Figure 3.1: Schematic of the processes which may alter the ice-nucleating ability of a mineral dust during transport.

3.2 Methods

3.2.1 Project overview

The Barbados Ice-nucleating particle Concentration Experiment (B-ICE) was conducted at Ragged point which is the most easterly point of Barbados (see Fig. 3.1). The air at this location is relatively pristine and not influenced heavily by local sources with the air masses mostly coming from an easterly direction over the Atlantic. For this reason, it is a chosen site for the Advanced Global Atmospheric Gases Experiment (AGAGE). The University of Miami also has infrastructure on sight which includes a ~20m sampling tower on which aerosol samplers and meteorological instrumentation collect data. The tower is situated on the cliff edge and was built to minimize the sampling of local sea spray aerosol (SSA) produced at the base of the cliff. July-August are when Barbados typically experiences the most mineral dust plume occurrences and so B-ICE ran during these months (July 24th to August 24th).

3.2.2 Aerosol sampling and measurements

Three MESA PQ100 aerosol samplers were used during the campaign and placed atop the 20 m sampling tower. 47mm, 0.4 μm pore sized, polycarbonate Whatmann track-etched filters were used at a flow rate of 16.7 Lpm with an aerosol cut off size of PM 10. The samplers were left to run for varying periods of time both during the day and at night. The flow rate and sampling

duration of each sampler was recorded by an inbuilt mass flow controller. Often two MESA samplers were run side by side to obtain two filters which collected similar aerosol. Where possible, one filter would be used for the on-site ice nucleation experiments (see section 3.2.3) and the other would be sealed, frozen and shipped to Leeds to conduct scanning electron microscopy. The methodology for SEM analysis is the same as that described by Sanchez-Marroquin et al. (2019). For one case study a cascade impactor (MOUDI) was also used to collect size segregated aerosol using the same polycarbonate filters as the mesa samplers.

Throughout the campaign handling filter blanks would also be taken by placing a clean filter in the filter holder, removing it and analysing it as mentioned in section 3.2.3. For some handling blanks a HEPA filter was used instead of the inlet head and air sampled for a duration of time before removing the filter and analysing.

A TSI 3321 Aerodynamic Particle Sizer (APS) was placed in a weather sealed container on top of the tower with no cut off inlet to take particle size distribution measurements in the range of 0.5-20 microns. A vertical inlet, which led to a laboratory directly below the tower, was used to sample to an SMPS (TSI 3938), owned by Max-Planck institute, for measurements in the size range of 1nm - 1 μ m. Both the SMPS and APS were run 24/7 with sporadic power outages or maintenance. SMPS and APS datasets were converted to volume equivalent diameters as to merge the two datasets to cover the full range of the size distributions. The data sets were merged in the same way as described by Mohler et al. (2008) with a particle density of 2.6 gcm⁻³ and shape correction factor of 1.3.

3.2.3 Ice nucleation experiments

The time between collection and analysis has unknown effects on INP and can change their ice-nucleating ability (O'Sullivan et al., 2018; Stopelli et al., 2014). To reduce the unknown effects of storage on our samples we prepared and analysed them on site within the IcePod portable laboratory. This has been employed in a previous INP field study by O'Sullivan et al. (2018).

A well characterised immersion mode drop assay technique, μ L-NIPI, was then used for all ice nucleation experiments (Harrison et al., 2016; O'Sullivan et al., 2014; Whale et al., 2015). Previously, this method has been used for the analysis of filter collected aerosol samples (O'Sullivan et al., 2018), based on the filter sampling and subsequent particle suspension in

water described by DeMott et al. (2016). At the start of each day a blank experiment with pure HPLC grade water was conducted to determine the background of the experiment before conducting experiments with filter collected aerosol. HPLC wash water from the rinsing of a handling blank filter were also periodically run to determine the extent of contamination during the sampling process. The handling blanks and baselines were in agreement with one another although there was a large degree of variability across all blanks (~ 4 °C at T50). This variability was attributed to the contamination of the HPLC water, most likely from aerosol present in the working environment. As these backgrounds were variable, they were compiled to ascertain a more comprehensive representation of the background. See text S1 for a full description of the protocol.

Some samples were heated to test for the presence of biological INP as ice active proteins associated with some classes of biological INP can be denatured with heat, causing a decrease in their ice-nucleating ability (Christner et al., 2008; Garcia et al., 2012; O'Sullivan et al., 2018). A selection of suspensions were heated to 100 °C for 1 hour, by immersing a suspension in a sealed vial in boiling water. The INP content of this suspension was determined before and after heating, therefore providing a qualitative test for the presence of biological INP.

The data presented in the following sections has had the pure water background subtracted from each data point (unless specified). Data points which had error bars that spanned more than four orders of magnitude, are indicated with open symbols and should be considered as upper limits. A description of the background subtraction and the calculation of the errors is found in text S1.

3.3 Results and discussion

3.3.1 Ice-nucleating particle concentrations and activity

Figure 3.2a displays the INP concentrations measured during the campaign in comparison with those measured in the ETA. The back trajectories for the aerosol collected for the filters in Fig. 3.2a can be found in Fig. S4. There is at least one order of magnitude in variability in the concentration of INP at this location with a mode INP concentration active at -20°C of $\sim 0.1 \text{ L}^{-1}$, Fig. 2a. In contrast, at the same temperature, Price et al. (2018) found between ~ 1 and 100 L^{-1} in the ETA. There are no direct measurements of INP concentrations in Barbados in the literature, but Haarig et al. (2019) have recently estimated INP concentrations using a

combination of lidar derived aerosol size distributions and literature parameterisations. They predict that at a few hundred meters altitude above Barbados the INP concentrations are around $2 \times 10^{-2} \text{ L}^{-1}$ at -25°C . Our measured concentration at this activation temperature is between about 1 and 10 L^{-1} . The mass concentration and surface area of dust aerosol decreases on transport across the Atlantic (Velasco-Merino et al., 2018) which is consistent with these observations of the INP concentration decreasing as we cross the Atlantic, although not by as much as Haarig et al. (2019) predicts. This is qualitatively consistent with the measured size distributions where we see that the integrated surface area is $10\text{-}40 \mu\text{m}^2 \text{ cm}^{-3}$ versus $25\text{-}1800 \mu\text{m}^2 \text{ cm}^{-3}$ in the boundary layer in the ETA.

On heating of a selection of aerosol suspensions it is observed that in most cases there is no significant decrease in ice-nucleating activity (Figure 3.3,S5). The lack of sensitivity to heat treatment suggests that there is not a major biological INP component in most samples. A breakdown of the heat tests conducted can be seen in figure S5 along with results from a cascade impactor. There are instances, such as on the 2nd of August, where deactivation on heating was observed which we attribute to the likely presence of marine organics. The heat tests and information collected from SEM and XRD analysis (section 3.3.2) are consistent with mineral dust being the major source of INP in this region with some more minor contributions from biogenic (most likely marine organic) sources.

In order to assess whether the ice-nucleating ability of the mineral dust has changed on transport across the Atlantic we have derived the active sites per unit surface area, n_s , for our collected aerosol samples. We estimate n_s using the INP concentration and the surface area of dust. We assume that the surface area derived from the size distribution measurements is equal to the surface area of mineral dust. This is a fair assumption, since our electron microscope analysis showed that on average mineral dust made up $>90\%$ of the aerosol surface area (see section 3.3.2 and Fig. S7). In figure 3.2b we present $n_s(T)$ for both the ETA (Price et al., 2018) and Barbados allowing us to compare the relative ice-nucleating activities of the dusts sampled at these locations. Figure 2b demonstrates that the active site density of the mineral dust in Barbados is lower than that measured in the ETA with the active site density at -22°C being between 1.8×10^6 to $1.1 \times 10^8 n_s(\text{m}^{-2})$ and 1.5×10^7 to $1.1 \times 10^8 n_s(\text{m}^{-2})$ in Barbados and Cape Verde respectively. This would suggest that the desert dust has deactivated during transport

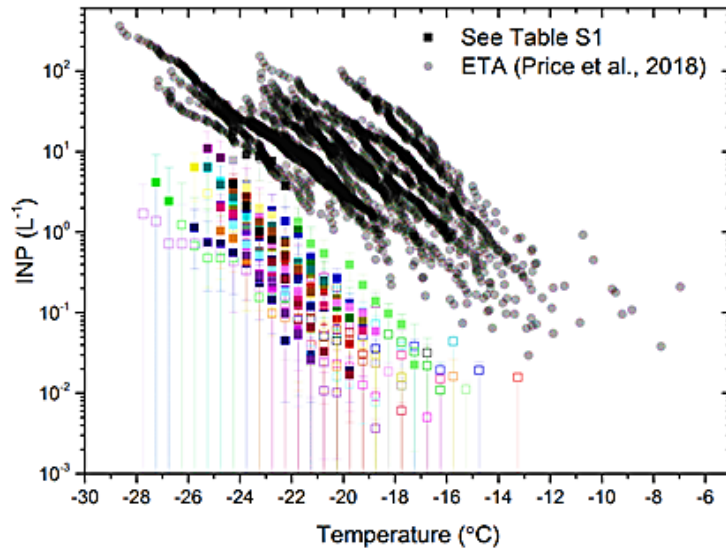
across the Atlantic and that the low INP concentrations in Barbados cannot be fully explained by lower amounts of mineral dust reaching the island.

Other mineral dust n_s values for relatively fresh desert dust collected in various locations are also plotted in figure 3.2b. It can be seen that mineral dust sampled at Barbados has the lowest activity of any of these other mineral dust samples. It should be noted that the other mineral dusts plotted are closer to dust source regions than Barbados and so the effect of transportation on mineral dust may relate to the lower activity observed at Barbados. Boose et al. (2016b) demonstrated that airborne mineral dusts, on average, have a lower ice-nucleating ability than ground collected dusts which gives evidence for the reduction of mineral dusts ability to nucleate ice when suspended in air. This loss of activity of airborne mineral dusts may then relate to transportation processes and be time dependent, i.e. the longer the mineral dust is suspended in air the larger the decrease in its ability to nucleate ice.

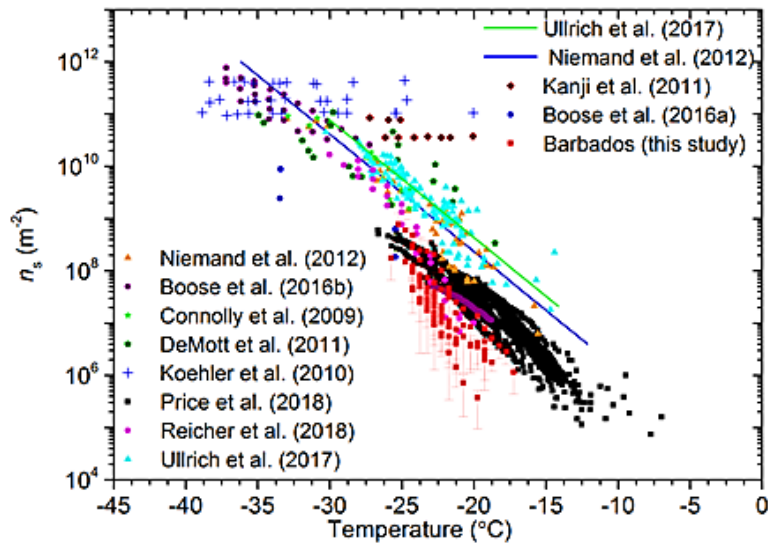
A cascade impactor was employed to sample aerosol on the 24th of August and showed that the dominant INP were found in the 3.2-5.6 μm size range (figure 3.2c) which also displayed no significant sensitivity to heat treatment (Figure S5). Below 1 μm there was a much smaller contribution to the INP population suggesting that the super micron mode was responsible for the aerosol activity. The correlation of ice-nucleating ability and aerosol size may be of potential significance given that the largest particles will be the first to gravitationally settle out of suspension on transport.

There is a 3 °C variability at INP concentrations of 0.01L^{-1} during the campaign. This variability in INP concentration cannot be correlated with any meteorological factors (wind direction, temperature, relative humidity or atmospheric pressure), see Figure S6.

a) Measured INP concentrations at Barbados and in the Eastern Tropical Atlantic



b) Active site density measurements of mineral dusts



c) Size resolved active site densities from the 24th of August 2017

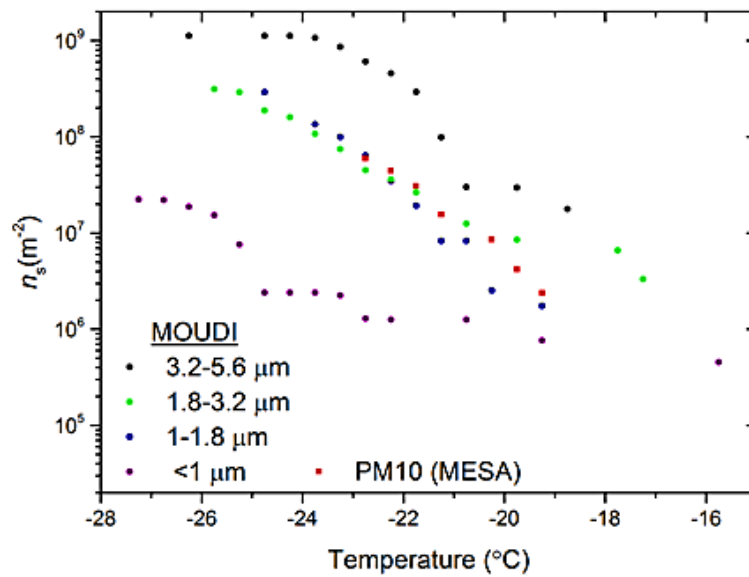


Figure 3.2: INP measurements from Barbados from the 24th July-24th August. a) INP concentrations from Barbados and the ETA, around the Cape Verde region(Price et al., 2018). Data points which were consistent with background signal are displayed as hollow points and should be considered as upper limits. b) The active site density measurements made of mineral dusts at various locations including the measurements made from this study in Barbados and those made by (Price et al., 2018) in the ETA. It should be noted that data points which were consistent with the baseline were removed from the Barbados dataset. c) Size resolved active site density measurements made on the 24th of August 2017 from this study in Barbados. The measurements collected from the MESA aerosol sampler (PM10) for the same date and time are also presented.

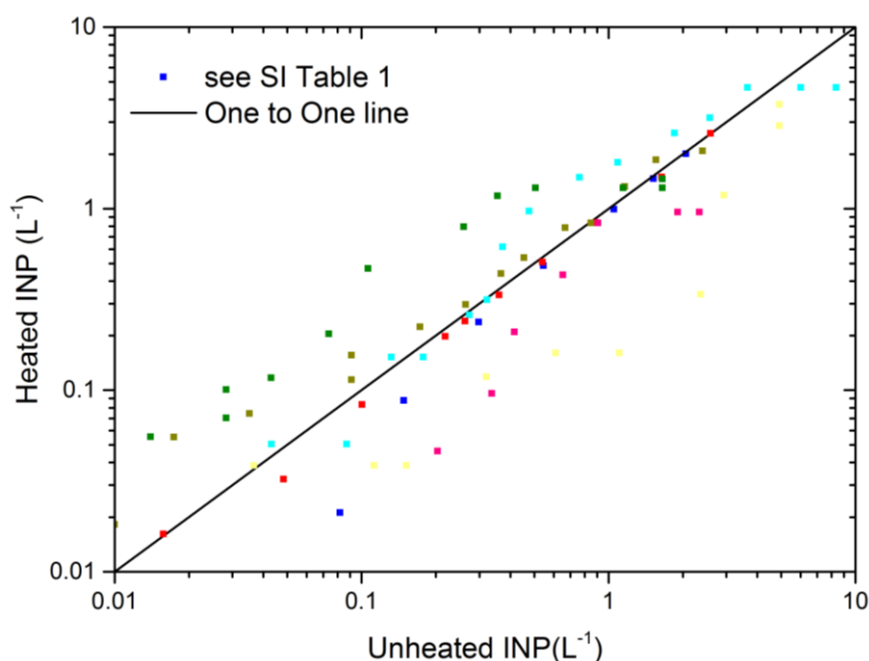


Figure 3.3: [INP] per litre for heated versus unheated samples. No background subtraction has been applied in this plot, however the background signal is the same for heated versus unheated suspensions and so the background signal does not influence the relative trends.

3.3.2 Characterisation of aerosol in Barbados

SEM analysis of four filters shows that on average 92% of the aerosol surface area is attributable to mineral dust with sea salt also present (Figure S7). XRD analysis of dust

collected in rain water collectors (between the 03/08/17-04/08/17) showed that kaolinite (57.8%) dominated the aerosol population with muscovite (27%), quartz (9.1%), plagioclase (3.6%) and calcite (2.6%) also being present (Figure S8). K-feldspar was low in concentration, below the detection limit of the method ($< \sim 2\%$) (Hillier, 1999; Maters et al., 2019). K-feldspar being in concentrations below 2 wt% is in agreement with measurements at Barbados of 1.7 wt% made by Glaccum and Prospero (1980) and ~ 1 wt% by Kandler et al. (2018).

The aerosol size distribution remained fairly constant throughout the campaign of which a composite of the size distributions can be seen in figure 3.4. It should be considered that particles above $10 \mu\text{m}$ were not observed in our aerosol samples whereas the study by Price et al. (2018) did not have an aerosol cut off and saw particles larger than $20 \mu\text{m}$. This may have some impacts on the mineralogy of the sample and therefore the activity as minerals, such as quartz and feldspar, may be found in these larger grain sizes and may also be the first to settle out of suspension on transport. This has similar implications when comparing the results presented here to surface collected samples.

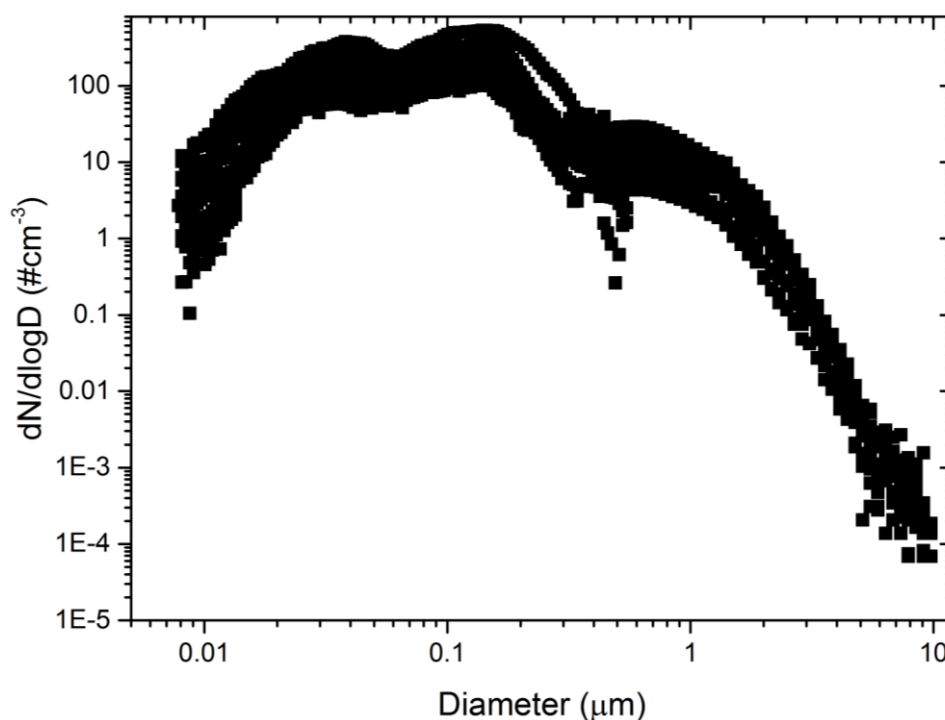


Figure 3.4: Composite of the merged size distributions (from both the APS and SMPS) for the duration of the campaign. The APS and SMPS data have been converted into volume equivalent diameters.

3.3.3 Discussion of what leads to the lower activity of dust in Barbados

There are several potential processes that might lead to a reduced activity of dust on long-range transport (see Fig. 3.1). These include the depletion of K-feldspar in transported dust, acid aging and internal mixing with NaCl. We start with the internal mixing with NaCl hypothesis. It has been shown that relatively small concentrations (~ 0.015 M, i.e. where the melting point depression is only of a few tenths of a degree) of NaCl decreases the activity of K-feldspar by $\sim 5^\circ\text{C}$ (Whale et al., 2018). In order to understand whether sea salt could cause a significant loss of ice-nucleating ability in our samples we decided to conduct a simple experiment. A suspension of 0.1wt% K-feldspar and 6.6×10^{-4} wt% aquarium salt (Marine salt, Tetra) was tested for its ice-nucleating ability. This concentration of sea salt was used based on the upper concentration of sea salt in the atmosphere, measured by Prospero (1979), being $8.71 \mu\text{g m}^{-3}$. Assuming this concentration of sea salt had been sampled on to a filter for four hours (at 16.7Lpm) and diluted into 6 mL of Milli-Q water we would expect to have a sea salt concentration of 6.6×10^{-4} wt% in our aerosol suspension. These values were chosen to represent a typical aerosol suspension collected and analysed in this field study. No observable change in the ice-nucleating ability of K-feldspar was seen with this atmospherically relevant concentration of sea salt (Figure S11) and so we suggest that sea salt has a negligible effect on the deactivation of the transported mineral dust observed at Barbados.

Acid aging is harder to rule out. Laboratory experiments have shown that the activity of mineral dust decreases on exposure to acids (Augustin-Bauditz et al., 2014; Kumar et al., 2018; Kumar et al., 2019; Sullivan et al., 2010; Wex et al., 2014), but simulating the conditions a dust particle experiences in the atmosphere is very challenging and hence we are unable to say how important this effect may be. This leaves us with the hypothesis that the K-feldspar content in transported desert dust is depleted.

In order to address the depleted K-feldspar hypothesis we use an aerosol transport model (GLOMAP) to simulate the INP concentrations at Barbados. This model represents desert dust INP (by representing K-feldspar) and sea spray INP, as described in Vergara-Temprado et al. (2017). An advantage of using this model is that it represents the K-feldspar component of desert dust, based on mineral composition in the dust source regions (Atkinson et al., 2013), and therefore allows the dust to become less active on transport as the coarse mode aerosol, where the K-feldspar is enriched, is removed. This results in the activity of the dust decreasing

on transport. This model was used by Price et al. (2018) to show good agreement with the observed INP concentrations around the Cape Verde region, where the INP population was clearly dominated by relatively fresh desert dust.

A comparison between model predictions and measured INP concentrations at Barbados during the campaign period are shown in Figure 3.5a. The mineral dust INP concentrations were predicted using two K-feldspar parameterisations; the old parameterisation (Atkinson et al., 2013) and the new parameterisation based on the newly available literature data (Harrison et al., 2019). We also show the marine organic INP concentration associated with sea spray based on the parameterisation in Wilson et al. (2015). Overall, the slope of the INP data is consistent with the K-feldspar predictions, albeit shifted to lower temperatures, rather than the marine organics. It is noticeable that the Atkinson et al. (2013) parameterisation over predicts the measurements by roughly an order of magnitude with the parameterisation by Harrison et al. (2019) being in much better agreement with the observations. However, the Harrison et al. (2019) parameterisation still over predicts roughly half the data. Marine organics are found to be of secondary importance until temperatures above ~ -20 °C. Similar to the findings with n_s above we find that the activity of the dust, as defined by the measurements in this location, is lower than we would have expected. We now take a closer look at the K-feldspar content of the dust and the amount of dust in the model predictions.

GLOMAP predicted ~ 7 wt% of the total aerosol mass was K-feldspar, with ~ 8 wt% of the mineral dust mass component being attributed to K-feldspar (Figure S9). The XRD analysis from this study and previous studies (Glaccum and Prospero, 1980; Kandler et al., 2018) show the K-feldspar concentration to be ~ 1 wt% which provides evidence to suggest that the GLOMAP prediction of the K-feldspar content is too high. The average aerosol mass predicted in the GLOMAP simulations during the campaign was $14.8 \pm 8.2 \mu\text{g m}^{-3}$ which is consistent with, albeit slightly lower than, the average aerosol mass measured by the APS of $20.8 \pm 11.2 \mu\text{g m}^{-3}$ (Figure S10). The aerosol mass simulated in GLOMAP is generally lower than that observed and so cannot explain the over estimation of INP in the model. This suggests that the over prediction of K-feldspar may explain the discrepancy.

The XRD analysis of aerosol collected in rain water, from the 3rd-4th of August 2017, shows a K-feldspar content below detection ($< \sim 2\%$) opposed to the ~ 7 wt% predicted in GLOMAP. Given this information, we can make the assumption that 1wt% or less of the aerosol is K-

feldspar and combine this assumption with the Harrison et al. (2019) parameterisation and the range of aerosol surface area concentrations measured during this sampling period. In doing so we predict the INP concentrations well (Fig. 3.5b). From Figure 3.5b we can see that other minerals present in the aerosol cannot account for the INP concentrations but 0.1 wt% to 1 wt% K-feldspar can estimate explain the INP concentrations. The presence of 1 wt% K-feldspar is in good agreement with the recent work of Kandler et al. (2018) who sampled during the same months as this study. A few data points (with large uncertainties), at the very warmest temperatures ($> -20^{\circ}\text{C}$) are not predicted by this estimate of K-feldspar. However, the marine organics prediction from GLOMAP encompasses all but one of these data points. Over this particular period there was some evidence for biogenic material in the warmest regime as the first freezing events were heat sensitive (Figure S5). These data points may then be explained by the presence of biogenic material, perhaps associated with sea spray, but no strong conclusion can be drawn due to the large uncertainty of these data points.

Given the previous case studies agreement with 1 wt% K-feldspar we can aim to predict the activity (n_s) of the dust observed at Barbados for the entire campaign. Assuming that 1% of the aerosol population is K-feldspar, we can predict the activity of the dust, figure 3.5c. Displayed by the red band, in figure 3.5c, is the variability of the ice-nucleating ability of K-feldspar proposed by Harrison et al. (2019). In reality the variability in the observations will likely be a combination of both the variability in the amount of K-feldspar present and the variability of K-feldspar at nucleating ice, but given this assumption we predict the measured n_s of dust in Barbados with exceptional agreement.

Mineralogical measurements are non-trivial which leads to a large range in reported values for the K-feldspar content in mineral dusts. However, Atkinson et al. (2013) reports an average K-feldspar content of 3 % for airborne mineral dusts. Measurements of mineral dusts at Cape Verde suggest a K-feldspar content between ~ 2 % (Glaccum and Prospero, 1980) and 20 ± 5 % (Kandler et al., 2011), which is higher than the 1 % K-feldspar thought to exist at Barbados. This combined with the previous results gives strong evidence that a low weight percent of K-feldspar in the dust collected at Barbados is responsible for the discrepancy in the ice-nucleating ability of the comparable mineral dusts from Cape Verde and Barbados. This suggests that there is a process which preferentially removes K-feldspar from mineral dusts during transport across the Atlantic Ocean and thus leads to a lower concentration of K-feldspar

available to act as an INP. Consequently this results in the deactivation of the mineral dust's ice-nucleating ability. This is consistent with measurements that show K-feldspar concentrations below detection for mineral dusts which have been transported large distances from source regions (Arnold et al., 1998; Atkinson et al., 2013; Blank et al., 1985; Leinen et al., 1994).

We hypothesise that processes such as precipitation and gravitational settling of large grain sizes (of which feldspar is a common component) may result in the preferential removal of K-feldspar. There are two aspects to this. First, processes such as ice formation and subsequent precipitation may preferentially remove K-feldspar more effectively than the aerosol generally. The second is that the wet and dry size dependent removal processes will preferentially remove larger aerosol and therefore the assumed size distribution of the K-feldspar will critically influence the transport of K-feldspar. Perlwitz et al. (2015) suggest that Atkinson et al. (2013) places too large a proportion of the K-feldspar content in the fine mode relative to the coarse mode, which results in too much transported K-feldspar. GLOMAP defines the size distribution of K-feldspar based on the mineralogical maps presented in Nickovic et al. (2012), which provides the coarse (silt) mode feldspar content, but not in the fine (clay) mode. An assumption is then made that the ratio of K-feldspar in the fine mode to the coarse mode is the same ratio as for quartz (which is reported by Nickovic et al. (2012)). Hence, the amount of K-feldspar which undergoes long range transport is likely to be dependent on the size distribution of K-feldspar at source, a term which is unfortunately poorly defined (Perlwitz et al., 2015). This is something that needs to be explored in the global model in more detail, ideally with measurements of the size resolved mineralogy at source and at remote locations such as Barbados.

With this said, although though we cannot quantitatively rule out the effect of acid ageing on the transported mineral dust at Barbados, the low amount of K-feldspar does appear to account for the full loss of activity observed. We therefore attribute the deactivation of the mineral dust at Barbados to the scavenging of K-feldspar and that the amount of sea salt may simply correlate with the time the aerosol spent over the ocean, and thus may also correlate with the depletion of K-feldspar. The scavenging of K-feldspar appears to be underrepresented in models leading to an over prediction of the K-feldspar content and therefore INP concentration.

This scavenging processes needs to be better constrained in climate models in order to improve predictions of INP.

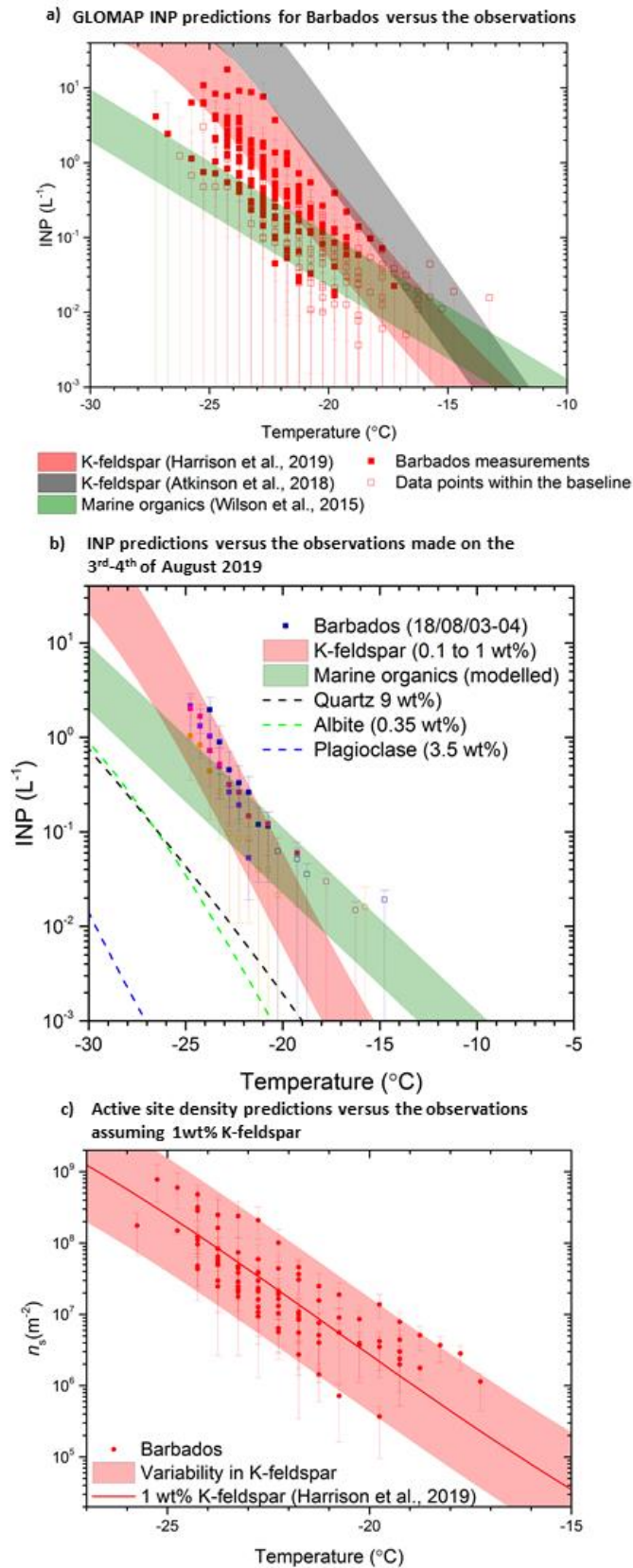


Figure 3.5: Predictions versus the observations at Barbados. Data points represented as hollow symbols have large uncertainties and are consistent with the baseline. a) GLOMAP INP concentration predictions for marine organics and K-feldspar based on various parameterisations along with the observed INP concentrations. b) Calculated INP concentrations using parameterisations for K-feldspar, plagioclase, quartz and albite developed by Harrison et al. (2019). The parameterisations are scaled using the XRD measurements in section 3.2 and K-feldspar is assumed to be 1 wt% - 0.1 wt%. The GLOMAP simulated INP concentration as a result of marine organics is also plotted. c) Predicted active site density (n_s) assuming 1 wt% K-feldspar using the Harrison et al. (2019) K-feldspar parameterisation. The red band demonstrates the variability in the ice-nucleating ability of K-feldspar as presented by Harrison et al. (2019). The observed n_s from this study is plotted for comparison with the data points consistent with the baseline excluded.

3.4 Conclusions

The measured INP concentration in Barbados is found to be 0.4 to 4 INP L⁻¹ at -24 °C. This is roughly one and a half orders of magnitude lower than measured in the eastern tropical Atlantic. The activity, expressed as active sites per unit surface area, of the mineral dust collected in Barbados is also lower than that measured in the ETA which suggests a deactivation of the dust during transport across the Atlantic Ocean. GLOMAP simulations over predict the observations at Barbados which we attribute to the over estimation of the K-feldspar content in the global model. The measured K-feldspar content (using XRD analysis of rain collected aerosol) is below 2 wt%. When the predictions of INP are scaled to this low content of K-feldspar a good agreement is found between the observations and the predictions. We hypothesise that removal of K-feldspar results in the reduction of the ice-nucleating ability of transported mineral dust at this location. This hypothesis may also explain observations by Si et al. (2019) and Iwata and Matsuki (2018) who correlate a reduction in INP activity with sea salt. The amount of sea salt may be related to the time the aerosol has been transported (over sea) and hence is a proxy for the degree of removal of K-feldspar. We therefore suggest that future studies take care in assessing the mineralogy of mineral dusts and incorporate accurate representations of mineral components in to models.

References

- Ansmann, A., Tesche, M., Seifert, P., Althausen, D., Engelmann, R., Fruntke, J., Wandinger, U., Mattis, I., and Müller, D.: Evolution of the ice phase in tropical altocumulus: SAMUM lidar observations over Cape Verde, *Journal of Geophysical Research: Atmospheres*, 114, D17208, 2009.
- Arnold, E., Merrill, J., Leinen, M., and King, J.: The effect of source area and atmospheric transport on mineral aerosol collected over the North Pacific Ocean, *Global and Planetary Change*, 18, 137-159, 1998.
- Atkinson, J. D., Murray, B. J., Woodhouse, M. T., Whale, T. F., Baustian, K. J., Carslaw, K. S., Dobbie, S., O'Sullivan, D., and Malkin, T. L.: The importance of feldspar for ice nucleation by mineral dust in mixed-phase clouds, *Nature*, 498, 355-358, 2013.
- Augustin-Bauditz, S., Wex, H., Kanter, S., Ebert, M., Niedermeier, D., Stolz, F., Prager, A., and Stratmann, F.: The immersion mode ice nucleation behavior of mineral dusts: A comparison of different pure and surface modified dusts, *Geophysical Research Letters*, 41, 7375-7382, 2014.
- Blank, M., Leinen, M., and Prospero, J. M.: Major Asian aeolian inputs indicated by the mineralogy of aerosols and sediments in the western North Pacific, *Nature*, 314, 84-86, 1985.
- Boose, Y., Baloh, P., Plötze, M., Ofner, J., Grothe, H., Sierau, B., Lohmann, U., and Kanji, Z. A.: Heterogeneous ice nucleation on dust particles sourced from nine deserts worldwide – Part 2: Deposition nucleation and condensation freezing, *Atmospheric Chemistry and Physics*, 19, 1059-1076, 2019.
- Boose, Y., Sierau, B., Garcia, I. M., Rodriguez, S., Alastuey, A., Linke, C., Schnaiter, M., Kupiszewski, P., Kanji, Z. A., and Lohmann, U.: Ice nucleating particles in the Saharan Air Layer, *Atmos. Chem. and Phys.*, 16, 9067-9087, 2016a.

Boose, Y., Welti, A., Atkinson, J., Ramelli, F., Danielczok, A., Bingemer, H. G., Plötze, M., Sierau, B., Kanji, Z. A., and Lohmann, U.: Heterogeneous ice nucleation on dust particles sourced from nine deserts worldwide – Part 1: Immersion freezing, *Atmospheric Chemistry and Physics*, 16, 15075-15095, 2016b.

Boucher, O., Randall, D., Artaxo, P., Bretherton, C., Feingold, G., Forster, P., Kerminen, V.-M., Kondo, Y., Liao, H., and Lohmann, U.: Clouds and aerosols. In: *Climate change 2013: The physical science basis. Contribution of working group I to the fifth assessment report of the intergovernmental panel on climate change*, Cambridge University Press, 2013.

Christner, B. C., Morris, C. E., Foreman, C. M., Cai, R., and Sands, D. C.: Ubiquity of biological ice nucleators in snowfall, *Science*, 319, 1214, 2008.

Connolly, P. J., Möhler, O., Field, P. R., Saathoff, H., Burgess, R., Choularton, T., and Gallagher, M.: Studies of heterogeneous freezing by three different desert dust samples, *Atmos. Chem. Phys.*, 9, 2805-2824, 2009.

Cziczo, D. J., DeMott, P. J., Brock, C., Hudson, P. K., Jesse, B., Kreidenweis, S. M., Prenni, A. J., Schreiner, J., Thomson, D. S., and Murphy, D. M.: A method for single particle mass spectrometry of ice nuclei, *Aerosol Science and Technology*, 37, 460-470, 2003.

DeMott, P. J., Hill, T. C., McCluskey, C. S., Prather, K. A., Collins, D. B., Sullivan, R. C., Ruppel, M. J., Mason, R. H., Irish, V. E., Lee, T., Hwang, C. Y., Rhee, T. S., Snider, J. R., McMeeking, G. R., Dhaniyala, S., Lewis, E. R., Wentzell, J. J., Abbatt, J., Lee, C., Sultana, C. M., Ault, A. P., Axson, J. L., Diaz Martinez, M., Venero, I., Santos-Figueroa, G., Stokes, M. D., Deane, G. B., Mayol-Bracero, O. L., Grassian, V. H., Bertram, T. H., Bertram, A. K., Moffett, B. F., and Franc, G. D.: Sea spray aerosol as a unique source of ice nucleating particles, *Proceedings of the National Academy of Sciences of the United States of America*, 113, 5797-5803, 2016.

DeMott, P. J., Prenni, A. J., Liu, X., Kreidenweis, S. M., Petters, M. D., Twohy, C. H., Richardson, M. S., Eidhammer, T., and Rogers, D. C.: Predicting global atmospheric ice nuclei distributions and their impacts on climate, *Proceedings of the National Academy of Sciences, USA*, 107, 11217-11222, 2010.

Emersic, C., Connolly, P. J., Boulton, S., Campana, M., and Li, Z.: Investigating the discrepancy between wet-suspension- and dry-dispersion-derived ice nucleation efficiency of mineral particles, *Atmos. Chem. Phys.*, 15, 11311-11326, 2015.

Eriksen Hammer, S., Mertes, S., Schneider, J., Ebert, M., Kandler, K., and Weinbruch, S.: Composition of ice particle residuals in mixed-phase clouds at Jungfrauoch (Switzerland): enrichment and depletion of particle groups relative to total aerosol, *Atmospheric Chemistry and Physics*, 18, 13987-14003, 2018.

Field, C. B., Barros, V. R., Mach, K. J., Mastrandrea, M. D., Aalst, M. v., Adger, W. N., Arent, D. J., Barnett, J., Betts, R., Bilir, T. E., Birkmann, J., Carmin, J., Chadee, D. D., Challinor, A. J., Chatterjee, M., Cramer, W., Davidson, D. J., Estrada, Y. O., Gattuso, J. P., Hijjoka, Y., Hoegh-Guldberg, O., Huang, H. Q., Insarov, G. E., Jones, R. N., Kovats, R. S., Lankao, P. R., Larsen, J. N., Losada, I. J., Marengo, J. A., McLean, R. F., Mearns, L. O., Mechler, R., Morton, J. F., Niang, I., Oki, T., Olwoch, J. M., Opondo, M., Poloczanska, E. S., Pörtner, H. O., Redster, M. H., Reisinger, A., Revi, A., Schmidt, D. N., Shaw, M. R., Solecki, W., Stone, D. A., Stone, J. M. R., Strzepek, K. M., Suarez, A. G., Tschakert, P., Valentini, R., Vicuña, S., Villamizar, A., Vincent, K. E., Warren, R., White, L. L., Wilbanks, T. J., Wong, P. P., and Yohe, G. W.: Technical Summary. In: *Climate Change 2014: Impacts, Adaptation, and Vulnerability. Part A: Global and Sectoral Aspects. Contribution of Working Group II to the Fifth Assessment Report of the Intergovernmental Panel on Climate Change*, Field, C. B., Barros, V. R., Dokken, D. J., Mach, K. J., Mastrandrea, M. D., Bilir, T. E., Chatterjee, M., Ebi, K. L., Estrada, Y. O., Genova, R. C., Girma, B., Kissel, E. S., Levy, A. N., MacCracken, S., Mastrandrea, P. R., and White, L. L. (Eds.), Cambridge University Press, Cambridge, United Kingdom and New York, NY, USA, 2014.

Garcia, E., Hill, T. C. J., Prenni, A. J., DeMott, P. J., Franc, G. D., and Kreidenweis, S. M.: Biogenic ice nuclei in boundary layer air over two U.S. High Plains agricultural regions, *Journal of Geophysical Research-Atmospheres*, 117, 2012.

Glaccum, R. A. and Prospero, J. M.: Saharan aerosols over the tropical North Atlantic — Mineralogy, *Marine Geology*, 37, 295-321, 1980.

Haarig, M., Walser, A., Ansmann, A., Dollner, M., Althausen, D., Sauer, D., Farrell, D., and Weinzierl, B.: CCN concentration and INP-relevant aerosol profiles in the Saharan Air Layer over Barbados from polarization lidar and airborne in situ measurements, *Atmospheric Chemistry and Physics Discussions*, doi: 10.5194/acp-2019-466, 2019. 1-24, 2019.

Harrison, A. D., Lever, K., Sanchez-Marroquin, A., Holden, M. A., Whale, T. F., Tarn, M. D., McQuaid, J. B., and Murray, B. J.: The ice-nucleating ability of quartz immersed in water and its atmospheric importance compared to K-feldspar, *Atmospheric Chemistry and Physics Discussions*, doi: 10.5194/acp-2019-288, 2019. 1-23, 2019.

Harrison, A. D., Whale, T. F., Carpenter, M. A., Holden, M. A., Neve, L., apos, Sullivan, D., Vergara Temprado, J., and Murray, B. J.: Not all feldspars are equal: a survey of ice nucleating properties across the feldspar group of minerals, *Atmospheric Chemistry and Physics*, 16, 10927-10940, 2016.

Herbert, R. J., Murray, B. J., Dobbie, S. J., and Koop, T.: Sensitivity of liquid clouds to homogenous freezing parameterizations, *Geophysical Research Letters*, 42, 1599-1605, 2015.

Hillier, S.: Quantitative Analysis of Clay and other Minerals in Sandstones by X-Ray Powder Diffraction (XRPD), doi: 10.1002/9781444304336.ch11, 1999. 213-251, 1999.

Hoose, C., Kristjánsson, J., and Burrows, S.: How important is biological ice nucleation in clouds on a global scale?, *Environmental Research Letters*, 5, 024009, 2010.

Iwata, A. and Matsuki, A.: Characterization of individual ice residual particles by the single droplet freezing method: a case study in the Asian dust outflow region, *Atmospheric Chemistry and Physics*, 18, 1785-1804, 2018.

Kandler, K., Schneiders, K., Ebert, M., Hartmann, M., Weinbruch, S., Prass, M., and Pöhlker, C.: Composition and mixing state of atmospheric aerosols determined by electron microscopy: method development and application to aged Saharan dust deposition in the Caribbean boundary layer, *Atmospheric Chemistry and Physics*, 18, 13429-13455, 2018.

Kandler, K., SchÜTZ, L., JÄCKel, S., Lieke, K., Emmel, C., MÜLLer-Ebert, D., Ebert, M., Scheuven, D., Schladitz, A., ŠEgviĆ, B., Wiedensohler, A., and Weinbruch, S.: Ground-based off-line aerosol measurements at Praia, Cape Verde, during the Saharan Mineral Dust Experiment: microphysical properties and mineralogy, *Tellus*, 63B, 459-474, 2011.

Koehler, K. A., Kreidenweis, S. M., DeMott, P. J., Petters, M. D., Prenni, A. J., and Möhler, O.: Laboratory investigations of the impact of mineral dust aerosol on cold cloud formation, *Atmospheric Chemistry and Physics*, 10, 11955-11968, 2010.

Kumar, A., Marcolli, C., Luo, B., and Peter, T.: Ice nucleation activity of silicates and aluminosilicates in pure water and aqueous solutions – Part 1: The K-feldspar microcline, *Atmospheric Chemistry and Physics*, 18, 7057-7079, 2018.

Kumar, A., Marcolli, C., and Peter, T.: Ice nucleation activity of silicates and aluminosilicates in pure water and aqueous solutions – Part 3: Aluminosilicates, *Atmospheric Chemistry and Physics*, 19, 6059-6084, 2019.

Leinen, M., Prospero, J. M., Arnold, E., and Blank, M.: Mineralogy of aeolian dust reaching the north Pacific-Ocean. 1. Sampling and analysis, *J. Geophys. Res.*, 99, 21017-21023, 1994.

Lohmann, U., Koren, I., and Kaufman, Y. J.: Disentangling the role of microphysical and dynamical effects in determining cloud properties over the Atlantic, *Geophysical Research Letters*, 33, 2006.

Maters, E. C., Dingwell, D. B., Cimorelli, C., Müller, D., Whale, T. F., and Murray, B. J.: The importance of crystalline phases in ice nucleation by volcanic ash, *Atmospheric Chemistry and Physics*, 19, 5451-5465, 2019.

Möhler, O., Benz, S., Saathoff, H., Schnaiter, M., Wagner, R., Schneider, J., Walter, S., Ebert, V., and Wagner, S.: The effect of organic coating on the heterogeneous ice nucleation efficiency of mineral dust aerosols, *Environmental Research Letters*, 3, 2008.

Murray, B. J., O'Sullivan, D., Atkinson, J. D., and Webb, M. E.: Ice nucleation by particles immersed in supercooled cloud droplets, *Chemical Society Reviews*, 41, 6519-6554, 2012.

Nickovic, S., Vukovic, A., Vujadinovic, M., Djurdjevic, V., and Pejanovic, G.: Technical Note: High-resolution mineralogical database of dust-productive soils for atmospheric dust modeling, *Atmos. Chem. Phys.*, 12, 845-855, 2012.

Niedermeier, D., Augustin-Bauditz, S., Hartmann, S., Wex, H., Ignatius, K., and Stratmann, F.: Can we define an asymptotic value for the ice active surface site density for heterogeneous ice nucleation?, *Journal of Geophysical Research: Atmospheres*, 120, 5036-5046, 2015.

Niemand, M., Möhler, O., Vogel, B., Vogel, H., Hoose, C., Connolly, P., Klein, H., Bingemer, H., DeMott, P. J., Skrotzki, J., and Leisner, T.: A particle-surface-area-based parameterization of immersion freezing on desert dust particles, *Journal of the Atmospheric Sciences*, 69, 2012.

O'Sullivan, D., Adams, M. P., Tarn, M. D., Harrison, A. D., Vergara-Temprado, J., Porter, G. C. E., Holden, M. A., Sanchez-Marroquin, A., Carotenuto, F., Whale, T. F., McQuaid, J. B., Walshaw, R., Hedges, D. H. P., Burke, I. T., Cui, Z., and Murray, B. J.: Contributions of biogenic material to the atmospheric ice-nucleating particle population in North Western Europe, *Sci Rep*, 8, 13821, 2018.

O'Sullivan, D., Murray, B. J., Malkin, T. L., Whale, T. F., Umo, N. S., Atkinson, J. D., Price, H. C., Baustian, K. J., Browse, J., and Webb, M. E.: Ice nucleation by fertile soil dusts: relative importance of mineral and biogenic components, *Atmos. Chem. Phys.*, 14, 1853-1867, 2014.

Pachauri, R. K., Allen, M. R., Barros, V. R., Broome, J., Cramer, W., Christ, R., Church, J. A., Clarke, L., Dahe, Q., Dasgupta, P., Dubash, N. K., Edenhofer, O., Elgizouli, I., Field, C. B., Forster, P., Friedlingstein, P., Fuglestvedt, J., Gomez-Echeverri, L., Hallegatte, S., Hegerl, G., Howden, M., Jiang, K., Jimenez Cisneroz, B., Kattsov, V., Lee, H., Mach, K. J., Marotzke, J., Mastrandrea, M. D., Meyer, L., Minx, J., Mulugetta, Y., O'Brien, K., Oppenheimer, M., Pereira, J. J., Pichs-Madruga, R., Plattner, G. K., Pörtner, H. O., Power, S. B., Preston, B., Ravindranath, N. H., Reisinger, A., Riahi, K., Rusticucci, M., Scholes, R., Seyboth, K., Sokona, Y., Stavins, R., Stocker, T. F., Tschakert, P., van Vuuren, D., and van Ypserle, J. P.: *Climate Change 2014: Synthesis Report. Contribution of Working Groups I, II and III to the Fifth Assessment Report of the Intergovernmental Panel on Climate Change*, IPCC, Geneva, Switzerland, 2014.

Peckhaus, A., Kiselev, A., Hiron, T., Ebert, M., and Leisner, T.: A comparative study of K-rich and Na/Ca-rich feldspar ice-nucleating

particles in a nanoliter droplet freezing assay, *Atmospheric Chemistry and Physics*, 16, 11477-11496, 2016.

Perlwitz, J. P., Pérez García-Pando, C., and Miller, R. L.: Predicting the mineral composition of dust aerosols – Part 1: Representing key processes, *Atmos. Chem. Phys.*, 15, 11593-11627, 2015.

Pratt, K. A., DeMott, P. J., French, J. R., Wang, Z., Westphal, D. L., Heymsfield, A. J., Twohy, C. H., Prenni, A. J., and Prather, K. A.: In situ detection of biological particles in cloud ice-crystals, *Nature Geosci*, 2, 398-401, 2009.

Price, H. C., Baustian, K. J., McQuaid, J. B., Blyth, A., Bower, K. N., Choulaton, T., Cotton, R. J., Cui, Z., Field, P. R., Gallagher, M., Hawker, R., Merrington, A., Miltenberger, A., Neely Iii, R. R., Parker, S. T., Rosenberg, P. D., Taylor, J. W., Trembath, J., Vergara-Temprado, J., Whale, T. F., Wilson, T. W., Young, G., and Murray, B. J.: Atmospheric Ice-Nucleating Particles in the Dusty Tropical Atlantic, *Journal of Geophysical Research: Atmospheres*, 123, 2175-2193, 2018.

Prospero, J. M.: Mineral and sea salt aerosol concentrations in various ocean regions, *Journal of Geophysical Research*, 84, 725, 1979.

Prospero, J. M., Bullard, J. E., and Hodgkins, R.: High-Latitude Dust Over the North Atlantic: Inputs from Icelandic Proglacial Dust Storms, *Science*, 335, 1078-1082, 2012.

Pruppacher, H. R. and Klett, J. D.: *Microphysics of Clouds and Precipitation*, Kluwer Academic Publishers, 1997.

Reicher, N., Segev, L., and Rudich, Y.: The Weizmann Supercooled Droplets Observation on a Microarray (WISDOM) and application for ambient dust, *Atmospheric Measurement Techniques*, 11, 233-248, 2018.

Riechers, B., Wittbracht, F., Hütten, A., and Koop, T.: The homogeneous ice nucleation rate of water droplets produced in a microfluidic device and the role of temperature uncertainty, *Physical Chemistry Chemical Physics*, 15, 5873-5887, 2013.

Sanchez-Marroquin, A., Hedges, D. H. P., Hiscock, M., Parker, S. T., Rosenberg, P. D., Trembath, J., Walshaw, R., Burke, I. T., McQuaid, J. B., and Murray, B. J.: Characterisation of the filter inlet system on the BAE-146 research aircraft and its use for size resolved aerosol composition measurements, *Atmospheric Measurement Techniques Discussions*, doi: 10.5194/amt-2019-196, 2019. 1-35, 2019.

Si, M., Evoy, E., Yun, J., Xi, Y., Hanna, S. J., Chivulescu, A., Rawlings, K., Veber, D., Platt, A., Kunkel, D., Hoor, P., Sharma, S., Leitch, W. R., and Bertram, A. K.: Concentrations, composition, and sources of ice-nucleating particles in the Canadian High Arctic, *Atmos. Chem. and Phys.*, 19, 3007-3024, 2019.

Stopelli, E., Conen, F., Zimmermann, L., Alewell, C., and Morris, C. E.: Freezing nucleation apparatus puts new slant on study of biological ice nucleators in precipitation, *Atmospheric Measurement Techniques*, 7, 129-134, 2014.

Storelvmo, T., Hoose, C., and Eriksson, P.: Global modeling of mixed-phase clouds: The albedo and lifetime effects of aerosols, *Journal of Geophysical Research: Atmospheres*, 116, D05207, 2011.

Sullivan, R. C., Petters, M. D., DeMott, P. J., Kreidenweis, S. M., Wex, H., Niedermeier, D., Hartmann, S., Clauss, T., Stratmann, F., Reitz, P., Schneider, J., and Sierau, B.: Irreversible loss of ice nucleation active sites in mineral dust particles caused by sulphuric acid condensation, *Atmos. Chem. Phys.*, 10, 11471-11487, 2010.

Tan, I., Storelvmo, T., and Zelinka, M. D.: Observational constraints on mixed-phase clouds imply higher climate sensitivity, *Science*, 352, 224-227, 2016.

Ullrich, R., Hoose, C., Möhler, O., Niemand, M., Wagner, R., Höhler, K., Hiranuma, N., Saathoff, H., and Leisner, T.: A New Ice Nucleation Active Site Parameterization for Desert Dust and Soot, *Journal of the Atmospheric Sciences*, 74, 699-717, 2017.

Vali, G., DeMott, P. J., Möhler, O., and Whale, T. F.: Technical Note: A proposal for ice nucleation terminology, *Atmos. Chem. Phys.*, 15, 10263-10270, 2015.

Velasco-Merino, C., Mateos, D., Toledano, C., Prospero, J. M., Molinie, J., Euphrasie-Clotilde, L., González, R., Cachorro, V. E., Calle, A., and de Frutos, A. M.: Impact of long-range transport over the Atlantic Ocean on Saharan dust optical and microphysical properties based on AERONET data, *Atmospheric Chemistry and Physics*, 18, 9411-9424, 2018.

Vergara-Temprado, J., Murray, B. J., Wilson, T. W., amp, apos, Sullivan, D., Browse, J., Pringle, K. J., Ardon-Dryer, K., Bertram, A. K., Burrows, S. M., Ceburnis, D., DeMott, P. J., Mason, R. H., amp, apos, Dowd, C. D., Rinaldi, M., and Carslaw, K. S.: Contribution of feldspar and marine organic aerosols to global ice nucleating particle concentrations, *Atmos. Chem. Phys.*, 17, 3637-3658, 2017.

Wex, H., DeMott, P. J., Tobo, Y., Hartmann, S., Rösch, M., Clauss, T., Tomsche, L., Niedermeier, D., and Stratmann, F.: Kaolinite particles as ice nuclei: learning from the use of different kaolinite samples and different coatings, *Atmos. Chem. Phys.*, 14, 5529-5546, 2014.

Whale, T. F., Holden, M. A., Wilson, T. W., O'Sullivan, D., and Murray, B. J.: The enhancement and suppression of immersion mode heterogeneous ice-nucleation by solutes, *Chem Sci*, 9, 4142-4151, 2018.

Whale, T. F., Murray, B. J., O'Sullivan, D., Wilson, T. W., Umo, N. S., Baustian, K. J., Atkinson, J. D., Workneh, D. A., and Morris, G. J.: A technique for quantifying heterogeneous ice nucleation in microlitre supercooled water droplets, *Atmos. Meas. Tech.*, 8, 2437-2447, 2015.

Wilson, T. W., Ladino, L. A., Alpert, P. A., Breckels, M. N., Brooks, I. M., Browse, J., Burrows, S. M., Carslaw, K. S., Huffman, J. A., Judd, C., Kilhau, W. P., Mason, R. H., McFiggans, G., Miller, L. A., Najera, J. J., Polishchuk, E., Rae, S., Schiller, C. L., Si, M., Temprado, J. V., Whale, T. F., Wong, J. P. S., Wurl, O., Yakobi-Hancock, J. D., Abbatt, J. P. D., Aller, J. Y., Bertram, A. K., Knopf, D. A., and Murray, B. J.: A marine biogenic source of atmospheric ice-nucleating particles, *Nature*, 525, 234-238, 2015.

Zolles, T., Burkart, J., Häusler, T., Pummer, B., Hitzemberger, R., and Grothe, H.: Identification of Ice Nucleation Active Sites on Feldspar Dust Particles, *The Journal of Physical Chemistry A*, 119, 2692-2700, 2015.

Supporting information for:

Ice-nucleating activity of desert dust decreases on transport across the Atlantic

A. D. Harrison¹, D. O'Sullivan¹, M. P. Adams¹, G. C. E. Porter¹, C. Brathwaite², R. Chewitt-Lucas², R. Hawker¹, O. O. Krueger^{3,4}, L. Neve¹, M. L. Pohlker³, C. Pohlker^{3,4}, U. Poschl^{3,4}, J. M. Prospero⁵, A. Sanchez-Marroquin¹, A. Sealy², P. Sealy², M. D. Tarn¹, S. Whitehall², J. B. McQuaid¹ and B. J. Murray¹

¹ School of Earth and Environment, University of Leeds, Leeds, England

²Caribbean Institute of Meteorology and Hydrology, Bridgetown, Barbados

³Max Planck Institute of Chemistry, Biogeochemistry Department, Mainz, Germany

⁴Max Planck Institute of Chemistry, Multiphase Chemistry Department, Mainz, Germany

⁵Rosenstiel School of Marine and Atmospheric Science, University of Miami, Miami, U.S.A

Contents of this file

Table S1

Text S1

Figures S1 to S11

Introduction

Table S1 provides the start and end times for all the filters during the campaign and the corresponding symbols used to represent the collected filters in figure 2a. Text S1 describes the methodology for creating a fit to the background INP signal for the experiments during the campaign and then the methodology to subtract this background and calculate the subsequent errors. Figures S1-3 are relatable to Text S1. Figure S4 shows back trajectories for the aerosol collected on to filters during the campaign. Figure S5 shows the heat sensitivity of aerosol suspensions collected during the campaign. Figure S6 shows a time series of the INP

concentration and meteorological conditions for the duration of the campaign. SEM and XRD analysis are shown in Figures S7 and S8. The ratio of K-feldspar to overall desert dust aerosol across the globe (as modelled by GLOMAP) is presented in Figure S9. The GLOMAP simulated aerosol mass (μgm^{-3}) versus the observed aerosol mass recorded via the APS during the campaign is shown in Figure S10. Results showing the solute effect of sea salt on K-feldspar (with sea salt concentrations relevant for the collected filter samples in this study) are presented in Figure S11.

Symbol	Start	End	Vol. Air sampled (Litres)	Aerosol surface area ($\mu\text{m}^2 \text{cm}^{-3}$)
■	24/08/17 11:30	24/08/17 18:00	6513	30.2
■	19/08/17 16:15	19/08/17 18:44	2488	N/A
■	19/08/17 11:16	19/08/17 16:06	4843	N/A
■	17/08/17 15:43	17/08/17 18:31	2805	N/A
■	17/08/17 11:02	18/08/17 11:17	24299	N/A
■	16/08/17 20:31	17/08/17 05:15	8750	N/A
■	15/08/17 20:38	15/08/17 23:02	2405	35.9
■	15/08/17 15:40	15/08/17 23:24	7749	40.0
■	13/08/17 13:40	14/08/17 02:31	12876	11.3
■	13/08/17 16:34	13/08/17 17:41	1119	13.0
■	10/08/17 02:05	10/08/17 05:37	3540	N/A
■	09/08/17 18:56	10/08/17 05:46	10855	N/A
■	09/08/17 10:15	09/08/17 12:57	2705	N/A
■	04/08/17 18:42	05/08/17 10:16	15598	N/A
■	04/08/17 10:21	04/08/17 18:37	8283	N/A
■	04/08/17 10:07	04/08/17 18:40	8567	N/A
■	03/08/17 09:49	03/08/17 19:27	9653	12.5
■	02/08/17 14:32	02/08/17 16:50	2305	24.1
■	02/08/17 10:44	02/08/17 20:47	10070	26.4
■	02/08/17 10:43	02/08/17 14:28	3758	29.1
■	01/08/17 10:20	01/08/17 22:50	12525	32.8
■	31/07/17 16:22	01/08/17 06:42	14362	25.9
■	31/07/17 16:22	31/07/17 18:05	1720	21.1
■	31/07/17 09:09	31/07/17 16:19	7164	20.5
■	29/07/17 14:47	31/07/17 03:08	36423	16.0
■	27/07/17 12:05	28/07/17 09:41	21643	19.0
■	26/07/17 10:15	27/07/17 11:44	25534	N/A
■	24/07/17 08:31	24/07/17 16:17	7766	35.2

Table S1: Sampling durations and the volume of air sampled for 28 runs and their corresponding symbols used in figure 3.2a.

Text S1. Background subtraction and errors calculation

To determine the contribution of impurities to the overall INP signal of the collected aerosol samples we first collated all of the blanks and handling blanks into a single dataset and produced a polynomial fit to represent the baseline. This was done by binning all of the data for the individual blank runs into 0.5 °C temperature intervals and calculating $k(T)$, the active site density per unit volume per temperature interval. Equation 1 was used to calculate $k(T)$:

$$k(T) = -\frac{1}{v \cdot \Delta T} \cdot \ln\left(1 - \frac{\Delta N}{N(T)}\right) \quad \text{Equation 1}$$

Where v is the volume of the droplets used, ΔT is the change in temperature (the temperature interval), ΔN is the number of droplets which have frozen in the temperature interval and N is the total number of droplets.

Temperature intervals which saw a freezing event occur but were separated from the bulk of the data by more than 1 °C were removed from the overall compilation of the baseline data as these data points had large uncertainties.

Once compiled, a polynomial fit to the data was applied and the standard deviation determined. The best approximation of the baseline was found to be $\log(k(T)) = -1.57 \times 10^{-2} T^2 - 9.46T - 11.22$, with a standard deviation of ± 0.3 , Figure S1.

The aerosol data was then binned (into 0.5 °C intervals) and $k(T)$ calculated and plotted against this representation of the baseline along with the associated errors. A code similar to that presented by Vali (2019) is used to calculate the errors for the temperature intervals by running a monte carlo simulation and calculating a Poisson distribution to find one standard deviation centred around the mean number of freezing events in the interval (the mean is assumed to be the same number as the number of recorded events in the temperature interval during the experiment). These error bars are then used to determine whether a data point is significantly above the baseline signal. If the $k(T)$ value of the data point, or the lower error bar, overlap with the one standard deviation band of the baseline then it is assumed that this data point is not statistically above the baseline, see Figure S2. Figure S2 shows two examples of aerosol

collected data versus the baseline (one example for a sample which falls completely within the baseline and one example for a sample which is mostly above the baseline).

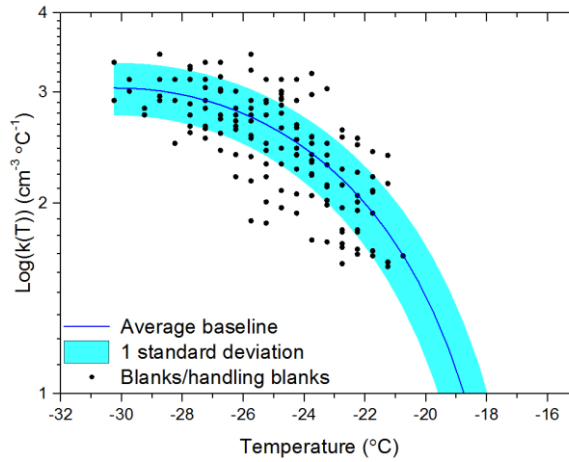


Figure S1: $\text{Log}(k(T))$ for the baselines of the experiments and the exponential fit and standard deviation used to represent the baseline in subsequent error calculations and background subtractions.

The data points which are not statistically above the baseline are noted so they may be represented as uncertain data points in the final plots. The data is then background subtracted using the previously calculated representation of the baseline.

To calculate the error bars for the background subtracted data the standard deviation in the baseline is combined with the Poisson errors to determine the overall error. A quadratic summation of the errors is used to achieve this, equation 2.

$$\text{Error}_{\text{Tot}} = \sqrt{\text{Error}_{\text{bas}}^2 + \text{Error}_{\text{pos}}^2} \quad \text{Equation 2}$$

Where $\text{Error}_{\text{bas}}$ is the error calculated for the baseline (the standard deviation in the baseline signal) and $\text{Error}_{\text{pos}}$ is the error calculated through the monte carlo simulations to represent the Poisson distribution.

These errors are then converted into the cumulative expression $K(T)$ (active sites per unit volume) through their summation, see Figure 34. This then allows for the errors to be calculated in other cumulative expressions such as $\text{INP} (\text{L}^{-1})$ and n_s .

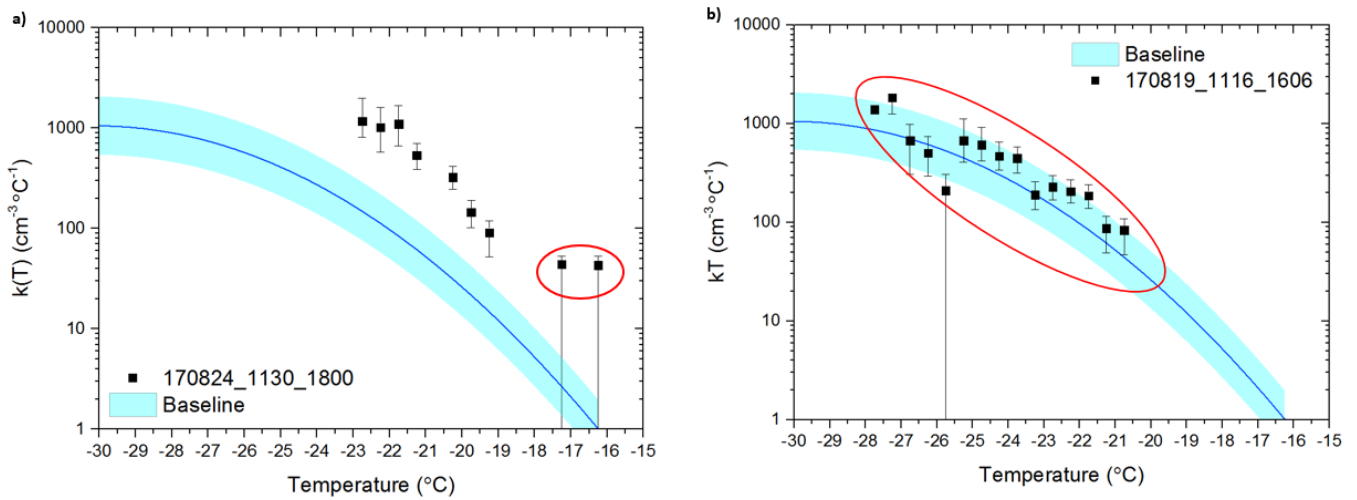


Figure S2: $k(T)$ versus temperature for two examples of collected aerosol. Also plotted is the representation of the baseline (background impurities). Data points which are highlighted by a red oval are thought to not be statistically above the background signal. a) An example when the majority of the data points are above the baseline. The first two freezing events (outlined by the red oval) have large uncertainties and so cannot be said to be statistically above the baseline. b) An example where the INP signal is not significantly above the background signal and so all data points are consistent with the baseline.

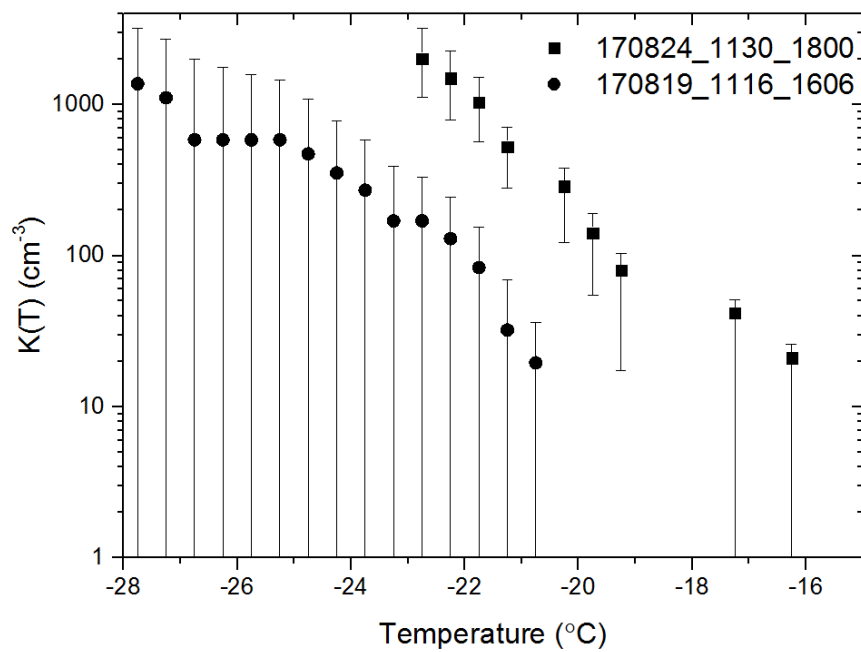
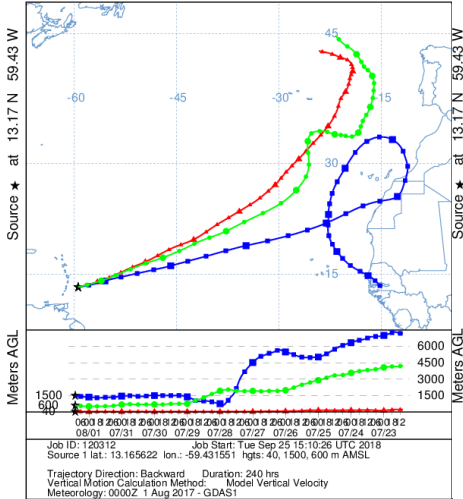
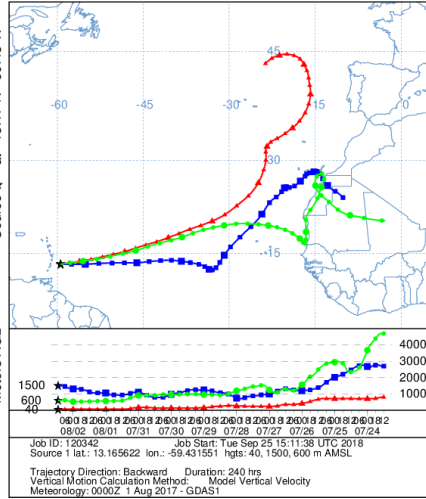


Figure S3: The calculated $K(T)$ values for the examples from Figure S2 and their corresponding errors.

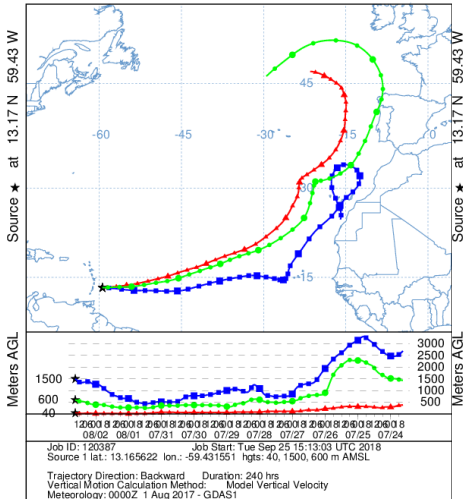
NOAA HYSPLIT MODEL
Backward trajectories ending at 1000 UTC 01 Aug 17
GDAS Meteorological Data



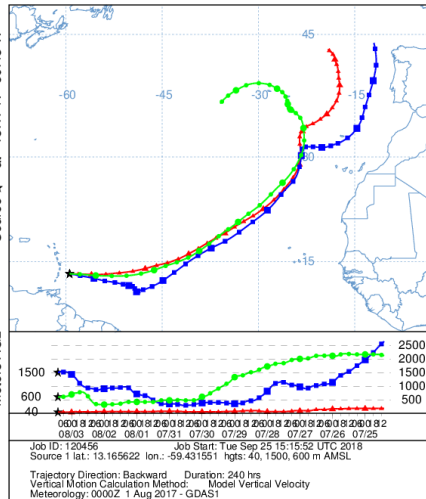
NOAA HYSPLIT MODEL
Backward trajectories ending at 1100 UTC 02 Aug 17
GDAS Meteorological Data



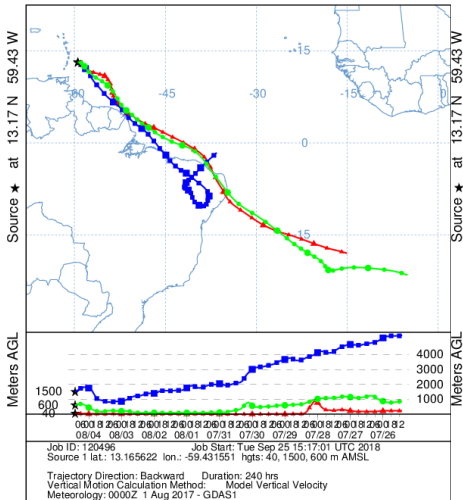
NOAA HYSPLIT MODEL
Backward trajectories ending at 1500 UTC 02 Aug 17
GDAS Meteorological Data



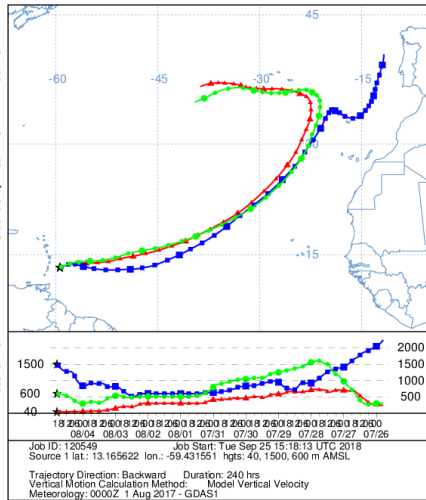
NOAA HYSPLIT MODEL
Backward trajectories ending at 1000 UTC 03 Aug 17
GDAS Meteorological Data



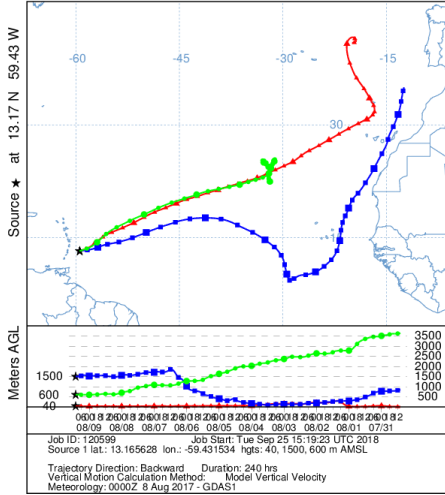
NOAA HYSPLIT MODEL
Backward trajectories ending at 1000 UTC 04 Aug 17
GDAS Meteorological Data



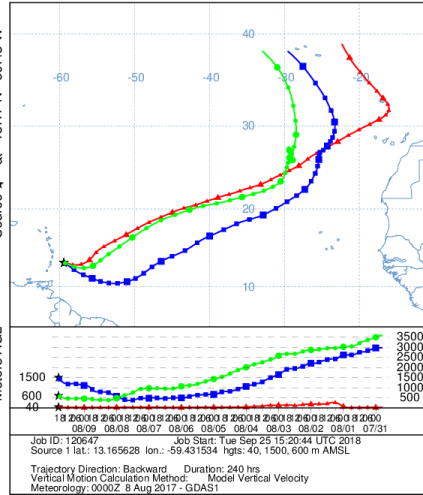
NOAA HYSPLIT MODEL
Backward trajectories ending at 1900 UTC 04 Aug 17
GDAS Meteorological Data



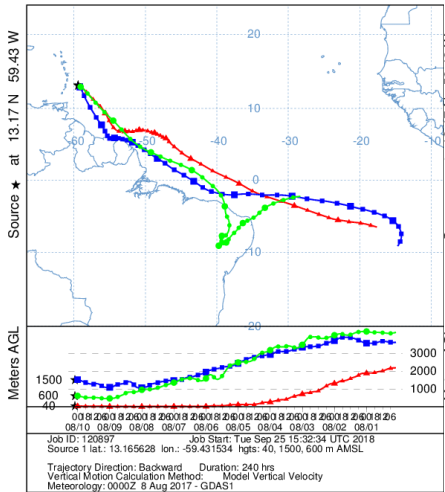
NOAA HYSPLIT MODEL
Backward trajectories ending at 1000 UTC 09 Aug 17
GDAS Meteorological Data



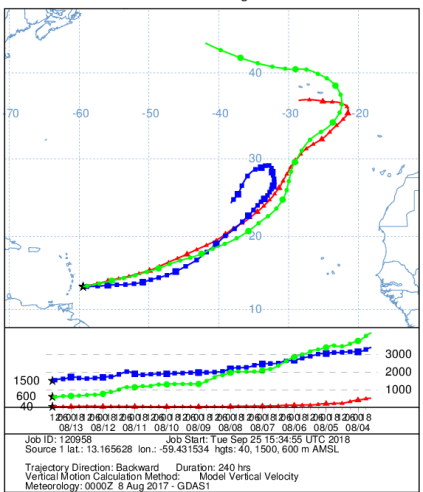
NOAA HYSPLIT MODEL
Backward trajectories ending at 1900 UTC 09 Aug 17
GDAS Meteorological Data



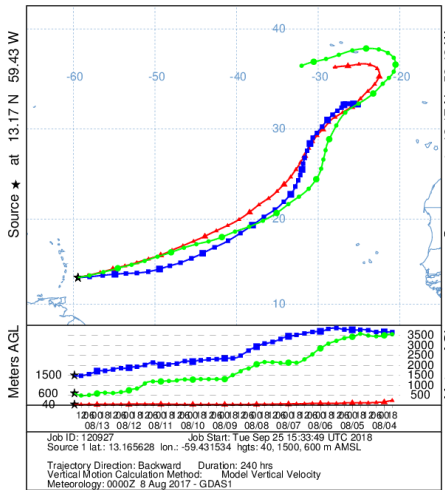
NOAA HYSPLIT MODEL
Backward trajectories ending at 0200 UTC 10 Aug 17
GDAS Meteorological Data



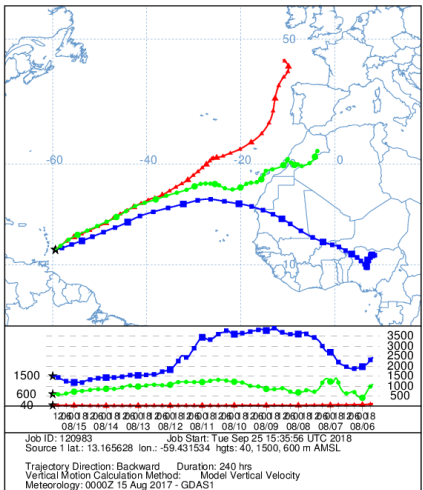
NOAA HYSPLIT MODEL
Backward trajectories ending at 1400 UTC 13 Aug 17
GDAS Meteorological Data



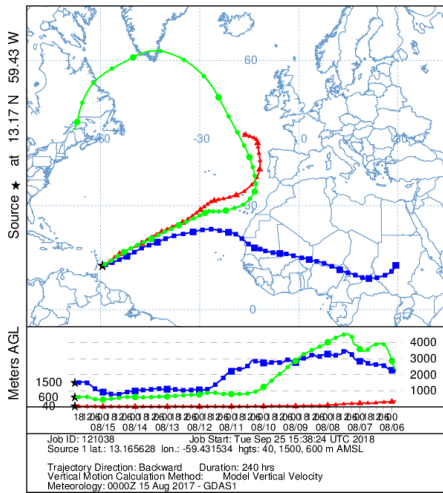
NOAA HYSPLIT MODEL
Backward trajectories ending at 1700 UTC 13 Aug 17
GDAS Meteorological Data



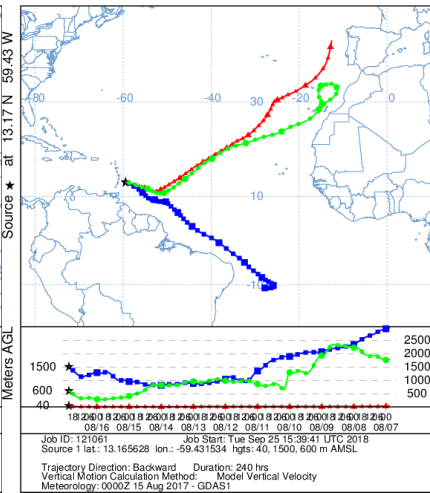
NOAA HYSPLIT MODEL
Backward trajectories ending at 1600 UTC 15 Aug 17
GDAS Meteorological Data



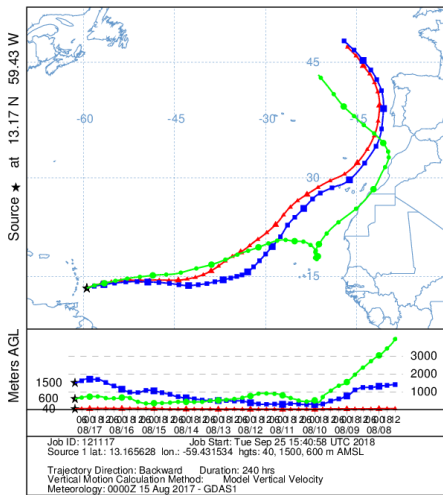
NOAA HYSPLIT MODEL
Backward trajectories ending at 2100 UTC 15 Aug 17
GDAS Meteorological Data



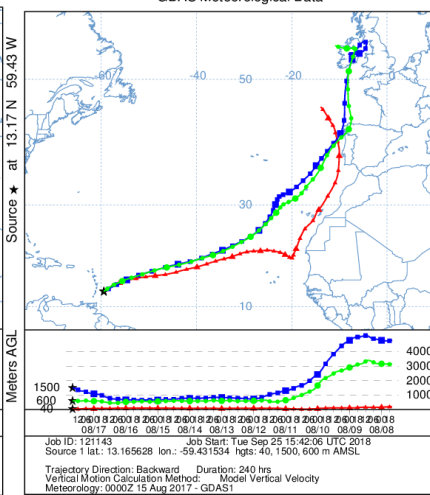
NOAA HYSPLIT MODEL
Backward trajectories ending at 2100 UTC 16 Aug 17
GDAS Meteorological Data



NOAA HYSPLIT MODEL
Backward trajectories ending at 1100 UTC 17 Aug 17
GDAS Meteorological Data



NOAA HYSPLIT MODEL
Backward trajectories ending at 1600 UTC 17 Aug 17
GDAS Meteorological Data



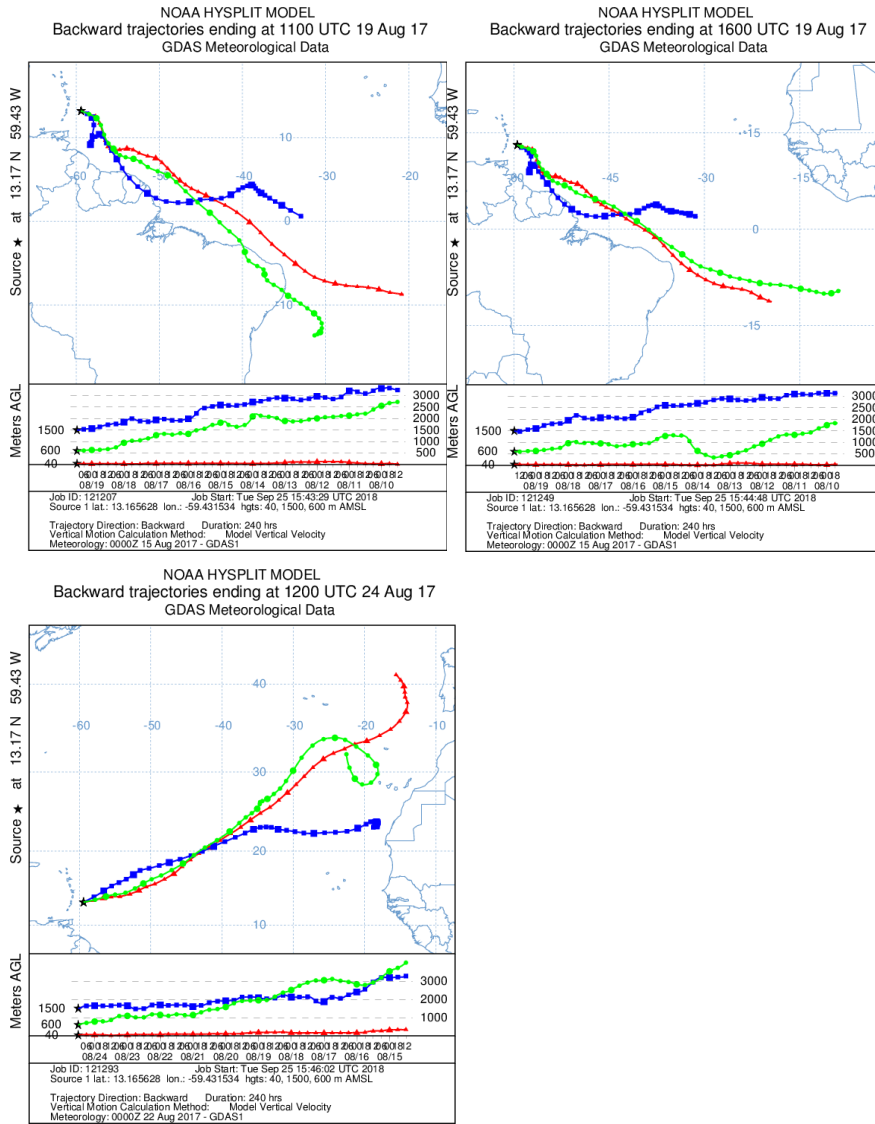


Figure S4: HYSPLIT back trajectories for the date and times of the filter samples in this study. Altitudes of 40m, 600m, and 1500m were chosen to represent the sampling height, boundary layer and Saharan air layer respectively.

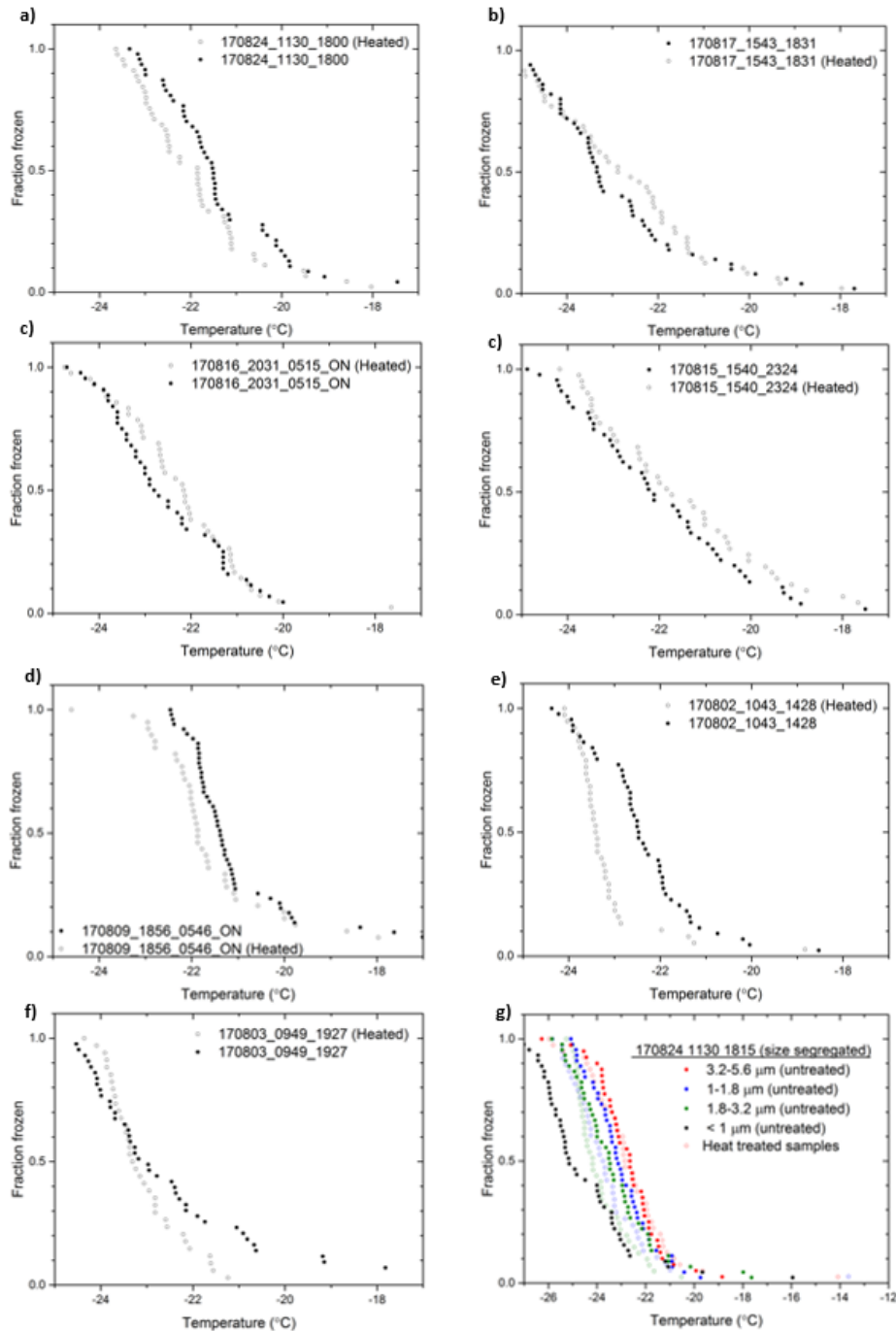


Figure S5: The fraction frozen curves for heated versus unheated suspensions. a-f) Fraction frozen curves for heated and unheated aerosol suspensions collected from the MESA PQ100 samplers with an aerosol cut off diameter of roughly 10 μm . g) Fraction frozen curves for heated versus unheated suspensions of size segregated aerosol in a MOUDI cascade impactor.

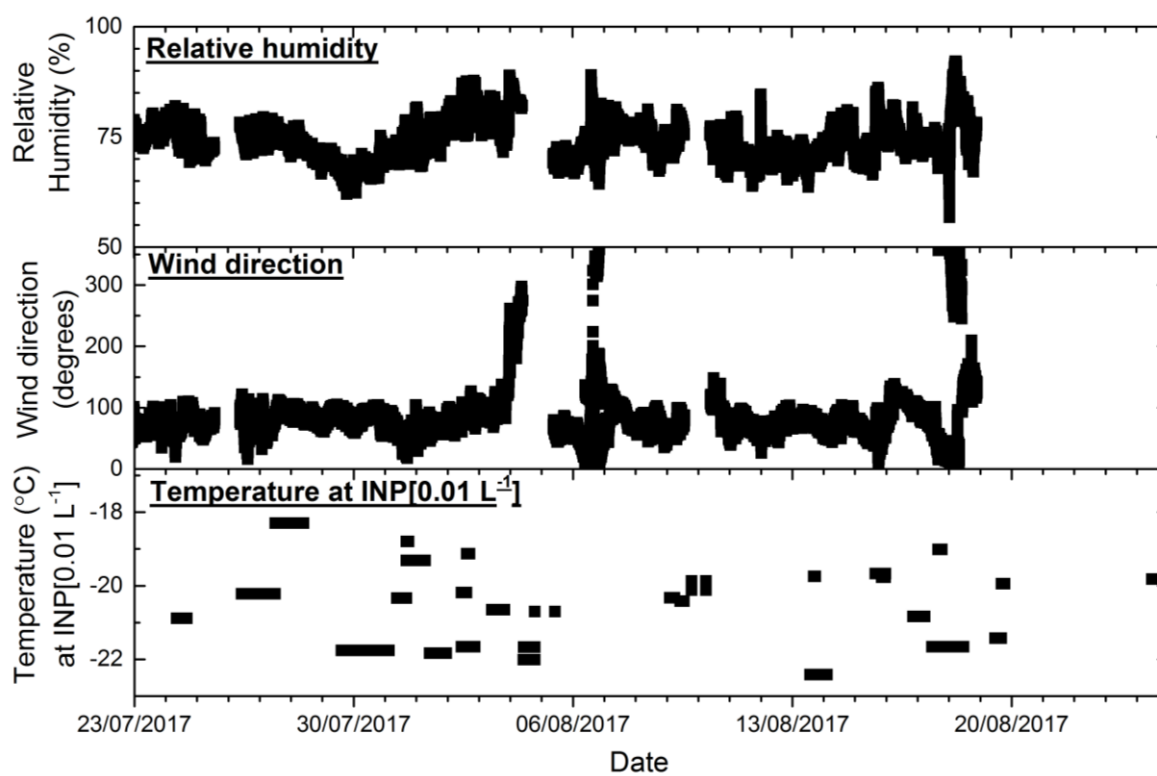


Figure S6: Time series for the relative humidity, wind direction and INP(T) at 0.01L^{-1} . It should be noted that the INP concentration has not been background subtracted in this plot.

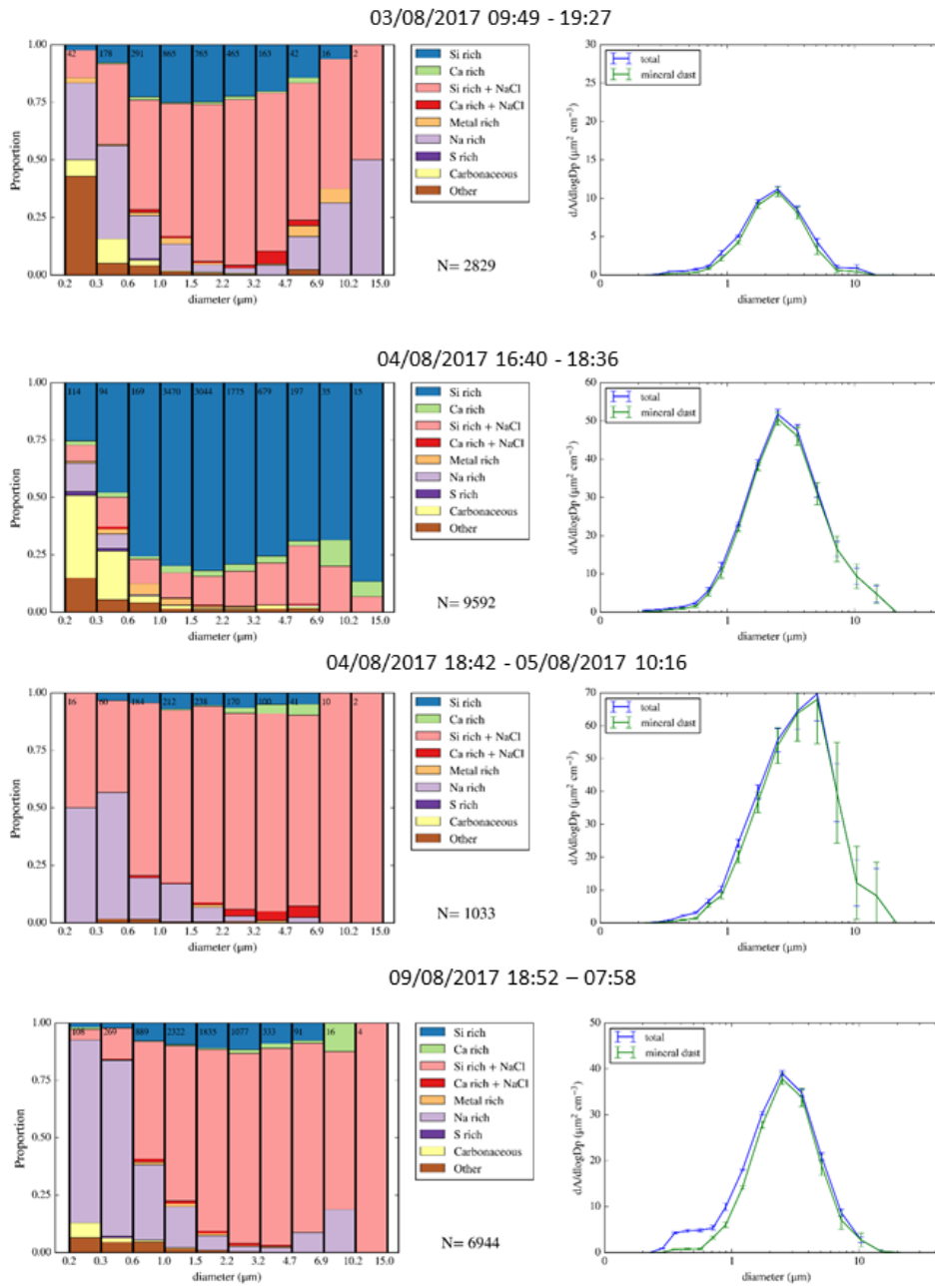


Figure S7: Compilation of the sized resolved composition and the contribution of mineral dust to the overall surface area retrieved from SEM analysis of four aerosol filter samples. N is the number of particles analysed on each filter.

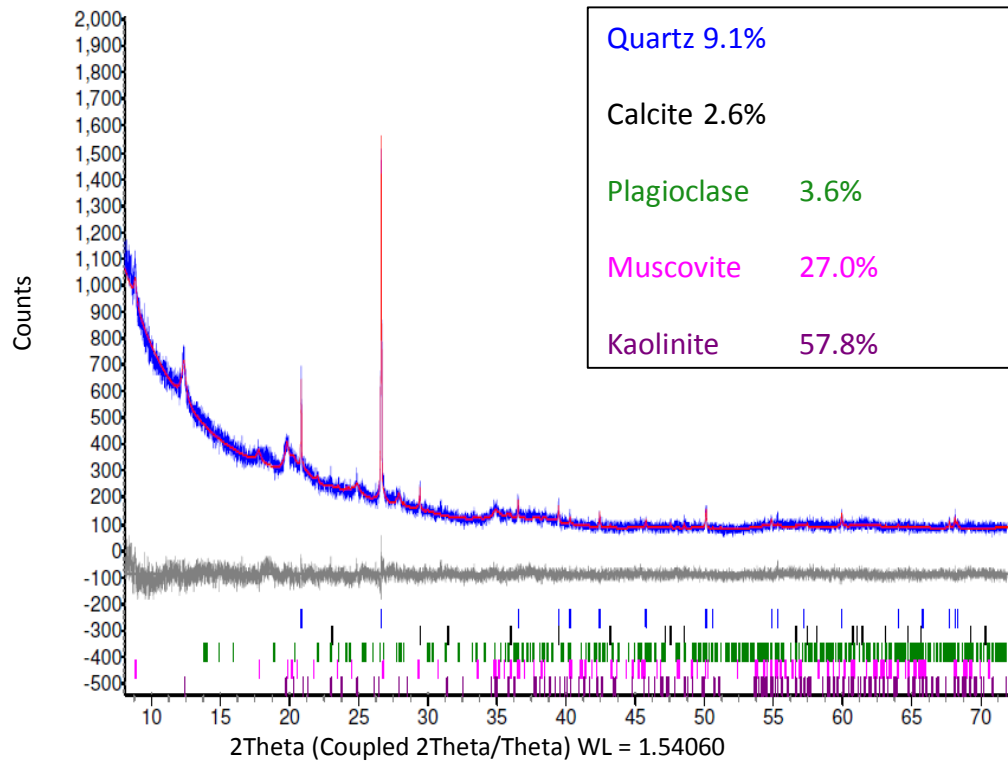


Figure S8: XRD analysis of aerosol collected in rain water from the 3rd-4th of August. The limit of detection of this technique was ~2%.

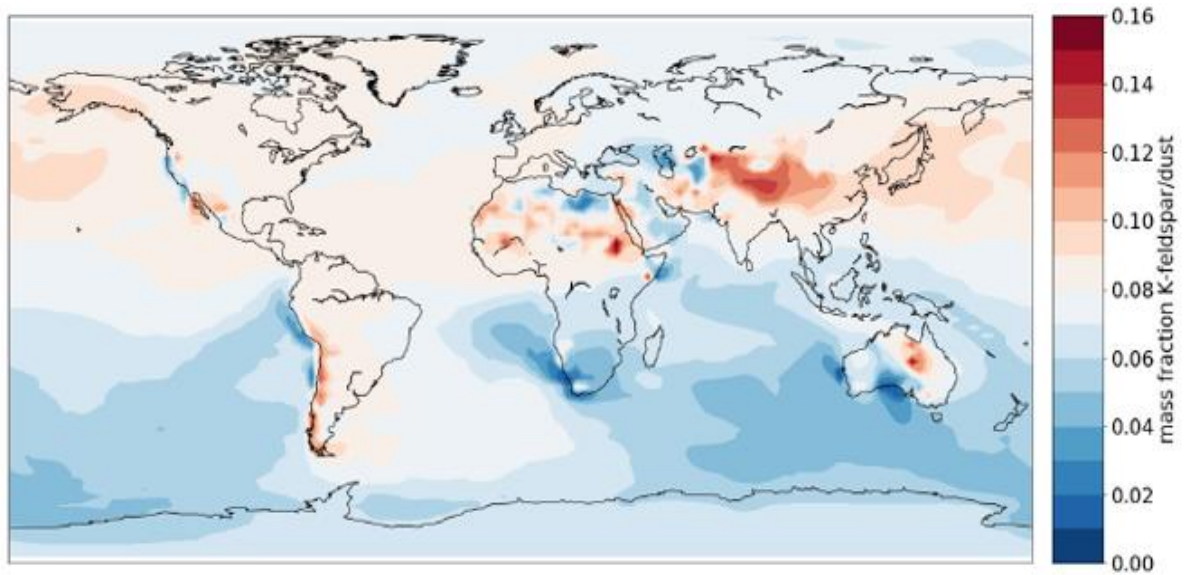


Figure S9: GLOMAP model simulation of the mass fraction of K-feldspar relative to aerosolised mineral dust. At Barbados it can be seen that K-feldspar is predicted to account for roughly 8% of the aerosolised mineral dust.

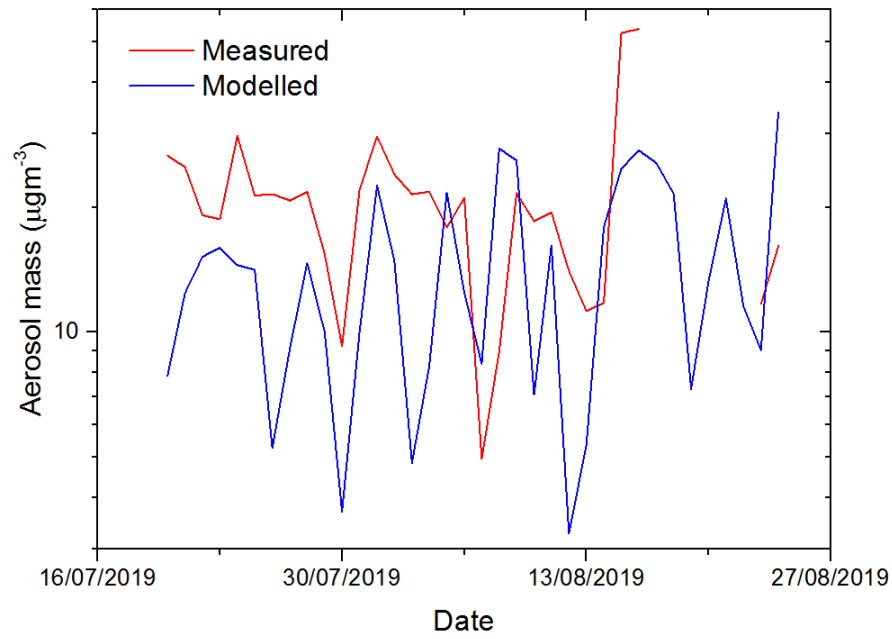


Figure S10: The GLOMAP simulated and APS measured aerosol mass daily averages for the duration of the campaign.

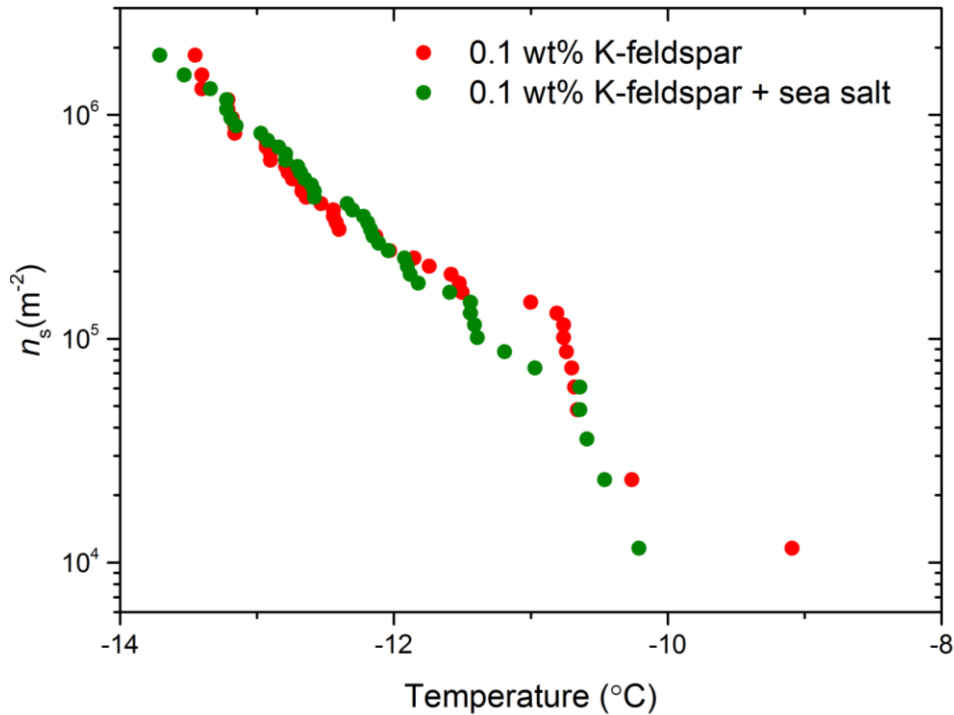


Figure S11: The effect of sea salt on K-feldspars ability to nucleate ice. The control experiment used a suspension of Milli-Q water and 0.1 wt% BCS376 K-feldspar. A suspension of 0.1wt% K-feldspar and 6.6×10^{-4} wt% aquarium salt (Marine salt, Tetra) was then tested for its ice-nucleating ability. This concentration of sea salt was used as the upper concentration of sea salt in the atmosphere measured by Prospero (1979) was $8.71 \mu\text{g m}^{-3}$. Assuming this concentration had been sampled on to a filter for four hours (at 16.7Lpm) and diluted into 6 mL of Milli-Q water we expect a sea salt concentration of 6.6×10^{-4} wt%. These values were chosen to represent a typical experiment collected and analysed in this field study. No observable change in the ice-nucleating ability of K-feldspar was seen with this atmospherically relevant concentration of sea salt.

References

Prospero, J. M.: Mineral and sea salt aerosol concentrations in various ocean regions, *Journal of Geophysical Research*, 84, 725, 1979.

Vali, G.: Revisiting the differential freezing nucleus spectra derived from drop-freezing experiments: methods of calculation, applications, and confidence limits, *Atmospheric Measurement Techniques*, 12, 1219-1231, 2019.

4. An instrument for quantifying heterogeneous ice nucleation in multiwell plates using infrared emissions to detect freezing

This chapter has been published in *Atmospheric Measurement Techniques* as:

Harrison, A. D., Whale, T. F., Rutledge, R., Lamb, S., Tarn, M. D., Porter, G. C. E., Adams, M. P., McQuaid, J. B., Morris, G. J., and Murray, B. J. ‘An instrument for quantifying heterogeneous ice nucleation in multiwell plates using infrared emissions to detect freezing’, published in *Atmospheric Measurement Techniques* (2018).

Abstract

Low concentrations of ice nucleating particles (INPs) are thought to be important for the properties of mixed-phase clouds, but their detection is challenging. Hence, there is a need for instruments where INP concentrations of less than 0.01 L^{-1} can be routinely and efficiently determined. The use of larger volumes of suspension in drop assays increases the sensitivity of an experiment to rarer INPs or rarer active sites due to the increase in aerosol or surface area of particulates per droplet. Here we describe and characterise the InfraRed-Nucleation by Immersed Particles Instrument (IR-NIPI), a new immersion freezing assay that makes use of IR emissions to determine the freezing temperature of individual $50 \mu\text{L}$ droplets each contained in a well of a 96-well plate. Using an IR camera allows the temperature of individual aliquots to be monitored. Freezing temperatures are determined by detecting the sharp rise in well temperature associated with the release of heat caused by freezing. In this paper we first present the calibration of the IR temperature measurement, which makes use of the fact that following ice nucleation aliquots of water warm to the ice-liquid equilibrium temperature (i.e. 0°C when water activity is ~ 1), which provides a point of calibration for each individual well in each experiment. We then tested the temperature calibration using $\sim 100 \mu\text{m}$ chips of K-feldspar, by immersing these chips in $1 \mu\text{L}$ droplets on an established cold stage (μL -NIPI) as well as in $50 \mu\text{L}$ droplets on IR-NIPI; the results were consistent with one another indicating no bias in the reported freezing temperature. In addition we present measurements of the efficiency of the mineral dust NX-illite and a sample of atmospheric aerosol collected on a filter in the city of Leeds. NX-illite results are consistent with literature data and the atmospheric INP concentrations were in good agreement with the results from the μL -NIPI instrument. This

demonstrates the utility of this approach, which offers a relatively high throughput of sample analysis and access to low INP concentrations.

4.1 Introduction

Cloud droplets can freeze homogeneously below about -33°C (Herbert et al., 2015), but the presence of ice-nucleating particles (INPs) can induce freezing at much warmer temperatures (Kanji et al., 2017). The glaciation of clouds at these warmer temperatures has a substantial impact on a cloud's reflective properties, lifetime and therefore the overall climate of the planet, but is poorly represented in many models (Hoose and Möhler, 2012; Vergara-Temprado et al., 2018). INPs can cause nucleation through a number of pathways (Vali et al., 2015), but in mixed-phase clouds it is thought that the pathways where particles become immersed in droplets is most important (Hande and Hoose, 2017; Hoose et al., 2010; Murray et al., 2012). Even small concentrations of INPs can influence cloud properties; for example, in a modelling study of Southern Ocean shallow mixed-phase clouds, Vergara-Temprado et al. (2018) showed that while concentrations of INPs greater than $\sim 1 \text{ L}^{-1}$ cause profound changes in cloud properties, clouds are sensitive to concentrations many orders of magnitude smaller.

The ability to quantify INP spectra (INP concentrations as a function of temperature) and test the efficiency of proxy materials for ice-nucleating efficiency is invaluable for improving our understanding of cloud glaciation and developing computationally inexpensive parameterisations for atmospheric models. However it is not a trivial task, in part because INP concentrations are low ($< 0.1 \text{ L}^{-1}$) (DeMott et al., 2010) and the sites on the surfaces which cause nucleation at warm temperatures (Vali, 2014; Whale et al., 2017) are rare. There are several different methods of conducting ice nucleation experiments that include Continuous Flow Diffusion Chambers (CFDC's) e.g. (Garimella et al., 2016; Kanji and Abbatt, 2009; Kohn et al., 2016; Rogers et al., 2001; Salam et al., 2006; Stetzer et al., 2008), cloud expansion chambers e.g. (Cotton et al., 2007; Niemand et al., 2012), wind tunnels e.g. (Diehl and Mitra, 1998; Pitter and Pruppacher, 1973) and droplet freezing assays e.g. (Beall et al., 2017; Budke and Koop, 2015; Häusler et al., 2018; Knopf and Alpert, 2013; Murray et al., 2011; Vali, 2008; Whale et al., 2015). Each of these methods has its limitations and advantages which must be understood and accounted for when conducting an experiment and interpreting the results. For example CFDCs cannot be used for measurements at temperatures warmer than about -11°C but they do allow for specific saturation conditions to be controlled, something which other

instruments cannot achieve. For more information on the capabilities and limitations of the various techniques see the comprehensive reviews and intercomparisons conducted by Hiranuma *et al.* (2015) and (DeMott *et al.*, 2018). Haüsler *et al.* (2018) also presents a summary of the features of various techniques.

A significant challenge in sampling INPs in the atmosphere is their low concentration. At present there is a dearth of published, atmospherically relevant, INP measurements globally (Kanji *et al.*, 2017; Vergara-Temprado *et al.*, 2017). Not only is the global spatial and temporal coverage of INPs inadequate, but the range of activation temperatures and INP concentrations covered in any one set of measurements is typically limited. No single instrument has the capability of measuring INP concentrations over the full range of conditions relevant to mixed-phase clouds. Online instruments, such as CFDCs, can measure over a wide range of relevant conditions but their detection limit is limited to $\sim 10^{-1} \text{ L}^{-1}$ (Al-Naimi and Saunders, 1985; DeMott *et al.*, 2010; Eidhammer *et al.*, 2010; Prenni *et al.*, 2009). This can be improved with aerosol concentrators (Prenni *et al.*, 2013; Tobo *et al.*, 2013), but is still above the INP concentrations models suggest influence the properties of certain cloud types, such as high latitude cold-sector clouds (Vergara-Temprado *et al.*, 2018). The alternative approach is therefore to increase the number of particles within each aliquot of water. In principle, increasing the number of particles per droplet, and therefore the surface area of nucleator, per droplet will increase the sensitivity of the experiment to rarer INP. This enables quantification of lower INP concentrations. To increase the number of aerosol particles per volume of liquid the time period over which an atmospheric sample is collected can be extended, but in doing so temporal resolution would be lost. A method of increasing the sensitivity of an immersion mode technique is to increase the volume of the collected suspension used in each aliquot, while maintaining the concentration of particles per unit volume. This increases the number of particles per aliquot of liquid and therefore makes it more likely that rarer INP will be detected. The use of larger volume droplet suspensions has been exploited in the past e.g. (Bigg, 1953; Vali, 1971), and has been the strategy employed in the development of some recent instruments e.g. (Beall *et al.*, 2017; Conen *et al.*, 2012; Du *et al.*, 2017; Stopelli *et al.*, 2014). These large volume assays capture the rarer, more active INP but often miss the more abundant but less active INP. Hence they should ideally be used alongside a smaller droplet instrument to generate complimentary datasets.

While many instruments use optical cameras to detect freezing events (Beall et al., 2017; Budke and Koop, 2015; Häusler et al., 2018; Whale et al., 2015), some researchers have used techniques to detect the release of latent heat associated with freezing. For example differential scanning calorimetry (Marcolli et al. 2007; Pinti et al. 2012) and infrared emissions (Zaragotas et al., 2016; Kunert et al. 2018) have been used. Zaragotas *et al.* (2016) use a thermal camera to measure the temperature of individual aliquots within a 96 multiwell plate partially submerged within an alcohol bath. This study investigated plant samples but suggested that the technique may be adapted for atmospheric purposes. Very recently, Kunert *et al.* (2018) presented a similar set up to investigate biological samples and collected aerosol. Unlike Zaragotas *et al.* (2016), Kunert *et al.* (2018) do not measure individual droplet temperatures via infrared emissions but instead use multiple thermistors embedded in the sample holders to infer temperature for the droplet array.

Here we propose a new technique, the IR Nucleation by Immersed Particle Instrument (IR-NIPI), for the detection of INPs using large volumes of sample in the immersion mode. This instrument is part of the NIPI suite of instruments that includes the μL -NIPI. When used together these devices allow measurements to be taken over a very wide range of INP concentrations. The use of an infrared camera allows temperature measurements to be made for individual droplets which helps reduce errors from horizontal gradients across the array of droplets and the effect of heat release on the temperature of neighbouring wells. The unique design, in combination with a Stirling engine-based chiller, is also compact making it ideal for field-based measurements and the use of multiwell plates lends itself to future automation.

4.2 Instrument Design

4.2.1 Operating principle

Drop assays have been used extensively for ice nucleation experiments e.g. (Budke and Koop, 2015; Conen et al., 2011; Garcia et al., 2012; Knopf and Forrester, 2011; Stopelli et al., 2014; Vali, 1995, 1971; Whale et al., 2015). This is partly due to their simplicity compared to other techniques but also the ability to scale the amount of nucleator with droplet size. In brief, aqueous suspensions are prepared and droplets of a well quantified size are placed onto a substrate or immersed in oil. These droplets tend to be monodispersed but polydispersed

experiments are also possible (Murray et al., 2011; Vali, 1971). The system is then cooled and the fraction of droplets frozen is recorded. The cooling can be conducted at a constant rate or with a stepped rate to hold the droplets at a specified temperature for a period of time (i.e. isothermally) to explore the time dependence aspect of ice nucleation (Herbert et al., 2014; Sear, 2014; Vali, 1994). The droplets are monitored and the freezing temperature of each droplet is recorded. The fraction of the droplet population frozen throughout the explored temperature range can then be determined, from which the ice-nucleating active site density or INP concentration can be derived (Vali et al., 2015).

If the surface area of nucleant per droplet is known then it is common to express the nucleating ability of a material as the density of active sites per unit surface area of nucleator, $n_s(T)$ (Connolly et al., 2009; DeMott, 1995). This approach is based on the assumption specific sites on a nucleator's surface are responsible for ice formation. n_s is a cumulative term, i.e. as you move to cooler temperatures there are more features which may behave as an active site as the energy barrier for ice formation decreases. $n_s(T)$ is calculated via equation (1).

$$n_s(T) = \frac{(-\ln(1 - \frac{n(T)}{N}))}{A} \quad (1)$$

Where $n(T)$ is the number of droplets frozen at a given temperature and N is the total number of droplets. A is the surface area of nucleator within each droplet. Nucleation is a time-dependent stochastic process, but in determining $n_s(T)$ the time dependence is neglected. This assumption is justified for many materials because the diversity in activity of active sites leads to a much greater spread in freezing temperatures than the shift in freezing temperatures associated with changes in cooling rate (Herbert et al., 2014; Vali, 2008).

4.2.2 IR-NIPI design

In brief an aqueous suspension is prepared and aliquots pipetted into the wells of a 96 multiwell plate which is then placed on a temperature controlled stage. The cold stage and multiwell plate are enclosed by a Perspex cover with an infrared camera mounted in its lid (Figure 4.1). The system is cooled at $\sim -1 \text{ }^\circ\text{C min}^{-1}$ until all droplets are frozen (typically in a temperature range of 0 to $-30 \text{ }^\circ\text{C}$). The temperature of the individual aliquots is monitored using the IR camera which records a temperature map every 20 seconds. The temperature map is then analysed with a semi-automated process using custom Python code to yield the freezing temperatures of individual wells.

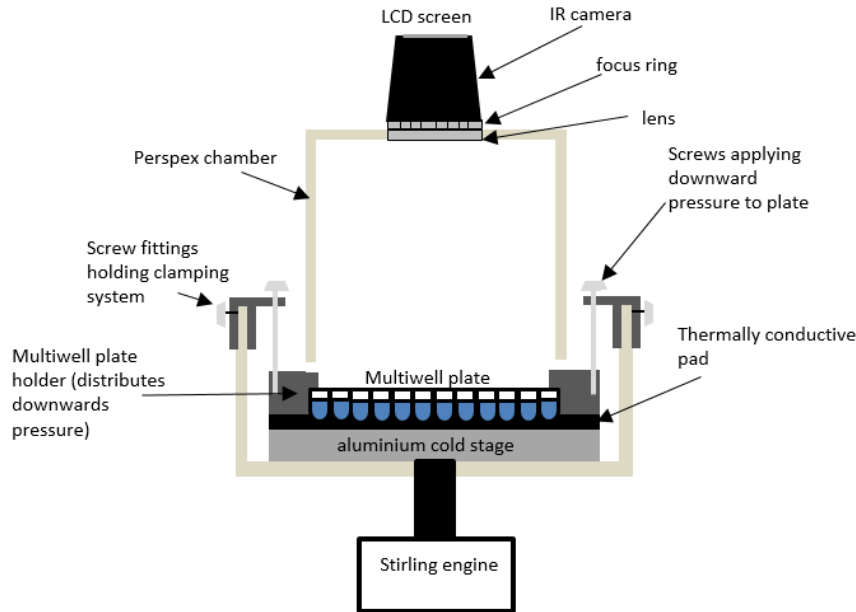


Figure 4.1: Schematic diagram of the IR-NIPI system (not to scale). The IR camera is positioned above the multiwell plate and monitors the freezing events as the cold stage cools.

The IR-NIPI has been designed around an Asymptote Ltd. VIA Freeze™ Stirling cryocooler (Figure 4.). The VIA Freeze uses a Stirling engine to provide a convenient means of cooling without refrigerants or circulating liquids and was primarily designed for use in cryopreservation applications. This chiller can achieve temperatures of $-90\text{ }^{\circ}\text{C}$, hence it has more than enough cooling capacity for our application, and has sufficiently low power requirements that allow it to be run from an automotive 12 V inverter. It also features an onboard datalogger and internal computer with touch screen control. The VIA Freeze has been developed to accommodate multiwell plates onto its aluminium cooling stage, which are ideal for large volume drop assays as they hold up to $200\text{ }\mu\text{L}$ per aliquot (for the 96 well plates), allow the separation of droplets to reduce interference across cells and can be supplied medically sterile. These multiwell plates have anywhere from 12-1536 wells (with maximum working volumes of 6.9 mL to $2\text{ }\mu\text{L}$, respectively). The most useful for this freezing assay are

the 96 x 200 μL or 384 x 50 μL aliquot arrays and in the tests reported here 50 μL droplets (~2300 μm volume equivalent diameter) are used in 96 well plates. We have used both polystyrene (Corning, CLS3788) and polypropylene plates (Greiner, M8060) and observed no difference in freezing results between the two. To aid thermal contact between the multiwell plate and the VIA Freeze a thermally conductive gap pad (RS components, 7073452) is located between the cold plate and the multiwell plate, while a clamping system with screw threads applies mechanical pressure to the multiwell plate to push the wells into the pad (Figure 4.1). A specially designed Perspex hood then encloses the system to reduce contamination from the surroundings. The IR camera slots into the hood and captures an image of the multiwell plate every 20 seconds (Figure 4.2), storing the corresponding temperature data (Figure 4.2b) on a removable memory card. The IR camera used here is a Fluke Ti9 Thermal Imager with 160 x 120 pixels. The Stirling engine chiller is then set to cool down at $1.3\text{ }^{\circ}\text{C min}^{-1}$ which corresponds to $1\text{ }^{\circ}\text{C min}^{-1} \pm 0.06\text{ }^{\circ}\text{C}$ in the wells due to a measured offset between the plate and aliquot temperatures. This ramp rate was selected based on preliminary runs and justification for this cooling rate being equivalent to $1\text{ }^{\circ}\text{C min}^{-1}$ can be seen in the well temperatures over time (Figure 4.2b). Once the system has initially cooled to $5\text{ }^{\circ}\text{C}$ the temperature is held for 5 min to allow time for the system to equilibrate. Following this the system continues to ramp down in temperature while recording IR heat maps of the multiwell plate.

In order to determine the temperature of individual wells, the analysis code locates a pixel centred in the middle of each well, reporting this temperature as the well temperature. Profiles of temperature versus time are shown in Figure 4.2b and c. The freezing temperature of each individual well is determined by comparing each temperature reading, for a certain well, with the temperature recorded 20 seconds prior. If the temperature reading increases by more than $2\text{ }^{\circ}\text{C}$ this is recorded as a freezing event (Figure 4.2c). The $2\text{ }^{\circ}\text{C}$ threshold occasionally needs to be optimised to capture freezing events while eliminating the detection of false freezing events. For example, samples that freeze above $-3\text{ }^{\circ}\text{C}$ are more difficult to detect because there is less heat released on initial freezing and crystallisation happens over a longer period of time (see section 4.2.4). Manual inspection is required in this temperature regime and the $2\text{ }^{\circ}\text{C}$ threshold adjusted accordingly. The code then prints out the number of events recorded, along with a time vs temperature plot (Figure 4.2b) and the corresponding event temperatures for the user to quality control check and then exports the data as a '.csv' file.

The whole process from sample preparation to final analysis takes approximately 1 hour. In order to achieve higher throughput of samples, albeit with a reduced number of replicates, multiple samples and internal blanks can be placed within one multiwell plate. For example, when performing dilutions we might run 12 wells as a handling blank and three lots of 28 wells that contain three different sample dilutions. This not only speeds up analysis, it also reduces the effect of any time-dependent aging processes such as the rapid deactivation of an albite sample suspended in water observed by Harrison et al. (2016).

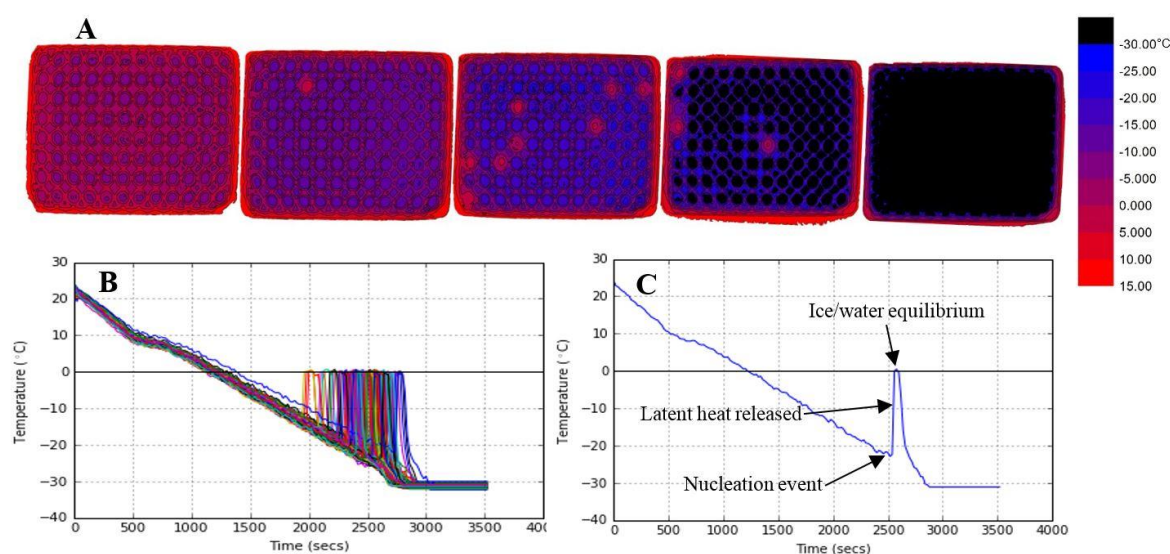


Figure 4.2: Illustration of the use of the IR camera to measure temperature and freezing events. (A) A sequence of colour maps taken during the course of an experiment. The leftmost image shows the start of an experiment with all droplets unfrozen, moving to all droplets frozen in the right most image. Warmer temperatures are represented in red, transitioning to blue for colder temperatures and finally black at $-30\text{ }^{\circ}\text{C}$ and below. Freezing events in individual wells are evident when they warm up to $0\text{ }^{\circ}\text{C}$. **(B)** An example of the output of an experiment with the temperature of each of the 96 wells plotted against time. The sharp increases in temperature are related to ice formation. The cooling rate was $1\text{ }^{\circ}\text{C min}^{-1}$. The calibration described in section 4.2.2 was applied here. Note that one well had a higher temperature than the others, likely due to poor thermal contact with the aluminium substrate. By using IR thermometry to measure the

temperature of each well individually such variability is accounted for. (C) Plot of temperature vs time for a single well within a multiwell plate containing a 50 μL aliquot of water.

4.2.3 Temperature measurements with an Infrared camera

By using an IR camera to view the thermal emission of each individual well of suspension we are able to obtain temperatures associated with individual wells. This contrasts with the approaches adopted in other experiments where the temperature is recorded and assumed to be representative for all droplets, for example when employing a cold stage housing an embedded thermocouple whose reading is used to represent the temperature of the droplet array. We note that in our system there was a lateral gradient across the entire multiwell plate in the IR-NIPI of up to 6 °C (in extreme cases). This is likely due to there not being an even thermal contact of the multiwell plate with the underlying cold plate. The typical gradient was 4 °C, hence temperature measurements of the individual wells was necessary.

4.2.4 Temperature calibration

The IR camera we use was quoted for use between -20 to +250 °C with an uncertainty of ± 5 °C and is intended for use in a wide range of applications with a range of materials of different emissivity. In our application, we only need to measure the temperature of one material, water, over a relatively narrow range of temperatures, hence we perform a calibration for our specific experimental setup. Our calibration is based on the fact that when an aliquot of water in a multiwell plate freezes, the released latent heat raises the temperature of the aliquot to the ice-water equilibrium temperature (0 °C when the water activity of the sample is ~ 1 , as it is in these experiments). This is illustrated in Figure 4.2c which shows the phases of crystallisation that the aliquots go through. Initially, the crystal growth is rapid with a rapid release of latent heat and a corresponding rise in temperature of the aliquot within the 20 s time between frames. Visual inspection of the live screen display of the IR camera revealed that the temperature reached a maximum within 1 s. The temperature of an ice-water mixture will necessarily be 0 °C, hence the aliquot cannot warm above 0 °C and the temperature will remain at 0 °C until all of the water has frozen and no more heat is evolved. The rate of crystallisation in this regime is determined by the loss of heat to the surroundings, in this case the cold stage, as well as to the surrounding droplets and the multiwell plate. This stage of crystallisation takes longer at higher freezing temperatures where the temperature differential between the cold stage and the

aliquot is smaller. Hence, freezing when nucleation takes place at $-12\text{ }^{\circ}\text{C}$ takes around 100 s, whereas when nucleation takes place at $-20\text{ }^{\circ}\text{C}$ freezing takes around 20-40 s. Once all of the water has frozen the temperature of the aliquot decreases rapidly back to that of the multiwell plate within 20-40 s. The fact that the aliquots spend 10s of seconds at $0\text{ }^{\circ}\text{C}$ provides a very useful calibration point for each individual well. In the following we describe a novel method for calibrating the IR temperature measurements that takes advantage of this process and proceed to justify this approach.

Using the analysis code, an event is identified and recorded. The code then reads the temperature of the frame directly after this freezing event and calculates the difference of this value compared to $0\text{ }^{\circ}\text{C}$ to give an offset correction value, i.e. if the frame after freezing read $2\text{ }^{\circ}\text{C}$ then the correction factor for this well would be $-2\text{ }^{\circ}\text{C}$. This offset value is then subtracted from all of the temperature recordings for that specific well. The average correction value calculated for the IR camera via this method is $-1.9\text{ }^{\circ}\text{C}$ with a standard deviation $\pm 0.5\text{ }^{\circ}\text{C}$. It should be noted that one of the limitations of the setup used by Zaragotas et al. (2016) was that the IR camera was calibrated only once by the factory, however our calibration method mitigates this limitation.

A standard freezing experiment was then performed and the thermocouple data was contrasted to that of the IR camera which was calibrated using the above method (Figure 4.3). The comparison in Fig. 4.3a shows that the IR and thermocouple temperature were in excellent agreement and this is also readily seen in residuals plotted in Fig. 4.3b. The scatter around the zero line in the residual plot is $\pm 0.9\text{ }^{\circ}\text{C}$ (two standard deviations) in the regime after the equilibrium step at $+5\text{ }^{\circ}\text{C}$ and before the first freezing event. We used this value as an estimate of the temperature uncertainty associated with the IR technique generally. We did not use data in the red and blue shaded areas of Fig. 4.3b to calculate this uncertainty. The temperature readings in the red shaded area were discarded as they had not been held at $+5\text{ }^{\circ}\text{C}$ for five minutes to equilibrate. Temperature readings after the initial freezing event were also discarded as thermal conductivity of ice is different to that of water and neighbouring wells release heat on freezing which influence the temperature of surrounding wells.

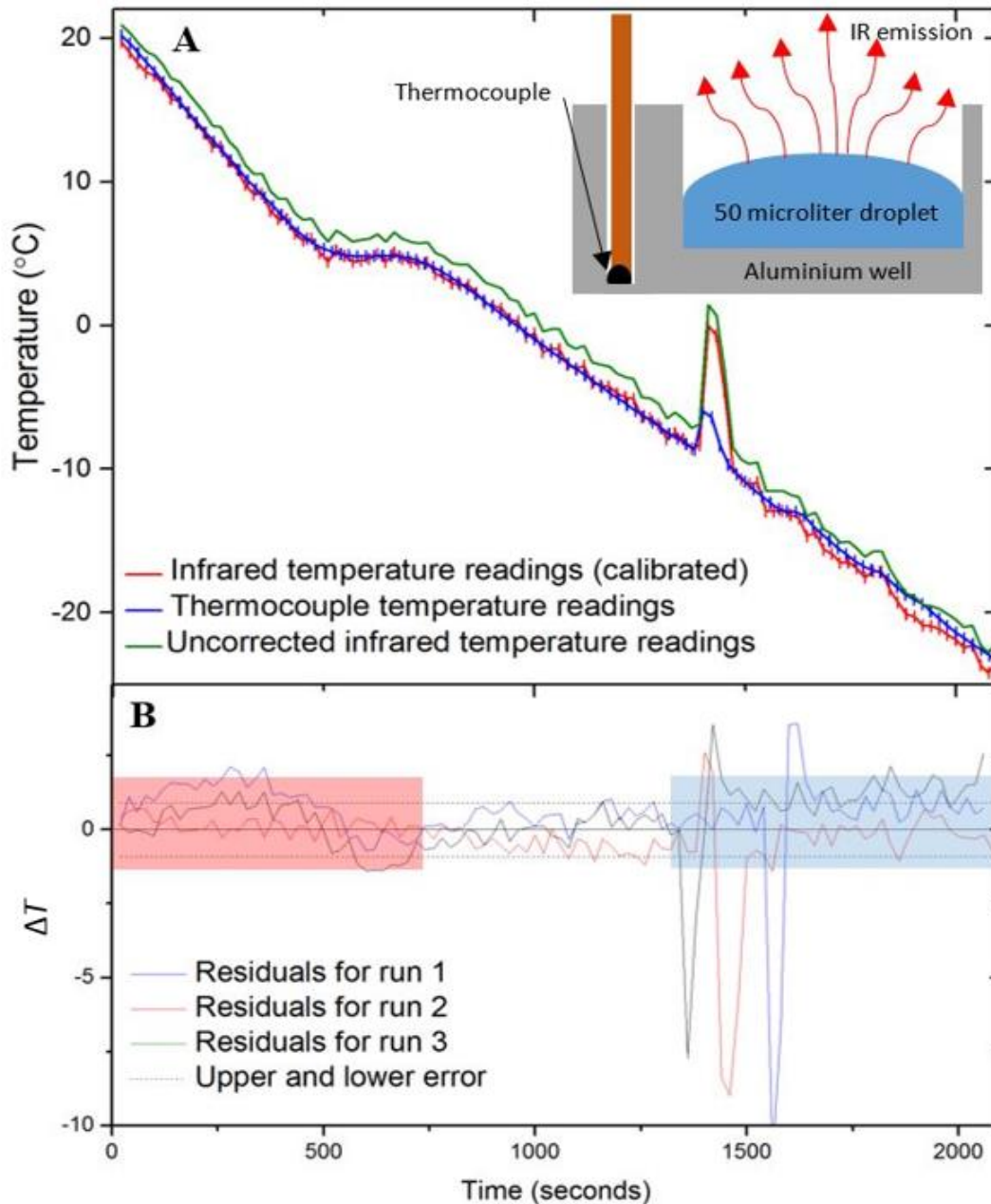


Figure 4.3: Tests of the IR temperature measurement using aluminium wells with embedded thermocouples. (A) The temperature measurement from a thermocouple (shown in blue) placed within an aluminium well vs infrared measurements taken using the IR camera. Uncorrected IR data is shown in green, whilst corrected IR data following the calibration described in section 4.2.2 is shown in red. Inset is a schematic of the experimental setup. (B) The difference in temperature (residual; ΔT) between the thermocouple readings for three aluminium wells and the corresponding IR data ($\Delta T = T_{\text{IR}} - T_{\text{Thermocouple}}$). The negative spikes are a result of the IR camera directly reading

the water temperature as it is heated by ice formation whereas the thermocouple measurement is reading the temperature of the aluminium well which is less affected by the latent heat release. The estimated error in temperature for the IR camera of $\pm 0.9^{\circ}\text{C}$ is indicated with dashed lines. The range over which freezing occurs is highlighted with a blue rectangle as this is where the thermal properties of ice and the initiation of heat release affect the temperature readings. Highlighted in red is the section of data before the well has equilibrated and so the IR camera is likely reading a warmer surface temperature than the thermocouple. See text for discussion.

We also tested the IR temperature measurement using T type thermocouples distributed in specific wells of a polypropylene multiwell plate. The IR camera could not take an accurate reading of wells that had a thermocouple placed inside them, therefore neighbouring unfrozen wells were assumed to be representative of each other (see inset in Figure 4.4). As mentioned above, there is a gradient across the entire plate (Fig. 4.2a) and so a series of preliminary experiments were undertaken to find suitable placement locations for the thermocouples in which the surrounding wells displayed similar temperature readings compared to one another. The thermocouples were placed in the base of the well along with 50 μL of Milli-Q grade water and four surrounding well temperatures were measured using the IR system. The thermocouple wire crossed one of the four IR measured wells and so only three wells adjacent to the thermocouple monitored well were used for comparison.

A total of six IR measurements were recorded with the corresponding thermocouple readings over a series of experiments spanning a temperature range of 20°C to -25°C . An example of a thermocouple measurement contrasted to three IR measurements can be seen in Figure 4.4a. The residual temperatures for all six thermocouple temperatures are also shown (Figure 4.4b). The IR temperature uncertainty derived from the aluminium well experiment is also plotted and shows that the multiwell temperature data is consistent with an uncertainty of $\pm 0.9^{\circ}\text{C}$.

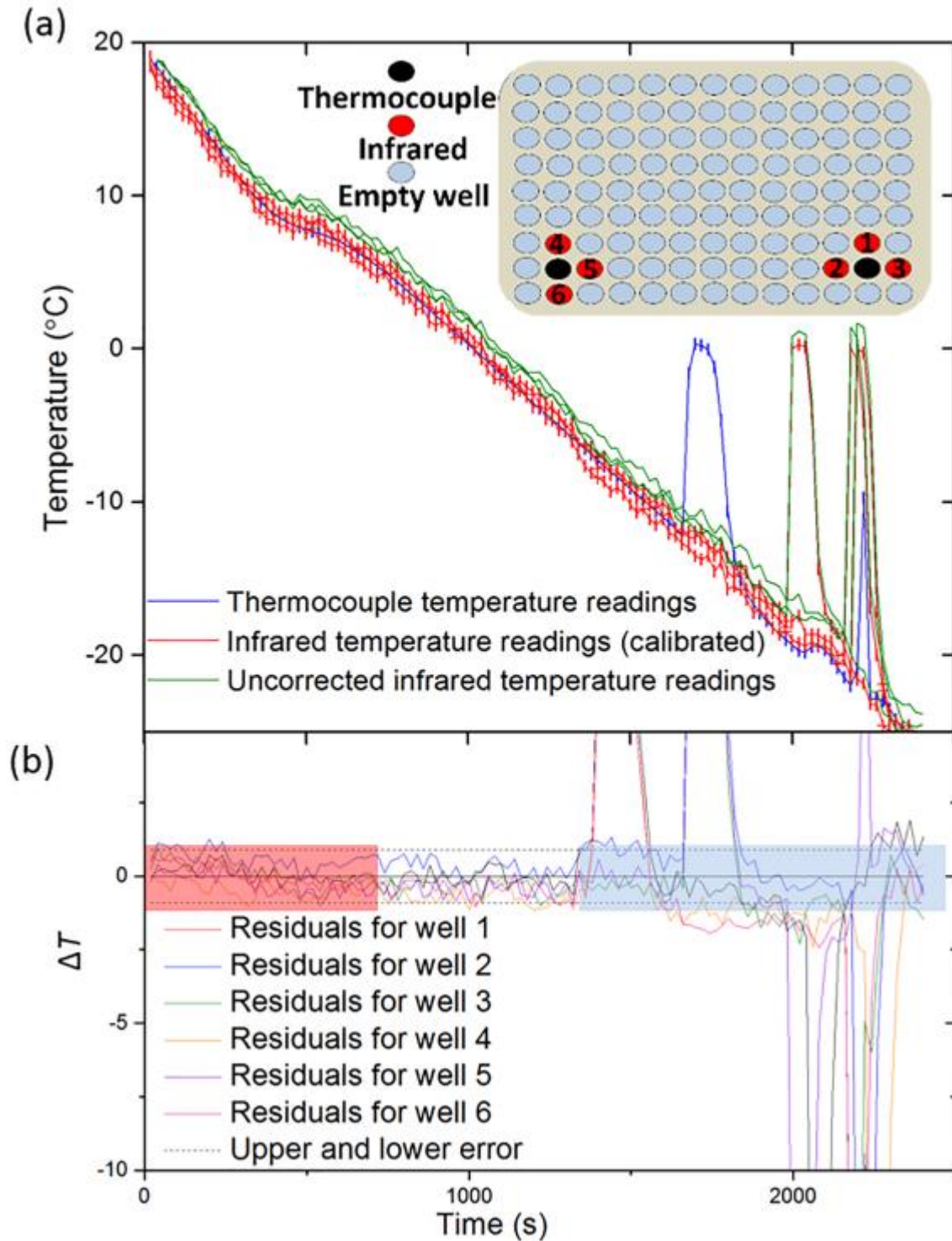


Figure 4.4: Tests of the IR temperature measurements using thermocouples positioned in a multiwall plate. (A) The temperature measurement from a thermocouple placed within a polyethylene well versus three IR measurements of surrounding wells corrected using the calibration described in section 4.2.2. The uncorrected IR data can be seen in green,

with the corrected IR data in red and the thermocouple readings in blue. A diagram of the wells within a 96 well plate chosen for the comparison of IR and thermocouple measurements is displayed as an inset. The numbers of the wells correspond to the residuals in part B. Red wells represent the wells measured with the infrared camera and black wells represent those measured with thermocouples. It should be noted that one of the four surrounding IR well temperature readings was discarded from each experiment as the thermocouple wire impeded the temperature measurement. Note that the freezing events at ~2000 s appear to cause some heating in the adjacent well. (B) Plot of the difference in temperature between the thermocouple readings for two wells and six corresponding wells measured with the IR camera as in Figure 4.3. The estimated error in temperature for the IR camera is indicated with dashed lines ($\pm 0.9^\circ\text{C}$). The range of freezing is highlighted in blue as this is where the thermal properties of ice and the initiation of heat release will affect the temperature readings. Highlighted in red is the section of data before the well had equilibrated and so the IR camera was likely reading a warmer surface temperature than the thermocouple.

4.3 Test experiments and analysis

4.3.1 Control experiments

In larger volume freezing assays (10s of microliters) it is extremely challenging to remove all background INPs from the water and substrates, hence freezing is typically observed at temperatures well above what one would expect for homogenous freezing (Koop and Murray, 2016). Homogeneous nucleation is expected to result in 50 % of 50 μL droplets freezing at around -33°C , whereas 50 % of the Milli-Q water droplets froze around -22°C in our control experiments (

Figure 4.5). Filtering of the Milli-Q water to $0.2\ \mu\text{m}$ reduced the temperature at which pure water droplets froze by $2\text{-}3^\circ\text{C}$. Sartorius Ministart, non-pyrogenic, single use filters were used for this (product code 17597-K). Blanks were run initially with entire 96 well plates and then 12 wells of each experiment thereafter were allocated for an internal blank when testing samples of INPs (i.e. 12 aliquots of Milli-Q water and 84 aliquots of sample suspension). Comparison of fraction frozen curves for typical IR-NIPI blanks with curves obtained for droplets containing various ice-nucleating materials (discussed below) show that there is a clear heterogeneous freezing signal (

Figure 4.5). We hope to improve the baseline in the future, through further improvements in the cleanliness of the system (Polen et al., 2018), but for the purpose of these experiments the nucleants tested were active at sufficiently warm temperatures to be well above the baseline.

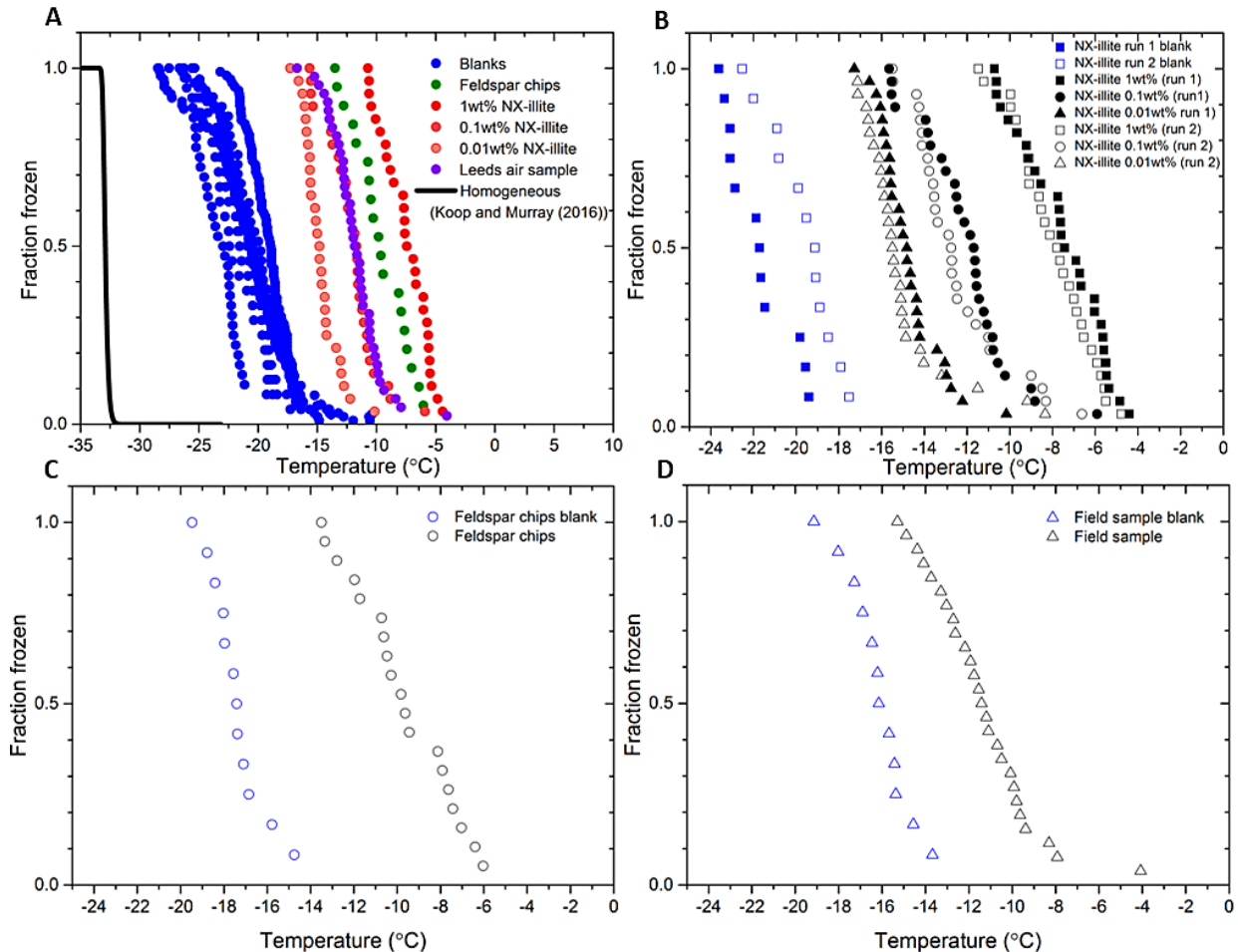


Figure 4.5: The fraction of droplets frozen as a function of temperature on cooling for a range of samples. (A) The fraction frozen curves for the IR-NIPI experiment showing standard blank runs and the sample runs from this study. The homogeneous freezing of water as predicted with the Koop and Murray (2016) parameterisation is also shown in black. (B) Fraction frozen plot for the internal blanks versus the corresponding NX-illite runs. (C) Fraction frozen plot for the internal blank versus the corresponding feldspar chips run. (D) Fraction frozen plot for the internal blank versus the corresponding field sample run.

4.3.3 Feldspar chips

To further test the temperature readings from the IR-NIPI instrument a set of experiments was performed where each droplet contained a single $\sim 100\ \mu\text{m}$ sized grain of K-feldspar in both the IR-NIPI and contrasted to the standard μL -NIPI employing $1\ \mu\text{l}$ droplets. The μl -NIPI is a well-established technique (Whale et al., 2015) which compares well with other similar instruments (DeMott et al., 2018; Hiranuma et al., 2015). The purpose of this experiment was to have the same amount of material per droplet in each experiment and to have the material at the base of the droplet so that the results from the two instruments could be directly compared. In doing so we could investigate the extent to which the gradient within the $50\ \mu\text{L}$ wells might be a problem. This experiment was adapted from the procedure described by Whale *et al.* (2018) and involved taking K-feldspar rich chips from a bulk rock of pegmatite and selecting individual grains (pegmatite is an igneous intrusive rock rich in K-feldspar with large grain sizes often being larger than $2.5\ \text{cm}$ and hence easy to separate). This material was chosen because K-feldspar is known to exhibit excellent ice-nucleating properties (Atkinson et al., 2013; Harrison et al., 2016; Peckhaus et al., 2016). A total of 19 grains were $\sim 100\ \mu\text{m}$ in diameter were separated by eye, assigned a number and their position tracked through the course of each experiment. The same feldspar chips were tested in both the μL -NIPI and the IR-NIPI. For the IR-NIPI experiments single grains of feldspar were placed into the bottom of a multiwell plate and $50\ \mu\text{L}$ of Milli-Q water was then pipetted into each well. The experiment was then carried out as normal and the freezing temperatures of the wells were recorded. The grains were then used in the μL -NIPI experiment by placing the grains onto a glass cover slip atop a cold plate and pipetting a single $1\ \mu\text{L}$ droplet onto each grain, before carrying out a standard μL -NIPI experiment. Briefly, the temperature of the cold plate was reduced at $1\ ^\circ\text{C}\ \text{min}^{-1}$ and the temperature of the droplet freezing events recorded via a camera. The resulting fraction frozen plot for this experiment can be seen in figure 4.6a and the corresponding correlation plot is shown in Figure 4.6b. The two instruments yielded similar fraction frozen curves and the individual feldspar grains nucleated ice at a similar temperature in both experiments. The correlation plot in Figure 4.6b shows that the freezing temperatures of a single grain were not identical in the two experiments, which is consistent with the stochastic nature of nucleation at active sites that have a characteristic freezing temperature (Vali, 2014, 2008). The agreement between the two instruments suggests that the temperature measurement

and calibration of the IR-NIPI were robust and that there is no major temperature gradient within the aliquots in the multiwell plates.

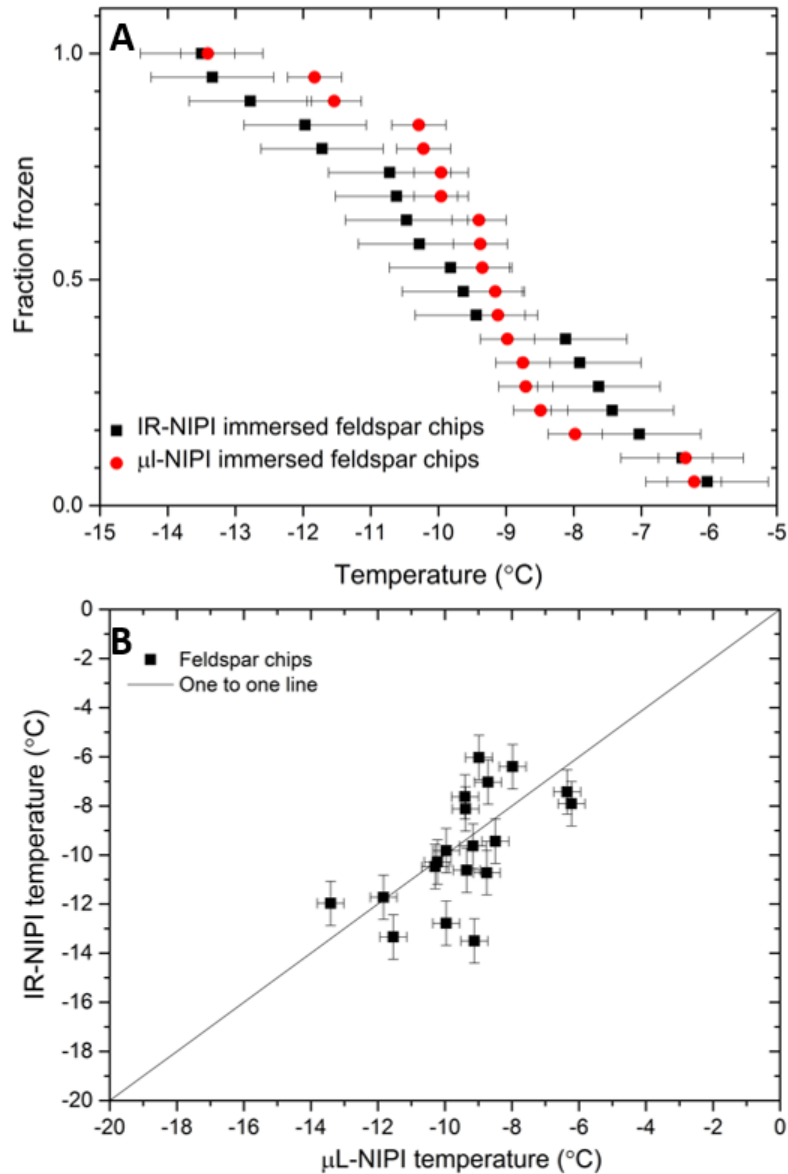


Figure 4.6: Comparison of nucleation induced by feldspar chips in the IR-NIPI and μ L-NIPI instruments. (A) The fraction frozen curves for single feldspar particles per droplet in both the μ L-NIPI (using 1 μ L droplets) and IR-NIPI (using 50 μ L droplets) experiments. The error bars indicate the error in temperature measurement on both instruments, respectively. (B) Shows the freezing temperature for the individual feldspar chips as measured by the IR-NIPI and μ L-NIPI instruments.

4.3.4 NX-illite

The mineral dust NX-illite was chosen as a test sample as it has been used in an extensive intercomparison study (Hiranuma et al. 2015) and contains some common components which are found in atmospheric mineral dusts (Broadley et al., 2012). NX-illite was taken from the same batch as that used by the Leeds group in the Hiranuma et al. (2015) intercomparison and no further processing of the material was carried out. Aqueous suspensions of the sample were prepared by weighing a known amount of material and suspending it in a corresponding volume of water to make up a weight percent suspension (i.e. 0.1 g of mineral in 9.9 g of water to yield a 1 wt% suspension). NX-illite concentrations of 0.01, 0.1 and 1 wt% were prepared in this manner, and in each case a Teflon-coated magnetic stirrer bar was used to keep the particles suspended whilst the sample was pipetted into the wells of the multiwell plate. Each concentration of NX-illite was tested using the IR-NIPI and the resultant fraction frozen curves are shown in Fig. 4.5.

By employing a suspension of known concentration and composed of a material with a known specific surface area, the surface area of nucleator per droplet can be calculated and used alongside the fraction frozen curves to determine $n_s(T)$, as described in equation (1). The $n_s(T)$ derived from IR-NIPI with 0.01, 0.1 and 1 wt% NX-illite are shown in figure 4.7a. They are in good agreement with one another with lower wt% suspensions yielding data at lower temperatures and higher $n_s(T)$ values, as expected. The few data points from the 0.01wt% NX-illite run 2 which appear as outliers may indicate that the particles were not evenly distributed throughout the droplets. Further to this a freeze thaw experiment of 0.1wt% suspension was conducted where the sample was frozen once, thawed and then frozen again (see figure 4.8). The agreement between the two runs show that the material did not alter on freezing.

The values of $n_s(T)$ for NX-illite derived from 0.01-1 wt% suspensions are shown in Figure 4.7a together with the literature data for this material in Figure 4.7b. This material has also been investigated by Beall *et al.* (2017) using an instrument that also uses 50 μ L droplets: the Automated Ice Spectrometer (AIS). The results of Beall *et al.* (2017) are therefore directly comparable to the results from the IR-NIPI. All of the wet suspension techniques have been grouped together in black in Fig. 4.7b, apart from the AIS data shown in green and the IR-NIPI data in red. Both the IR-NIPI and AIS data are in good agreement with one another. It can be seen that the larger volume assays (IR-NIPI and AIS) give results towards the upper spread of

literature data but are still consistent with other results (Figure 4.7b). Dry dispersed techniques have also been plotted as unfilled blue squares in Fig. 4.7b, but none of these techniques are sensitive in the range of $n_s(T)$ seen by the large droplet instruments. The new data from the IR-NIPI has extended the dataset for NX-illite to warmer temperatures than in previous measurements, illustrating the utility of the technique.

It should be noted that in preliminary experiments some discrepancies between dilutions of NX-illite were observed which highlighted the importance of accurately making up suspensions. In the following we note some issues that had to be solved. In some initial experiments the dilutions of a suspension would yield a higher than expected $n_s(T)$. On further investigation this issue was resolved via gravimetrically weighing suspensions (i.e. preparing a known mass of a sample in a known mass of water) rather than diluting a bulk stock suspension. Further to this great care was taken when sampling from the bulk NX-illite sample as to make sure no bias was introduced when selecting material since a powder can separate on the basis of grain size. This was avoided by shaking the container horizontally and selecting material from the centre of the bulk sample. Magnetic stirrer bars were used to keep particles suspended but when it came to collecting the suspension using a pipette the suspension was taken from the magnetic stirrer plate to stop the vortex within the vial. As the suspension was not stirring for a short period of time it meant that particles did not have time to fallout of suspension and there was no longer a vortex created by the stirrer bar which could bias particle distribution when sampling. The above emphasises the importance of selecting samples in a reproducible way and may explain some of the variability between the literature data seen in Fig. 4.7b.

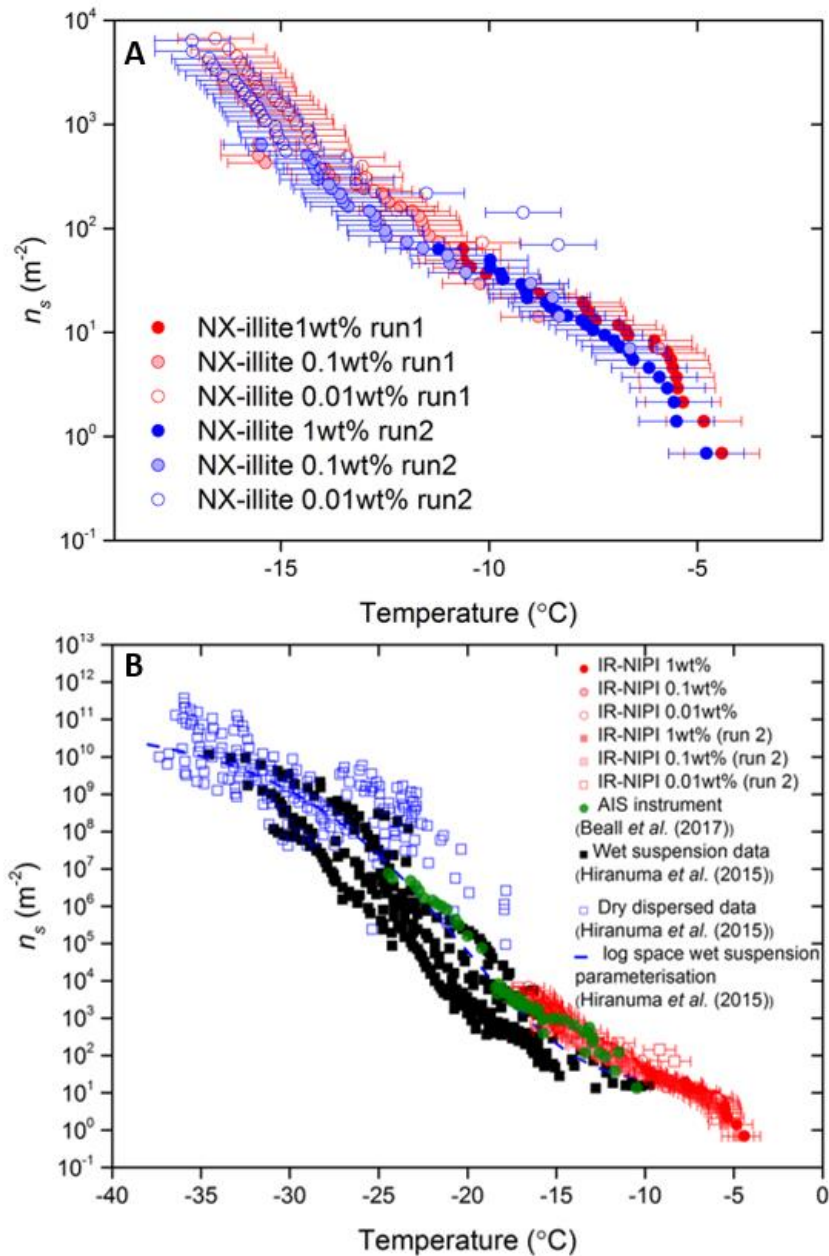


Figure 4.7: Active site densities, $n_s(T)$, for NX-illite. (A) The active site density for a dilution series of NX-illite run on the IR-NIPI instrument for a range of concentrations. The data for a repeat experiment is also shown. The error bars represent the temperature error of $\pm 0.9^{\circ}\text{C}$. (B) The active site density for NX-illite from this study compared to literature data. Data from wet dispersed techniques are displayed in black with the IR-NIPI highlighted in red and Automated Ice Spectrometer (AIS) in green. Data from dry dispersed techniques are also plotted as hollow blue squares.

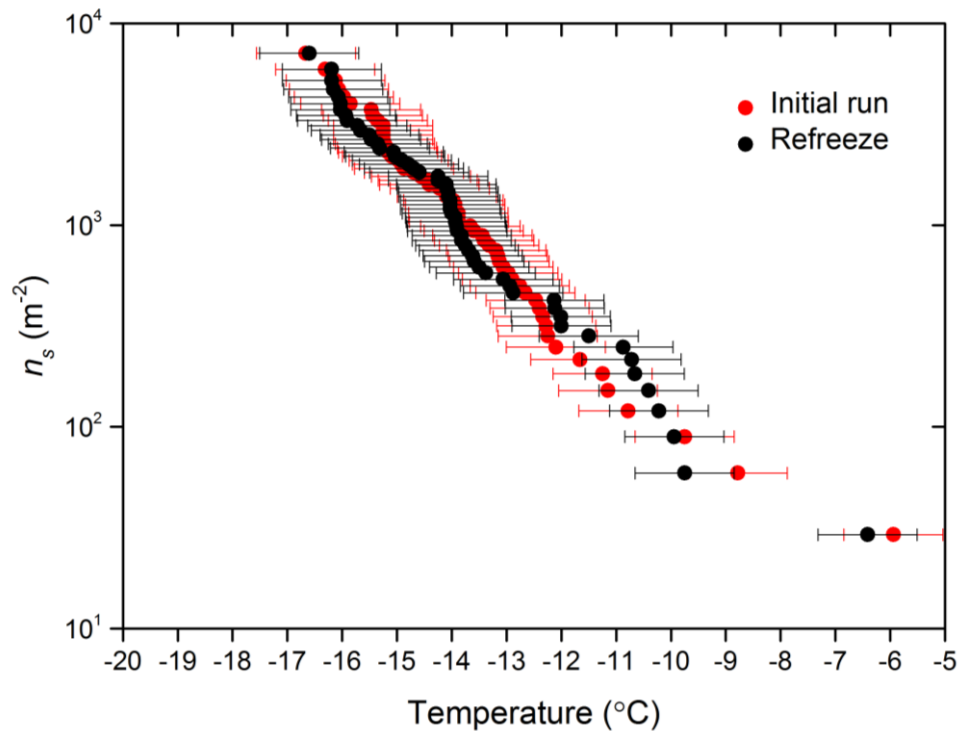


Figure 4.8: The active site density, $n_s(T)$, for a 0.01wt% NX-illite suspension and $n_s(T)$ from a corresponding second freezing run with the same droplets after they had been thawed out and refrozen.

4.3.4 Atmospheric aerosol sample

In order to demonstrate the utility of this approach for atmospheric aerosol samples, a filter sample was collected in Leeds as part of a field campaign held on the evening of the 5th November. A sample of atmospheric aerosol was collected using a Mesa PQ100 air sampler for 100 min. An inlet head with an upper cut-off of 10 μ m was utilised and air was sampled at 16.7 L min⁻¹ on to a 0.4 μ m polycarbonate track-etched Whatman filter, with a total of 1670 L of air sampled. The filter was then placed into 6 mL of Milli-Q water and vortexed for 5 min to wash the particles from the filter and into suspension.

The aqueous sample was then analysed on the IR-NIPI and μ L-NIPI (Whale et al., 2015). The concentration of INPs per litre of air, $[INP]_T$, was subsequently calculated using equation (2) (DeMott et al., 2016).

$$[INP]_T = -\ln\left(\frac{N_u(T)}{N}\right)\left(\frac{V_w}{V_a V_s}\right) \quad (2)$$

Where $N_u(T)$ is the number of unfrozen droplets at a given temperature, N is the total number of droplets, V_w is the volume of wash water, V_a is the volume of an aliquot and V_s is the volume of air sampled.

The resulting INP concentrations from the combination of these two instruments spanned four orders of magnitude and covered a temperature range of 20 °C (see figure 4.9). The data from both instruments was in good agreement and yielded complementary information. This illustrates how the IR-NIPI can be used to extend the measurements of INP concentrations to higher temperatures and lower INP concentrations. Since high-resolution regional modelling of the effect of INP on shallow clouds suggests that 0.1 to 1 INP L⁻¹ is a critical concentration and much lower concentrations still impact clouds (Vergara-Temprado et al., 2018), measurements with IR-NIPI will be extremely useful, particularly in environments with low INP concentrations.

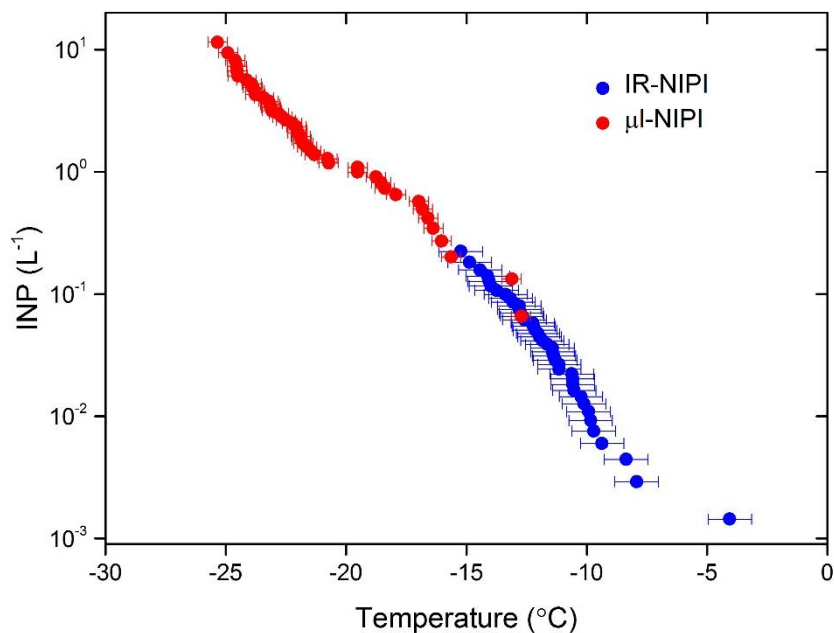


Figure 4.9. INP concentrations per litre of air samples on the 5th November 2017 in Leeds. Aerosol were collected onto filters for later extraction into water and analysis of the resulting suspensions with the IR-NIPI and μ L-NIPI instruments.

4.4 Summary and conclusions

The IR-NIPI technique is a novel approach to measuring freezing events in immersion mode nucleation studies. We demonstrate that IR thermometry is a sound method for determining the freezing temperature of 50 μ L water droplets in multiwell plates. This method overcomes potential distorting influences such as thermal gradients across the plate, the effect of freezing wells warming surrounding wells and poor thermal contact to the underlying cold plate. A freezing event is detected as a sharp rise in freezing temperature to the equilibrium melting point and a novel calibration method has been proposed which relies on the return of water droplets to the equilibrium melting temperature of water, 0 °C, after initial freezing. This gives an individual calibration for every run and every well. When comparing this calibration technique to thermocouple readings the data is consistent to within ± 0.9 °C. The use of this calibration method is further supported when looking at experiments using single grains of feldspar, with the results being consistent with those of the established μ L-NIPI instrument that employs 1 μ L droplets on a cold stage. Results for the ice nucleating ability of NX-illite with

the IR-NIPI, a mineral dust which has been the subject of an extensive inter-comparison, are consistent with literature measurements. In particular, the IR-NIPI is in good agreement with another well-characterised large droplet instrument (AIS) (Beall et al., 2017). However, it is unclear why both of these large volume instruments produce n_s results at the high end of the range of n_s values reported previously. The utility of IR-NIPI for the analysis of atmospheric samples was also demonstrated by collecting and analysing an aerosol sample from the city of Leeds, England. The sample was analysed simultaneously with the μ L-NIPI instrument. Results from the two instruments were in good agreement with one another. The IR-NIPI instrument extended the range of INP concentrations shown by the μ L-NIPI by two orders of magnitude, covering a regime critical for cloud formation with a modest sampling time of just 100 mins at 16.67 L min⁻¹.

Data availability: Data collected for the IR-NIPI temperature measurements, blank runs, NX-illite experiments and field collected sample are available at <http://dx.doi.org/10.5285/858a4b439d7d4466b82ea5215614f135>.

Acknowledgements: We would like to take the opportunity to thank David Harrison for the assembly of the IR camera automatic shutter trigger. We would also like to thank Antony Windross and Stephen Burgess for construction of the camera housing and multiwell plate mount. The authors acknowledge the European Research Council (MarineIce: 648661, CryoProtect: 713664 and IceControl: 632272), and the Natural Environment Research Council (NE/M010473/1) for funding this research.

References

- Al-Naimi, R. and Saunders, C. P. R.: Measurements of natural deposition and condensation-freezing ice nuclei with a continuous flow chamber, *Atmos. Environ.*, 19, 1871-1882, 1985.
- Atkinson, J. D., Murray, B. J., Woodhouse, M. T., Whale, T. F., Baustian, K. J., Carslaw, K. S., Dobbie, S., O'Sullivan, D., and Malkin, T. L.: The importance of feldspar for ice nucleation by mineral dust in mixed-phase clouds, *Nature*, 498, 355-358, 2013.

- Beall, C. M., Stokes, M. D., Hill, T. C., DeMott, P. J., DeWald, J. T., and Prather, K. A.: Automation and heat transfer characterization of immersion mode spectroscopy for analysis of ice nucleating particles, *Atmospheric Measurement Techniques*, 10, 2613-2626, 2017.
- Bigg, E. K.: The supercooling of water, *Proc.Phys. Soc.*, 66, 688-694, 1953.
- Broadley, S. L., Murray, B. J., Herbert, R. J., Atkinson, J. D., Dobbie, S., Malkin, T. L., Condliffe, E., and Neve, L.: Immersion mode heterogeneous ice nucleation by an illite rich powder representative of atmospheric mineral dust, *Atmos. Chem. Phys.*, 12, 287-307, 2012.
- Budke, C. and Koop, T.: BINARY: an optical freezing array for assessing temperature and time dependence of heterogeneous ice nucleation, *Atmos. Meas. Tech.*, 8, 689-703, 2015.
- Conen, F., Henne, S., Morris, C. E., and Alewell, C.: Atmospheric ice nucleators active $\geq -12^{\circ}\text{C}$ can be quantified on PM10 filters, *Atmospheric Measurement Techniques*, 5, 321-327, 2012.
- Conen, F., Morris, C. E., Leifeld, J., Yakutin, M. V., and Alewell, C.: Biological residues define the ice nucleation properties of soil dust, *Atmos. Chem. Phys.*, 11, 9643-9648, 2011.
- Connolly, P. J., Möhler, O., Field, P. R., Saathoff, H., Burgess, R., Choularton, T., and Gallagher, M.: Studies of heterogeneous freezing by three different desert dust samples, *Atmos. Chem. Phys.*, 9, 2805-2824, 2009.
- Cotton, R. J., Benz, S., Field, P. R., Mohler, O., and Schnaiter, M.: Technical note: A numerical test-bed for detailed ice nucleation studies in the AIDA cloud simulation chamber, *Atmos. Chem. Phys.*, 7, 243-256, 2007.
- DeMott, P. J.: Quantitative Descriptions of Ice Formation Mechanisms of Silver Iodide-Type Aerosols, *Atmospheric Research*, 38, 63-99, 1995.
- DeMott, P. J., Hill, T. C., McCluskey, C. S., Prather, K. A., Collins, D. B., Sullivan, R. C., Ruppel, M. J., Mason, R. H., Irish, V. E., Lee, T., Hwang, C. Y., Rhee, T. S., Snider, J. R., McMeeking, G. R., Dhaniyala, S., Lewis, E. R., Wentzell, J. J., Abbatt, J., Lee, C., Sultana, C. M., Ault, A. P., Axson, J. L., Diaz Martinez, M., Venero, I., Santos-Figueroa, G., Stokes, M. D., Deane, G. B., Mayol-Bracero, O. L., Grassian, V. H., Bertram, T. H., Bertram, A. K., Moffett, B. F., and Franc, G. D.: Sea spray aerosol as a unique source of ice nucleating

particles, *Proceedings of the National Academy of Sciences of the United States of America*, 113, 5797-5803, 2016.

DeMott, P. J., Möhler, O., Cziczo, D. J., Hiranuma, N., Petters, M. D., Petters, S. S., Belosi, F., Bingemer, H. G., Brooks, S. D., Budke, C., Burkert-Kohn, M., Collier, K. N., Danielczok, A., Eppers, O., Felgitsch, L., Garimella, S., Grothe, H., Herenz, P., Hill, T. C. J., Höhler, K., Kanji, Z. A., Kiselev, A., Koop, T., Kristensen, T. B., Krüger, K., Kulkarni, G., Levin, E. J. T., Murray, B. J., Nicosia, A., amp, apos, Sullivan, D., Peckaus, A., Polen, M. J., Price, H. C., Reicher, N., Rothenberg, D. A., Rudich, Y., Santachiara, G., Schiebel, T., Schrod, J., Seifried, T. M., Stratmann, F., Sullivan, R. C., Suski, K. J., Szakáll, M., Taylor, H. P., Ullrich, R., Vergara-Temprado, J., Wagner, R., Whale, T. F., Weber, D., Welti, A., Wilson, T. W., Wolf, M. J., and Zenker, J.: The Fifth International Workshop on Ice Nucleation phase 2 (FIN-02): Laboratory intercomparison of ice nucleation measurements, *Atmospheric Measurement Techniques Discussions*, doi: 10.5194/amt-2018-191, 2018. 1-44, 2018.

DeMott, P. J., Prenni, A. J., Liu, X., Kreidenweis, S. M., Petters, M. D., Twohy, C. H., Richardson, M. S., Eidhammer, T., and Rogers, D. C.: Predicting global atmospheric ice nuclei distributions and their impacts on climate, *Proceedings of the National Academy of Sciences, USA*, 107, 11217-11222, 2010.

Diehl, K. and Mitra, S. K.: A laboratory study of the effects of a kerosene-burner exhaust on ice nucleation and the evaporation rate of ice crystals, *Atmospheric Environment*, 32, 3145-3151, 1998.

Du, R., Du, P., Lu, Z., Ren, W., Liang, Z., Qin, S., Li, Z., Wang, Y., and Fu, P.: Evidence for a missing source of efficient ice nuclei, *Sci Rep*, 7, 39673, 2017.

Eidhammer, T., DeMott, P. J., Prenni, A. J., Petters, M. D., Twohy, C. H., Rogers, D. C., Stith, J., Heymsfield, A., Wang, Z., Pratt, K. A., Prather, K. A., Murphy, S. M., Seinfeld, J. H., Subramanian, R., and Kreidenweis, S. M.: Ice Initiation by Aerosol Particles: Measured and Predicted Ice Nuclei Concentrations versus Measured Ice Crystal Concentrations in an Orographic Wave Cloud, *Journal of the Atmospheric Sciences*, 67, 2417-2436, 2010.

Garcia, E., Hill, T. C. J., Prenni, A. J., DeMott, P. J., Franc, G. D., and Kreidenweis, S. M.: Biogenic ice nuclei in boundary layer air over two U.S. High Plains agricultural regions, *Journal of Geophysical Research-Atmospheres*, 117, 2012.

Garimella, S., Kristensen, T. B., Ignatius, K., Welti, A., Voigtländer, J., Kulkarni, G. R., Sagan, F., Kok, G. L., Dorsey, J., Nichman, L., Rothenberg, D., Rösch, M., Kirchgäßner, A., Ladkin, R., Wex, H., Wilson, T. W., Ladino, L. A., Abbatt, J. P. D., Stetzer, O., Lohmann, U., Stratmann, F., and Cziczo, D. J.: The SPectrometer for Ice Nuclei (SPIN): An instrument to investigate ice nucleation, *Atmos. Meas. Tech. Discuss.*, 2016, 1-37, 2016.

Hande, L. B. and Hoose, C.: Partitioning the primary ice formation modes in large eddy simulations of mixed-phase clouds, *Atmospheric Chemistry and Physics*, 17, 14105-14118, 2017.

Harrison, A. D., Whale, T. F., Carpenter, M. A., Holden, M. A., Neve, L., apos, Sullivan, D., Vergara Temprado, J., and Murray, B. J.: Not all feldspars are equal: a survey of ice nucleating properties across the feldspar group of minerals, *Atmospheric Chemistry and Physics*, 16, 10927-10940, 2016.

Häusler, T., Witek, L., Felgitsch, L., Hitzenberger, R., and Grothe, H.: Freezing on a Chip—A New Approach to Determine Heterogeneous Ice Nucleation of Micrometer-Sized Water Droplets, *Atmosphere*, 9, 140, 2018.

Herbert, R. J., Murray, B. J., Dobbie, S. J., and Koop, T.: Sensitivity of liquid clouds to homogenous freezing parameterizations, *Geophysical Research Letters*, 42, 1599-1605, 2015.

Herbert, R. J., Murray, B. J., Whale, T. F., Dobbie, S. J., and Atkinson, J. D.: Representing time-dependent freezing behaviour in immersion mode ice nucleation, *Atmospheric Chemistry and Physics*, 14, 8501-8520, 2014.

Hiranuma, N., Augustin-Bauditz, S., Bingemer, H., Budke, C., Curtius, J., Danielczok, A., Diehl, K., Dreischmeier, K., Ebert, M., Frank, F., Hoffmann, N., Kandler, K., Kiselev, A., Koop, T., Leisner, T., Möhler, O., Nillius, B., Peckhaus, A., Rose, D., Weinbruch, S., Wex, H., Boose, Y., DeMott, P. J., Hader, J. D., Hill, T. C. J., Kanji, Z. A., Kulkarni, G., Levin, E. J. T., McCluskey, C. S., Murakami, M., Murray, B. J., Niedermeier, D., Petters, M. D., O'Sullivan, D., Saito, A., Schill, G. P., Tajiri, T., Tolbert, M. A., Welti, A., Whale, T. F.,

Wright, T. P., and Yamashita, K.: A comprehensive laboratory study on the immersion freezing behavior of illite NX particles: a comparison of 17 ice nucleation measurement techniques, *Atmos. Chem. Phys.*, 15, 2489-2518, 2015.

Hoose, C., Kristjánsson, J. E., Chen, J.-P., and Hazra, A.: A Classical-Theory-Based Parameterization of Heterogeneous Ice Nucleation by Mineral Dust, Soot, and Biological Particles in a Global Climate Model, *Journal of the Atmospheric Sciences*, 67, 2483-2503, 2010.

Hoose, C. and Möhler, O.: Heterogeneous ice nucleation on atmospheric aerosols: a review of results from laboratory experiments, *Atmos. Chem. Phys.*, 12, 9817-9854, 2012.

Kanji, Z. A. and Abbatt, J. P. D.: The University of Toronto Continuous Flow Diffusion Chamber (UT-CFDC): A Simple Design for Ice Nucleation Studies, *Aerosol Science and Technology*, 43, 730-738, 2009.

Kanji, Z. A., Ladino, L. A., Wex, H., Boose, Y., Burkert-Kohn, M., Cziczo, D. J., and Krämer, M.: Overview of Ice Nucleating Particles, *Meteorological Monographs*, 58, 1.1-1.33, 2017.

Knopf, D. A. and Alpert, P. A.: A water activity based model of heterogeneous ice nucleation kinetics for freezing of water and aqueous solution droplets, *Faraday Discuss*, 165, 513-534, 2013.

Knopf, D. A. and Forrester, S. M.: Freezing of Water and Aqueous NaCl Droplets Coated by Organic Monolayers as a Function of Surfactant Properties and Water Activity, *J. Phys. Chem. A*, 115, 5579-5591, 2011.

Kohn, M., Lohmann, U., Welti, A., and Kanji, Z. A.: Immersion mode ice nucleation measurements with the new Portable Immersion Mode Cooling chamber (PIMCA), *Journal of Geophysical Research: Atmospheres*, 121, 4713-4733, 2016.

Koop, T. and Murray, B. J.: A physically constrained classical description of the homogeneous nucleation of ice in water, *J Chem Phys*, 145, 211915, 2016.

Kunert, A. T., Lamneck, M., Helleis, F., Pöhlker, M. L., Pöschl, U., and Fröhlich-Nowoisky, J.: Twin-plate ice nucleation assay (TINA) with infrared detection for high-throughput

droplet freezing experiments with biological ice nuclei in laboratory and field samples, *Atmospheric Measurement Techniques Discussions*, doi: 10.5194/amt-2018-230, 2018. 1-25, 2018.

Murray, B. J., Broadley, S. L., Wilson, T. W., Atkinson, J. D., and Wills, R. H.: Heterogeneous freezing of water droplets containing kaolinite particles, *Atmospheric Chemistry and Physics*, 11, 4191-4207, 2011.

Murray, B. J., O'Sullivan, D., Atkinson, J. D., and Webb, M. E.: Ice nucleation by particles immersed in supercooled cloud droplets, *Chemical Society Reviews*, 41, 6519-6554, 2012.

Niemand, M., Möhler, O., Vogel, B., Vogel, H., Hoose, C., Connolly, P., Klein, H., Bingemer, H., DeMott, P., Skrotzki, J., and Leisner, T.: A Particle-Surface-Area-Based Parameterization of Immersion Freezing on Desert Dust Particles, *Journal of the Atmospheric Sciences*, 69, 3077-3092, 2012.

Peckhaus, A., Kiselev, A., Hiron, T., Ebert, M., and Leisner, T.: A comparative study of K-rich and Na/Ca-rich feldspar ice-nucleating particles in a nanoliter droplet freezing assay, *Atmos. Chem. Phys.*, 16, 11477-11496, 2016.

Pinti, V., Marcolli, C., Zobrist, B., Hoyle, C. R., and Peter, T.: Ice nucleation efficiency of clay minerals in the immersion mode, *Atmos. Chem. Phys. Discuss.*, 12, 3213-3261, 2012.

Pitter, R. L. and Pruppacher, H. R.: Wind-tunnel investigation of freezing of small water drops falling at terminal velocity in air, *Quarterly Journal of the Royal Meteorological Society*, 99, 540-550, 1973.

Polen, M., Brubaker, T., Somers, J., and Sullivan, R. C.: Cleaning up our water: reducing interferences from non-homogeneous freezing of "pure" water in droplet freezing assays of ice nucleating particles, *Atmospheric Measurement Techniques Discussions*, doi: <https://doi.org/10.5194/amt-2018-134>, 2018. 1-31, 2018.

Prenni, A. J., Demott, P. J., Rogers, D. C., Kreidenweis, S. M., McFarquhar, G. M., and Zhang, G.: Ice nuclei characteristics from M-PACE and their relation to ice formation in clouds, *Tellus*, 61, 436-448, 2009.

- Prenni, A. J., Tobo, Y., Garcia, E., DeMott, P. J., Huffman, J. A., McCluskey, C. S., Kreidenweis, S. M., Prenni, J. E., Pöhlker, C., and Pöschl, U.: The impact of rain on ice nuclei populations at a forested site in Colorado, *Geophysical Research Letters*, 40, 227-231, 2013.
- Rogers, D. C., DeMott, P. J., Kreidenweis, S. M., and Chen, Y. L.: A continuous-flow diffusion chamber for airborne measurements of ice nuclei, *J. Atmos. Ocean. Tech.*, 18, 725-741, 2001.
- Salam, A., Lohmann, U., Crenna, B., Lesins, G., Klages, P., Rogers, D., Irani, R., MacGillivray, A., and Coffin, M.: Ice nucleation studies of mineral dust particles with a new continuous flow diffusion chamber, *Aerosol. Sci. Tech.*, 40, 134-143, 2006.
- Sear, R. P.: Quantitative studies of crystal nucleation at constant supersaturation: experimental data and models, *CrystEngComm*, 16, 6506-6522, 2014.
- Stetzer, O., Baschek, B., Lüönd, F., and Lohmann, U.: The Zurich Ice Nucleation Chamber (ZINC)-A new instrument to investigate atmospheric ice formation, *Aerosol Science and Technology*, 42, 64-74, 2008.
- Stopelli, E., Conen, F., Zimmermann, L., Alewell, C., and Morris, C. E.: Freezing nucleation apparatus puts new slant on study of biological ice nucleators in precipitation, *Atmospheric Measurement Techniques*, 7, 129-134, 2014.
- Tobo, Y., Prenni, A. J., DeMott, P. J., Huffman, J. A., McCluskey, C. S., Tian, G., Pöhlker, C., Pöschl, U., and Kreidenweis, S. M.: Biological aerosol particles as a key determinant of ice nuclei populations in a forest ecosystem, *Journal of Geophysical Research: Atmospheres*, 118, 10,100-110,110, 2013.
- Vali, G.: Freezing Rate Due to Heterogeneous Nucleation, *Journal of the Atmospheric Sciences*, 51, 1843-1856, 1994.
- Vali, G.: Interpretation of freezing nucleation experiments: singular and stochastic; sites and surfaces, *Atmospheric Chemistry and Physics*, 14, 5271-5294, 2014.

Vali, G.: Principles of Ice Nucleation. In: Biological Ice Nucleation and Its Applications, Lee Jr, R., Warren, G. J., and Gusta, L. V. (Ed.), American Phytopathological Society, St. Paul, Mn, USA, 1995.

Vali, G.: Quantitative Evaluation of Experimental Results on the Heterogeneous Freezing Nucleation of Supercooled Liquids, *Journal of the Atmospheric Sciences*, 28, 402-409, 1971.

Vali, G.: Repeatability and randomness in heterogeneous freezing nucleation, *Atmos. Chem. Phys.*, 8, 5017-5031, 2008.

Vali, G., DeMott, P. J., Möhler, O., and Whale, T. F.: Technical Note: A proposal for ice nucleation terminology, *Atmos. Chem. Phys.*, 15, 10263-10270, 2015.

Vergara-Temprado, J., Miltenberger, A. K., Furtado, K., Grosvenor, D. P., Shipway, B. J., Hill, A. A., Wilkinson, J. M., Field, P. R., Murray, B. J., and Carslaw, K. S.: Strong control of Southern Ocean cloud reflectivity by ice-nucleating particles, *Proceedings of the National Academy of Sciences of the United States of America*, 115, 2687-2692, 2018.

Vergara-Temprado, J., Murray, B. J., Wilson, T. W., and Sullivan, D., Browse, J., Pringle, K. J., Ardon-Dryer, K., Bertram, A. K., Burrows, S. M., Ceburnis, D., DeMott, P. J., Mason, R. H., and Dowd, C. D., Rinaldi, M., and Carslaw, K. S.: Contribution of feldspar and marine organic aerosols to global ice nucleating particle concentrations, *Atmos. Chem. Phys.*, 17, 3637-3658, 2017.

Whale, T. F., Holden, M. A., Kulak, A. N., Kim, Y. Y., Meldrum, F. C., Christenson, H. K., and Murray, B. J.: The role of phase separation and related topography in the exceptional ice-nucleating ability of alkali feldspars, *Phys Chem Chem Phys*, 19, 31186-31193, 2017.

Whale, T. F., Holden, M. A., Wilson, T. W., O'Sullivan, D., and Murray, B. J.: The enhancement and suppression of immersion mode heterogeneous ice-nucleation by solutes, *Chem Sci*, 9, 4142-4151, 2018.

Whale, T. F., Murray, B. J., O'Sullivan, D., Wilson, T. W., Umo, N. S., Baustian, K. J., Atkinson, J. D., Workneh, D. A., and Morris, G. J.: A technique for quantifying heterogeneous ice nucleation in microlitre supercooled water droplets, *Atmos. Meas. Tech.*, 8, 2437-2447, 2015.

Zaragotas, D., Liolios, N. T., and Anastassopoulos, E.: Supercooling, ice nucleation and crystal growth: a systematic study in plant samples, *Cryobiology*, 72, 239-243, 2016.

5. Conclusions

5.1 Overview

In this thesis I outlined the need to understand mineral dusts as ice-nucleating particles in the atmosphere. In order to further our knowledge in this area I defined three objectives; the first objective was to improve our understanding of how the chemical and physical characteristics of a mineral may affect its ability to nucleate ice and how this then translates to which minerals are important for the glaciation of clouds in the atmosphere. The second objective was to make use of field observations to constrain our INP model predications, which use laboratory based parameterisations related to objective one. In particular we wanted to see if our model could predict the INP concentration of an environment which was exposed to transported mineral dust which may have undergone processing, such as acid ageing. The final objective was to develop an immersion mode drop assay capable of detecting low concentrations of INP which are relevant for cloud glaciation at higher temperatures, as field studies are lacking data in the regime above $-15\text{ }^{\circ}\text{C}$ which has significance for secondary ice multiplication processes, e.g. the Hallett-Mossop process.

5.2 Objective one: Mineral characteristics and their influence on the ice-nucleating ability of mineral dust

From the introduction we introduced the concept that there are many different mineral components that can be found in mineral dusts in the atmosphere. The relative proportions of these components and the overall mineralogy of these dusts vary globally and so it is important to understand the ice-nucleating ability of the various components of mineral dust rather than treat all mineral dusts as a single material. This may explain why some generalised mineral dust parameterisations cannot explain field observations of INP, see chapters two and three. The three major components of aerosolised mineral dusts are the clays, quartz and feldspar group of minerals. Atkinson et al. (2013) showed K-feldspar to be the dominant ice-nucleating material in typical mineral dusts. However, the ice-nucleating ability of quartz had not been well characterised in the literature although it makes up a large proportion of mineral dusts (on average quartz is a factor of five more in abundance than K-feldspar). Previous studies have shown quartz to be ice active but the number of representative samples for the atmosphere are

low (Atkinson et al., 2013; Holden et al., 2019; Isono and Ikebe, 1960; Kumar et al., 2019; Losey et al., 2018; Zolles et al., 2015). There are also other minerals which are present in the atmosphere which have not been well characterised but may potentially have importance when considering other potential mineral dust INP sources. Minerals such as pyroxene and amphibole have not been extensively researched in the literature yet could have potential significance for mineral INP in aerosol such as volcanic ashes or mineral dusts sourced from volcanic regions (e.g. Iceland). The potential significance of such minerals is suggested in the recent work of Maters et al. (2019), however in this thesis I have focused on the most common minerals found in typical mineral dusts. I propose that work continues to grow the current understanding of ice nucleation by various minerals, in particular those which have yet to be extensively surveyed and well characterised, such as pyroxene and amphibole. Pyroxene would be of particular interest as it also exhibits phase separation, similar to K-feldspar, and hence it is plausible that certain pyroxene minerals may also have microtextures which are beneficial for ice nucleation. If other minerals are explored for their ice-nucleating ability, and sufficiently characterised, it will help the community explore the nature of active sites and the influence of microtexture and crystal formation on the development of active sites for ice nucleation.

With this in mind, here (chapter two) I have tested 10 well characterised, atmospherically relevant, α -quartz samples for their ice-nucleating ability as they have previously been underrepresented in ice nucleation studies of mineral dust components. The 10 samples show a large degree of variability in the ice-nucleating ability of the quartz mineral group. Given the similar crystal structure of all these samples of α -quartz I attribute these variable ice-nucleating abilities to the minor impurities found in the quartz sample and/or its geological history. I suggest that the minor impurities may lead to fracturing of the sample in a manner which is beneficial to the exposure of sites for ice nucleation. The possible influence of grinding minerals (and thus fracturing) on the ice-nucleating ability of quartz has been seen previously via the increased activity of ground samples (Kumar et al., 2019; Zolles et al., 2015). We also hypothesise that the geological history of the sample may lead to defects which act as sites/or expose sites for nucleation, i.e. a quartz sample which has been subjected to stresses at a shear zone may exhibit defects which act as/expose sites for ice nucleation.

The effect of the geological formation conditions has also been suggested to be important for K-feldspars, in that it determines the extent of phase separation in the alkali feldspars which is currently thought to be responsible, in part, for the ice-nucleating ability of this mineral group (Whale et al., 2017). It is becoming more apparent that the geological history of the mineral is key in determining its ability to nucleate ice. Not only does it influence its composition and polymorph type but also its development of microstructures. It is then apparent that new studies that relate the crystal formation histories to the ice-nucleating ability of minerals would be important in the understanding of the development of active sites. New studies should explore the concepts proposed in this thesis in order to quantify the effect that the geological history of a mineral has on its ability to nucleate ice. For example, a study which investigates the ice-nucleating ability of strained quartz versus a quartz sample which has undergone very little deformation/stress, would be important to understand the role of post processing on a mineral's ability to nucleate. If key processes, such as crystallisation cooling rates and deformation, were understood in relation to their influence on the nature of active sites, then it would be a pivotal step towards being able to predict what makes a good nucleator.

In chapter two we also show the sensitivity of the ice-nucleating activity of quartz to the exposure of water which is in agreement with previous observations (Kumar et al., 2019; Zolles et al., 2015). Kumar et al. (2019) completed experiments in both glass and polypropylene vials and saw that only quartz within glass vials deactivated. They proposed that the leaching of silica from the glass vial caused the quartz particles to grow and therefore alter the surface of the particles and deactivate its ice-nucleating ability. This is consistent with most of the results presented in Chapter two although this hypothesis does not explain the deactivation of some quartz samples in air nor does it explain why the Bombay Chalcedony sample did not deactivate. This suggests there are different sites on these samples of quartz which have differing sensitivities to ageing processes. It is hypothesised here that the active sites for nucleation are potentially unstable high energy sites, which is supported by computational studies by Pedevilla et al. (2017), and are typically the most sensitive to reactions. Berner and Holdren et al. (1979) proposed that high energy sites, related to defects in the crystal structure, would be the first areas to be altered by weathering/ageing processes and so it is conceivable that the activity of minerals may change with ageing as the high energy active sites are altered.

However, the relative insensitivity of the highly active Bombay chalcedony sample provides evidence that not all active sites have the same sensitivity to ageing processes and so it becomes complicated in determining how a specific mineral may react to various processes. Work by Kumar et al. (2018), Whale et al. (2018) and Boose et al. (2019) has also shown the potential significance of other ageing processes in the atmosphere, such as the effect of acid coatings and solutes. With so many processes that may affect the ice-nucleating ability of minerals in the atmosphere (which may interact in complex ways) we currently have to assume that ageing is negligible when making INP predications.

At present we understand that K-feldspar is the dominant INP in mineral dusts which has been supported by the development and use of new parameterisations to represent the various components of mineral dusts in chapter two. Given the assumption that ageing is minimal for K-feldspar in the atmosphere and that the parameterisations created for quartz, albite and plagioclase (in chapter two) are expressions of the maximum possible activity for these mineral groups, I show that K-feldspar is the dominant INP globally. This is supported by the good agreement between predicted INP concentrations and field observations (chapter two and three). Assuming typical concentrations of minerals in aerosolised mineral dusts I find that quartz, albite and plagioclase feldspar are all of second order importance. Even in relatively low concentrations (0.1% of the mineral dust population, or even lower) K-feldspar dominates ice nucleation. These findings are consistent with the original work by Atkinson et al. (2013). Only in rare instances can any other mineral compete with K-feldspar. The work presented in chapter three demonstrates that the new K-feldspar parameterisation can be used to predict INP concentrations extremely well given that the mineralogy of the aerosol is known. It is hoped that these newly developed parameterisations will be used by the community to predict and model INP. These parameterisations have already proved useful for the interpretation of the nucleating components of volcanic ash (Maters et al., 2019). In addition to this, further field measurements would be useful to test the robustness of these parameterisations so that they may be used more confidently in global models in future.

As discussed previously, we currently make the assumption that minerals are not greatly impacted by ageing processes in the atmosphere when modelling INP. Fortunately, K-feldspar has been shown to be the dominant mineral INP in most instances and it has shown little

sensitivity to time left in water and air (Harrison et al., 2016; Kumar et al., 2018). However, K-feldspar is potentially sensitive to acids and solutes (Kumar et al., 2018; Whale et al., 2018). Sea salt has been proposed to be a source of solutes (including NaCl) which have the ability to deactivate transported mineral dusts (Iwata and Matsuki, 2018, Si et al., 2019). However, in chapter three we present a simple experiment which suggests that natural concentrations of sea salt have no impact on the ice-nucleating ability of K-feldspar. With this in mind, and given the good agreement of INP predictions compared to observations, it would then suggest that using laboratory based parameterisations for fresh, minimally aged K-feldspar to represent mineral dusts in the atmosphere is a reasonable assumption. This assumption is in agreement with the results presented in chapter three and previous studies (O'Sullivan et al., 2018; Price et al., 2018). However, it is possible in some locations that this assumption may not hold true, i.e. if acid ageing were to occur. There is then a need for future work into the effect of ageing processes on mineral dusts. Solute have been shown to both decrease and increase the activity of feldspar (Whale et al, 2018), while acids have shown to decrease the activity all cases (Kumar et al., 2018, Kumar et al., 2019a, Kumar et al., 2019b, Wex et al., 2014, Sullivan et al., 2010) and coatings on the surface of mineral particles are generally thought to inhibit the ice-nucleating ability of aerosol (Möhler et al., 2008). Acids, solutes and coatings may all effect the activity of INP in the atmosphere and interact with the aerosol in complex ways. The work from this thesis has demonstrated that reasonable predictions of INP concentrations using lab based parameterisations can be made but there is now a new step (the effect of ageing processes) that needs to be considered to further improve these predictions.

It should also be noted that weathering processes create mineral dusts and continue to process them over millions of years. We hypothesise in chapter two that the energetic saltation process is somewhat comparable to the grinding of mineral powders in the laboratory and could lead to fresh surfaces/sites for nucleation in the atmosphere. Knowing the extent of ageing on a mineral dust before it is emitted to the atmosphere is key to determining the influence of ageing processes in the atmosphere. An interesting study would be to take aged mineral dust and subject it to the saltation process, for example in a wind tunnel, to see if the saltation impactions give rise to fresh mineral surfaces before emission to the atmosphere, e.g. breaking down reaction products on the surface. The overall effect of ageing on mineral dusts can be tackled

with both laboratory investigations and field measurements, of which there are currently very limited datasets. This then leads us on to the second objective in which we aim to make field measurements of transported, and processed, mineral dust.

5.3 Objective two: Taking field measurements of transported mineral dust and constraining INP predictions

Given the discussion in section 5.2 we can now see the importance of understanding the effect of transportation on mineral dust. However, there are a dearth of field observations from which we can infer the effect of transport. Iwata and Matsuki (2018) characterise single particles for their ice-nucleating ability and suggest a deactivation of mineral dust sampled in the Asian dust outflow region when comparing the sampled aerosol to the Arizona Test Dust (ATD) standard and K-feldspar. This study suggests that an internal mixing of sea salt may be the cause of the deactivation in this instance as a solute effect may occur which is similar to that described by Whale et al. (2018). This observation is supported by the work of Si et al. (2019) who correlate sea salt tracers to a deactivation of mineral dust in the high Arctic. However, there is yet to be a study which investigates two comparable dusts which represent different stages of transport, i.e. a dust which is close to source versus a dust which has been transported for roughly one week.

With this in mind we chose to sample mineral dust at Barbados and compare the results to observations made in the eastern tropical Atlantic, around the Cape Verde region (Price et al. 2018). This allowed for the first study of transported desert dust to be compared to observations of a similar, minimally transported, desert dust which was sampled close to known dust sources. This study showed a deactivation of the mineral dust on transport similar to Si et al. (2019) and Iwata and Matsuki (2018) with sea salt being commonly found disseminated across filters. Initial model predictions overestimated the INP concentrations at Barbados and so it was originally hypothesised that the sea salt may be having a solute effect as this is not considered in the model. However, a preliminary experiment investigating the effect of typical sea salt concentrations on K-feldspar showed no effect, chapter three. This pragmatic experiment had a number of assumptions involved and so it would be beneficial for a more extensive and focused study on the effect of sea salt on mineral dusts ice-nucleating ability. Ideally this work could be incorporated with the parameterisations developed in chapter two to

represent the activity of INP globally, i.e. provide a correction factor for the reduction in activity (if any) as a result of sea salt.

Assuming a typical concentration of aerosolised K-feldspar in Barbados leads to an over estimation of the INP concentrations at this location. However, when investigating the mineralogy of the aerosol at Barbados I find evidence for a lower than average K-feldspar content (< 2 wt%) for the aerosolised mineral dust sampled. When combining this mineralogical information with the newly improved K-feldspar parameterisation developed in chapter two, and assuming K-feldspar is the dominant mineral INP, I find I can predict the INP concentrations at Barbados. It is then clear from chapter three that knowing the mineralogy of a mineral dust is key to predicting its capacity to nucleate ice. This has highlighted areas for improvement in both our global model (GLOMAP) and sampling strategies employed in the field. GLOMAP was seen to over predict the K-feldspar content at Barbados in its simulations by roughly a factor of 7. We attribute this over estimation to the subsequent over estimation of the INP concentrations at Barbados. The XRD analysis of rain water collected aerosol proved valuable for determining this discrepancy between the predictions and the observations. I therefore suggest that future INP field studies look to determine the mineralogy of the aerosol they collect in order to understand the components which may lead to nucleation. Without this understanding of the mineralogy of the desert dust at Barbados I would have been limited in my ability to explain the discrepancies seen and as such would have hypothesised sea salt or acid ageing as the main cause of the deactivation of the mineral dust. At present identification of the mineralogy of aerosol collected samples is not routinely carried out in most ice nucleation studies. Further to this, the mineralogy of the samples is limited and often groups key mineral components together, e.g. albite is often grouped with the rest of the plagioclase series although they have different ice-nucleating abilities. It would be advantageous to the community to make robust characterisations of the mineralogy of aerosol alongside INP measurements as it will allow for a better interpretation of the results. This will also make it easier to probe the influence of ageing processes in the atmosphere.

Although I cannot definitely rule out the effect of acid ageing (or sea salt) at Barbados, all of the observations can be explained when constrained by the mineralogical composition of the aerosol. Hence, I propose that scavenging of the K-feldspar component on transport, i.e.

through precipitation and gravitational settling, reduces the K-feldspar content and thus reduces the amount of INP available and hence decreases the mineral dusts ice-nucleating ability. This hypothesis may also explain the previous observations by Si et al. (2019) and Iwata and Matsuki (2018). Si et al. (2019) correlated a decrease in aerosol activity to an increase in the amount of sea salt, however this increase in sea salt may also be a function of the time the aerosol was transported. If the aerosol had been transported over the ocean for longer periods of time it would have time to collect more sea salt. It is then possible that these longer transportation times correlate with larger degrees of scavenging and hence could explain the decrease in activity of the aerosol as a function of the K-feldspar component being removed. This is also true for Iwata and Matsuki (2018) who find sea salt in their samples. It should be noted that Iwata and Matsuki (2018) attribute the activity of particles that froze above $-30\text{ }^{\circ}\text{C}$ to particles that resemble clays in nature. This may then suggest that the K-feldspar component was in low concentrations or that it had been deactivated by the presence of solutes from the sea salt. It is however hard to say whether the lower than expected activity of the sampled mineral dust aerosol was a result of a low K-feldspar content or as a result of the deactivation of the mineral particles as a result of the presence of sea salt. A deeper investigation into the role of sea salt and K-feldspar would be beneficial to shed light on this topic.

From GLOMAP simulations it is apparent that the removal of K-feldspar is underrepresented in the model. We hypothesise that this is, in part, due to the K-feldspar component being overrepresented in the clay size aerosol mode, and so a larger proportion of K-feldspar stays suspended for longer. It is hoped that the work presented in chapter three can guide future improvements to the GLOMAP model so that it may better represent the removal of K-feldspar on transport and thus better simulate INP concentrations in locations such as Barbados. It is also apparent that further field studies are needed to provide more evidence for the effect of scavenging and ageing processes on transported mineral dusts in order to guide how we handle K-feldspar in global aerosol models. If future work can build on these findings and quantify the removal of K-feldspar from mineral dusts and the role of ageing processes then it will be beneficial for global models in order to more accurately predict INP concentrations.

5.4 Objective three: Develop an immersion mode instrument capable of detecting rare INP

In chapter four I present the newly developed large volume assay, the IR-NIPI. This instrument uses large droplet sizes, 50 μL , and so it is sensitive to rare populations of INP which are low in concentration and active at the warmest temperatures ($>-15\text{ }^\circ\text{C}$). This was seen by the extension of the dataset to warmer temperatures when analysing aerosol collected from Leeds city centre. The data collected from a 1 μL instrument (μL -NIPI) was limited to temperatures below $-12\text{ }^\circ\text{C}$. The IR-NIPI extended this dataset to include INPs active at $-5\text{ }^\circ\text{C}$ and one and a half orders of magnitude lower in concentration. The benefit of accessing these high temperature regimes is reflected by the recent surge in the use of large volume assays (Beall et al., 2017, Kunert et al., 2018, David et al., 2019).

Both vertical (Beall et al., 2017) and horizontal temperature gradients (David et al., 2019) across an array of large volume droplets have been noted in the literature. The use of an infrared camera in the IR-NIPI allowed for the individual monitoring of temperature for droplets in a multiwell plate which reduced the bias in temperature measurements as a result of a horizontal gradient across the cold plate. Other groups in the ice nucleation community may look to use infrared technology in a similar way as it removes the uncertainty from horizontal gradients from the experiment. The use of feldspar chips at the base of the droplets in the IR-NIPI suggests a minor influence of the vertical gradient on the temperature measurement of freezing events and it was found to be within the uncertainties of the experiment. However, these gradients will become problematic if larger droplets were to be used which may become an issue as experiments look to reach even rarer INP active at higher temperatures.

The introduction of a novel temperature calibration, using the ice-liquid equilibrium as a calibration point, gave accurate temperature measurements with an error of $\pm 0.9\text{ }^\circ\text{C}$. This calibration could be beneficial to other ice nucleation assays as no experimental setup self-calibrates for every new experiment or has a unique calibration for every droplet. This novel calibration method would be of particular use to the setup of (Zaragotas et al., 2016) as they use an infrared camera. The instrument presented in Zaragotas et al. (2016) was limited by the use of a factory standard calibration which had large errors and was not routinely calibrated.

It should be highlighted that even with a robust temperature measurement a discrepancy in the freezing temperatures for NX-illite suspensions was seen in the IR-NIPI. Upon dilution of the NX-illite suspension the temperature at which the droplets froze did not decrease as expected.

From vigorous temperature calibrations I ruled out an error in the temperature measurement of the system. By gravimetrically weighing suspensions rather than diluting a stock suspension I was able to mitigate this discrepancy. I attribute this discrepancy on dilution to the uneven distribution of particles in the dilutions/droplets which is dependent on the material. This material dependency may be due to the size distribution of the material or the way in which it flocculates in suspension. When probing literature data this discrepancy is seen in other large volume instruments (Beall et al., 2017; David et al., 2019) and so forms an interesting problem which relates to the volume of the droplets in the instrument and the material investigated. This problem has been tentatively presented in the literature with no study addressing this issue head on. The paper presented in chapter four describes this problem in the literature for the first time to make other research groups aware of this phenomena. Future studies should aim to explore this discrepancy as it may help explain the discrepancies seen between other instruments, i.e. wet versus dry dispersion techniques (Hiranuma et al., 2015).

Finding agreement between instrumental setups is key in order to interpret data from various studies. At present there is no robust and routinely used standard material in the ice-nucleating community. Currently, the most commonly used material is NX-illite. However, NX-illite is a mixture of various minerals which may not be homogeneously distributed through a batch of samples. This poses issues when considering, for example, that the ice-nucleating ability of a sample of clay with 1 wt% K-feldspar opposed to 0.1wt% K-feldspar would lead to one order of magnitude difference in measured activity. I propose that a standard material which is homogenous and well characterised be used as a standard to characterise the various instruments. This is a crucial step in then being able to understand the discrepancies in results from large volume instruments and smaller volume instruments.

If the aforementioned volume dependence discrepancy can be understood then the IR-NIPI (and other large volume instruments) can be reliably used to extend INP datasets to warmer temperatures which becomes particularly important for field studies. With this said, there are still improvements which could be made to the IR-NIPI to increase its potential. One of the changes I would like to make to the IR-NIPI would be the resolution and specs of the IR camera. Currently the resolution is the limiting factor in the number of droplets we can monitor at a given time. We could use a variety of multiwell plates and push the number of droplets

from 96 droplets to 1536 droplets if the IR camera had sufficient resolution. Increasing the resolution and specs of the camera may also help lower the ± 0.9 °C temperature uncertainty. If given time I would also like to work on the automation of the system. Ideally, an automatic pipetting system could be fitted to the shell of the IR-NIPI to reduce the amount of manual time needed per experiment. The custom analysis software could also be integrated into the on board computer which is found in the ViaFreeze stirling engine. With more time the custom python software could be modified to perform further analysis (e.g. calculate INP concentrations and n_s) and output graphs for the user to see on the inbuilt screen. Overall, the IR-NIPI is a neat, compact system but still has room for further adjustments to improve its usability and capabilities.

5.5 Concluding remarks

The project detailed above has furthered our understanding of the ice-nucleating ability of common components of mineral dusts. Here I have focused on the most common aerosolised mineral components and have supported the consensus that K-feldspar dominates the INP population in most mineral dusts. It should be considered that there will be instances where this may not be the case, for example in dust emissions from volcanic sources where K-feldspar is not present. In these instances other mineral components may become important and so a deeper understanding of all atmospherically relevant minerals as INPs is important. I have also shown that there is the possibility for minerals to lose their ability to nucleate ice and highlighted the potential impact of atmospheric processes on mineral INP.

Using both laboratory and field measurements I have hypothesised that long range transport of a mineral dust leads to the removal of the K-feldspar component and therefore results in a decrease in the ice-nucleating ability of a mineral dust on transport. The effect of sea salt and acid ageing is still unclear and further investigations are needed to determine whether atmospheric solutes and acids play a role in the deactivation of mineral dusts. Further field studies are then needed to provide information on the effect of transportation on mineral dusts.

With this in mind I have developed the IR-NIPI instrument which may be deployed in future campaigns to extend INP datasets to lower concentrations of INP active at warmer temperatures than are currently observable in the μL -NIPI setup. However, there is a large volume

discrepancy for some materials seen in the IR-NIPI (and other instruments in the literature) which is not currently understood. This issue should be investigated and resolved in order to confidently use these instruments for certain materials.

References

Atkinson, J. D., Murray, B. J., Woodhouse, M. T., Whale, T. F., Baustian, K. J., Carslaw, K. S., Dobbie, S., O'Sullivan, D., and Malkin, T. L.: The importance of feldspar for ice nucleation by mineral dust in mixed-phase clouds, *Nature*, 498, 355-358, 2013.

Augustin-Bauditz, S., Wex, H., Kanter, S., Ebert, M., Niedermeier, D., Stolz, F., Prager, A., and Stratmann, F.: The immersion mode ice nucleation behavior of mineral dusts: A comparison of different pure and surface modified dusts, *Geophysical Research Letters*, 41, 7375-7382, 2014.

Beall, C. M., Stokes, M. D., Hill, T. C., DeMott, P. J., DeWald, J. T., and Prather, K. A.: Automation and heat transfer characterization of immersion mode spectroscopy for analysis of ice nucleating particles, *Atmospheric Measurement Techniques*, 10, 2613-2626, 2017.

Berner, R. A., and Holdren, G. R.: Mechanism of feldspar weathering—ii. Observations of feldspars from soils, *Geochim. Cosmochim. Acta*, 43, 1173-1186, [http://dx.doi.org/10.1016/0016-7037\(79\)90110-8](http://dx.doi.org/10.1016/0016-7037(79)90110-8), 1979.

Boose, Y., Baloh, P., Plötze, M., Ofner, J., Grothe, H., Sierau, B., Lohmann, U., and Kanji, Z. A.: Heterogeneous ice nucleation on dust particles sourced from nine deserts worldwide – Part 2: Deposition nucleation and condensation freezing, *Atmospheric Chemistry and Physics*, 19, 1059-1076, 2019.

David, R. O., Cascajo Castresana, M., Brennan, K. P., Rösch, M., Els, N., Werz, J., Weichlinger, V., Boynton, L. S., Bogler, S., Borduas-Dedekind, N., Marcolli, C., and Kanji, Z. A.: Development of the DRoplet Ice Nuclei Counter Zürich (DRINCZ): Validation and application to field collected snow samples, *Atmospheric Measurement Techniques Discussions*, doi: 10.5194/amt-2019-213, 2019. 1-35, 2019.

Harrison, A. D., Whale, T. F., Carpenter, M. A., Holden, M. A., Neve, L., apos, Sullivan, D., Vergara Temprado, J., and Murray, B. J.: Not all feldspars are equal: a survey of ice nucleating properties across the feldspar group of minerals, *Atmospheric Chemistry and Physics*, 16, 10927-10940, 2016.

Hiranuma, N., Augustin-Bauditz, S., Bingemer, H., Budke, C., Curtius, J., Danielczok, A., Diehl, K., Dreischmeier, K., Ebert, M., Frank, F., Hoffmann, N., Kandler, K., Kiselev, A., Koop, T., Leisner, T., Möhler, O., Nillius, B., Peckhaus, A., Rose, D., Weinbruch, S., Wex, H., Boose, Y., DeMott, P. J., Hader, J. D., Hill, T. C. J., Kanji, Z. A., Kulkarni, G., Levin, E. J. T., McCluskey, C. S., Murakami, M., Murray, B. J., Niedermeier, D., Petters, M. D., O'Sullivan, D., Saito, A., Schill, G. P., Tajiri, T., Tolbert, M. A., Welti, A., Whale, T. F., Wright, T. P., and Yamashita, K.: A comprehensive laboratory study on the immersion freezing behavior of illite NX particles: a comparison of 17 ice nucleation measurement techniques, *Atmos. Chem. Phys.*, 15, 2489-2518, 2015.

Holden, M. A., Whale, T. F., Tarn, M. D., O'Sullivan, D., Walshaw, R. D., Murray, B. J., Meldrum, F. C., and Christenson, H. K.: High-speed imaging of ice nucleation in water proves the existence of active sites, *Sci. Adv.*, 2019. 2019.

Isono, K. and Ikebe, Y.: On the Ice-nucleating Ability of Rock-forming Minerals and Soil Particles&lowast, *Journal of the Meteorological Society of Japan. Ser. II*, 38, 213-230, 1960.

Iwata, A. and Matsuki, A.: Characterization of individual ice residual particles by the single droplet freezing method: a case study in the Asian dust outflow region, *Atmospheric Chemistry and Physics*, 18, 1785-1804, 2018.

Kumar, A., Marcolli, C., Luo, B., and Peter, T.: Ice nucleation activity of silicates and aluminosilicates in pure water and aqueous solutions – Part 1: The K-feldspar microcline, *Atmospheric Chemistry and Physics*, 18, 7057-7079, 2018.

Kumar, A., Marcolli, C., and Peter, T.: Ice nucleation activity of silicates and aluminosilicates in pure water and aqueous solutions – Part 2: Quartz and amorphous silica, *Atmospheric Chemistry and Physics*, 19, 6035-6058, 2019a.

Kumar, A., Marcolli, C., and Peter, T.: Ice nucleation activity of silicates and aluminosilicates in pure water and aqueous solutions – Part 3: Aluminosilicates, *Atmos. Chem. Phys.*, 19, 6059-6084, 10.5194/acp-19-6059-2019, 2019b.

Kunert, A. T., Lamneck, M., Helleis, F., Pöhlker, M. L., Pöschl, U., and Fröhlich-Nowoisky, J.: Twin-plate ice nucleation assay (TINA) with infrared detection for high-throughput droplet freezing experiments with biological ice nuclei in laboratory and field samples, *Atmospheric Measurement Techniques Discussions*, doi: 10.5194/amt-2018-230, 2018. 1-25, 2018.

Losey, D. J., Sihvonen, S. K., Veghte, D. P., Chong, E., and Freedman, M. A.: Acidic processing of fly ash: chemical characterization, morphology, and immersion freezing, *Environ Sci Process Impacts*, 20, 1581-1592, 2018.

Maters, E. C., Dingwell, D. B., Cimarelli, C., Müller, D., Whale, T. F., and Murray, B. J.: The importance of crystalline phases in ice nucleation by volcanic ash, *Atmospheric Chemistry and Physics*, 19, 5451-5465, 2019.

Möhler, O., Benz, S., Saathoff, H., Schnaiter, M., Wagner, R., Schneider, J., Walter, S., Ebert, V., and Wagner, S.: The effect of organic coating on the heterogeneous ice nucleation efficiency of mineral dust aerosols, *Environ. Res. Lett.*, 3, 025007, doi:10.1088/1748-9326/3/2/025007, 2008

O'Sullivan, D., Adams, M. P., Tarn, M. D., Harrison, A. D., Vergara-Temprado, J., Porter, G. C. E., Holden, M. A., Sanchez-Marroquin, A., Carotenuto, F., Whale, T. F., McQuaid, J. B., Walshaw, R., Hedges, D. H. P., Burke, I. T., Cui, Z., and Murray, B. J.: Contributions of biogenic material to the atmospheric ice-nucleating particle population in North Western Europe, *Sci Rep*, 8, 13821, 2018.

Pedevilla, P., Fitzner, M., and Michaelides, A.: What makes a good descriptor for heterogeneous ice nucleation on OH-patterned surfaces, *Physical Review B*, 96, 2017.

Price, H. C., Baustian, K. J., McQuaid, J. B., Blyth, A., Bower, K. N., Choulaton, T., Cotton, R. J., Cui, Z., Field, P. R., Gallagher, M., Hawker, R., Merrington, A., Miltenberger, A., Neely, R. R., Parker, S. T., Rosenberg, P. D., Taylor, J. W., Trembath, J., Vergara-Temprado, J., Whale, T. F., Wilson, T. W., Young, G., and Murray, B. J.: Atmospheric Ice-Nucleating Particles in the Dusty Tropical Atlantic, *Journal of Geophysical Research: Atmospheres*, 123, 2175-2193, 2018.

Si, M., Evoy, E., Yun, J., Xi, Y., Hanna, S. J., Chivulescu, A., Rawlings, K., Veber, D., Platt, A., Kunkel, D., Hoor, P., Sharma, S., Leaitch, W. R., and Bertram, A. K.: Concentrations, composition, and sources of ice-nucleating particles in the Canadian High Arctic, *Atmos. Chem. and Phys.*, 19, 3007-3024, 2019.

Sullivan, R. C., Petters, M. D., DeMott, P. J., Kreidenweis, S. M., Wex, H., Niedermeier, D., Hartmann, S., Clauss, T., Stratmann, F., Reitz, P., Schneider, J., and Sierau, B.: Irreversible loss of ice nucleation active sites in mineral dust particles caused by sulphuric acid condensation, *Atmos. Chem. Phys.*, 10, 11471–11487, doi:10.5194/acp-10-11471-2010, 2010.

Wex, H., DeMott, P. J., Tobo, Y., Hartmann, S., Rösch, M., Clauss, T., Tomsche, L., Niedermeier, D., and Stratmann, F.: Kaolinite particles as ice nuclei: learning from the use of different kaolinite samples and different coatings, *Atmos. Chem. Phys.*, 14, 5529-5546, 2014

Whale, T. F., Holden, M. A., Kulak, A. N., Kim, Y. Y., Meldrum, F. C., Christenson, H. K., and Murray, B. J.: The role of phase separation and related topography in the exceptional ice-nucleating ability of alkali feldspars, *Phys Chem Chem Phys*, 19, 31186-31193, 2017.

Whale, T. F., Holden, M. A., Wilson, T. W., O'Sullivan, D., and Murray, B. J.: The enhancement and suppression of immersion mode heterogeneous ice-nucleation by solutes, *Chem Sci*, 9, 4142-4151, 2018.

Zaragotas, D., Liolios, N. T., and Anastassopoulos, E.: Supercooling, ice nucleation and crystal growth: a systematic study in plant samples, *Cryobiology*, 72, 239-243, 2016.

Appendix 1

Not all feldspars are equal: a survey of ice nucleating properties across the feldspar group of minerals

Alexander D. Harrison^{1†}, Thomas F. Whale^{1*†}, Michael A. Carpenter², Mark A. Holden¹, Lesley Neve¹, Daniel O'Sullivan¹, Jesus Vergara Temprado¹, Benjamin J. Murray^{1*}

¹School of Earth and Environment, University of Leeds, Leeds, LS2 9JT, UK

² Department of Earth Sciences, University of Cambridge, Downing Street, Cambridge CB2 3EQ, UK

[†]Both authors contributed equally to the paper

Abstract

Mineral dust particles from wind-blown soils are known to act as effective ice nucleating particles in the atmosphere and are thought to play an important role in the glaciation of mixed phase clouds. Recent work suggests that feldspars are the most efficient nucleators of the minerals commonly present in atmospheric mineral dust. However, the feldspar group of minerals is complex, encompassing a range of chemical compositions and crystal structures. To further investigate the ice-nucleating properties of the feldspar group we measured the ice nucleation activities of 15 characterised feldspar samples. We show that alkali feldspars, in particular the potassium feldspars, generally nucleate ice more efficiently than feldspars in the plagioclase series which contain significant amounts of calcium. We also find that there is variability in ice nucleating ability within these groups. While five out of six potassium-rich feldspars have a similar ice nucleating ability, one potassium rich feldspar sample and one sodium-rich feldspar sample were significantly more active. The hyper-active Na-feldspar was found to lose activity with time suspended in water with a decrease in mean freezing temperature of about 16°C over 16 months; the mean freezing temperature of the hyper-active K-feldspar decreased by 2°C over 16 months, whereas the 'standard' K-feldspar did not change activity within the uncertainty of the experiment. These results, in combination with a review of the available literature data, are consistent with the previous findings that potassium feldspars are important components of arid or fertile soil dusts for ice nucleation. However,

we also show that there is the possibility that some alkali feldspars may have enhanced ice nucleating abilities, which could have implications for prediction of ice nucleating particle concentrations in the atmosphere.

1 Introduction

Clouds containing supercooled liquid water play an important role in our planet's climate and hydrological cycle, but the formation of ice in these clouds remains poorly understood (Hoose and Möhler, 2012). Cloud droplets can supercool to below -35°C in the absence of particles capable of nucleating ice (Riechers et al., 2013; Herbert et al., 2015), hence clouds are sensitive to the presence of ice nucleating particles (INPs). A variety of aerosol types have been identified as INPs (Murray et al., 2012; Hoose and Möhler, 2012), but mineral dusts from deserts are thought to be important INPs over much of the globe and in a variety of cloud types (DeMott et al., 2003; Hoose et al., 2008; Hoose et al., 2010; Niemand et al., 2012; Atkinson et al., 2013).

Atmospheric mineral dusts are composed of weathered mineral particles from rocks and soils, and are predominantly emitted to the atmosphere in arid regions such as the Sahara (Ginoux et al., 2012). The composition and relative concentrations of dust varies spatially and temporally but it is generally made up of only a handful of dominant minerals. The most common components of dust reflect the composition of the continental crust and soil cover, with clay minerals, feldspars and quartz being major constituents. Until recently, major emphasis for research has been placed on the most common minerals in transported atmospheric dusts, the clays. It has now been shown that, when immersed in water, the feldspar component nucleates ice much more efficiently than the other main minerals that make up typical desert dust (Atkinson et al., 2013; Augustin-Bauditz et al., 2014; O'Sullivan et al., 2014; Niedermeier et al., 2015; Zolles et al., 2015). This is an important finding as it has been demonstrated that feldspar is a common component of aerosolised mineral dusts (Glaccum and Prospero, 1980; Kandler et al., 2009; Kandler et al., 2011; Atkinson et al., 2013; Perlwitz et al., 2015). Feldspar particles in the atmosphere tend to be larger than clay particles and so will have shorter lifetimes in the atmosphere, however aerosol modelling work has suggested that feldspar particles can account

for many observations of INP concentrations around the world (Atkinson et al., 2013). Work conducted below water saturation using a continuous flow diffusion chamber has also concluded that feldspars, particularly orthoclase feldspars, nucleate ice at lower relative humidity in the deposition mode than other common dust minerals (Yakobi-Hancock et al., 2013). While all available evidence indicates that feldspars are very effective INPs, it must also be recognised that feldspars are a group of minerals with differing compositions and crystal structures. Therefore, in this study we examine immersion mode ice nucleation by a range of feldspar samples under conditions pertinent to mixed phase clouds.

An additional motivation is that determining the nature of nucleation sites is of significant fundamental mechanistic interest and is likely to help with further understanding of ice nucleation in the atmosphere (Vali, 2014; Freedman, 2015; Slater et al., 2015). By characterising a range of feldspars and associating them with differences in ice nucleation activity it might be possible to build understanding of the ice nucleation sites on feldspars. Some work has been conducted in this area already. Augustin-Bauditz et al. (2014) concluded that microcline nucleates ice more efficiently than orthoclase on the basis of ice nucleation results looking at a microcline feldspar and several mixed dusts. Zolles et al. (2015) recently found that a plagioclase and an albite feldspar nucleated ice less well than a potassium feldspar and suggested that the difference in the ice nucleation activity of these feldspars is related to the difference in ionic radii of the cations and the local chemical configuration at the surface. They suggested that only potassium feldspar will nucleate ice efficiently because the K^+ is kosmotropic (structure making) in the water hydration shell while Ca^{2+} and Na^+ are chaotropic (structure breaking).

There has been much interest in the study of ice nucleation using molecular dynamics simulations (e.g. (Hu and Michaelides, 2007; Cox et al., 2012; Reinhardt and Doye, 2014; Lupi and Molinero, 2014; Lupi et al., 2014; Zielke et al., 2015; Cox et al., 2015a, b; Fitzner et al., 2015). To date there has been little overlap between work of this nature and laboratory experiments. This has been due to difficulties in conducting experiments on similar timescales and spatial extents between real-world and computational systems. While these obstacles are likely to remain in place for some time, the feldspars may offer the opportunity to address this deficit by providing qualitative corroboration between computational and laboratory results.

For instance, it may be possible to study ice nucleation on different types of feldspar computationally. If differences in nucleation rate observed also occur in the laboratory greater weight may be placed on mechanisms determined by such studies and so a mechanistic understanding of ice nucleation may be built up.

In this paper we have surveyed 15 feldspar samples with varying composition for their ice nucleating ability in the immersion mode. It will be shown that feldspars rich in alkali metal cations tend to be much better at nucleating ice than those rich in calcium. First, we introduce the feldspar group of minerals.

2 The feldspar group of minerals

The feldspars are tectosilicates (also called framework silicates) with a general formula of $XAl(Si,Al)Si_2O_8$, where X is usually potassium, sodium or calcium (Deer et al., 1992). Unlike clays, which are phyllosilicates (or sheet silicates), tectosilicates are made up of three dimensional frameworks of silica tetrahedra. Substitution of Si with Al in the structure is charge balanced by cation addition or replacement within the cavities in the framework. This leads to a large variability of composition in the feldspars and means that most feldspars in rocks have compositions between end-members of sodium-, calcium- or potassium-feldspars (Deer et al., 1992; Wenk and Bulakh, 2004). A ternary representation of feldspar compositions is shown in Figure 1. All feldspars have very similar crystal structures, but the presence of different ions and degrees of disorder related to the conditions under which they crystallised from the melt (lava or magma) yields subtle differences which can result in differing symmetry.

There are three polymorphs (minerals with the same composition, but different crystal structure) of the potassium end-member, which are microcline, orthoclase and sanidine. The polymorphs become more disordered in terms of Al placement in the tetrahedra from microcline to sanidine, respectively. The structures of feldspars which form from a melt vary according to their cooling rate. If cooling is fast (volcanic), sanidine is preserved. If cooling is slow, in some granites for example, microcline may be formed. Feldspars formed in metamorphic rocks have high degrees of Al/Si order. The sodium end-member of the feldspars

is albite and the calcium end-member is anorthite. Feldspars with compositions between sodium and calcium form a solid solution and are collectively termed the plagioclase feldspars with specific names for different composition ranges. Feldspars between sodium and potassium end-members are collectively termed the alkali feldspars and can be structurally complex. A solid solution series exists between high albite and sanidine ('high' refers to high temperature character which is preserved on fast cooling), but not between low albite and microcline ('low' refers to low temperature character which is indicative of slow cooling rates). In contrast to the series between sodium and calcium, and sodium and potassium, there are no feldspars between calcium and potassium end-members because calcium and potassium ions do not actively substitute for one another within the framework lattice due their difference in size and ionic charge (Deer et al., 1992; Wenk and Bulakh, 2004).

There is limited information about the composition of airborne atmospheric mineral dusts (Glaccum and Prospero, 1980; Kandler et al., 2007; Kandler et al., 2009); where mineralogy is reported the breakdown of the feldspar family has only been done in a limited way. Atkinson et al. (2013) compiled the available measurements and grouped them into K-feldspars and plagioclase feldspars (see the Supplementary Table 1 in Atkinson et al. (2013)). This compilation indicates that the feldspar type is highly variable in atmospheric dusts, with K-feldspars ranging from 1 to 25% by mass (with a mean of 5%) and plagioclase feldspars ranging from 1 to 14% (with a mean of 7%). The feldspar component of airborne dusts is highly variable and the nucleating ability of the various components needs to be investigated.

In order to aid the discussion and representation of the data we have grouped the feldspars into three groups: the plagioclase feldspars (not including albite), albite (the sodium rich corner of the ternary diagram) and potassium (K-) feldspars (microcline, sanidine and orthoclase). The K-feldspars contain varying amounts of sodium, but their naming is determined by their crystal structure. We also collectively refer to albite and potassium feldspars as alkali feldspars.

3 Samples and sample preparation

A total of 15 feldspars were sourced for this study. Details of the plagioclase feldspars tested are in Table 1 and details of the alkali feldspars are in Table 2. We have made use of a series

of characterised plagioclase feldspars which were assembled for previous studies (Carpenter et al., 1985; Carpenter, 1986; Carpenter, 1991). The other samples were sourced from a range of repositories, detailed in Tables 1 and 2. The naming convention we have used in this paper is to state the identifier of the specific sample followed by the mineral name. For example, BCS 376 microcline is a microcline sample from the Bureau of Analysed Samples with sample code 376. In other cases, such as Amelia Albite, the sample is from a traceable source and is commonly referred to with this name and when a code is used, such as 97490 plagioclase, the code links to the cited publications.

Anorthite glass and synthetic anorthite ANC 68 were tested for ice nucleating efficiency to investigate the impact of crystal structure in feldspar. The anorthite glass was produced by Carpenter (1991) by melting natural calcite with reagent grade SiO_2 and Al_2O_3 at 1680°C for 3 hours. The melt was then stirred before air cooling. The resulting glass was then annealed at 800°C to relieve internal stresses. The composition of the resulting glass was shown to be stoichiometric $\text{CaAl}_2\text{Si}_2\text{O}_8$. Synthetic anorthite ANC 68 was produced by heating a sample of this glass to 1400°C for 170 hours. As these two samples are chemically identical, differing only in that one is amorphous and the other crystalline, comparison of the ice nucleating efficiency of the two samples has the potential to reveal information about the impact of feldspar crystal structure on ice nucleating efficiency. Feldspars 148559, 21704a, 67796b and 97490 plagioclase and Amelia albite are natural samples that form a solid solution series covering the plagioclase series from nearly pure anorthite to nearly pure albite as seen in Table 1.

The alkali feldspars used here have not previously been characterised. Rietveld refinement of powder XRD patterns was carried out using TOtal Pattern Analysis Solutions (TOPAS) to determine the phase of the feldspar present. The results of this process are presented in Table 2. The surface areas of all the feldspars were measured by Brunauer-Emmett-Teller (BET) nitrogen gas adsorption (see Sect. 4). All samples, unless otherwise stated, were ground to reduce the particle size and increase the specific surface area using a mortar and pestle which were scrubbed with pure quartz then cleaned with deionised water and methanol before use. Grinding of most samples was necessary in order to make the particles small enough for our experiments. Amelia albite was the only material tested both in an unground state (or at least

not a freshly ground state) and a freshly ground state. Suspensions of known concentration were made up gravimetrically using Milli-Q water (18.2 M Ω .cm). Except where stated otherwise the suspensions were then mixed for a few minutes using magnetic stirrers prior to use in ice nucleation experiments.

The activity of Amelia albite and TUD #3 microcline decrease during repeat experiments conducted approximately 30 minutes after initial experiments. Based on this observation three samples, the BCS 376 microcline, ground Amelia albite and TUD #3 microcline, were tested for changes in ice nucleating efficiency with time, when left in suspension at room temperature. BCS 376 microcline was chosen as it has been previously studied and the activity decrease was not seen on the time scale of ~ 30 minutes previously. Ice nucleation efficiency was quantified at intervals over 11 days. Between experiments the suspensions were left at room temperature without stirring and then stirred to re-suspend the particulates for the ice nucleation experiments. Suspensions of the three dusts were also tested 16 months after initial experiments were performed to determine the long term impact of contact with water on ice nucleation efficiency.

4 Experimental method and data analysis

In order to quantify the efficiency with which a range of feldspar dusts nucleate ice we made use of the microliter Nucleation by Immersed Particle Instrument (μ l-NIPI). This system has been used to make numerous ice nucleation measurements in the past and has been described in detail by Whale et al. (2015). Briefly, 1 ± 0.025 μ l droplets of an aqueous suspension, containing a known mass concentration of feldspar particles are pipetted onto a hydrophobic coated glass slide. This slide is placed on a temperature controlled stage and cooled from room temperature at a rate of 5 $^{\circ}\text{C min}^{-1}$ to 0 $^{\circ}\text{C}$ and then at 1 $^{\circ}\text{C min}^{-1}$ until all droplets are frozen. Dry nitrogen is flowed over the droplets at 0.2 l min^{-1} to prevent frozen droplets from affecting neighbouring liquid droplets, droplets evaporate slowly during experiments however this has been shown to have no detectable effect on freezing temperatures (Whale et al., 2015). Whale et al. (2015) demonstrated that a dry nitrogen flow prevents condensation and frost accumulating on the glass slide so ice from a frozen droplet cannot trigger freezing in

neighbouring droplets. Freezing is observed with a digital camera, allowing determination of the fraction of droplets frozen as a function of temperature. Multiple experiments have been combined to produce single sets of data for each mineral. Suspensions of the feldspars were made up gravimetrically and specific surface areas of the samples were measured using the Brunauer–Emmett–Teller (BET) N₂ adsorption method using a Micromeritics TriStar 3000. Here the μ l-NIPI technique is used to for immersion mode nucleation experiments.

To allow comparison of the ability of different materials to nucleate ice, the number of active sites is normalised to the surface area available for nucleation. This yields the ice nucleation active site density, $n_s(T)$. $n_s(T)$ is the number of ice nucleating sites that become active per surface area on cooling from 0°C to temperature T and can be calculated using (Connolly et al., 2009):

$$\frac{n(T)}{N} = 1 - \exp(-n_s(T)A) \quad (1)$$

Where $n(T)$ is the number of droplets frozen at temperature T , N is the total number of droplets in the experiment and A is the surface area of nucleator per droplet.

Active sites may be related to imperfections in a crystal structure, such as cracks or defects, or may be related to the presence of quantities of other more active materials located in specific locations at a surface. While the fundamental nature of active sites is not clear, and may be different for different materials, n_s is a pragmatic parameter which allows us to empirically define the ice nucleating efficiency of a range of materials (Vali, 2014).

This description is site specific and does not include time dependence. The role of time dependence in ice nucleation has recently been extensively discussed (Vali, 2014; Vali et al., 2014; Vali, 2008; Herbert et al., 2014; Wright et al., 2013). For feldspar (at least for BCS 376 microcline) it is thought that the time dependence of nucleation is relatively weak and that the particle to particle, or active site to active site, variability is much more important (Herbert et al., 2014). The implication of this is that specific sites on the surface of most nucleators, including feldspars, nucleate ice more efficiently than the majority of the surface. As this study is aimed at comparing and assessing the relative ice nucleating abilities of different feldspars we have not determined the time dependence of observed ice nucleation in this work, although this would be an interesting topic for future study.

By assuming that the BET surface area of the feldspar powders is made up of monodisperse particles it can be estimated that droplets containing 1 wt% of feldspar will each contain around 10^6 particles. While there will be a distribution of particle sizes we assume that there are enough particles per droplet that the uncertainty in surface area per droplet due to the distribution of particles through the droplets is negligible. In contrast, it has been suggested that ice nucleation data could be explained by variability of nucleator surface area through the droplet population (Alpert and Knopf, 2016). Our assumption that each droplet contains a representative surface area is supported by our previous work where we show that n_s derived from experiments with a range of feldspar concentrations are consistent with one another (Whale et al., 2015; Atkinson et al., 2013). If the particles were distributed through the droplets in such a way that some droplet contained a much larger surface area of feldspar than others we would expect the slope of n_s with temperature to be artificially shallow. The slope would be artificially shallow because droplets containing more than the average feldspar surface area would tend to freeze at higher temperatures and vice versa. However, the fact that n_s data for droplets made from suspensions made up with a wide range of different feldspar concentrations all line up shows that the droplet to droplet variability in feldspar surface area is minor (Atkinson et al., 2013; Whale et al., 2015). Hence, the droplet to droplet variability in feldspar surface area is neglected and the uncertainty in surface area per droplet in these experiments is estimated from the uncertainties in weighing, pipetting and specific surface area of the feldspars. Indeed, Murray et al (2011) found that even with picolitre droplets containing 10^7 's of particles per droplet median nucleation temperatures scaled well with surface area per droplet calculated in the way used in this work.

In order to estimate the uncertainty in $n_s(T)$ due to the randomness of the distribution of the active sites in droplet freezing experiments, we conducted Monte Carlo simulations. Wright and Petters (2013) previously adopted a similar approach to simulate the distribution of active sites in droplet freezing experiments. In these simulations, we generate a list of possible values for the number of active sites per droplet (μ). The theoretical relationship between the fraction of droplets frozen and μ can be derived from the Poisson distribution:

$$\frac{n(T)}{N} = 1 - \exp(-\mu) \quad (2)$$

The simulation works in the following manner. First, we take a value of μ and we simulate a corresponding random distribution of active sites through the droplet population for an experiment. Every droplet containing one or more active sites is then considered to be frozen. In this way, we can obtain a simulated value of the fraction frozen for a certain value of μ . Repeating this process many times and for all the possible values of μ , we obtain a distribution of possible values of μ that can explain each value of the observed fraction frozen. This resulting distribution is neither Gaussian nor symmetric, so in order to propagate the uncertainty to $n_s(T)$ values, we take the following steps. First, we generate random values of μ following the corresponding previously simulated distribution for each value of the fraction frozen. Then, we simulate random values of A following a Gaussian distribution centred on the value derived from the specific surface area per droplet with the standard deviation derived from the uncertainty in droplet volume and specific surface area. We assume that each droplet contains a representative surface area distribution as discussed above. This process results in two distributions, one for A and one for μ , with these distributions we can calculate the resultant distribution of $n_s(T)$ values, and from that distribution we obtain the 95% confidence interval.

5 Results and discussion

5.1 Ice nucleation efficiencies of plagioclase and alkali feldspars

Droplet fraction frozen from μ l-NIPI for the 15 feldspar samples are shown in Figure 2. The values of $n_s(T)$ derived from these experiments are shown in Figure 3 along with the $n_s(T)$ parameterisation from Atkinson et al. (2013) for BCS 376 microcline. The various groups of feldspars are indicated by colour which corresponds to the regions of the phase diagram in Figure 1. We define potassium (K-) feldspars (red) as those rich in K including microcline, orthoclase and sanidine; the Na end-member is albite (green); and plagioclase series feldspars (blue) are a solid solution between albite and the calcium end-member, anorthite.

Out of the six K-feldspars studied, five fall on or near the line defined by Atkinson et al. (2013). These include three microcline samples and one sanidine sample, which have different crystal structures. Sanidine has disordered Al atoms, microcline has ordered Al atoms and orthoclase

has intermediate order; these differences result in differences in symmetry and hence space group (see Tables 1 and 2). The freezing results indicate that Al disordering does not play an important role in nucleation for the analysed weight concentration range. However, one K-feldspar sample, TUD#3 microcline, was substantially more active. This indicates that crystal structure and composition are not the only factors dictating the ice nucleating ability of K-feldspars.

All plagioclase feldspars tested were less active ice nucleators than the K-feldspars which were tested. There was relatively little variation in the ice nucleation activities of the plagioclase solid solution series characterised by Carpenter (1986) and Carpenter et al. (1985). For instance, of those feldspars that possess the plagioclase structure, greater sodium content does not systematically increase effectiveness of ice nucleation. Overall, the results for plagioclase feldspars indicate that they have an ice nucleating ability much smaller than that of the K-feldspars.

It is also interesting to note that the ANC 68 synthetic anorthite had different nucleating properties to the anorthite glass from which it was crystallised (and had the same composition). The ANC 68 synthetic anorthite sample has a much more shallow $n_s(T)$ curve than the glass. This is noteworthy, because the composition of these two materials is identical, but the phase of the material is different. It demonstrates that crystallinity is not required to cause nucleation, but the presence of crystallinity can provide rare active sites which can trigger nucleation at much higher temperatures. In a future study it would be interesting to attempt to probe the nature of these active sites.

We tested three predominantly Na-feldspars (albite). Amelia albite was found to be highly active, approaching that of TUD#3 microcline. The others, BCS 375 albite, and TUD#2 albite were less active, intermediate between the K-feldspars and plagioclase feldspars.

To ensure that the high activity of Amelia albite and microcline TUD#3 was not caused by contamination from biological INPs the samples were heated to 100°C in Milli-Q water for 15 minutes. This treatment will disrupt any protein based nucleators present (O'Sullivan et al., 2015). No significant reduction in freezing temperatures (beyond what would be expected from the activity decay described in Sect. 5.2) was observed suggesting that the highly active INPs

present are associated with the feldspars rather than biological protein contamination. Certain biological nucleators have been observed to retain their ice nucleating activity despite heat treatment of this type (Pummer et al., 2012; O'Sullivan et al., 2014; Tobo et al., 2014) however, to the best of our knowledge, no biological species has been observed to nucleate ice at such warm temperatures after heat treatment. This behaviour does not seem consistent with biological nucleators, unless the biological entity is within the Amelia albite particles and is somehow dispersed through the particle population during grinding. While we cannot exclude the possibility that some unknown biological species is present on microcline TUD#3 and Amelia albite it seems more likely that the minerals themselves are responsible for the observed ice nucleation activity. Additionally, it is known that certain organic molecules can nucleate ice efficiently (Fukuta, 1966). It is not possible to exclude the possibility of the presence of these or other, unknown, heat resistant contaminants that nucleate ice very efficiently.

It has been noted by Vali (2014) that there is an indication that nucleators which are more active at higher temperatures tend to have steeper slopes of $\ln J$ (nucleation rate). We have observed this trend here in the data shown in Figure 3 ($n_s(T)$ is proportional to J for a single component). The slopes of experiments where freezing occurred at lower temperatures (plagioclases) generally being flatter than those where freezing took place at higher temperatures (alkali feldspars). Vali (2014) suggests that this maybe the result of different observational methods. In this study we have used a single method for all experiments so the trend is unlikely to be due to an instrument artefact. The implication is that active sites with lower activity tend to be more diverse in nature. This may indicate that there are fewer possible ways to compose an active site that is efficient at nucleating ice and that there will be less variation in these sites as a result. The active sites of lower activity may take a greater range of forms and so encompass a greater diversity of freezing temperatures. The lower diversity in the sites active at higher temperatures may explain the steep slopes in n_s seen, however it should be noted that classical nucleation theory also predicts steeper slopes at higher temperatures assuming a single contact angle.

To summarise, plagioclase feldspars tend to have relatively poor ice nucleating abilities, all K-feldspars we tested are relatively good at nucleating ice and the albites are variable in their nucleating activity. Out of the six K-feldspars tested, five have very similar activities and are

well approximated by the parameterisation of Atkinson et al. (2013) in the temperature- n_s regime we investigated here. However, we have identified two alkali feldspar samples, one K-feldspar and one albite, which are much more active than the others indicating that a factor or factors other than the polymorph or composition determines the efficiency of alkali feldspars as ice nucleators.

5.2 The stability of active sites

It was observed that the ice nucleation activity of ground Amelia albite and ground TUD #3 microcline declined over the course of ~30 minutes. Only the initial run is shown in Figure 3 where the feldspar had spent only about 10 minutes in suspension. This decay in activity over the course of ~30 mins was not seen in the other feldspars. To investigate this effect samples of BCS 376 microcline, Amelia albite and TUD #3 microcline were left in water within a sealed vial and tested at intervals over the course of 16 months, with a focus on the first 11 days. TUD #3 microcline and Amelia albite were chosen for this experiment as they contained highly active sites, represented two different types of feldspar and were the only feldspars observed to exhibit this rapid decay in activity. BCS 376 microcline was also included in this activity decay experiment as it had provided consistent data over repeated runs and served as a standard in the Atkinson et al. (2013) paper which could therefore be tested. The results of these experiments are shown in Figure 4. The median freezing temperature of the Amelia albite sample was most sensitive to time spent in water, decreasing by 8 °C in 11 days and by 16 °C in 16 months. The TUD#3 microcline sample decreased by about 2 °C in 16 months, but the freezing temperatures of the BCS 376 did not change significantly over 16 months (within the temperature uncertainty of $\pm 0.4^\circ\text{C}$). Clearly, the stability of the active sites responsible for ice nucleation in these samples is highly variable.

Amelia albite is a particularly interesting case, where the highly active sites are also highly unstable. For Amelia albite we observed that the ice nucleation ability of the powder directly as supplied (the sample had been ground many years prior to experiments) was much lower than the freshly ground sample. The n_s values for the ‘as-supplied’ Amelia albite are shown in Figure 4. This suggests that the active sites on Amelia albite are unstable and in general are sensitive to the history of the sample. We note that from previous work that BCS 376 feldspar ground to varied extents nucleates ice similarly (Whale et al., 2015) and we have not observed

a decay of active sites of the BCS 376 microcline sample when stored in a dry vial over the course of two years. It is also worth noting that freshly ground BCS 376 microcline did not nucleate ice as efficiently as Amelia albite or TUD#3 microcline. These results indicate that BCS 376 microcline contains very active sites, but that these sites are much more stable than those found in Amelia albite. This result is in agreement with the observation that albite weathers faster than microcline in soils as Na^+ is more readily substituted for hydrogen than K^+ (Busenberg and Clemency, 1976; Blum, 1994).

Zolles et al. (2015) have suggested that grinding can lead to active sites being revealed, or the enhancement of existing active sites. It was shown in Whale et al. (2015) that differently ground samples of BCS 376 microcline nucleate ice similarly. In contrast Hiranuma et al. (2014) show that ground hematite nucleates ice more efficiently (normalised to surface area) than cubic hematite. The evidence suggests that the ice nucleating efficiencies of different materials respond differently to grinding processes. Indeed, it is evident from this study that highly active sites in Amelia albite are generated by grinding but lose activity when exposed to liquid water, and probably lose activity during exposure to (presumably wet) air, returning to an activity level comparable to that of the plagioclase feldspars. TUD#3 microcline also possesses a highly active site type sensitive to water exposure but falls back to a level of activity higher than the other K-feldspars we have tested. This second, less active site type is shown to be stable in water over the course of 16 months. TUD#3 must possess populations of both more active, unstable sites and less active (although still relatively active compared to the sites on other K-feldspars) stable sites. Amelia albite possesses only unstable sites and much less active sites similar to those found on the plagioclase feldspars we have tested.

These results indicate something of the nature of the active sites on feldspars. Throughout this paper we refer to nucleation occurring on active sites, or specific sites, on the surface of feldspar. It is thought that nucleation by most ice active minerals is consistent with nucleation on active sites with a broad spectrum of activities (Marcolli et al., 2007; Lüönd et al., 2010; Niedermeier et al., 2010; Augustin-Bauditz et al., 2014; Herbert et al., 2014; Vali, 2014; Wex et al., 2014; Wheeler et al., 2015; Hiranuma et al., 2015; Niedermeier et al., 2015; Hartmann et al., 2016). However, the nature of these active sites is not known. It is postulated that active sites are related to defects in the structure and therefore that each site has

a characteristic nucleation ability, producing a spectrum of active sites. Defects are inherently less stable than the bulk of the crystal and we might expect these sites to be affected by dissolution processes, or otherwise altered, in preference to the bulk of the crystal (Parsons et al., 2015). The fact that we observe ice nucleation by populations of active sites with different stabilities in water implies that these sites have different physical or chemical characteristics. Furthermore, the fact that some populations of active sites are sensitive to exposure to water suggests that the history of particles can be critical in determining the ice nucleating ability of mineral dusts. This raises the question of whether differences in ice nucleation efficiency observed by different instruments (Emersic et al., 2015; Hiranuma et al., 2015), could be related to the different conditions particles experience prior to nucleation.

5.3 Comparison to literature data

We have compared the $n_s(T)$ values for various feldspars from a range of literature sources with data from this study in Figure 5. Inspection of this plot confirms that K-feldspars nucleate ice more efficiently than the plagioclase feldspars. Also, with the exception of the hyper-active Amelia albite sample, the K-feldspars are more active than the albites.

Results for BCS 376 microcline have been reported in several papers (Atkinson et al., 2013; O'Sullivan et al., 2014; Whale et al., 2015; Emersic et al., 2015). There is a discrepancy between the cloud chamber data from Emersic et al. (2015) and the picolitre droplet cold stage experiments at around -18°C , whereas the data at about -25°C are in agreement. Emersic et al. (2015) attribute this discrepancy to aggregation of feldspar particles in microlitre scale droplet freezing experiments reducing the surface area of feldspar exposed to water leading to a lower $n_s(T)$ value. It is unlikely that this effect can account for the discrepancy because in the temperature range of the Emersic et al. (2015) data the comparison is being made to results from picolitre droplet freezing experiments which Emersic et al. (2015) argue should not be affected by aggregation because there are not enough particles present in each droplet to result in significant aggregation. Atkinson et al. (2013) estimated that on average even the largest droplets only contained a few 10s of particles. We also note that our microscope images of droplets show many individual particles moving independently around in the picolitre droplets in those experiments, indicating that the feldspar grains do not aggregate substantially. Hence,

the discrepancy between the data of Emersic et al. (2015) and Atkinson et al. (2013) at around -18°C cannot be accounted for by aggregation. Furthermore, Atkinson et al. (2013) report that the surface area determined from the laser diffraction size distribution of BCS 376 microcline in suspension is 3.5 times smaller than that derived by the gas adsorption measurements (see supplementary Figure 5 in Atkinson et al. (2013) and the corresponding discussion). This difference in surface area can be accounted for by the fact that feldspar grains are not smooth spheres, as assumed in the analysis of the laser diffraction data. Feldspar grains are well-known to be rough and aspherical (Hodson et al., 1997). Atkinson et al. (2013) also note that the laser diffraction technique lacks sensitivity to the smallest particles in the distribution which will also lead to an underestimate in surface area. Nevertheless, the data presented by Atkinson et al. (2013) suggests that aggregation of feldspar particles leading to reduced surface area is at most a minor effect. As such the discrepancy between different instruments remains unexplained and more work is needed on this topic.

Ice nucleation by single size-selected particles of TUD#1 microcline has been investigated by Niedermeier et al. (2015) at temperatures below -23°C . We found that TUD#1 microcline was in good agreement with the K-feldspar parameterisation from Atkinson et al. (2013) between about -6 and -11°C . Between -23 and -25°C , the $n_s(T)$ values produced by Niedermeier et al. (2015) are similar (lower by a factor of roughly 4) to that of the Atkinson et al. (2013) parameterisation, despite the different sample types. Niedermeier et al. (2015) used the Leipzig Aerosol Cloud Interaction Simulator (LACIS), in which they size selected particles, activated them to cloud droplets and then quantified the probability of freezing at a particular temperature. It is interesting that the Niedermeier et al. (2015) $n_s(T)$ values curve off at lower temperatures to a limiting value which they term n_s^* , indicating that nucleation by K-feldspars may hit a maximum value and emphasises why we need to be cautious in extrapolating $n_s(T)$ parameterisations beyond the range of experimental data.

The data for a microcline, a plagioclase (andesine) and albite from Zolles et al. (2015) is consistent with our finding that plagioclase feldspars are less effective nucleators than K-feldspars. It is also consistent with Atkinson et al. (2013) who found that albite is less efficient at nucleating ice than microcline. However, the data for K-feldspar from Zolles et al. (2015) sits below the line from Atkinson et al. (2013) for BCS 376 microcline and are lower than the

points from Niedermeier et al. (2015) for TUD#1 microcline. Their measurements involved making up suspensions (2-5wt%) and then creating a water-in-oil emulsion where droplets were between 10-40 μm . They quote their particle sizes as being between 1-10 μm for the feldspars. Atkinson et al. (2013) worked with 0.8 wt% suspensions, with droplets of 9 to 19 μm where the mode particle size was ~ 700 nm. Hence, Zolles et al. (2015) worked with more concentrated suspensions and larger particles than used by Atkinson et al. (2013). In principle, n_s should be independent of droplet volume and particle concentration, but differences between instruments and methods have been reported (Hiranuma et al., 2015). Additionally, Zolles et al. (2015) estimated the surface area of their feldspar particles using a combination of SEM images and the BET surface area of quartz. This leads to an unspecified uncertainty in their n_s values. However, it is not possible to determine whether the observed difference in n_s is due to differences in the sample or the techniques used, but may mean that certain K-feldspars nucleate ice less well than those defined by the Atkinson et al. (2013) line in this temperature regime. This would be a very interesting result as it may provide a point of difference that could provide insight into why K-feldspars nucleate ice efficiently. There has been relatively little work on what makes feldspar a good nucleator of ice. Zolles et al. (2015) suggest that only K-feldspars will nucleate ice well on the basis that Ca^{2+} and Na^+ are chaotropic (structure breaking in water) while K^+ is kosmotropic (structure making in water). We have only observed one feldspar that contains little K^+ but nucleates ice relatively efficiently, Amelia albite. This feldspar loses its activity quickly in water and eventually becomes more comparable to the plagioclase feldspars. It may be that the strong nucleation observed is associated with the small amount of K^+ it contains and that once this dissolves away the feldspar behaves like a plagioclase.

Augustin-Bauditz et al. (2014) tentatively concluded that microcline may nucleate ice more efficiently than orthoclase at $n_s(T)$ values above about 10^6 cm^{-2} and at temperatures below -23°C , the conditions where they performed their measurements. They arrived at this conclusion by noting that NX-illite and Arizona test dust both contain orthoclase (8 and 20%, respectively), but the $n_s(T)$ values they report for these materials are more than one order less than microcline.

Within the surface area regime examined in this study we have observed some variability amongst the K-feldspars (see Figure 2), but no difference between sanidine and four out of five microclines which fall around the line defined by Atkinson et al. (2013). As discussed above, the Al in sanidine is the least ordered, with microcline the most ordered and orthoclase at an intermediate order, hence we observe no clear dependency on the ordering of Al in K-feldspars. Further investigations of the ice nucleating ability of the various K-feldspar phases at low temperature would be valuable. We could not do this in the present study with the samples used here because we did not have sufficient quantities of the samples.

6 Conclusions

In this study we have analysed the ice nucleating ability of 15 characterised feldspar samples. These minerals include plagioclase feldspars (in the solid solution series between Ca and Na end-members), the K-feldspars (sanidine and microcline) and albite (the Na end-member). The results indicate that the alkali feldspars, including albite and K-feldspars, tend to nucleate ice more efficiently than plagioclase feldspars. The plagioclase feldspars nucleate ice at the lowest temperatures with no obvious dependence on the Ca-Na ratio. The albites have a wide variety of nucleating abilities, with one sample nucleating ice much more efficiently than the microcline sample Atkinson et al. (2013) studied. This hyper-active albite lost its activity over time while suspended in water. Five out of six of the K-feldspar samples we studied nucleated ice with a similar efficiency to the BCS 376 microcline studied by Atkinson et al. (2013). A single K-feldspar we studied had a very high activity, nucleating ice as warm as -2°C in our microliter droplet assay. The striking activity of this hyperactive microcline decayed with time spent in water, but not to the same extent as the hyperactive albite sample. While the hyperactive sites are sensitive, to varying degrees, to time spent in water, the activity of the BCS 376 microcline sample used by Atkinson et al. (Atkinson et al., 2013) did not change significantly. We have not excluded the possibility that other entities on the surfaces of the feldspar may be responsible for the ice nucleation observed.

In light of these findings, we suggest that there are at least three classes of active site present in the feldspars studied here: *i*) sites of relatively low activity associated with plagioclase

feldspars; *ii*) sites which are more active associated with K-feldspars that are stable in water over the course of many months; *iii*) hyper-active sites associated with one albite and one K-feldspar that we studied that loses activity when exposed to water. It is possible that the sites of type *i* are present on the typical K-feldspars, but we do not observe them because ice nucleates on more active sites. Whether these different sites are all related to similar features on the surfaces or if they are each related to different types of features is not known. Nevertheless, it appears that feldspars are characterised by a range of active site types with varying stability and activity.

The specific details of these active sites continue to elude us, although it appears that they are only present in alkali feldspars and in particular, the K-feldspars. Unlike the plagioclase feldspars which form a solid solution, the Na and K feldspars in alkali feldspars are often exsolved, possessing intergrowths of the Na and K feldspars referred to as microtexture (Parsons et al., 2015). It is possible that the boundaries between the two phases in the intergrowth provide sites for nucleation that are not present in plagioclase feldspars. If the high energy defects along exsolution boundaries are responsible for higher ice nucleation activity of K-feldspars then this may offer an insight into acid passivation of ice nucleating ability observed in laboratory studies (Wex et al., 2014; Augustin-Bauditz et al., 2014). Berner and Holdren (1979) suggest that the acid mediated weathering of feldspar occurs in multiple stages and suggest dissolution of feldspars is concentrated at high surface energy sites such as dislocations and crystal defects, sites which may be related to ice nucleation. More work is needed to explore the significance of exsolution, microtexture and the impact of weathering on feldspars with respect to ice nucleation activity.

In a previous study Atkinson et al. (2013) used an $n_s(T)$ parameterisation of a single K-feldspar (BCS 376 microcline) to approximate the ice nucleating properties of desert dust in a global aerosol model. Given that five out of six of the K-feldspars we studied here have very similar ice nucleating abilities, this approximation seems reasonable. However, we have identified two hyper-active feldspars and do not know how representative these samples are of natural feldspars in dust emission regions. We also note that the active sites on these feldspars are less stable than those of BCS 376 microcline. Nevertheless, there is the possibility that the

parameterisation used by Atkinson et al. (2013) underestimates the contribution of feldspars at higher temperatures above about -15°C .

In the longer term it may be possible to identify what it is that leads to the variation in ice nucleation activity between the different feldspar classes. In particular, the nature of the active sites in the hyper-active feldspars and the reason plagioclase is so much poorer at nucleating ice are subjects of interest. The instability of the active sites in the hyperactive feldspars may be related to dissolution of feldspar in water and investigation of this process may allow progress towards understanding of nucleation by feldspars. The results presented here are empirical in nature and do not provide a thorough underpinning understanding of the nature of the active sites. Nevertheless, the fact that the feldspar group of minerals have vastly different ice nucleating properties despite possessing very similar crystal structures may provide us with a means of gaining a fundamental insight to heterogeneous ice nucleation.

Acknowledgments

We would like to acknowledge Theodore Wilson and Alexei Kiselev for helpful discussions and John Morris for introducing TFW and MAC. We are grateful to Alexei Kiselev and Martin Ebert for providing the TUD samples. Alex Harrison thanks the School of Earth and Environment for an Undergraduate Research Scholarship which allowed him to make many of the measurements presented in this paper. We would like to thank the National Environmental Research Council, (NERC, NE/I013466/1; NE/I020059/1; NE/K004417/1; NE/I019057/1; NE/M010473/1) the European Research Council (ERC, 240449 ICE; 632272 IceControl; 648661 MarineIce), and the Engineering and Physical Sciences Research Council (EPSRC, EP/M003027/1) for funding.

Alpert, P. A., and Knopf, D. A.: Analysis of isothermal and cooling-rate-dependent immersion freezing by a unifying stochastic ice nucleation model, *Atmos. Chem. Phys.*, 16, 2083-2107, 10.5194/acp-16-2083-2016, 2016.

Atkinson, J. D., Murray, B. J., Woodhouse, M. T., Whale, T. F., Baustian, K. J., Carslaw, K. S., Dobbie, S., O'Sullivan, D., and Malkin, T. L.: The importance of feldspar for ice nucleation by mineral dust in mixed-phase clouds, *Nature*, 498, 355-358, 10.1038/nature12278, 2013.

Augustin-Bauditz, S., Wex, H., Kanter, S., Ebert, M., Niedermeier, D., Stolz, F., Prager, A., and Stratmann, F.: The immersion mode ice nucleation behavior of mineral dusts: A comparison of different pure and surface modified dusts, *Geophys. Res. Lett.*, 41, 7375-7382, 10.1002/2014gl061317, 2014.

Berner, R. A., and Holdren, G. R.: Mechanism of feldspar weathering—ii. Observations of feldspars from soils, *Geochim. Cosmochim. Acta*, 43, 1173-1186, [http://dx.doi.org/10.1016/0016-7037\(79\)90110-8](http://dx.doi.org/10.1016/0016-7037(79)90110-8), 1979.

Blum, A. E.: Feldspars in weathering, in: *Feldspars and their reactions*, Springer, 595-630, 1994.

Busenberg, E., and Clemency, C. V.: The dissolution kinetics of feldspars at 25 c and 1 atm co₂ partial pressure, *Geochim. Cosmochim. Acta*, 40, 41-49, 1976.

Carpenter, M.: Experimental delineation of the “e” \rightleftharpoons i\bar{1} and “e” \rightleftharpoons c\bar{1} transformations in intermediate plagioclase feldspars, *Phys Chem Minerals*, 13, 119-139, 10.1007/bf00311902, 1986.

Carpenter, M. A., McConnell, J. D. C., and Navrotsky, A.: Enthalpies of ordering in the plagioclase feldspar solid solution, *Geochim. Cosmochim. Acta*, 49, 947-966, [http://dx.doi.org/10.1016/0016-7037\(85\)90310-2](http://dx.doi.org/10.1016/0016-7037(85)90310-2), 1985.

Carpenter, M. A.: Mechanisms and kinetics of al-si ordering in anorthite; i, incommensurate structure and domain coarsening, *American Mineralogist*, 76, 1110-1119, 1991.

Connolly, P. J., Möhler, O., Field, P. R., Saathoff, H., Burgess, R., Choulaton, T., and Gallagher, M.: Studies of heterogeneous freezing by three different desert dust samples, *Atmos. Chem. Phys.*, 9, 2805-2824, 10.5194/acp-9-2805-2009, 2009.

Cox, S. J., Kathmann, S. M., Purton, J. A., Gillan, M. J., and Michaelides, A.: Non-hexagonal ice at hexagonal surfaces: The role of lattice mismatch, *Phys. Chem. Chem. Phys.*, 14, 7944-7949, 10.1039/c2cp23438f, 2012.

Cox, S. J., Kathmann, S. M., Slater, B., and Michaelides, A.: Molecular simulations of heterogeneous ice nucleation. I. Controlling ice nucleation through surface hydrophilicity, *The Journal of Chemical Physics*, 142, 184704, doi:<http://dx.doi.org/10.1063/1.4919714>, 2015a.

Cox, S. J., Kathmann, S. M., Slater, B., and Michaelides, A.: Molecular simulations of heterogeneous ice nucleation. II. Peeling back the layers, *The Journal of Chemical Physics*, 142, 184705, doi:<http://dx.doi.org/10.1063/1.4919715>, 2015b.

Deer, W. A., Howie, R. A., and Zussman, J.: *An introduction to the rock forming minerals*, 2nd ed., Addison Wesley Longman, Harlow, UK, 1992.

DeMott, P. J., Sassen, K., Poellot, M. R., Baumgardner, D., Rogers, D. C., Brooks, S. D., Prenni, A. J., and Kreidenweis, S. M.: African dust aerosols as atmospheric ice nuclei, *Geophys. Res. Lett.*, 30, 1732, 10.1029/2003GL017410, 2003.

Emersic, C., Connolly, P. J., Boulton, S., Campana, M., and Li, Z.: Investigating the discrepancy between wet-suspension- and dry-dispersion-derived ice nucleation efficiency of mineral particles, *Atmos. Chem. Phys.*, 15, 11311-11326, 10.5194/acp-15-11311-2015, 2015.

Fitzner, M., Sosso, G. C., Cox, S. J., and Michaelides, A.: The many faces of heterogeneous ice nucleation: Interplay between surface morphology and hydrophobicity, *J. Am. Chem. Soc.*, 137, 13658-13669, 10.1021/jacs.5b08748, 2015.

Freedman, M. A.: Potential sites for ice nucleation on aluminosilicate clay minerals and related materials, *The Journal of Physical Chemistry Letters*, 2015.

Fukuta, N.: Experimental studies of organic ice nuclei, *J. Atmos. Sci.*, 23, 191-196, doi:10.1175/1520-0469(1966)023<0191:ESOOIN>2.0.CO;2, 1966.

Ginoux, P., Prospero, J. M., Gill, T. E., Hsu, N. C., and Zhao, M.: Global-scale attribution of anthropogenic and natural dust sources and their emission rates based on modis deep blue aerosol products, *Rev. Geophys.*, 50, RG3005, 10.1029/2012rg000388, 2012.

Glaccum, R. A., and Prospero, J. M.: Saharan aerosols over the tropical north-atlantic - mineralogy, *Mar. Geol.*, 37, 295-321, 10.1016/0025-3227(80)90107-3, 1980.

Hartmann, S., Wex, H., Clauss, T., Augustin-Bauditz, S., Niedermeier, D., Rösch, M., and Stratmann, F.: Immersion freezing of kaolinite: Scaling with particle surface area, *J. Atmos. Sci.*, 73, 263-278, doi:10.1175/JAS-D-15-0057.1, 2016.

Herbert, R. J., Murray, B. J., Whale, T. F., Dobbie, S. J., and Atkinson, J. D.: Representing time-dependent freezing behaviour in immersion mode ice nucleation, *Atmos. Chem. Phys.*, 14, 8501-8520, 10.5194/acp-14-8501-2014, 2014.

Herbert, R. J., Murray, B. J., Dobbie, S. J., and Koop, T.: Sensitivity of liquid clouds to homogenous freezing parameterizations, *Geophys. Res. Lett.*, 42, 1599-1605, 10.1002/2014gl062729, 2015.

Hiranuma, N., Hoffmann, N., Kiselev, A., Dreyer, A., Zhang, K., Kulkarni, G., Koop, T., and Möhler, O.: Influence of surface morphology on the immersion mode ice nucleation efficiency of hematite particles, *Atmos. Chem. Phys.*, 14, 2315-2324, 10.5194/acp-14-2315-2014, 2014.

Hiranuma, N., Augustin-Bauditz, S., Bingemer, H., Budke, C., Curtius, J., Danielczok, A., Diehl, K., Dreischmeier, K., Ebert, M., Frank, F., Hoffmann, N., Kandler, K., Kiselev, A., Koop, T., Leisner, T., Möhler, O., Nillius, B., Peckhaus, A., Rose, D., Weinbruch, S., Wex, H., Boose, Y., DeMott, P. J., Hader, J. D., Hill, T. C. J., Kanji, Z. A., Kulkarni, G., Levin, E. J. T., McCluskey, C. S., Murakami, M., Murray, B. J., Niedermeier, D., Petters, M. D., O'Sullivan, D., Saito, A., Schill, G. P., Tajiri, T., Tolbert, M. A., Welti, A., Whale, T. F., Wright, T. P., and Yamashita, K.: A comprehensive laboratory study on the immersion freezing behavior of illite particles: A comparison of 17 ice nucleation measurement techniques, *Atmos. Chem. Phys.*, 15, 2489-2518, 10.5194/acp-15-2489-2015, 2015.

Hodson, M. E., Lee, M. R., and Parsons, I.: Origins of the surface roughness of unweathered alkali feldspar grains, *Geochim. Cosmochim. Acta*, 61, 3885-3896, 10.1016/s0016-7037(97)00197-x, 1997.

Hoose, C., Lohmann, U., Erdin, R., and Tegen, I.: The global influence of dust mineralogical composition on heterogeneous ice nucleation in mixed-phase clouds, *Environ. Res. Lett.*, 3, 10.1088/1748-9326/3/2/025003, 2008.

Hoose, C., Kristjánsson, J. E., Chen, J.-P., and Hazra, A.: A classical-theory-based parameterization of heterogeneous ice nucleation by mineral dust, soot, and biological particles in a global climate model, *J. Atmos. Sci.*, 67, 2483-2503, 10.1175/2010jas3425.1, 2010.

Hoose, C., and Möhler, O.: Heterogeneous ice nucleation on atmospheric aerosols: A review of results from laboratory experiments, *Atmos. Chem. Phys.*, 12, 9817-9854, 10.5194/acp-12-9817-2012, 2012.

Hu, X. L., and Michaelides, A.: Ice formation on kaolinite: Lattice match or amphotericism?, *Surface Science*, 601, 5378-5381, 10.1016/j.susc.2007.09.012, 2007.

Kandler, K., Benker, N., Bundke, U., Cuevas, E., Ebert, M., Knippertz, P., Rodríguez, S., Schütz, L., and Weinbruch, S.: Chemical composition and complex refractive index of saharan mineral dust at izana, tenerife (spain) derived by electron microscopy, *Atmos. Environ.*, 41, 8058-8074, 2007.

Kandler, K., Schütz, L., Deutscher, C., Ebert, M., Hofmann, H., Jäckel, S., Jaenicke, R., Knippertz, P., Lieke, K., Massling, A., Petzold, A., Schladitz, A., Weinzierl, B., Wiedensohler, A., Zorn, S., and Weinbruch, S.: Size distribution, mass concentration, chemical and mineralogical composition and derived optical parameters of the boundary layer aerosol at tinfou, morocco, during samum 2006, *Tellus*, 61B, 32-50, 10.1111/j.1600-0889.2008.00385.x, 2009.

Kandler, K., SchÜTz, L., JÄCkel, S., Lieke, K., Emmel, C., MÜLler-Ebert, D., Ebert, M., Scheuvens, D., Schladitz, A., ŠEgviĆ, B., Wiedensohler, A., and Weinbruch, S.: Ground-based off-line aerosol measurements at praia, cape verde, during the saharan mineral dust experiment: Microphysical properties and mineralogy, *Tellus*, 63B, 459-474, 10.1111/j.1600-0889.2011.00546.x, 2011.

Lüönd, F., Stetzer, O., Welti, A., and Lohmann, U.: Experimental study on the ice nucleation ability of size-selected kaolinite particles in the immersion mode, *J. Geophys. Res.*, 115, D14201, 10.1029/2009jd012959, 2010.

Lupi, L., Hudait, A., and Molinero, V.: Heterogeneous nucleation of ice on carbon surfaces, *J. Am. Chem. Soc.*, 136, 3156-3164, 10.1021/ja411507a, 2014.

Lupi, L., and Molinero, V.: Does hydrophilicity of carbon particles improve their ice nucleation ability?, *J. Phys. Chem. A*, 118, 7330-7337, 10.1021/jp4118375, 2014.

Marculli, C., Gedamke, S., Peter, T., and Zobrist, B.: Efficiency of immersion mode ice nucleation on surrogates of mineral dust, *Atmos. Chem. Phys.*, 7, 5081-5091, 10.5194/acp-7-5081-2007, 2007.

Murray, B. J., Broadley, S. L., Wilson, T. W., Atkinson, J. D., and Wills, R. H.: Heterogeneous freezing of water droplets containing kaolinite particles, *Atmos. Chem. Phys.*, 11, 4191-4207, 10.5194/acp-11-4191-2011, 2011.

Murray, B. J., O'Sullivan, D., Atkinson, J. D., and Webb, M. E.: Ice nucleation by particles immersed in supercooled cloud droplets, *Chem. Soc. Rev.*, 41, 6519-6554, 10.1039/C2CS35200A, 2012.

Niedermeier, D., Hartmann, S., Shaw, R. A., Covert, D., Mentel, T. F., Schneider, J., Poulain, L., Reitz, P., Spindler, C., Clauss, T., Kiselev, A., Hallbauer, E., Wex, H., Mildenerger, K., and Stratmann, F.: Heterogeneous freezing of droplets with immersed mineral dust particles - measurements and parameterization, *Atmos. Chem. Phys.*, 10, 3601-3614, 10.5194/acp-10-3601-2010, 2010.

Niedermeier, D., Augustin-Bauditz, S., Hartmann, S., Wex, H., Ignatius, K., and Stratmann, F.: Can we define an asymptotic value for the ice active surface site density for heterogeneous ice nucleation?, *Journal of Geophysical Research: Atmospheres*, 120, 5036-5046, 10.1002/2014jd022814, 2015.

Niemand, M., Möhler, O., Vogel, B., Vogel, H., Hoose, C., Connolly, P., Klein, H., Bingemer, H., DeMott, P. J., Skrotzki, J., and Leisner, T.: A particle-surface-area-based parameterization of immersion freezing on desert dust particles, *J. Atmos. Sci.*, 69, 10.1175/jas-d-11-0249.1, 2012.

O'Sullivan, D., Murray, B. J., Malkin, T. L., Whale, T. F., Umo, N. S., Atkinson, J. D., Price, H. C., Baustian, K. J., Browse, J., and Webb, M. E.: Ice nucleation by fertile soil dusts: Relative importance of mineral and biogenic components, *Atmos. Chem. Phys.*, 14, 1853-1867, 10.5194/acp-14-1853-2014, 2014.

O'Sullivan, D., Murray, B. J., Ross, J. F., Whale, T. F., Price, H. C., Atkinson, J. D., Umo, N. S., and Webb, M. E.: The relevance of nanoscale biological fragments for ice nucleation in clouds, *Sci. Rep.*, 5, 10.1038/srep08082, 2015.

Parsons, I., Fitz Gerald, J. D., and Lee, M. R.: Routine characterization and interpretation of complex alkali feldspar intergrowths, *American Mineralogist*, 100, 1277-1303, 10.2138/am-2015-5094, 2015.

Perlwitz, J. P., Pérez García-Pando, C., and Miller, R. L.: Predicting the mineral composition of dust aerosols – part 1: Representing key processes, *Atmos. Chem. Phys.*, 15, 11593-11627, 10.5194/acp-15-11593-2015, 2015.

Pummer, B. G., Bauer, H., Bernardi, J., Bleicher, S., and Grothe, H.: Suspendable macromolecules are responsible for ice nucleation activity of birch and conifer pollen, *Atmos. Chem. Phys.*, 12, 2541-2550, 10.5194/acp-12-2541-2012, 2012.

Reinhardt, A., and Doye, J. P. K.: Effects of surface interactions on heterogeneous ice nucleation for a monatomic water model, *Journal of Chemical Physics*, 141, 10.1063/1.4892804, 2014.

Riechers, B., Wittbracht, F., Hütten, A., and Koop, T.: The homogeneous ice nucleation rate of water droplets produced in a microfluidic device and the role of temperature uncertainty, *Phys. Chem. Chem. Phys.*, 15, 5873-5887, 10.1039/C3CP42437E, 2013.

Slater, B., Michaelides, A., Salzmann, C. G., and Lohmann, U.: A blue-sky approach to understanding cloud formation, *B. Am. Meteorol. Soc.*, 10.1175/bams-d-15-00131.1, 2015.

Tobo, Y., DeMott, P. J., Hill, T. C. J., Prenni, A. J., Swoboda-Colberg, N. G., Franc, G. D., and Kreidenweis, S. M.: Organic matter matters for ice nuclei of agricultural soil origin, *Atmos. Chem. Phys.*, 14, 8521-8531, 10.5194/acp-14-8521-2014, 2014.

Umo, N. S., Murray, B. J., Baeza-Romero, M. T., Jones, J. M., Lea-Langton, A. R., Malkin, T. L., O'Sullivan, D., Neve, L., Plane, J. M. C., and Williams, A.: Ice nucleation by combustion ash particles at conditions relevant to mixed-phase clouds, *Atmos. Chem. Phys.*, 15, 5195-5210, 10.5194/acp-15-5195-2015, 2015.

Vali, G.: Repeatability and randomness in heterogeneous freezing nucleation, *Atmos. Chem. Phys.*, 8, 5017-5031, 10.5194/acp-8-5017-2008, 2008.

Vali, G.: Interpretation of freezing nucleation experiments: Singular and stochastic; sites and surfaces, *Atmos. Chem. Phys.*, 14, 5271-5294, 10.5194/acp-14-5271-2014, 2014.

Vali, G., DeMott, P., Möhler, O., and Whale, T.: Ice nucleation terminology, *Atmospheric Chemistry and Physics Discussions*, 14, 22155-22162, 2014.

Wenk, H.-R., and Bulakh, A.: *Minerals: Their constitution and origin*, Cambridge University Press, 2004.

Wex, H., DeMott, P. J., Tobo, Y., Hartmann, S., Rösch, M., Clauss, T., Tomsche, L., Niedermeier, D., and Stratmann, F.: Kaolinite particles as ice nuclei: Learning from the use of different kaolinite samples and different coatings, *Atmos. Chem. Phys.*, 14, 5529-5546, 10.5194/acp-14-5529-2014, 2014.

Whale, T. F., Murray, B. J., O'Sullivan, D., Wilson, T. W., Umo, N. S., Baustian, K. J., Atkinson, J. D., Workneh, D. A., and Morris, G. J.: A technique for quantifying heterogeneous ice nucleation in microlitre supercooled water droplets, *Atmos. Meas. Tech.*, 8, 2437-2447, 10.5194/amt-8-2437-2015, 2015.

Wheeler, M. J., Mason, R. H., Steunenberg, K., Wagstaff, M., Chou, C., and Bertram, A. K.: Immersion freezing of supermicron mineral dust particles: Freezing results, testing different

schemes for describing ice nucleation, and ice nucleation active site densities, *The Journal of Physical Chemistry A*, 119, 4358-4372, 10.1021/jp507875q, 2015.

Wittke, W., and Sykes, R.: *Rock mechanics*, Springer Berlin, 1990.

Wright, T. P., and Petters, M. D.: The role of time in heterogeneous freezing nucleation, *J. Geophys. Res.-Atmos.*, 118, 3731-3743, 10.1002/jgrd.50365, 2013.

Wright, T. P., Petters, M. D., Hader, J. D., Morton, T., and Holder, A. L.: Minimal cooling rate dependence of ice nuclei activity in the immersion mode, *J. Geophys. Res.-Atmos.*, 118, 10535-10543, 10.1002/jgrd.50810, 2013.

Yakobi-Hancock, J. D., Ladino, L. A., and Abbatt, J. P. D.: Feldspar minerals as efficient deposition ice nuclei, *Atmos. Chem. Phys.*, 13, 11175-11185, 10.5194/acp-13-11175-2013, 2013.

Zielke, S. A., Bertram, A. K., and Patey, G. N.: Simulations of ice nucleation by kaolinite (001) with rigid and flexible surfaces, *The Journal of Physical Chemistry B*, 10.1021/acs.jpcc.5b09052, 2015.

Zolles, T., Burkart, J., Häusler, T., Pummer, B., Hitzenberger, R., and Grothe, H.: Identification of ice nucleation active sites on feldspar dust particles, *The Journal of Physical Chemistry A*, 119, 2692-2700, 10.1021/jp509839x, 2015.

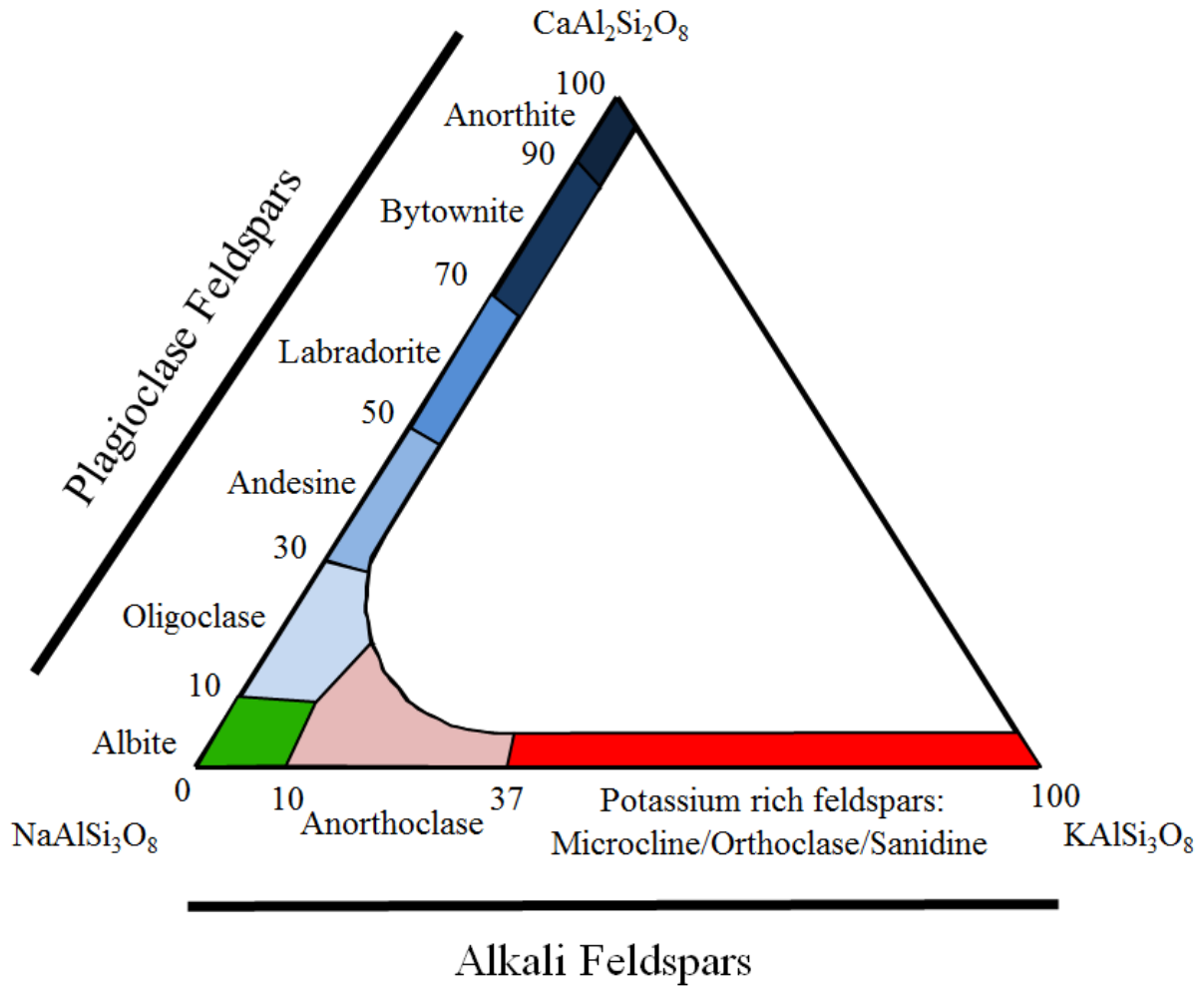


Figure 5: The ternary composition diagram for the feldspars group based on similar figures in the literature (Wittke and Sykes, 1990; Deer et al., 1992).

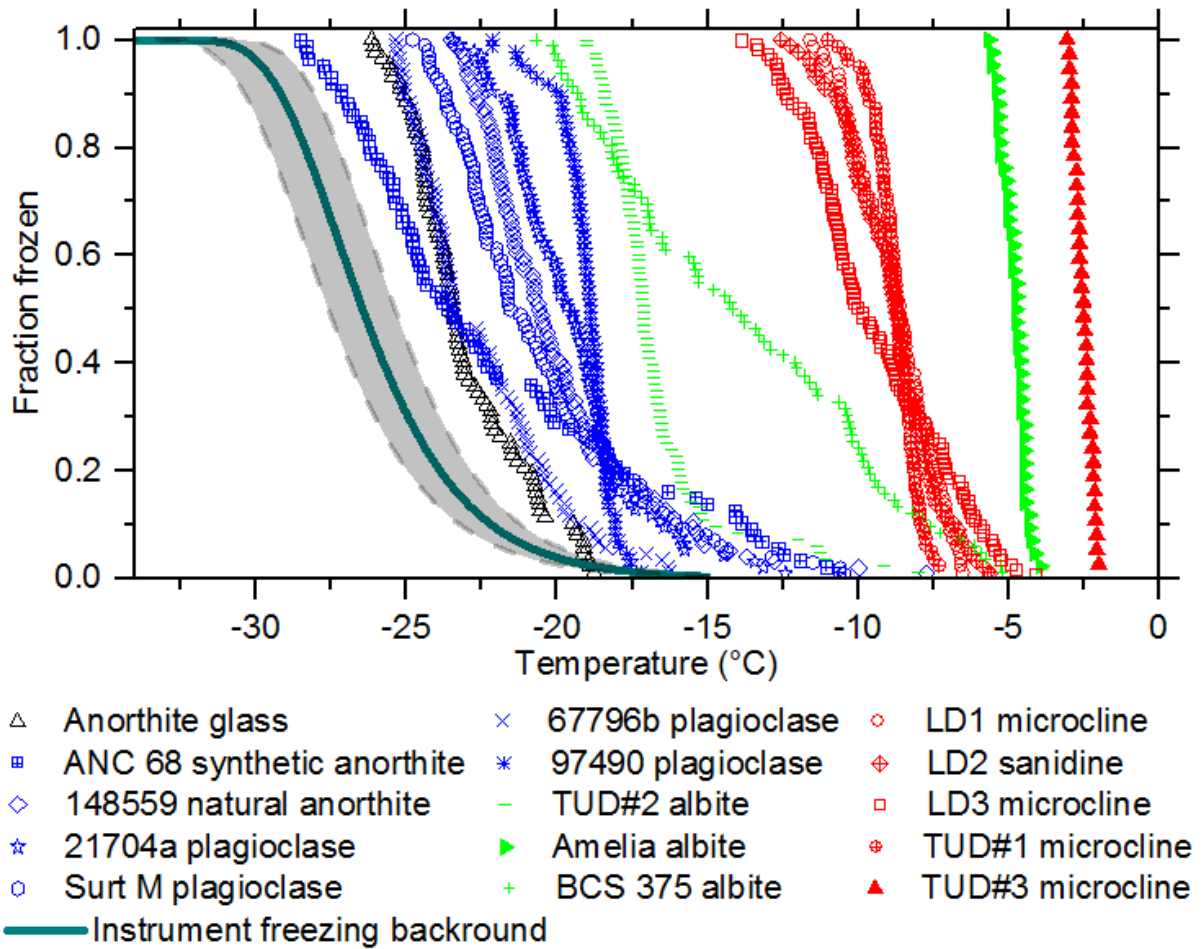


Figure 6: Droplet fraction frozen as a function of temperature for 1 wt% suspensions of ground powders of various feldspar samples. The K-feldspars are coloured red, the plagioclase feldspars are coloured blue, the albites are coloured green and the feldspar glass is coloured black. A fit to the background freezing of pure MilliQ water in the μ -NIPI instrument used by Umo et al. (2015) is also included. The shaded area around this fit shows 95% confidence intervals for the fit. It can be seen that all the feldspar samples tested nucleate ice more efficiently than the background freezing of the instrument.

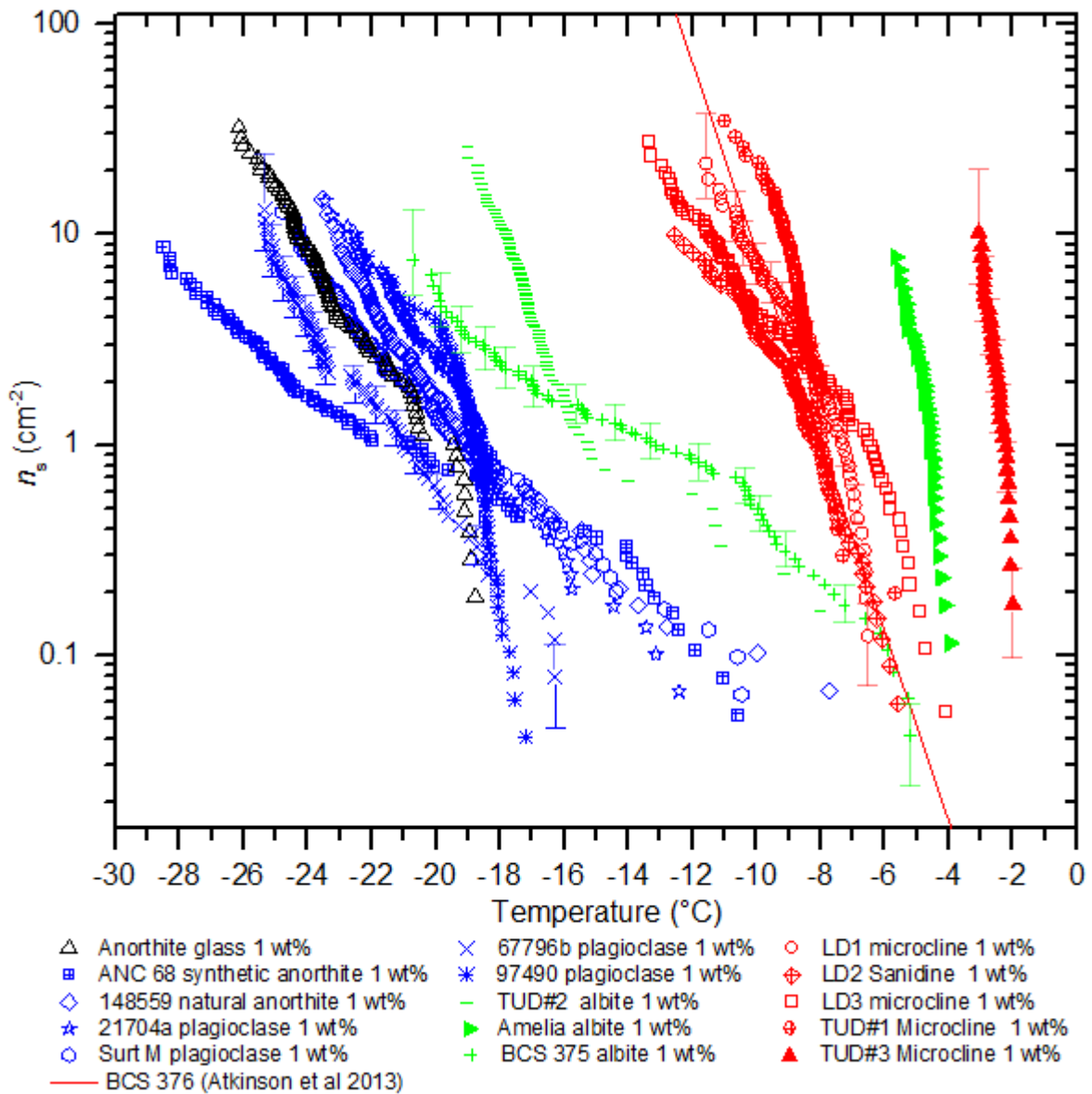


Figure 7: Ice nucleation efficiency expressed as $n_s(T)$ for the various feldspars tested in this study. The K-feldspars are coloured red, the plagioclase feldspars are coloured blue, the albites are coloured green and the feldspar glass is coloured black. Except for Amelia albite and TUD#1 microcline all samples were tested twice and the data from the two runs combined. Sample information can be found in tables 1 and 2. Temperature uncertainty is $\pm 0.4^{\circ}\text{C}$. Y-Error bars calculated using the Poisson Monte Carlo procedure described in Sect. 4. Data points with large uncertainties greater than an order of magnitude have been removed, these are invariably the first one or two freezing events of a given experiment. For clarity error bars have only been included on a selection of datasets

(TUD#3 microcline, LD1 microcline, BCS 375 albite and 67796b plagioclase). The error bars shown are typical.

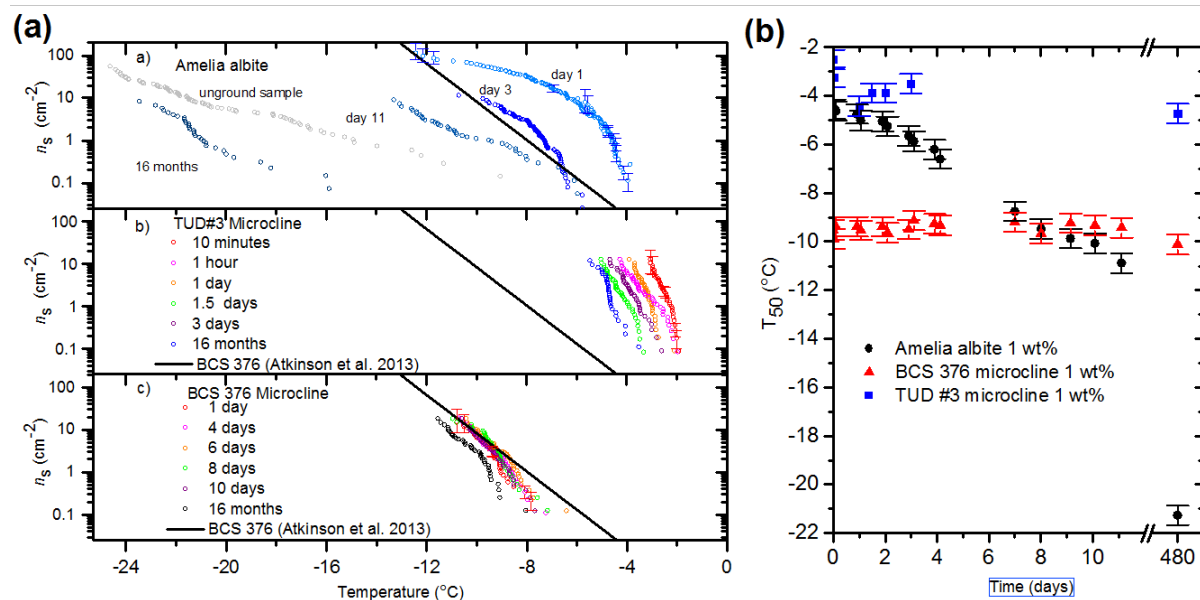


Figure 8: (a) The dependence of n_s on time spent in water for three feldspar samples. The time periods indicate how long samples were left in contact with water. Fresh samples were tested minutes after preparation of suspensions. Note that ice nucleation temperatures of BCS 376 are almost the same after 16 months in water while those of Amelia albite decreases by around 16°C. TUD #3 microcline loses activity quickly in the first couple of days of exposure to water but total decrease in nucleation temperatures after 16 months is only around 2°C. (b) Median freezing temperature against time left in suspension for BCS 376 microcline, TUD#3 microcline and Amelia albite.

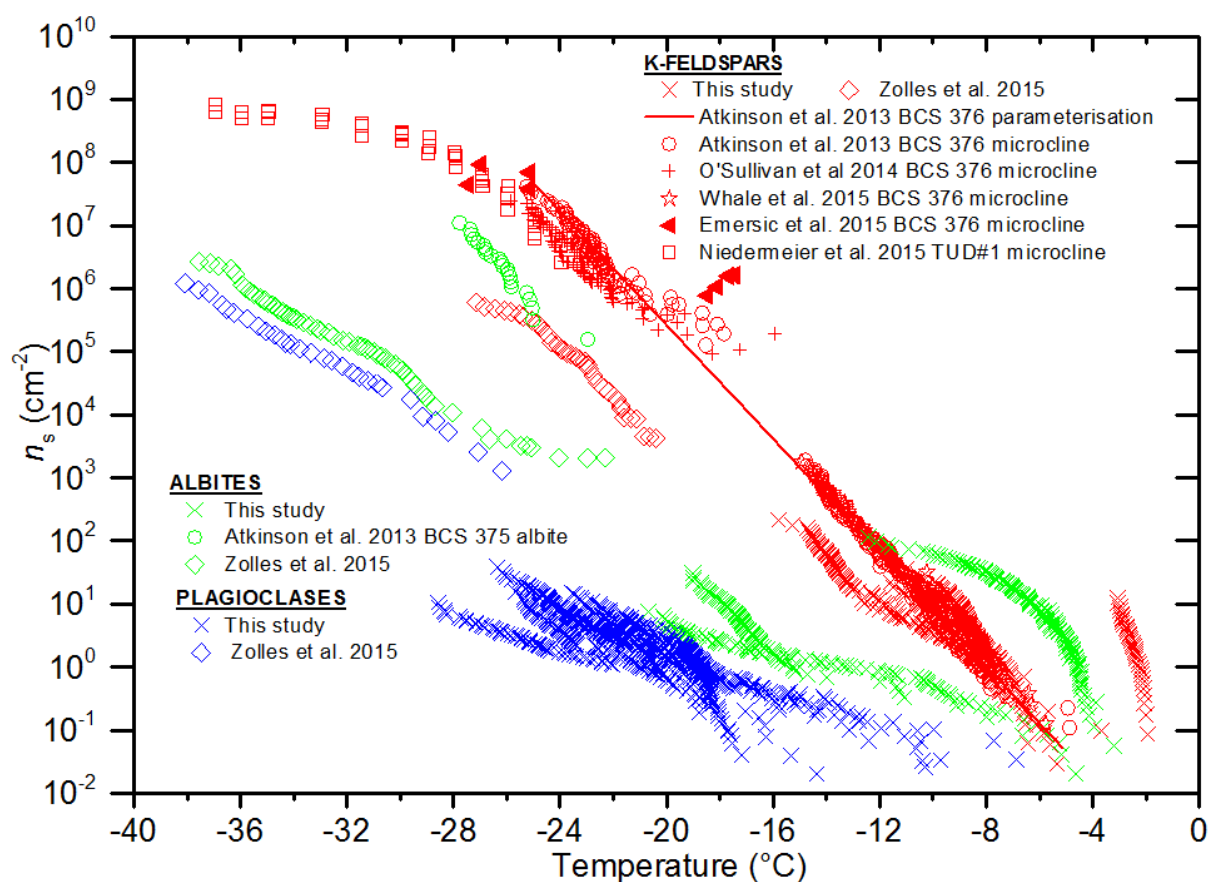


Figure 9: Comparison of literature data from Atkinson et al. (2013), Emersic et al. (2015), Niedermeier et al. (2015) and Zolles et al. (2015) with data from this study. Feldspars are coloured according to their composition, as in Figure 3. 0.1 wt% data for Amelia albite and LD1 microcline, which is not shown in figure 3, has been included. Where samples are known to lose activity with time the most active runs have been shown. Note that data from Niedermeier et al. (2015) includes some data from Augustin-Bauditz et al. (2014).

Table 1. Plagioclase feldspars used in this study.

Sample	Composition*	Source location	Source of composition/phase data	Space group	P o i n t g r o u p	Crystal system
Anorthite glass	An ₁₀₀	Synthetic sample	(Carpenter, 1991)	-	-	-
ANC 68	An ₁₀₀	Synthetic sample	(Carpenter, 1991) describes similar feldspars	P $\bar{1}$	$\bar{1}$	triclinic
148559	An _{99.5} Ab _{0.5}	University of Cambridge mineral collection	-----	P $\bar{1}$	$\bar{1}$	triclinic
21704a	An ₈₆ Ab ₁₄	Viakfontein, Bushveld complex, Transvaal (Harker collection no. 21704)	(Carpenter et al., 1985)	P $\bar{1}$ - $\bar{1}$	$\bar{1}$	triclinic
Surt M	An ₆₄ Ab ₃₆	Surtsey (no. 7517, Iceland Natural History Museum) Phenocrysts from volcanic ejecta	(Carpenter, 1986)	C $\bar{1}$	$\bar{1}$	triclinic

67796b	An ₆₀ Or ₁ Ab ₃₉	Gulela Hills, Tanzania (Harker collection no. 67796)	(Carpenter et al., 1985)	Incommen- surate order	-	triclinic
97490	An ₂₇ Or ₁ Ab ₇₁	Head of Little Rock Creek, Mitchell co., N. Carolina (P. Gay, U.S.N.M. no. 97490)	(Carpenter et al., 1985)	Incommen- surate order	-	triclinic

*This refers to the chemical makeup of the feldspars. An stands for anorthite, the calcium end-member, Ab stands for albite, the sodium end-member and Or stands for orthoclase, the potassium end-member.

Table 2. Alkali feldspars used in this study.

Sample	Dominant feldspar phase	Source location	Source of composition/phase data	Space group	Point group	Crystal system
LD1 microcline	microcline	University of Leeds rock collection	XRD	$C\bar{1}$	$\bar{1}$	triclinic
LD2 sanidine	sanidine	University of Leeds rock collection	XRD	$C2/m$	$2/m$	monoclinic
LD3 microcline	microcline	University of Leeds rock collection	XRD	$C\bar{1}$	$\bar{1}$	triclinic
BCS 376 microcline	microcline	Bureau of Analysed Samples Ltd	Reference sample/XRD (Atkinson et al., 2013)	$C\bar{1}$	$\bar{1}$	triclinic
Amelia Albite (un-ground)	albite	Amelia Courthouse, Amelia Co.,	(Carpenter et al., 1985)	$C\bar{1}$	$\bar{1}$	triclinic

		Virginia (Harker mineral collection)				
Amelia Albite ground	albite	Amelia Courthouse, Amelia Co., Virginia (Harker mineral collection)	(Carpenter et al., 1985)	$C\bar{1}$	$\bar{1}$	triclinic
TUD#1 microcline	microcline	Minas Gerais, Brazil	XRD	$C\bar{1}$	$\bar{1}$	triclinic
TUD#2 albite	albite*	Norway	XRD	$C\bar{1}$	$\bar{1}$	triclinic
TUD#3 microcline	microcline	Mt. Maloso, Malawi	XRD	$C\bar{1}$	$\bar{1}$	triclinic
BCS 375 albite	albite	Bureau of Analysed Samples Ltd	Reference sample/XRD (Atkinson et al., 2013)	$C\bar{1}$	$\bar{1}$	triclinic

* We note that the XRD pattern was also consistent with oligoclase, which is close to albite in composition. The identification of albite is consistent with that of Alexei Kiselev (Personal communication).